JUNE 2021 | HydrocarbonProcessing.com

HYDROCARBON PROCESSING®

HYDROCARBON PROCESSING®

JUNE 2021 | Volume 100 Number 6
HydrocarbonProcessing.com

18

SPECIAL FOCUS: PROCESS OPTIMIZATION

CATALYSTS

SUSTAINABILITY

DIGITALIZATION

PROCESS CONTROLS, INSTRUMENTATION AND AUTOMATION

MAINTENANCE AND RELIABILITY

DEPARTMENTS

COLUMNS

WEB EXCLUSIVE

GAS PROCESSING SUPPLEMENT

Cover Image: Twilight view of a petrochemical plant. Photo courtesy of Honeywell Process Solutions.

99TH ANNIVERSARY 1922–2021

HP Industry Perspectives

Hydrocarbon Processing to showcase the latest in processing technologies and market dynamics

This month, *Hydrocarbon Processing* will be hosting two events—one to showcase the latest in processing technologies in the refining and petrochemicals markets, and the other to provide an update on the latest trends, initiatives and capital project investments in the global hydrocarbon processing industry (HPI).

IRPC Process Technologies. By the time our readers receive this publication, *Hydrocarbon Processing's* International Refining and Petrochemicals Conference (IRPC) will have already been broadcast to more than 1,200 people around the world.

IRPC Process Technologies highlighted the latest technological advancements in conventional and energy transition technologies taking place in the refining and petrochemicals industries. These two routes to transportation fuels and petrochemicals products production will be instrumental in the future of the HPI.

IRPC Process Technologies' conventional refining and petrochemical processing technologies sessions focused on alkylation, desulfurization, ethylene and propylene production, fluid catalytic cracking, hydrocracking, coking and refining-petrochemical integration.

The event's energy transition technologies examined the latest in alternative fuels, biofuels and green petrochemicals production, along with refining and petrochemicals sustainability, the circular economy and plastics recycling technologies.

Although the event has passed, presentations are archived on the event site—www.IRPC-Process.com—and can be viewed on demand.

Industry market outlook. On June 17, *Hydrocarbon Processing's* Editor-in-Chief/Associate Publisher, Lee Nichols, will present an update to the publication's *HPI Market Data 2021*.

Over the past several years, the world has witnessed significant downstream capacity growth in all sectors of the HPI. However, the COVID-19 pandemic caused a considerable decline in demand for fuels and certain petrochemical value chains, leading to low utilization rates, forced capacity closures, and delays or cancellations of capital project investments.

This outlook will provide a mid-year update on capital projects around the world, as well as major economic, environmental and political market trends that are shaping and influencing the HPI in the near term. From new regulations on carbon intensity, sulfur limits in transportation fuels and the increase in biofuels and renewable fuels production to demand scenarios for petrochemical value chains and global LNG trade, the *HPI Market Data 2021* update will provide a global outlook on the forces affecting the HPI and how they are shaping investments globally. Viewers can register at HydrocarbonProcessing.com/Webcasts. HP

HYDROCARBON PROCESSING®
www.HydrocarbonProcessing.com

P. O. Box 2608
Houston, Texas 77252-2608, USA
Phone: +1 (713) 529-4301
Fax: +1 (713) 520-4433
Editors@HydrocarbonProcessing.com

PUBLISHER Catherine Watkins

EDITOR-IN-CHIEF/ ASSOCIATE PUBLISHER Lee Nichols

EDITORIAL

Executive Editor	Adrienne Blume
Managing Editor	Mike Rhodes
Digital Editor	Stephanie Bartels
Technical Editor	Sumedha Sharma
Reliability/Equipment Editor	Heinz P. Bloch
Contributing Editor	Alissa Leeton
Contributing Editor	ARC Advisory Group
Contributing Editor	Anthony Sofronas

MAGAZINE PRODUCTION / +1 (713) 525-4633

Vice President, Production	Sheryl Stone
Manager, Advertising Production	Cheryl Willis
Manager, Editorial Production	Angela Bathe Dietrich
Assistant Manager, Editorial Production	Melissa DeLucca
Graphic Designer	Krista Norman

ADVERTISING SALES
See Sales Offices, page 89.

CIRCULATION / +1 (713) 520-4498 / Circulation@GulfEnergyInfo.com
Director, Circulation: Suzanne McGehee

SUBSCRIPTIONS
Subscription price (includes both print and digital versions): One year $399, two years $679, three years $897. Airmail rate outside North America $175 additional a year. Single copies $35, prepaid.

Hydrocarbon Processing's Full Data Access subscription plan is priced at $1,995. This plan provides full access to all information and data *Hydrocarbon Processing* has to offer. It includes a print or digital version of the magazine, as well as full access to all posted articles (current and archived), process handbooks, the *HPI Market Data* book, Construction Boxscore Database project updates and more.

Because *Hydrocarbon Processing* is edited specifically to be of greatest value to people working in this specialized business, subscriptions are restricted to those engaged in the hydrocarbon processing industry, or service and supply company personnel connected thereto.

Hydrocarbon Processing is indexed by Applied Science & Technology Index, by Chemical Abstracts and by Engineering Index Inc. Microfilm copies available through University Microfilms, International, Ann Arbor, Mich. The full text of *Hydrocarbon Processing* is also available in electronic versions of the Business Periodicals Index.

DISTRIBUTION OF ARTICLES
Published articles are available for distribution in a PDF format or as professionally printed handouts. Contact Foster Printing at Mossberg & Co. for a price quote and details about how you can customize with company logo and contact information.

For more information, contact Jill Kaletha with Foster Printing at Mossberg & Co. at +1 (800) 428-3340 x 149 or jkaletha@mossbergco.com.

Hydrocarbon Processing (ISSN 0018-8190) is published monthly by Gulf Energy Information, 2 Greenway Plaza, Suite 1020, Houston, Texas 77046. Periodicals postage paid at Houston, Texas, and at additional mailing office. POSTMASTER: Send address changes to Hydrocarbon Processing, P.O. Box 2608, Houston, Texas 77252.

Gulf Energy Information

BPA WORLDWIDE

President/CEO	John Royall
CFO	Alan Millis
Vice President, Upstream and Midstream	Andy McDowell
Vice President, Finance and Operations	Pamela Harvey
Vice President, Production	Sheryl Stone
Vice President, Downstream	Catherine Watkins

Publication Agreement Number 40034765 Printed in USA

Other Gulf Energy Information titles include: *Gas Processing™, Petroleum Economist®, World Oil®, Pipeline & Gas Journal* and *Underground Construction.*

LEE NICHOLS, EDITOR-IN-CHIEF/ASSOCIATE PUBLISHER
Lee.Nichols@HydrocarbonProcessing.com

Optimization: Advancing the industry's evolution and benefits to the masses

Optimization—the action of making the best or most effective use of a situation or resource—is not a term that the hydrocarbon processing industry (HPI) takes lightly: it is a way of life.

Throughout the history of the HPI, engineers, inventors, entrepreneurs, executives and other personnel have strived to optimize plant and business operations. This constant drive for improving existing technologies, workflows and supply chains has led to increased efficiency, safety and profitability. However, most importantly, this effort has advanced modern life for billions of people around the world.

Refining. Advancements in the global refining industry have provided transportation fuels to significantly advance the ability to travel incredible distances in a short amount of time. Who would have known that experiments with kerosene would lead to the development of gasoline and diesel to power the internal combustion engine? These processes led to the development of jet fuel and a better propulsion method other than steam to power marine vessels. Do you think the Wright brothers could have envisioned present-day air travel during their historic first flight in 1903? During the last flight of the day, Wilbur Wright stayed in the air for nearly 1 min. and traveled slightly over 850 ft. Fast forward 118 yr and advancements in jet propulsion and fuel technologies enable commercial carriers to travel more than 9,500 mi in a single flight—that is more than 18 hr in the air.

Throughout the history of the refining industry, engineers, scientists, lab technicians and many more have found ways to optimize the fuels that are used in every part of the world. Advancements in new processing technologies are leading to the production of gasoline, diesel and jet fuel with little to no sulfur content. Technology licensors are partnering with owner-operators to develop alternative fuels, biofuels, renewable fuels and sustainable jet fuels. These initiatives and investments in research and development are optimizing the way the world consumes energy, as well as leading to the mitigation of carbon emissions and increasing sustainable operations.

Petrochemicals. The optimization of refining processes has also produced a plethora of petrochemical value chains that have advanced lifestyles and provided lifesaving care for billions around the world. Modern life would not be possible without the work that has been done within this industry.

Although much of the global public is unaware of the petrochemical industry's products, they use these resources every day. For example, when is the last time you used a computer, smartphone or tablet? Did you take any medications today? Has a family member, friend or colleague needed advanced medical care—an all too common occurrence since the outbreak of COVID-19—to help save their life or cure an ailment? Do you live in a home, use modern plumbing systems, drive a car, wear clothes, store food in plastic containers, use plastics packaging, wear makeup, etc.? The list goes on and on. However, the point is that our industry must optimize the message being broadcast to the public.

Optimizing the message. The refining and petrochemical industry is composed of some of the brightest and hardworking people in the history of the world. Their devotion, knowledge and ingenuity have helped advance humankind, and the work being done within these industries is providing better mobility, energy, conveniences and life-improving products. These advancements and benefits to society are the themes that need to be broadcast to the masses outside the industry. HP

INSIDE THIS ISSUE

M. SANCHES, Airswift

Attracting digital talent for petrochemicals: You need a new brand strategy

According to Deloitte, the future success of most chemical companies relies on three areas: growth and innovation, performance and cost optimization, and sustainability and the circular economy. Central to much of this success is industrial digitalization, a hugely exciting transformation that is rapidly stimulating jobs growth. Respondents to the Global Energy Talent Index (GETI) 2021 agree: more than two thirds of industry professionals stated that advances in engineering techniques and technologies present the most important opportunity to the sector, while a further third identified new digitally enabled skills and competencies as another (FIG. 1).

Altogether, these new growth areas—and opportunities for petrochemical companies to get ahead—are creating a surge in demand for digitally minded employees that can help accelerate digitalization within the hydrocarbon processing industry.

COVID-19, digitalization and talent acquisition. Despite this excitement for the future, COVID-19 has created a year of mixed fortunes for the petrochemicals industry. While it is positive that most pure-play petrochemicals companies fared rather well, even seeing an uptick in demand for certain products, this has certainly not been the case for all. The reality is that many boards at larger integrated energy companies were faced with making difficult decisions, including layoffs, pay and benefits cuts, and restructuring that significantly impacted their employee base and company culture, and ultimately tarnished their brand.

In any industry, talent acquisition is predicated on the ability of a company to weave a compelling narrative of its brand and its core values. Yet, while the petrochemicals industry is no stranger to rebounding from downturns and healing its image

FIG. 1. Industry data from the Global Energy Talent Index (GETI) 2021 report.

with digital transformation underway, the landscape is beginning to look quite different.

Companies in the hydrocarbons sector must get closer to the pool of candidates that they want to hire to meet their digital transformation goals. Every candidate is a consumer, and almost all consumers are inspired by innovation.

In the context of digital transformation, the industry faces stiff competition from inspiring brands in rival sectors, such as renewables and consumer-tech, as well as the Googles and Amazons that all equally need bright, digitally minded hires. If petrochemicals companies want to obtain a competitive advantage to attract the best talent, do they now need to position themselves as the SpaceX of the tech world?

If digital transformation is a top priority for the company, then the short answer is, "Yes." Particularly for today's college graduates, the state of a company's brand can make or break whether they will be attracted to working with that company. One way to satisfy this need is to make the company more widely relevant and position it as a leader of the future. For that, you need a multi-brand approach.

Becoming widely relevant. Companies in the hydrocarbons sector must get closer to the pool of candidates that they want to hire to meet their digital transformation goals. Every candidate is a consumer, and almost all consumers are inspired by innovation. In fact, interest in the sector and innovation were the second and third most popular reasons—after career progression—why respondents to GETI 2021 said they chose to work in the petrochemicals industry.

That said, the story of innovation can be a difficult one to tell for a large, historically industrial petrochemicals company with a single or few brands. So, a multi-brand approach to brand strategy can comprise splitting the brand up to connect better with consumers and positioning the business as a pioneering, attractive employer.

This allows those companies to showcase their technology partners and product innovations, helping candidates connect the dots from what they experience in the world back to the petrochemicals industry.

Thousands of petrochemicals applications can be found in the home and everyday life—from the iPhone in our pocket to the tires on our car—but few consumers stop to think about the supplier of the raw materials. Petrochemicals companies can gain substantially from making their brands more relevant by coloring in that dotted line between their products and everyday life to help potential hires better understand the business.

Some companies are doing this phenomenally well. When you interact with them digitally through their website or LinkedIn, for example, you gain a real understanding of the impact of the products that they manufacture, as well as how they approach corporate social responsibility (CSR), be it diversity and inclusion, environmental programs, carbon recapture projects or product lifecycle.

Society recognizes that all companies must be in the race to net-zero, so having planned CSR goals, progress and results visible to all is very powerful—it is what connects with today's consumer, and today's talent. There is no longer a question about whether employees would rather work for a responsible and environmentally friendly company: it is a given.

So, it follows that companies that fail to create a strong digital presence and brand strategy to bring consumers on their sustainability journey will be overlooked. So many of us now make our buying decisions based on our digital experiences and research, often without even contacting the company. This situation is no different for petrochemicals companies when competing to attract, hire and retain the best talent in our very competitive digital world.

Sustainable credentials. Similarly, a multi-brand approach can also help petrochemicals companies leverage the environmental credentials of certain products to improve talent acquisition. Many of today's college graduates are deeply interested in improving the world around them and having a positive impact on sustainability. A 2019 study by Fast Company found that three quarters of millennials would accept a smaller salary to work for a company that is more environmentally responsible. At the same time, the petrochemicals industry is doing a huge amount of work to improve sustainability and the lifecycle impact of its products; yet those results are often buried in a CSR report only ever to be read by investors.

By being able to demonstrate sustainable product innovation through a multi-brand approach, petrochemicals businesses can better connect with bright and curious minds through the values that matter most to them.

If a multi-brand approach does not make sense in the context of the business, the alternative is to have a strong angle on the product applications that raw materials are developed into. Where possible, choosing "on trend" product applications—such as the petrochemical components in electric vehicles, for example—will again drive a greater sense of relevance, while tying the brand to innovation.

As with previous shocks to the sector, once the dust settles from COVID-19, petrochemicals companies will want to take stock of any damage to their brand. However, for those with industrial digitalization ambitions, it will not simply be about repair. As graduate hiring programs ramp up once more, now is the opportune time to realign brands to attract the hires needed for digitalization. A refreshed brand strategy will be crucial for success, and not just one that can edge out other petrochemical companies, but one that can compete for digital talent on the global stage. HP

MICHAEL SANCHES is the Consultancy Director, Management Consulting, and Global Sales Director for Airswift, leading the company's consultancy practice across the Americas. He works as a client partner to scope, improve or build contingent workforce solutions and talent acquisition services that include executive and professional search and selection via engaged search, retained search and RPO methodologies; benchmarking; talent mapping; market intelligence research; and managed solutions, including MSP and RPO. Mr. Sanches has worked with executives, HR practitioners and operational leaders across many sectors, including petrochemicals, refining, midstream and pipeline, pulp and paper, wind and solar, biogas, nitrogen, and mining and metals. As a client partner, he assesses recruitment and workforce strategies, rationalizes supplier bases, implements change and develops employer value propositions that speak to targeted talent and hiring campaigns.

HEINZ P. BLOCH, RELIABILITY/EQUIPMENT EDITOR
Heinz.Bloch@HydrocarbonProcessing.com

Exploring better compressor sour seal oil traps

An interesting case involving sour seal oil traps in an offshore application recently came to our attention. One of the platforms has several compressors with fluid film mechanical seals and, as is usually the case, whatever portion of H_2S-containing gas that comes into contact with the fluid film seals must be given special treatment. In essence, before the oil can be reused in the compressor's bearings and seals, the entrained gas must be separated from the oil. The separation process involves sour seal oil traps or "drainers" (located as shown in FIG. 1 and FIG. 2) that operate on the same principles as condensate traps in steam piping systems.

When it became clear that the degassing system did not adequately remove the sour gas, a troubleshooting exercise determined that the originally supplied sour seal oil traps did not work properly. With "sour"—meaning contaminated with H_2S—gas remaining entrained within the seal oil system, the density of the sour seal oil was lower than anticipated. The floats associated with the sour seal oil traps (or drainers) were apparently too heavy and did not lift as the liquid level in the sour seal oil traps increased. Lighter-weight floats were then provided by the compressor manufacturer; these compensated for the lower-density sour seal oil. They worked properly, and no further seal oil system problems were reported (FIG. 2).

Questions and answers. Whether traps constructed with a wider range of adjustability could have been supplied in the first place is not known. The experience seems to relate to an infrequent occurrence.

An appropriate note to the various bidders should alert them to application constraints that deal with gas entrainment in seal oils. Vendor experience checks are appropriate and should be done for sour seal oil traps. For the reliability-focused among us, this failure incident would have been the trigger event causing us to explore superior-quality sour seal oil traps. We would have followed up by researching styles or models based on the principles embodied in free-floating steam condensate traps.

Free-floating designs can be problem-solvers; they have lifetimes that harmonize with the run length extension needed for reliable facilities and high profitability. One vendor claims that successful similar applications include fluid specific gravities as low as 0.55, while another led us to believe that suitable designs cover the full range of specific gravities found in modern process gas compressors.

Nonetheless, vendor experience should be established before we would consider purchasing sour seal oil traps for the turbomachinery installed in our highly reliability-focused user facility. With a continuous focus on reliability, frankly, it would not matter what kinds of seals are in our machines and whether or not the entrained gas had corrosive properties.

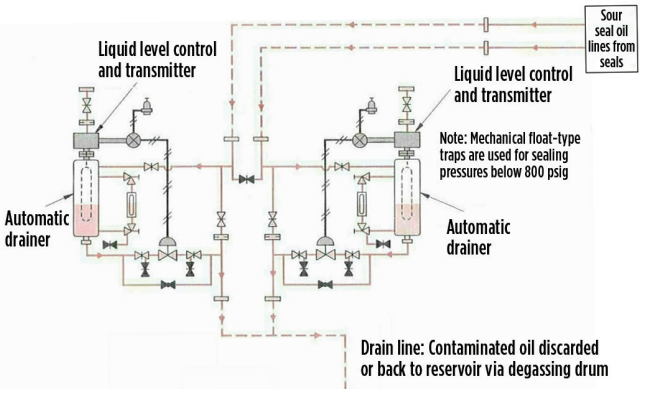

FIG. 1. Separation process for entrained gas involving sour seal oil traps.

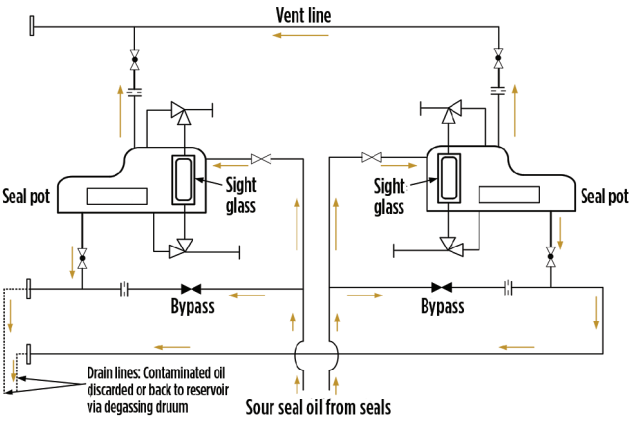

FIG. 2. Manual seal oil drain system.

Remember that best-in-class (BiC) users work with innovative designers and manufacturers. Instead of only hoping that the innovators present their products to the BiCs, the self-starters at BiCs will likely approach the four most prominent compressor manufacturers and ask them for the names of two cooperative, high-quality trap manufacturers. Cultivate them early and find solutions to potential trap problems. HP

HEINZ P. BLOCH resides in Montgomery, Texas. His professional career commenced in 1962 and included long-term assignments as Exxon Chemical's Regional Machinery Specialist for the U.S. He is an ASME Life Fellow and one of 10 inaugural inductees into the New Jersey Institute of Technology's Hall of Fame, which honors its most distinguished alumni. Among his 23 books on fluid machine reliability improvement is *Optimized Equipment Lubrication, Oil Mist Technology and Storage Preservation,* which describes many lubrication-related traditions that should have been phased out long ago. An expanded and slightly revised second edition is scheduled for release in early 2022.

A. DAVID
Endress+Hauser, Indianapolis, Indiana

Safety, simplicity and productivity provide the value needed in plant operations

In today's manufacturing environment, process automation professionals must choose from a multitude of widgets and innovations to help their plants run more smoothly. This raises questions as to what makes a new technology or widget useful and not just another PowerPoint slide detailing features and benefits.

When researching the universe of process automation technologies, it is easy to get excited about something new and innovative. However, investing in new technology for the plant environment is much harder than upgrading to the newest smartphone. Many different aspects and effects of proposed improvements must be considered, including compatibility with existing systems, ease-of-use, cost/benefit ratio and other factors.

Before deciding to install the newest widget in the market, it is important to evaluate the everyday work and demands of the process automation professionals who are the end users of the equipment. How can this new technology make their lives easier, and why should they care about this new tool? While the reasoning may change depending on who in the plant one is talking to, simplicity, safety and productivity are interconnected points that provide a solid basis for evaluating new technologies. This sentiment is shown in the following examples.

Improving instrument commissioning and operation. Smartphone apps are a relatively new tool in the industrial arena, although they have been in use for more than a decade in the consumer and commercial sectors.

Many process plants experience problems with instrument commissioning and with ongoing operations due to a lack of readily available diagnostics. Existing tools—ranging from pen and paper to frequent field visits—are not up to the task. To address these and other issues, some instrument vendors have introduced smartphone apps, allowing plant personnel to interact with process instruments via Bluetooth.

The following details how this new technology can be used to improve safety, simplicity and productivity.

Safety. Instrument apps make interactions with instruments safer. Technicians do not need to open electrical panels or instrument housings to establish the connectivity required for commissioning and diagnostics. Commissioning wizards walk a technician through the entire startup process, while ensuring that no steps are skipped. This is especially important for startup and verification of safety systems, where completing every step is essential for devices to function as intended. Bluetooth provides connectivity up to 30 ft, eliminating the need for a lift in certain cases, while decreasing fall risks and job site accidents.

When combined with onboard monitoring and verification software, technicians can see process data and diagnostics in real time. This empowers them to make predictive maintenance decisions on the spot, further decreasing the possibility of job site accidents due to equipment failure or product contamination.

An often-overlooked aspect of safety is cybersecurity, which should be provided along with any Bluetooth app intended for use in industrial applications. Features to look for include:

- Connectivity with a security level rating of at least "High" from an independent security specialist [e.g., the Fraunhofer Institute for Applied and Integrated Safety (AISEC)], which provides a level of security just below that of passports and credit cards.
- Passwords are never stored on the app or the instrument.
- Instruments can only be accessed wirelessly using the app.

Once paired with a handheld device, basic information—such as tag number, PV and instrument status—are visible to the technician without the need for a password. This provides visibility to basic information but with no ability to alter settings without the password.

Simplicity. Smartphone apps make instrument interactions simpler. Bluetooth communication eliminates the need for handheld communicators, which may require periodic updates. Guided commissioning ensures all bases are covered, converting a complex set of steps to a simple procedure.

The ability to access the reports generated by verification and monitoring software makes documentation much simpler, as well. Rather than manually filling out a report each time a setting is changed or when an instrument is checked, technicians can generate an "As Found" file before and an "As Left" file after assessing the instrument. This eliminates any questions about who made the adjustment or why it was made, which provides homogeneity among technicians.

Productivity. Imagine walking all the way across a plant to the instrument shop, grabbing a communicator (if one is available), walking back to the other side of the plant and then climbing up the side of a tank only to discover that the handheld does not have the proper EDD or DTM file loaded to communicate with the instrument requiring service. This problem becomes even more pronounced in petrochemical plants and refineries because they are often spread out over wide areas and require a lot of time to traverse from one side to the other.

Once the technician has gone back to the instrument shop—either updating the drivers or grabbing a different handheld that has been preloaded—and trekked back to the instrument,

diagnostic information can be accessed from the device. However, even after the diagnostic code(s) has been retrieved, another trip to the instrument shop may be needed to look up the diagnostic information, unless the technician makes a habit of carrying around all the manuals required for each instrument. Once a decision is made about what to do with the instrument, it may require a part replacement or a call to technical support, forcing another trip back to the instrument shop.

Implementing the latest widget or tool in the market only matters if it provides intrinsic value to plant personnel.

Loading all the information contained in a manual into an app that is updated and easily accessible keeps technicians from having to go back and forth, increasing productivity and reducing frustration. The ability to access all technical information, manuals and diagnostic codes for specific devices through an app allows technicians to handle everything in a single trip to the instrument, as well as provides them the ability to retrieve any part number(s) or technical support they may need right then and there.

Verification and monitoring software provides homogenous report generation, so technicians can document issues without having to type or open a separate laptop or other device. Everything is at their fingertips, quite literally. One single problem that may have lasted the entire workday now can be solved in a fraction of the time.

Takeaway. While a smartphone app, along with verification and monitoring software, were used in this example, the guidelines of safety, simplicity and productivity can be used to evaluate any new instrument or innovation. Implementing the latest widget or tool in the market only matters if it provides intrinsic value to plant personnel. Investment in new products requires a specific need to be met, along with justification for changing standard operating procedures that may have been in place for decades. When the above criteria are satisfied, enhancements are much more likely to provide expected improvements in productivity. HP

ASHLEY DAVID is a Product Marketing Manager for Endress+Hauser. She is focused on providing strategic vision, leadership and marketing direction for Endress+Hauser's level and pressure products, as well as leading and managing the development of business portfolio concepts and marketing plans. Previously, Ms. David served as a Regional Business Driver specializing in pressure, temperature and system products for Endress+Hauser. She has also spent time working in technical support and application engineering, creating expertise in customer processes and manufacturing.

N. LIU, Shell Catalysts & Technologies,
The Hague, the Netherlands

Increasing blue hydrogen production affordability

Large-scale, affordable, "blue" hydrogen (H_2) production from natural gas, along with carbon capture, utilization and storage (CCUS), is necessary to bridge the gap until large-scale H_2 production using renewable energy becomes economic. The cost of carbon dioxide (CO_2) already makes blue H_2 via steam methane reforming (SMR) competitive against gray H_2 (without CCUS), and a newly available process[a] based on gas partial oxidation (POX) technology and pre-combustion CO_2 capture solvent technology further increases the affordability of blue H_2 for greenfield projects.

Why blue H_2? A growing number of national governments and energy companies, including Shell,[1] have announced net-zero-emissions ambitions. Although renewable electricity is expanding rapidly, without low-carbon H_2 as a clean-burning, long-term-storable, energy-dense fuel, a net-zero goal is difficult to achieve, especially when it comes to decarbonizing fertilizer production and hard-to-abate heavy industries such as steel manufacturing and power generation. H_2 also has potential as a transport and heating fuel that could repurpose existing gas distribution infrastructure or be introduced into existing natural gas supplies.

Consequently, H_2 plays an important part in many green strategies. The EU's H_2 strategy,[2] published in July 2020, describes it as "…essential to support the EU's commitment to reach carbon neutrality by 2050 and for the global effort to implement the Paris Agreement while working towards zero pollution."

Momentum is building with a succession of commitments to H_2 by various companies and governments. For example, in June 2020, Germany announced a €9-B H_2 strategy,[3] and the International Energy Agency stated, "Now is the time to scale up technologies and bring down costs to allow hydrogen to become widely used."[4] Over the past 3 yr, the number of companies with membership in the international Hydrogen Council—which predicts a tenfold increase in H_2 demand by 2050[5]—has jumped from 13 to 81 and includes oil and gas companies, automobile manufacturers, trading companies and banks.

In 2018, global H_2 production was 70 MMtpy.[4] Today's demand is split between use for upgrading refined hydrocarbon products and as a feedstock for ammonia production for nitrogen fertilizers. Nearly all H_2 production comes from fossil fuels: it accounts for 6% of natural gas and 2% of coal consumption, as well as 830 MMtpy of CO_2 emissions[6]—more than double the UK's emissions.[7] Gray H_2 is a major source of CO_2 emissions. If H_2 is to contribute to carbon neutrality, it must be produced on a much larger scale and with far lower emissions levels.

Over the long term, the answer is likely to be "green" H_2, which is produced from the electrolysis of water powered by renewable energy. This supports the integration of renewable electricity generation by decoupling production from use. H_2 becomes a convertible currency, enabling electrical energy to be stored and used as an emissions-free fuel and chemical feedstock.

Green H_2 projects are starting. For example, a Shell-led consortium is at the feasibility stage of the NortH2 wind-to-H_2 project in the North Sea, and a Shell–Eneco consortium secured the right to build the 759-MW Hollandse Kust Noord project at a subsidy-free Dutch offshore wind auction in July 2020; this project will include a green H_2 technology demonstration.

However, electrolysis alone will not meet the forecast demand. It is expensive at present, and there is insufficient renewable energy available to support large-scale green H_2 production. To put the scale of the task into perspective, meeting today's H_2 demand through electrolysis would require 3,600 TWh of electricity, more than the EU's annual use.[4] Moreover, using the current EU electricity mix would produce gray H_2 from electrolysis with 2.2 times the greenhouse gas emissions of producing gray H_2 from natural gas.[8] This is because nearly half (45.5%) of the net electricity generated in the EU comes from burning natural gas, coal and oil,[9] and generating electricity from natural gas, for example, has a 44% efficiency.[10]

An alternative is blue H_2 produced from natural gas, coupled with CCUS. H_2 production via electrolysis has a similar efficiency to blue H_2 production, but the levelized cost of production is significantly higher for electrolysis at €66/MWh, compared with €47/MWh for SMR–CCUS.[11]

In addition, it is widely acknowledged that scaling up blue H_2 production will be easier than delivering green H_2. For example, the EU strategy[2] states, "Other forms of low-carbon hydrogen [i.e., blue] are needed, primarily to rapidly reduce emissions … and support the parallel and future uptake of renewable [green] hydrogen."

However, the strategy goes on to claim that neither green nor blue H_2 production is cost-competitive against gray; the H_2 costs estimated for the EU are €1.5/kg for gray, €2/kg for blue and up to €5.5/kg for green.[4] These costs are based on an assumed natural gas price for the EU of €22/MWh, an electricity price of €35/MWh–€87/MWh and a capacity cost of €600/kW.

With the cost of CO_2 at $25/t–$35/t, blue H_2 becomes competitive against gray even with higher capital costs, and green H_2 still may be more than double the price of blue H_2 by 2030 (**FIG. 1**).[4] Some forecasts indicate that cost parity will occur around 2045.[12]

This competitiveness between blue and gray H_2 (when considering CO_2 costs) is based on SMR technology, but other technologies are available to further increase blue H_2 affordability for greenfield projects.

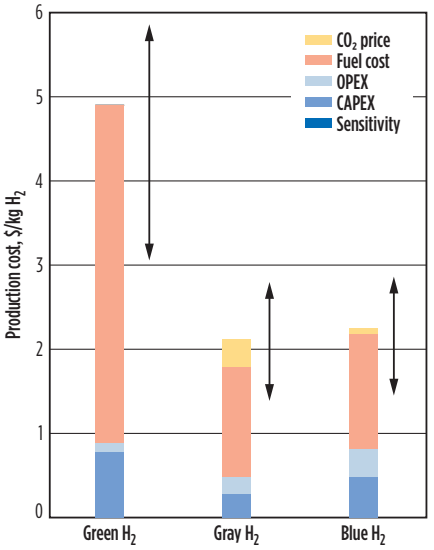

FIG. 1. Estimated H_2 production costs in 2030.

Greenfield technology options. This article considers three technology options for greenfield blue H_2 projects: SMR, autothermal reforming (ATR) and a proprietary gas POX technology[b] (**FIG. 2**).

SMR. SMR, a proven catalytic technology widely applied for gray H_2 production, uses steam in a multi-tubular reactor with external firing for indirect heating. More than 48% of H_2 production is from natural gas, with SMR being the most common production technology.[13] Post-combustion carbon capture[c] can be retrofitted to convert gray H_2 production to blue and is proven to capture nearly all the CO_2 (99%) from low-pressure, post-combustion flue gas.

However, for greenfield blue H_2 applications, oxygen (O_2)-based systems, such as ATR and gas POX technology, are more cost-effective than SMR (**FIG. 3**), a conclusion backed by numerous studies and reports.[14] **Note:** The cost of CO_2 makes gray H_2 via SMR more expensive than blue H_2 from SGP technology. The cost advantage of O_2-based systems over SMR increases with scale because the relative cost of the air separation unit decreases with increasing capacity. Another advantage is that more than 99.9% of the CO_2 can be captured using a lower-cost, pre-combustion solvent technology.[d]

ATR. ATR uses O_2 and steam with direct firing in a refractory-lined reactor with a catalyst bed. It is more cost-effective than SMR, but it requires a substantial feed gas pre-treatment investment, and the fired heater produces CO_2 emissions (**FIG. 2**). ATR can be combined with pre-combustion carbon-capture technology to convert gray H_2 production to blue.

Gas POX technology. Gas POX technology is also an O_2-based system with direct firing in a refractory-lined reactor, but it is a noncatalytic process that does not consume steam and has no direct CO_2 emissions. It, too, can be combined with pre-combustion carbon-capture technology for blue H_2 production. Compared with SMR, gas POX technology saves money by maximizing the carbon-capture efficiency and simplifying the process lineup, both of which offset the cost of O_2 production (**FIG. 4**).

POX vs. ATR for blue H_2. As O_2-based systems offer clear benefits over SMR, this article considers the advantages of the proprietary gas POX technology[b] over ATR for blue H_2 production.

A key advantage is that the POX reaction does not require steam as a reactant. Instead, high-pressure steam is generated by using waste heat from the reaction, which can satisfy the steam consumption within the blue H_2 process, as well as some internal power consumers.

With no need for feed gas pre-treatment, gas POX technology has a far simpler process lineup than ATR (**FIG. 2**). Also, as a noncatalytic, direct-fired system, it is robust against feed contaminants such as sulfur and can accommodate a large range of natural gas qualities, thereby giving refiners greater feed flexibility to decarbonize refinery fuel gas.

Gas POX technology[b] provides substantial savings compared with ATR—a 22% lower levelized cost of H_2 (**FIG. 5**). These savings come from a 17% lower CAPEX owing to the potential for a higher operating pressure leading to a smaller H_2 compressor (single-stage compression), CO_2 capture and CO_2 compressor units, and a 34% lower OPEX (exclud-

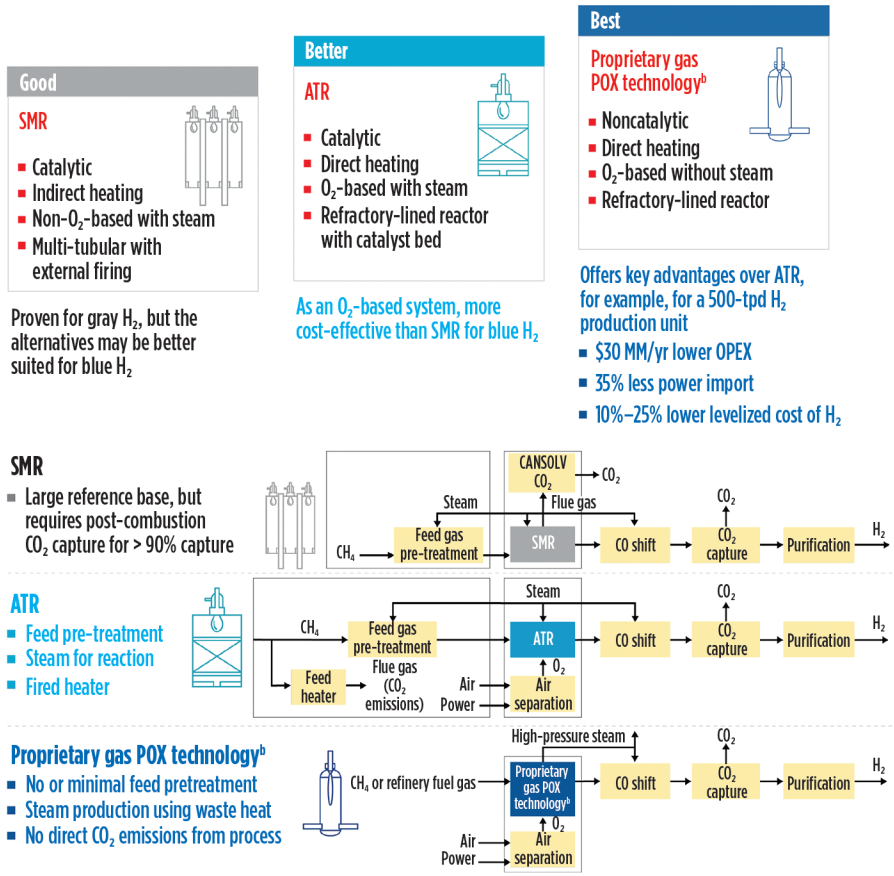

FIG. 2. Blue H_2 technologies and process lineups.

ing the natural gas feedstock price) from reduced compression duties and more steam generation for internal power. Gas POX technology consumes 6% more natural gas, but this is offset by power generation from the excess steam.

The proprietary blue H_2 process[a] is an end-to-end lineup that maximizes the integration of the gas POX and solvent technologies. Compared with an ATR unit, modeling shows (based on the parameters in **TABLE 1**) that a lineup producing 500 tpd of pure H_2 would have:

- $30 MM/yr lower OPEX
- 35% less power import
- > 99% CO_2 capture
- 10%–25% lower levelized cost of H_2.

The gas POX–solvent process is the best option for large-scale blue H_2 projects. **FIG. 6** shows the principle advantages of integrating it with other proprietary and open-source technologies.

The choice between a methanator or a pressure-swing absorption (PSA) unit for the H_2 purification step depends on the required H_2 purity. For example, a PSA unit is necessary to achieve the > 99.97% purity required for the H_2 used in fuel cells. The offgas is predominantly H_2, with trace containments such as CO, CO_2 and nitrogen. In the ATR process, this offgas is typically burned to preheat the natural gas, which produces direct CO_2 emissions.

In a methanator, the purity of the final H_2 is lower (> 98%, depending on the feed gas properties). However, it avoids the direct CO_2 emissions from burning the PSA offgas. The main advantage of choosing a methanator is that H_2 is not lost via the PSA offgas. Consequently, it reduces natural gas consumption for the same H_2 production. In addition, a methanator is commonly applied in industry, as it satisfies the H_2 purity requirements of most industrial consumers.

History of gas POX oxidation technology. The gas POX technology[b] is mature and "low-carbon," which makes it eligible for government funding. It has a long history of development and usage. For example, research into oil gasification was being conducted in Amsterdam, the Netherlands as early as 1956.

Today, the proprietary gas POX technology[b] has more than 30 active residue and gas gasification licensees, and more than 100 gasifiers using the technology

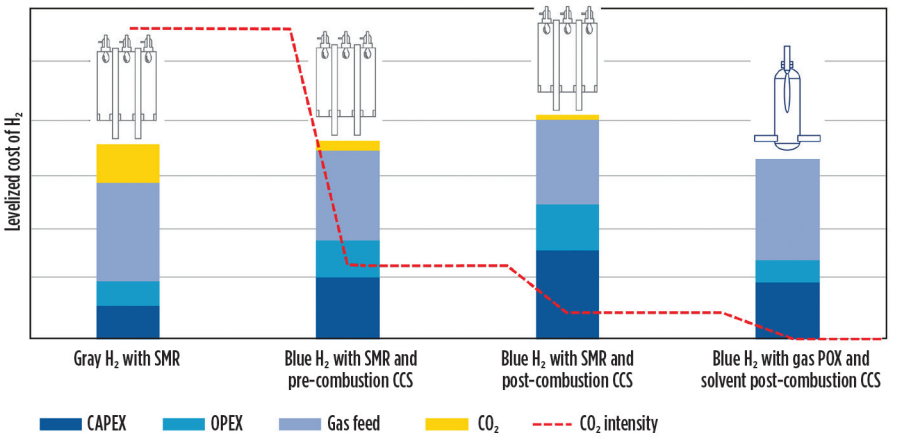

FIG. 3. Relative CO_2 intensity and cost of gray and blue H_2 via SMR with pre- and post-combustion capture, and blue H_2 via proprietary gas POX[a] and pre-combustion capture solvent[d] technologies.

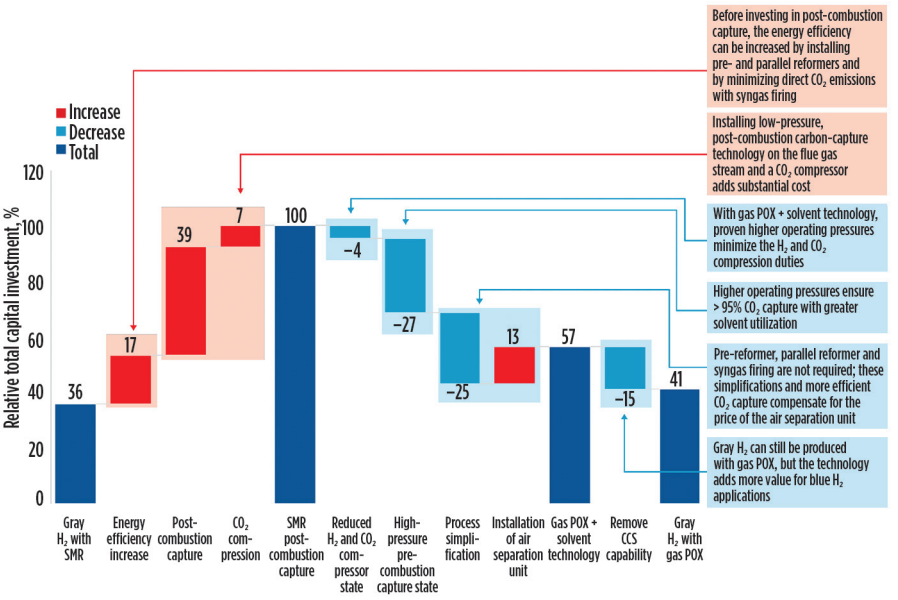

FIG. 4. Relative capital investment comparison between gray and blue H_2 via SMR and gas POX technology.

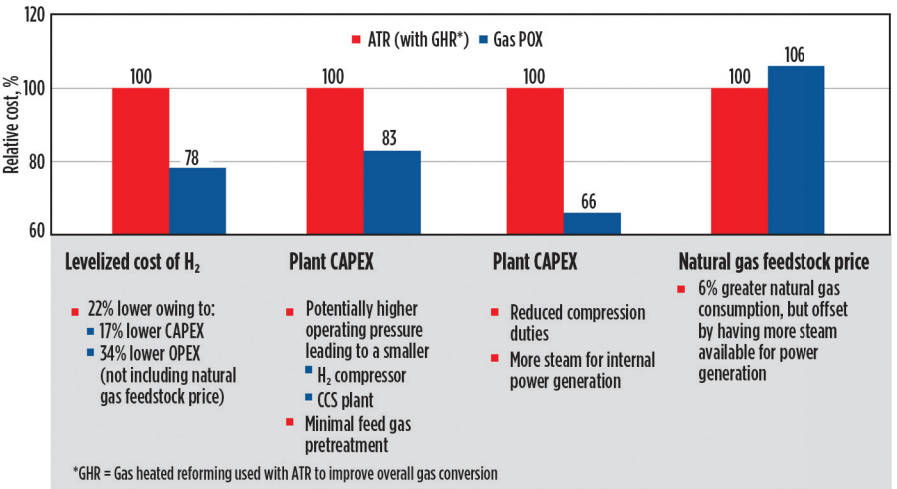

FIG. 5. The cost of gas POX technology relative to ATR.

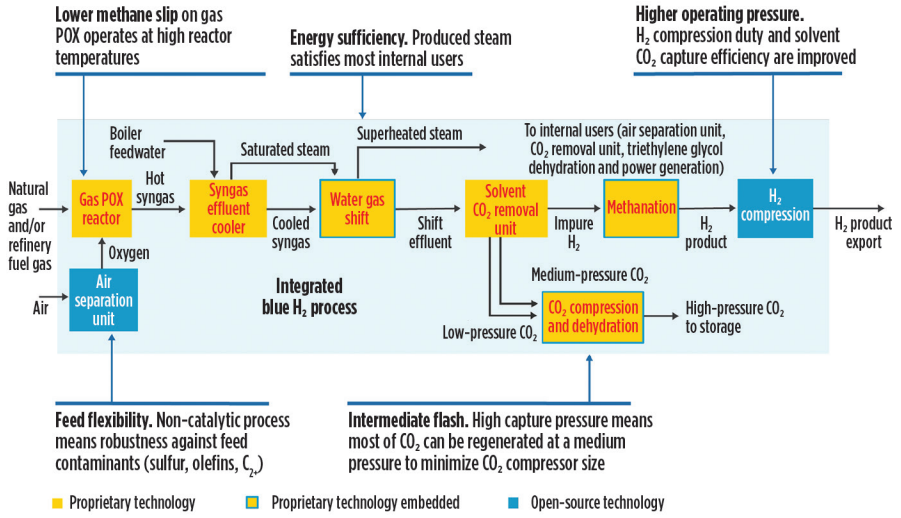

FIG. 6. The advantages of integrating the proprietary blue H_2 process with other technologies, with Shell as the master licensor.

TABLE 1. Modeling parameters

Pure H_2 production, tpd*	500
Natural gas cost, $/t equivalent	396
Demineralized water, $/t equivalent	8.4
Power import, $/MWh	86
H_2 discharge pressure, bara	72
CO_2 discharge pressure, bara	150
Plant availability, %	95

*Excluding inerts, methane, CO_2 and CO, which will also be present, depending on the final purification step. Solvent, triethylene glycol and catalyst costs are estimated.

have been built worldwide. For example, the Pearl gas-to-liquids (GTL) plant in Qatar has 18 trains, each with an equivalent pure H_2 production capacity of 500 tpd. Pearl GTL has been operating since 2011. The product is defined as pure H_2 production—i.e., not including any inerts, methane, CO_2 or CO, which will also be present, depending on the final purification step.

Since 1997, the Pernis refinery in the Netherlands has been operating a 1-MMtpy carbon-capture program using the technology. The CO_2 is used in local greenhouses. The CO_2 stream is an essential part of the Pernis CCS project.

No matter how cost-effective the H_2 production and carbon-capture technologies, without sequestering the CO_2 directly or through enhanced oil recovery, the H_2 remains gray. Many CCUS projects are in operation at various stages throughout the world. For example, since 2015, the Shell Quest facility in Canada has captured and stored more than 5 MMt of CO_2.

Key takeaways. H_2 will be part of the future energy mix, and several mature technologies are available for producing cost-effective, low-carbon blue H_2. For greenfield applications, SMR is an inefficient method of producing blue H_2 owing to poor CO_2 recovery and scalability; O_2-based systems offer better value (an independently backed conclusion).

The proprietary blue H_2 process[a], which integrates proprietary gas POX[b] and solvent[c] technologies, offers key advantages over ATR, including a 10%–25% lower levelized cost of H_2, a 20% lower CAPEX, a 35% lower OPEX (excluding natural gas feedstock price), > 99% CO_2 captured and overall process simplicity. The process, which is now available to third-party refiners, is proven at the 500-tpd scale. HP

NOTES

[a] Shell Blue Hydrogen Process (SBHP)
[b] Shell gas partial oxidation process (SGP)
[c] Shell CANSOLV CO_2 Capture System (CANSOLV is a Shell trademark)
[d] Shell ADIP ULTRA solvent technology

LITERATURE CITED

[1] Van Beurden, B., "A net zero emissions energy business," Shell, April 16, 2020, Online: https://www.shell.com/media/speeches-and-articles/2020/a-net-zero-emissions-energy-business.html
[2] European Commission, "A hydrogen strategy for a climate-neutral Europe," July 7, 2020, Brussels, Belgium.
[3] Press and Information Office of the German Federal Government, "German government adopts hydrogen strategy," June 10, 2020, Online: https://www.bundesregierung.de/breg-en/news/wasserstoffstrategie-kabinett-1758982
[4] International Energy Agency, "The future of hydrogen," June 2019.
[5] Hydrogen Council, "Hydrogen scaling up: A sustainable pathway for the global energy transition," November 13, 2017, Online: https://hydrogencouncil.com/en/study-hydrogen-scaling-up/
[6] International Energy Agency, "Hydrogen," 2021, Online: https://www.iea.org/fuels-and-technologies/hydrogen
[7] EU Science Hub, 2018, Online: https://ec.europa.eu/jrc/en
[8] Adolf, J. *et. al,* "Shell hydrogen study: Energy of the future? Sustainable mobility through fuel cells and hydrogen," January 2017.
[9] Europa, Eurostat, "Electricity production, consumption and market overview (based on 2018 data)," June 2020, Online: https://ec.europa.eu/eurostat/statistics-explained/index.php/Electricity_production,_consumption_and_market_overview#Electricity_generation
[10] U.S. Energy Information Administration, "Table 8.1: Average operating heat rate for selected energy sources," (Assuming a heat rate of 7,800 Btu/kWh for natural gas power plants), Online: https://www.eia.gov/electricity/annual/html/epa_08_01.html
[11] Pöyry Management Consulting, "Hydrogen from natural gas—The key to deep decarbonisation," July 2019, Online: https://www.poyry.com/sites/default/files/zukunft_erdgas_key_to_deep_decarbonisation_0.pdf
[12] European Zero Emission Technology and Innovation Platform, "Commercial scale feasibility of clean hydrogen," April 25, 2017, Online: https://zero-emissionsplatform.eu/wp-content/uploads/ZEP-Commercial-Scale-Feasibility-of-Clean-Hydrogen-report-25-April-2017-FINAL.pdf
[13] International Renewable Energy Agency (IRENA), "Hydrogen from renewable power: Technology outlook for the energy transition," September 2018, Online: https://www.irena.org/-/media/Files/IRENA/Agency/Publication/2018/Sep/IRENA_Hydrogen_from_renewable_power_2018.pdf
[14] IEA Greenhouse Gas R&D Programme (IEAGHG), "Reference data and supporting literature reviews for SMR based hydrogen production with CCS," IEAGHG Technical Review 2017-TR3, 2017, Online: https://ieaghg.org/publications/technical-reports/reports-list/10-technical-reviews/778-2017-tr3-reference-data-supporting-literature-reviews-for-smr-based-hydrogen-production-with-ccs

NAN LIU is the Licensing Technology Manager for Gasification at Shell Catalysts & Technologies. She has fulfilled roles throughout the project lifecycle, from initial feasibility and front-end development to project execution and plant operations, on major capital projects around the globe. These projects include the startup of the gasification unit at the Fujian refinery and ethylene project in China, as well as performance optimization at the gasification and hydrogen plant at Shell's Pernis refinery in the Netherlands. Ms. Liu has a strong commercial mindset and is a keen advocate of gasification as a value-adding investment.

J. S. KIM, H. J. DUNSHEATH and J. LOPEZ,
Covestro, Baytown, Texas

Vapor velocity guidelines for horizontal flare knockout drums

Flare knockout (KO) drums are important components of effluent handling systems. A horizontal drum is often considered more economical than a vertical one if the vapor flow is high and a large liquid holdup is required. The function of the flare KO drum is to remove liquid droplets in the range of 300 µm–600 µm from the vapor feed stream to the flare burner. Flare stacks should not discharge larger liquid droplets, as these can cause smoke or burning rain. Burning rain creates a significant safety hazard to people and can cause damage to structures and equipment. The most effective way to prevent burning rain is to install a properly designed KO drum.

American Petroleum Institute (API) Standard 521 presents a method for sizing horizontal flare KO drums based on a residence time method that does not verify vapor axial velocities. High axial vapor velocities are generally not desirable because the high axial vapor velocities may entrain the liquid droplets in the vapor phase. Therefore, the liquid droplets are carried along with the continuous vapor flow. The residence time method should be supplemented by vapor velocity limit guidelines for horizontal flare KO drums; however, there are presently no appropriate guidelines for the vapor velocity limits. This article proposes a new guideline for the axial vapor velocity in the horizontal flare KO drums.

Liquid droplet settling velocity. In horizontal flare KO drums, liquid droplets are separated from a continuous vapor phase. To separate the liquid droplets, the vapor phase velocity should be sufficiently low to allow the liquid droplets to settle (i.e., to fall out of the vapor). API 521 uses Eq. 1 to calculate the liquid droplet settling velocity in flare KO drums:[1]

$$u_d = 1.1547 \times \sqrt{\frac{g \times D_p \times \left(\rho_f - \rho_g\right)}{\rho_g \times C}} \quad (1)$$

where

u_d = the liquid droplet settling velocity, ft/sec
g = the acceleration due to gravity, 32.174 ft/sec^2
D_p = the liquid droplet diameter, ft
ρ_f = the density of liquid at operating conditions, lb/ft^3
ρ_g = the density of vapor at operating conditions, lb/ft^3
C = the drag coefficient (i.e., API 521, Figure 5).

API 521 Figure 5 relates the drag coefficient (C) to a function of the drag coefficient and Reynolds number.[1] The drag coefficient can also be obtained by a curve fit equation (Eq. 2):

$$C = EXP(6.494 - 1.158 \times ln(x) + 0.056 \times ln(x^2) - 0.00074 \times ln(x^3)) \quad (2)$$

$$x = C \times Re^2 = \frac{9.5 \times 10^7 \times \rho_g \times \left(\rho_f - \rho_g\right) \times D_p^3}{\mu_v^2} \quad (3)$$

where

μ_v = viscosity of vapor in cP.

The values obtained from Eq. 2 agree closely with those from API 521, Figure 5. The relationship between Eqs. 2 and 3 is shown in **FIG. 1.**

In vertical flare KO drums, API 521 recommends using the liquid droplet settling velocity from Eq. 1 as the limiting vapor velocity. For horizontal flare KO drums, API 521 uses the liquid droplet settling velocity as a starting point for optimizing the KO drum designs.

General vapor velocity guidelines for two-phase separators. The maximum vapor velocity for two-phase separators has been calculated using the empirical Sauders-Brown equation (Eq. 4). Walas recommended a K value of 0.14 ft/sec for vertical separators without a demister.[2] For sizing horizontal separators without a demister, it is recommended to use higher values by a factor of 1.25, since the upward drag of the vapor is largely absent in horizontal separators:

$$u_v = K \times \sqrt{\frac{\rho_f - \rho_g}{\rho_g}} \quad (4)$$

where

K = the vapor load empirical factor
u_v = the vapor velocity, ft/sec.

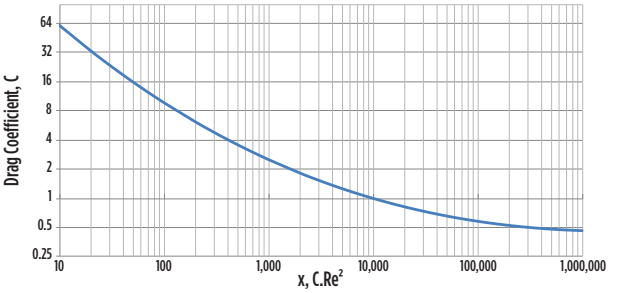

FIG. 1. Drag coefficient vs. Reynolds number.

API 12J provides ranges of *K* factors for vertical and horizontal vapor-liquid separators with demisters.[3] The values are presented in **TABLE 1.** The design of the internals (demister), separator orientation and separator dimensions affect the *K* factors. The Gas Processors Suppliers Association's *GPSA Engineering Data Book* indicates that the higher values of *K* for long horizontal separators are generally considered to be overly optimistic.[4] The *GPSA Engineering Data Book* indicates that $K = 0.5$ ft/sec is normally used as an upper limit for horizontal separators equipped with wire-mesh mist extractors.

Residence time method. The residence time method is used to design flare KO drums with sufficient vapor retention time for liquid droplets to settle. Therefore, the liquid droplet settling time is important in the design of flare KO drums. The liquid droplet settling time is shown in Eq. 5:

$$\theta = \frac{h_v}{u_d} \quad (5)$$

where

θ = the liquid droplet settling time, sec

h_v = the vertical drop height for liquid droplets (as shown in **FIG. 2**), ft.

The axial vapor velocity is calculated by using Eq. 6:

$$u_v = \frac{Q_v}{A_v} \quad (6)$$

where

Q_v = the vapor volumetric flowrate at KO drum operating conditions, ft³/sec

A_v = the vapor space cross-sectional area (as shown in **FIG. 2**), ft².

The vapor residence time is calculated by using Eq. 7:

$$\tau = \frac{L}{U_v} \quad (7)$$

where

τ = the vapor residence time in the KO drum, sec

TABLE 1. API 12J guidelines for vapor-liquid separator designs

Separator type	Height or length, ft	Typical *K* factor range
Vertical	5	0.12–0.24
	10	0.18–0.35
Horizontal	10	0.4–0.5
	Other lengths	$0.4–0.5 \times (L/10)^{0.56}$

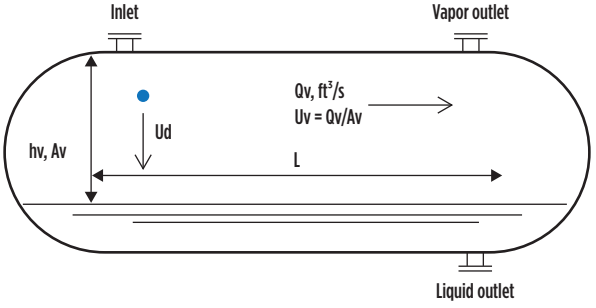

FIG. 2. Schematic of a typical horizontal KO drum.

L = the vapor flow path length (as shown in **FIG. 2**), ft

U_v = the axial vapor velocity in the KO drum, ft/sec.

API 521 uses this residence time method to size horizontal KO drums. The KO drum diameter and length are optimized—by trial and error—to provide a larger retention time than the liquid droplet settling time; however, no velocity considerations are involved in the optimizing process. As a result, the flare KO drums are often designed with axial vapor velocities exceeding the onset liquid re-entrainment velocity, as the method provided in API 521 does not check for possible liquid re-entrainment from the liquid surface. API 521 indicates that flare vapor velocities exceeding 9.8 ft/sec or 13.1 ft/sec could entrain liquid droplets up to 1,000 μm in size. Liquid droplets 300 μm and larger may drop out of the gas stream at less than 6.6 ft/sec. However, the API 521 sample calculations for a flare KO drum show an axial vapor velocity greater than 13.1 ft/sec. It was for this reason that this article was developed.

Preventing re-entrainment from the liquid surface in the KO drum. High axial vapor velocities can cause liquid re-entrainment across the liquid surface in the settled section of the KO drums. This re-entrainment should be checked to ensure that there is no liquid re-entrainment in the KO drums. Ishii and Grolmes[5] suggested Eq. 8 to estimate the onset liquid re-entrainment axial vapor velocity in horizontal lines:

$$u_{v-reentrainment} = 4.3105 \times \left[\frac{\rho_f}{\rho_g} \times \left(\frac{\sigma}{\rho_g}\right)^4 \times \left(\frac{g \times (\rho_f - \rho_g)}{\mu f}\right)^2\right]^{0.1} \quad (8)$$

where

$u_{v\,-\,reentrainment}$ = the onset liquid re-entrainment vapor velocity, ft/sec

σ = the liquid surface tension, lbm/sec²

μ_f = the viscosity of liquid in centipoise (cP).

The Center for Chemical Process Safety (CCPS) guidelines use this onset liquid re-entrainment velocity from Eq. 8 as a limiting axial vapor velocity to prevent liquid re-entrainment from the liquid surface in the flare KO drum.[6] However, the onset liquid re-entrainment vapor velocity obtained from Eq. 8 is only applicable to dry flare vapors if there are combustible liquids in the flare KO drum. For wet flare vapors, the maximum vapor velocity allowed is much less. This is to ensure that the fine liquid droplets in the wet vapors are removed prior to leaving the flare KO drum. The proposed vapor velocity limit guidelines for wet flare vapors are described in the following section.

New vapor velocity limit guidelines for wet (condensable) flare vapors. This method attempts to estimate a limit to the axial vapor velocity in horizontal flare KO drums. This method applies to wet flare vapors. The procedure is as follows:

1. Calculate the onset liquid re-entrainment vapor velocity, using Eq. 8.
2. Calculate the liquid droplet particle size, using Eq. 9 at the onset liquid re-entrainment vapor velocity, based on the critical Weber number (We). The Weber number represents the ratio of disruptive hydrodynamic forces to the stabilizing surface tension force. The liquid droplet starts to break up at the critical Weber number. According to Ishii and Grolmes, the critical

Weber number is approximately 17 and increases with increasing viscosity.[5] However, the Weber number (Eq. 10) does not include the influence of viscosity. Turner *et al.* also indicated that the critical Weber number for free-falling droplets in a vertical turbulent gas flow was found to be approximately 20–30.[7] Eq. 9 is obtained based on the critical Weber number of 17.

$$D = \frac{17 \times \sigma}{\rho_v \times u^2_{v-reentrainment}} \quad (9)$$

$$We = \frac{D \times \rho_g \times u^2}{\sigma} \quad (10)$$

3. Calculate the Froude number at the onset liquid re-entrainment vapor velocity conditions, using Eq. 11. The Froude number is a measure of the ratio of aerodynamic forces from the vapor phase to gravitational effects on the liquid phase. Therefore, liquid droplets settle when the Froude number is reduced as the vapor velocity decreases.

$$F_r = \frac{u^2_{v-reentrainment}}{g \times D} \times \frac{\rho_g}{\rho_f - \rho_g} \quad (11)$$

4. Calculate the axial vapor velocity limit at the target liquid droplet particle size, using Eq. 12. It is assumed that the Froude number at the onset liquid re-entrainment velocity is still valid for the target liquid droplet particle size to become suspended in the vapor phase. The axial vapor velocity expected is smaller than the onset liquid re-entrainment vapor velocity, since the target particle size is smaller.

$$u_{v-maxmum} = \sqrt{g \times D_p \times F_r \times \frac{\rho_f - \rho_g}{\rho_g}} \quad (12)$$

Rearranging Eq. 12—in terms of fluid physical properties—becomes Eq. 13, which can be used to estimate the maximum horizontal KO drum vapor velocity to remove the intended liquid droplets and prevent them from being entrained in the vapor phase. Eq. 13 is expressed in international system (SI) units in Eq. 14. In U.S. customary units:

$$u_{v-maximum} = 4.5064 \times \left[\rho_f \times \sigma^{1.5} \times \left(\frac{D_p}{\rho_g} \right)^{2.5} \times \left(\frac{g \times (\rho_f - \rho_g)}{\mu_f} \right)^2 \right]^{0.2} \quad (13)$$

where

$u_{v-maximum}$ = the axial vapor velocity limit, ft/sec
D_p = the liquid droplet diameter, ft
g = the acceleration due to gravity, 32.174 ft/sec^2
ρ_f = the density of liquid at operating conditions, lb/ft^3
ρ_g = the density of vapor at operating conditions, lb/ft^3
σ = the liquid surface tension, lbm/sec^2 (divide dynes/cm by 453.6 to convert to lbm/sec^2)
μ_f = the viscosity of liquid in cP.

In SI units:

$$u_{v-maximum} = 0.4839 \times \left[\rho_f \times \sigma^{1.5} \times \left(\frac{D_p}{\rho_g} \right)^{2.5} \times \left(\frac{g \times (\rho_f - \rho_g)}{\mu_f} \right)^2 \right]^{0.2} \quad (14)$$

where

$u_{v-maximum}$ = the axial vapor velocity limit, m/sec
D_p = the liquid droplet diameter, m
g = the acceleration due to gravity, 9.807 m/sec^2
ρ_f = the density of liquid at operating conditions, kg/m^3
ρ_g = the density of vapor at operating conditions, kg/m^3
σ = the liquid surface tension, mN/m (dyn/cm)
μ_f = the viscosity of liquid in millipascal-seconds (mPa-sec).

Comparison of various axial vapor velocity guidelines.

The following example for the API 521 sample calculations is used to compare the various vapor velocity guidelines. The operating conditions include the following:

- Vapor flowrate of 169,000 lb/hr, with a vapor density of 0.18 lb/ft^3
- Liquid flowrate of 31,000 lb/hr, with a liquid density of 31 lb/ft^3
- Drop size selected, as allowable: 300 μm (0.000984252 ft)
- Viscosity of the vapor: 0.01 cP
- Viscosity of the liquid: 0.5 cP (assumed for this evaluation)
- An assumed liquid surface tension of 20 dynes/cm (0.0441 lbm/sec^2)
- Flare vapors that are assumed wet and combustible for this evaluation.

TABLE 2 is a result of the API 521 optimized designs of the horizontal KO drum. The droplet settling velocity obtained from Eq. 1 is 2.35 ft/sec. The onset liquid re-entrainment velocity, obtained from Eq. 8, is 18.76 ft/sec. CCPS recommends limiting the axial vapor velocity below the onset liquid re-entrainment velocity to prevent re-entrainment from the liquid surface in the horizontal flare KO drum. However, the axial vapor velocities in trial numbers 3 and 4 exceed the liquid re-entrainment velocity because API 521 does not have any vapor velocity limit guidelines.

TABLE 3 shows comparisons of the axial vapor velocity guidelines presently available. The API 521 guidelines predict velocities that are too high and that could exceed the liquid re-entrainment limit. While the API 12J specification is not applicable for a horizontal separator without an internal demister,

TABLE 2. Optimizing results of the API 521 sample calculations

Trial no.	Drum diameter, ft	Drum length, ft	Vapor space area, ft^2	Vertical depth of vapor spaces, in.	Vapor retention time, sec	Axial vapor velocity, ft/sec	Minimum drum length, ft
1	8	19	20.43	41	1.45	12.76	18.5
2	7.5	20.5	16.52	36	1.28	15.78	20.2
3	7	22.5	13.29	31.7	1.13	19.62	22.1
4	6.5	25	10.51	27.6	0.98	24.82	24.3

these guidelines provide valuable information for vapor velocity criteria since they were based on test data. It is generally recognized that the allowable vapor velocity without a demister is lower than the vapor velocity with a demister. Therefore, the axial vapor velocity for a horizontal separator without an internal demister should be less than the vapor velocity recommended by API 12J. Walas' guideline is generally considered conservative. For horizontal flare KO drums, it is important to limit the axial vapor velocity below the maximum velocity limit from Eq. 13 to permit the liquid droplets to settle down prior to leaving the KO drums. In addition, the vapor residence time should be greater than the liquid droplets' settling time.

Takeaway. Horizontal flare KO drums are used to separate fine liquid droplets out of the flare vapor stream by gravity at relatively low velocities and low turbulence. The function of the flare KO drums is to remove liquid droplets in the range of 300 μm–600 μm from the vapor feed stream to the flare burner. Failures to remove these liquid droplets can cause smoke or burning rain (a significant safety hazard).

TABLE 3. Comparisons of various axial vapor velocity guidelines

Method	Axial vapor velocity, ft/s	Froude number
API 521 sample calculations	12.76–24.3	30–108.9
CCPS (re-entrainment limit)	18.76	64.91
API 12J (K = 0.5 ft/s)	6.54	7.89
Walas (K = 0.14 ft/s × 1.25)	2.29	0.97
Eq. 13	5.41	5.4

The most effective way to prevent burning rain is to install a properly designed KO drum. Although determining the maximum wet vapor velocity in the horizontal flare KO drums is important to ensure that the liquid droplets are removed, the wet vapor velocity guidelines are not well defined. The comparison of various axial vapor velocity guidelines in **TABLE 3** shows that the residence time method recommended by API 521 is not conservative and could lead to undersized flare KO drums that could fail to remove entrained liquid. The residence time method should be supplemented by the proposed vapor velocity limit guidelines for the horizontal flare KO drums. The vapor velocity estimated with Eq. 13 provides a reasonable prediction of the wet vapor velocity based on the API 521 indication. Flare vapor velocities exceeding 9.8 ft/sec or 13.1 ft/sec could entrain liquid droplets up to 1,000 μm in size, and liquid droplets 300 μm and larger may drop out of the gas stream at less than 6.6 ft/sec. Eq. 13 predicts 9.9 ft/sec for 1,000-μm liquid droplets and 5.41 ft/sec for 300-μm liquid droplets. The vapor velocity guidelines using Eq. 13 are in good agreement with the indication of API 521, Section 5.7.8.4. Consequently, the maximum axial vapor velocities of dry (non-condensable) vapors and wet (condensable) vapors in horizontal flare KO drums should be less than the calculated values obtained using Eq. 8 and Eq. 13, respectively. HP

LITERATURE CITED

[1] API, "Pressure-Relieving and Depressurizing Systems," API Standard 521, 7th Edition, June 2020.
[2] Walas, S. M., "Chemical Process Equipment Selection and Design," Butterworth-Heinemann, Houston, 1990.
[3] API, "Specification for Oil and Gas Separators," API Specification 12J, 8th Edition, October 2008.
[4] Gas Processors Suppliers Association, *GPSA Engineering Data Book,* Vol. 1, 12th Ed., GPA, Tulsa, Oklahoma, 2004.
[5] Ishii, M. and M. A. Grolmes, "Inception Criteria for Droplet Entrainment in Two-Phase Concurrent Film Flow," *AIChE Journal,* March 1975.
[6] Center for Chemical Process Safety, *Guidelines for Pressure Relief Effluent Handling Systems,* AIChE, New York, 1998.
[7] Turner, R. G., M. G. Hubbard and A. E. Dukler, "Analysis and Prediction of Minimum Flow Rate for the Continuous Removal of Liquids from Gas Wells," *Journal of Petroleum Technology,* 1969.

JUNG SEOB KIM is a Principal Pressure Safety Engineer at Covestro. He has more than 35 yr of experience in different roles within the petrochemical industry, including with ioMosaic, SK E&C USA, Bayer Technology Services, Samsung BP Chemicals, and Samsung Engineering. Mr. Kim is a member of AIChE and is a registered Professional Engineer in the State of Texas. He earned a BS degree in chemical engineering from the University of Seoul in South Korea.

HEATHER JEAN DUNSHEATH is an Explosion Safety Expert at Covestro. She has more than 14 yr of experience in process safety, including designing emergency relief systems and facilitating process hazard analysis studies. Ms. Dunsheath spent 3 yr in Covestro's Global Explosion Safety Group in Leverkusen, Germany. She earned a BS degree in chemical engineering from Rice University in Houston, Texas.

JUAN P. LOPEZ is a Senior Pressure Safety Engineer at Covestro. He has 8 yr of experience in process safety, including designing emergency relief systems and participating in process hazard analyses. He is a registered Professional Engineer in the State of Texas, and earned a BS degree in chemical engineering from Texas A&M University.

B. BLUM, Bazan Group, Haifa, Israel; **H. KISTER,** Fluor, Aliso Viejo, California; and **R. TSANG,** Koch-Glitsch, Stoke-on-Trent, UK

Good distributor design for high-velocity feed debottlenecks a crude preflash tower

Bazan Group's crude unit No. 3—not designed by any of the authors' companies—was bottlenecked by the preflash tower. The tower experienced frequent episodes—especially with light crudes (high naphtha percent)—in which the naphtha stream leaving the tower turned dark, accompanied by a high tower ΔP. Most likely, these episodes originated from crude entrainment and restricted the throughput of the entire crude unit.

From the lowest downcomer, a 4-in. pipe drains the liquid into the top shed deck. During two recent outages, the 4-in. pipe was found broken and falling, with a hole in the seal pan from which it originated. As the pipe was in front of a high-velocity feed entry, it was likely that feed impingement at high velocities generated vibration and caused the 4-in. pipe to break. It was believed that, due to the pipe breakage, the high feed vapor velocities picked up the descending liquid or rose up the bottom downcomer, causing the naphtha product to become dark. The initial solution sought was reorientation of the 4-in. pipe away from the feed.

Suspecting that there may be other issues, Bazan requested Fluor to assist with the problem analysis. Koch-Glitsch was later added to the team to consult on hardware changes. The analysis determined that the breakage of the 4-in. pipe was insufficient to explain the entrainment and dark naphtha. It was determined that the root cause was excessive feed velocities, with feed entry too close to the bottom tray.

To solve the problem, it was necessary to break the incoming momentum and to divert the feed to a lower point in the tower. This was achieved by a unique feed entry design for the very-high-velocity feed, by removing two segments of the top shed deck to permit feed entry at a lower point, and by adding a specially designed impingement baffle to break the incoming momentum.

When the tower returned to service, the dark naphtha episodes completely disappeared. The naphtha product rate could be raised significantly (by 20% and above) without any adverse effects on operation. No limit has been reached. The entrainment problem has been eliminated.

This article details the problem, analysis and solution.

Process and problem description.

The preflash tower (**FIG. 1**) is designed to receive crude feed at 160°C, which contains 4.8% vapor by weight. The tower operates at a pressure of 1.6 barg. Overhead vapor from the tower is condensed, and some is returned to the tower as reflux. The rest is naphtha overhead product that is sent to the main stabilizer tower. Bottom product is preflashed crude that goes to the heat exchangers, the crude heater and, finally, to the atmospheric tower.

The 2.1-m-diameter preflash tower contained 12 single-pass rectangular moving valve trays above the crude feed inlet and six shed decks with 34% open windows beneath the feed inlet. A connection permits stripping steam to be added below the stripping section, but this steam has not been used.

Since the 1990s, the tower experienced dark naphtha (about 2–3 episodes/yr) while distilling crudes with high naphtha content. Following a turnaround in 2018, the unit started running on September 9, 2018. Beginning November 11, 2018, the preflash tower experienced episodes of dark naphtha product. The dark naphtha episodes happened about 15 times/yr—with each dark naphtha event lasting approximately 12 hr, during which the naphtha was continuously dark. The dark naphtha was accompanied with a high pressure drop, which remained high throughout the episode. There was no problem of instability of the bottom level during the dark naphtha episodes; however, during these episodes, the bottom level dropped by approximately 20%.

The rest of the time, the tower was working as intended because the refinery limited the tower inlet temperature and the total amount of naphtha in the top. To get out of the event, the refinery needed to cut crude charge rates or the feed temperature. These episodes became the prime crude unit capacity bottleneck.

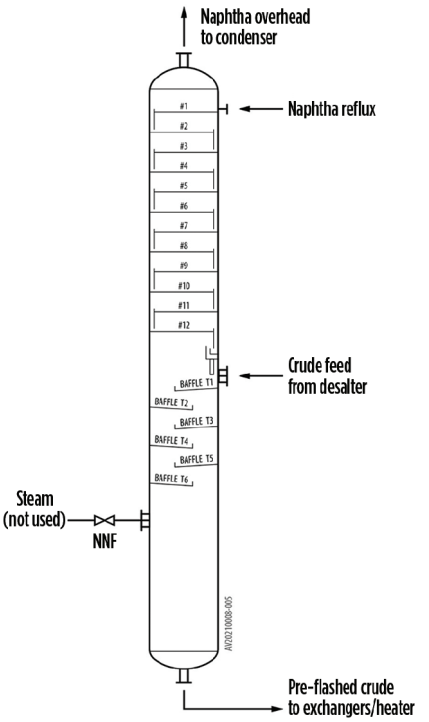

FIG. 1. Bazan's preflash tower.

In search of the root cause. The bottom seal pan arrangement is shown in **FIG. 2.** The bottom downcomer enters a 242-mm-wide primary seal pan, clearing its floor by 67 mm. Liquid from the primary seal pan overflows a 117-mm-tall overflow weir into the 386-mm-wide secondary seal pan. From the secondary seal pan, liquid descends onto the top shed deck via a 4-in.-diameter, 800-mm-long pipe. The overflow weir of the secondary seal pan rises 65 mm above the overflow weir of the primary seal pan, so no liquid should be overflowing the secondary seal pan unless the 4-in. pipe plugs. **FIG. 2** also shows the 10-in. crude feed nozzle at an elevation about two-thirds of the way down along the 4-in. pipe.

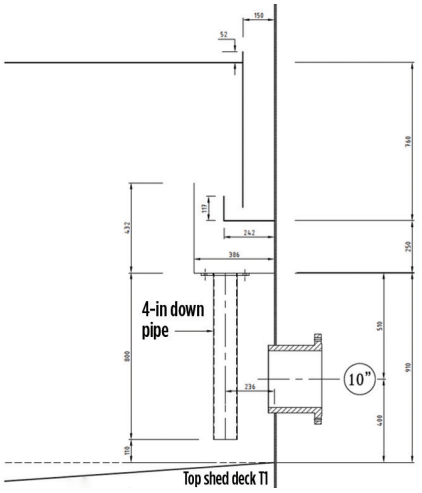

FIG. 2. Primary and secondary seal pan arrangement showing the 4-in. down pipe from the secondary seal pan to the top shed deck.

FIG. 3. Broken 4-in. down pipe and the 4-in. hole in the secondary seal pan floor.

When the tower was inspected during the 2018 turnaround, the 4-in. pipe was found broken and sitting on the top shed deck. It broke where it exited the secondary seal pan, leaving a crack and a 4-in. hole in the seal pan floor. The seal pan floor was repaired, and the pipe was reinstated. During the next turnaround in 2020, the tower was inspected and, once again, the 4-in. pipe was found broken at the same spot, leaving a crack and a 4-in. hole in the secondary seal pan floor (**FIG. 3**).

FIG. 4 shows the cause of the pipe breakage. It was in front of the flashing crude feed inlet, and the high feed velocities caused the pipe to vibrate and break. This breakage was linked to the entrainment experience in the tower. With the pipe broken, the high-velocity vapor was theorized to pick up the liquid descending from the secondary seal pan and entrain it up the tower, causing the naphtha to turn dark. A solution was sought to either relocate the 4-in. pipe or to extend the 10-in. inlet pipe—with baffling or a pipe distributor—to prevent impingement of the feed on the 4-in. pipe.

Bazan invited Fluor to join their task force to seek out the root cause of the problem. The joint task force review of the past experiences questioned the theory that entrainment of liquid falling from the secondary seal pan is capable of being the root cause for the dark naphtha. The liquid flowrate in the upper trays of preflash towers is small—in some cases, too small to keep the downcomers sealed. A 4-in. pipe does not transport much liquid. As long as the downcomers do not lose their seals, they will drain the liquid entrained from the broken 4-in. pipe. This small amount did not explain the flooding indicated by the observed pressure drop rise and its persistence for 12 hr. It would take a massive amount of liquid to explain the pressure drop rise and its staying elevated for 12 hr, and this can only come from the incoming crude.

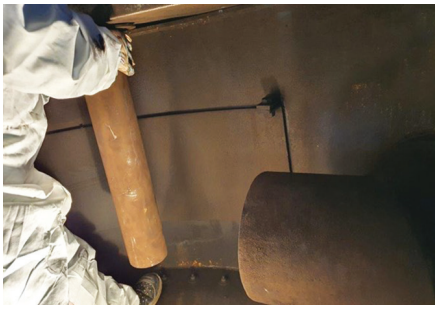

FIG. 4. The broken 4-in. down pipe hand-held in its location in front of the tower crude feed inlet pipe.

Another important observation is that the upper seal pan was not damaged, so the bottom downcomer will always remain sealed. This would permit the bottom tray to continue operating normally. Since the liquid flow rate in the rectifying trays is small, any entrainment of this liquid will be captured by the bottom tray and will descend via the upper seal pan into the lower seal pan (**FIG. 2**). It will then try to come out through the hole left by the broken pipe. If the rising vapor prevents this liquid from descending through the hole, it will overflow the weir on the secondary seal pan and, again, flooding will not occur.

The task force identified two mechanisms by which a massive carryover of crude is likely to occur. These include:

1. Preflash towers that often experience foaming[1,2] (a foam-over usually causes massive carryover of crude to the upper section)
2. High $\rho_M V_M^2$ (where ρ_M is the mixed phase density, kg/m^3; and V_M is the mixed phase velocity at the tower entrance, m/sec).

Both mechanisms are consistent with the observed dark naphtha, high pressure drop, and the drop in bottoms level. Foaming may be caused by components in the crude[1], desalter chemicals[2] or pockets of water that quickly vaporize upon entering the tower.

A weak argument against the foaming theory is the stability of the tower bottom level. In many cases where preflash foaming occurs, the bottom pump cavitates and the bottom level is unsteady. Neither was observed in the Bazan preflash tower.

The high inlet velocities and foam-over mechanisms are interconnected, as has been demonstrated by Barber and Wijn, who point out the significant influence of the feed inlet design on preflash foaming.[1] A common practice to cure or prevent foam-overs in preflash drums, towers and similar services is to pass the feed through vortex clusters.[3,4]

With the crude unit coming out of turnaround, adding vortex clusters was not an option. A quick solution was sought.

Hydraulic analysis and root cause. The flashing crude feed entered the tower via a 10-in. pipe, as seen in **FIG. 4.** The bottom of the 10-in. crude inlet pipe was

only 273 mm above the top shed deck. At the intended operating conditions, the feed mixture was 4.8% vapor by weight. By volume, the mixture was 89% vapor. It was entering at a significant feed mixture velocity of 16.7 m/sec. The $\rho_M V_M^2$ at the 10-in. pipe and nozzle was 26,600 kg/msec^2. This is about seven times higher than the common good-practice criterion of keeping it below 3,700 kg/msec^2. At this high $\rho_M V_M^2$—which signifies a high kinetic energy—and coming in so close to the shed deck floor, it is highly unlikely that the tower would have properly operated. The high velocity and kinetic energy would blow the liquid on the top shed deck (T1) right up the tower.

Two other factors further aggravated the situation. First, the open area of the top shed deck was low—approximately 34% of the tower cross-section area. Alone, this would not have been so bad, as there was only a small amount of vapor coming up through the window from underneath. However, with the feed pipe discharging so close to the floor, the top shed deck was holding a very foamy mix, which would have had difficulty descending via the small window. Second, based on the superficial area, the liquid velocity down the tower (below the feed entry) was 95 m^3/ hm^2. At this rate, the Barber and Wijn correlation[1] predicts a foam height of 1.7 m. Looking at **FIG. 2,** this foam will almost reach the bottom valve tray.

The task force concluded that the feed arrangement and discharge velocities were the root cause of the dark naphtha events.

Correction strategy. The corrective action needed was to lower the point of feed discharge into the tower, and to reduce the kinetic energy of the discharged feed, effectively separate the vapor from the liquid upon entry to prevent foaming, and prevent the feed from impinging on the top shed deck liquid. The conceptual process design of the new feed pipe was performed by Fluor, and the mechanical engineering and fabrication were done by Bazan. Kock-Glitsch joined the task force as a consultant on optimizing the feed piping design and on achieving a sound mechanical design. The mechanical design was a special challenge due to the very high kinetic energy of the feed mixture. Neither of the authors' companies had any involvement in the original design of this tower and its internals.

The new feed pipe is shown in **FIG. 5.** The 10-in. feed pipe was extended into the tower, ending in a tee that split the feed into two 10-in. laterals. The laterals had 93-mm-wide slots pointing downward at 37° to the horizontal (**FIG. 6**), discharging the feed onto a new vertical impingement baffle. This impingement baffle directed the liquid downward toward shed deck T2, with the vapor disengaging upward. To allow the free rise of vapor from the impingement baffle, two segments of the top shed deck (T1) were removed. The segment of T1 at the opposite end of the tower from T2 was kept and was used to collect liquid from the trays that descended from the secondary seal pan via the 4-in. pipe. To distribute this liquid, a 50-mm weir was installed at the end of the unremoved segment of the top shed deck T1.

Taking out the two segments of T1 was central to the success of the design. The vapor rises on the inside of the impingement baffle, so the region at the back of the impingement baffle (between the baffle and the tower shell) does not contribute an open area for vapor rise. The vapor velocity through the open area is expressed by the C-factor in Eq. 1:

$$C = U\sqrt{\rho_G} / (\rho_L - \rho_G) \quad (1)$$

where

C = the capacity factor (m/sec) based on the open area for vapor rise
U = the vapor superficial velocity based on the same open area, m/sec
ρ_G = gas density, kg/m^3
ρ_L = liquid density, kg/m^3.

With no T1 panels removed, the C-factor would have been 0.092 m/sec, which is too large for a foaming system. With two panels removed, the C-factor declined several-fold to an acceptable 0.02 m/sec.

The new feed entry design faced many challenges. First, before splitting to the tee, the feed mixture velocity in the extended feed pipe was a high 16.7 m/sec. The $\rho_M V_M^2$ at the 10-in. pipe was 26,600 kg/msec^2, about seven times higher than the common good-practice criterion of keeping it below 3,700 kg/msec^2. At this very high $\rho_M V_M^2$, which signifies a high kinetic energy, there would be intense hydraulic pounding of the pipe and a large bending moment. The tee was strongly anchored to the tower shell. The flanges on the feed entry pipe and the impingement plate supports were double-nutted

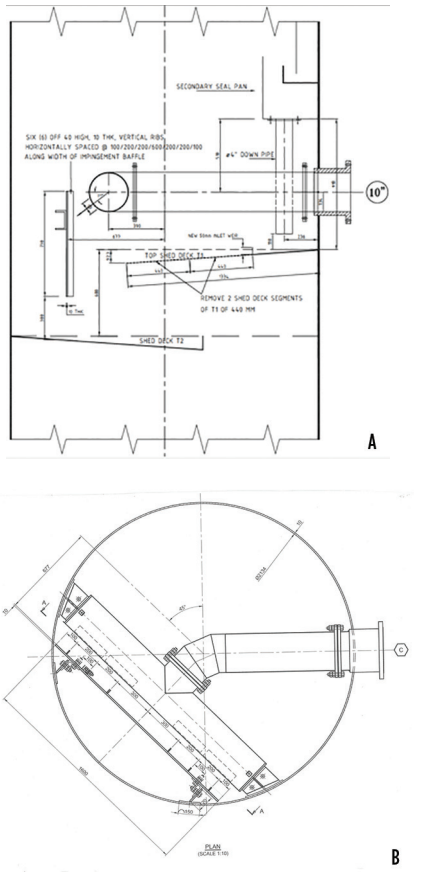

FIG. 5. New feed entry design: (A) elevation and (B) plan.

FIG. 6. The laterals with the slots that directed the feed toward the impingement baffle at 37° to the horizontal.

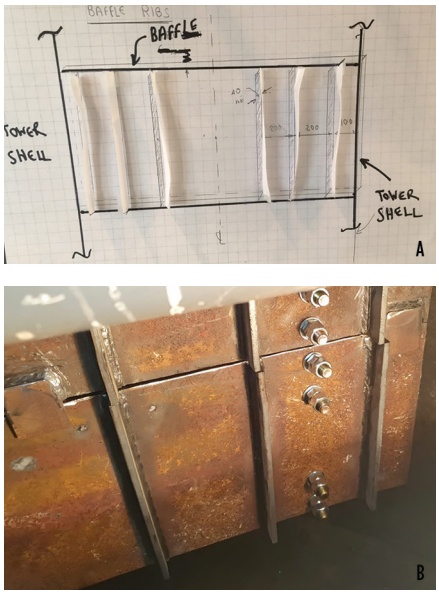

FIG. 7. The ribs installed on the impingement baffle to prevent the horizontal momentum of the feed mixture issuing from the slots from pushing the liquid and vapor toward the column shell: (A) a paper model, used during the design, to explain the concept to the fabricators; and (B) the ribs installed on the baffle.

to provide extra protection against vibration and hammering.

In the laterals, the mixture velocity was halved to 8.3 m/sec, and the $\rho_M V_M^2$ was four times lower (6,660 kg/msec^2). The slot velocity was set roughly the same as the velocity in the laterals, giving the same $\rho_M V_M^2$ (6,660 kg/msec^2). Even though this is a lot better than in the 10-in. main feed pipe, it is still about 80% above the recommended 3,700 kg/msec^2. However, this is the best that could be done with the tight space constraints in this 2.1-m-diameter tower.

Upon turning at the tee, the mixture momentum becomes horizontal, directed toward the blanked end of each lateral. This horizontal momentum will persist after the mixture exits the slots. The exiting feed mixture will hit the baffle with considerable momentum directed toward the shell ends of the baffle. The large amount of liquid descending in a small region at each end of the baffles near the shell is likely to generate foam upon impact on the T2 shed deck liquid, as well as liquid maldistribution on T2, with high flows near the shell and low flows in the center. The large amount of vapor rising near the shell ends of the baffle can generate entrainment. These hydraulic issues are likely to reduce the effectiveness of the new design and possibly even defeat its success.

FIG. 8. The laterals and the ribbed impingement baffle. The feed pipe entering the tee is obscured by an engineering drawing.

This scenario can be prevented by installing vertical ribs on the baffle. **FIG. 7** shows the ribs. The liquid flowing along the baffle toward the shell will be directed downward by the ribs, and the vapor will be deflected upward. This is a patented design.[5]

The installed laterals and baffle are shown in **FIG. 8.** As it was expected that the baffle will receive severe pounding by the feed mixture, it was fabricated from a 10-mm-thick plate and anchored strongly to the tower shell.

Takeaway. The tower was restarted on July 22, 2020. It was in operation until September 6 of last year, when the unit was shut down due to falling demand because of the COVID-19 pandemic. The unit was then restarted a few months later on November 20. Since that time, no incidents of dark naphtha have been experienced during operation. Additionally, the naphtha production rate was increased by more than 20% without any adverse effects on operation. Bazan has not yet pushed the unit to the maximum but intends to do so in the future. There was no limit in the preflash tower, even though naphtha production was increased by more than 20%. The entrainment problem has also been eliminated. The preflash tower is no longer a bottleneck of the crude unit.

A takeaway from this revamp is that the feed inlet design to the preflash towers can make or break not only the tower performance, but also that of the entire crude unit. Poor design of the inlet can severely bottleneck the tower and the entire crude unit. Judicious, low-cost modifications to the inlet design can largely improve performance, eliminate bottlenecks and provide trouble-free operation. HP

LITERATURE CITED

[1] Barber, A. D. and E. F. Wijn, "Foaming in Crude Distillation Units," IChemE Symposium, Ser. 56, 1979.
[2] Lieberman, N. P. and S. W. Golden, "Foaming is leading cause of tower flooding," *Oil & Gas Journal,* August 1989.
[3] Turner, J., R. J. Asquith and R. Atkinson, "Stop foaming on hydrotreater 'hot' separator," *Hydrocarbon Processing*, June 1999.
[4] Barletta, T., E. Hartman and D. J. Leake, "Foam control in crude units," *Petroleum Technology Quarterly,* Autumn 2004.
[5] Kister, H. Z. and W. J. Stupin, "Configurations and Methods for Ribbed Downcomer Wall," U.S. Patent 7,581,719 B2, September 2009.

BETZALEL BLUM is the Chief Process Technology Manager for the Bazan Group (Oil Refineries Ltd.). During his 35 yr with the Bazan Group, he has been the lead process engineer for some major revamps and debottlenecks of catalytic and distillation units. Mr. Blum has also been involved in fractionator process design, equipment design and optimization, the identification of flow regime patterns, and field troubleshooting. He earned a BSC degree in chemical engineering, along with an MS degree in oil and gas, from Technion—Israel Institute of Technology.

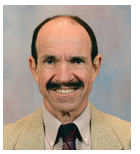

HENRY KISTER is a Senior Fellow and Director of Fractionation Technology for Fluor Corp. He has more than 35 yr of experience in design, troubleshooting, revamping, field consulting, and the control and startup of fractionation processes and equipment. He is the author of three books, along with the distillation equipment chapter in *Perry's Chemical Engineers' Handbook* (8th and 9th editions), the distillation chapter in the *Kirk-Othmer Encyclopedia of Chemical Technology,* and more than 120 articles. Mr. Kister has taught the IChemE-sponsored "Practical Distillation Technology" course over 530 times in 26 countries. He is a Fellow of both IChemE and AIChE, and is a member of the U.S. National Academy of Engineering. For more than 25 yr, he has also served on Fractionation Research Inc.'s (FRI's) Technical Advisory and Design Practices committees. Mr. Kister earned his BE and ME degrees from the University of New South Wales in Australia.

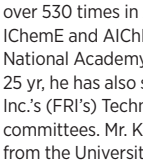

RAYMOND TSANG is the Process Engineering Manager at Koch-Glitsch, UK. He has more than 30 yr of experience in the design of fractionation equipment. Mr. Tsang earned a BS degree in chemical engineering from the University of Newcastle upon Tyne in the UK.

J. CHRISTIANSON and V. SCALCO,
General Atomics, San Diego, California

Separating from the competition: Recovering profits after the pandemic

As recovery from the COVID-19 pandemic begins, so will a return to normal life. However, fuel and petrochemical demand may never return to normal. Shelter-in-place orders have devastated global demand, and climate change policies are designed to maintain lower demand. In this ever-changing world, refiners must target profit improvements.

At the beginning of 2020, the refining industry anticipated a year of profitability, with projects anticipated to support refinery expansions, upgrades and new grassroot efforts. The global COVID-19 pandemic introduced an unseen assailant on the industry worldwide, with its effect on oil and gas production still reverberating throughout the refining community.

The pandemic shockwave. Even though global oil prices closed at previous-year averages of $51/bbl, 2020 remained a year of volatility spurred on by countries adopting climate change policies to limit carbon emissions, and by the growing global pandemic crisis. Starting in mid-2020, the refining industry desperately tried to reinvent itself as the pandemic destroyed fuel demand, exposing an unforeseen future reality of a world operating with a much lower hydrocarbon dependency. That reality portends a high probability that, in the coming years, hydrocarbon production could remain weak as recovery efforts from the pandemic begin to take hold.[1]

Therefore, to survive this volatility, the modern refinery must increase opportunities to remain profitable. Reducing lost profits from the refinery process and investing in more efficient technologies that improve profitability are of utmost urgency as the industry moves into post-virus stability.

Even before the events of 2020, a major topic of concern was the impending implementation of the International Maritime Organization's (IMO's) 2020 sulfur cap regulation, a marine fuel regulation mandating the reduction of sulfur content in marine fuels to a maximum of 0.5% and total ash content below 60 ppm. Although the IMO 2020 regulation was not fully enforceable because of the global pandemic, it has had an impact on refiners who are no longer working at peak capacity—and who are unable to make the investment in fuel oil and/or have been forced to close their facilities altogether.

During the post-pandemic shift, it is important that refiners evaluate key technologies to become more sustainable, target new market opportunities, and reduce operating costs to ensure that lost revenue can be obtained by the most efficient processes. The lack of refined product demand, coupled with refineries operating significantly below peak capacity, is delaying turnaround periods and postponing planned facility upgrade activities. Delaying these projects directly affects future profits and operating growth, particularly if key enabling technology improvements have been neglected because of the pandemic.[1]

The transition began before the pandemic. Saudi Arabia's decision to cut oil production and postpone expansion projects into 2021 reflects expectations for demand to weaken further as business operations across the globe continue to be impacted by the pandemic crisis. Reducing waste and stabilizing profits from key refining assets are paramount and are the only actualities that can support growth in 2021.[2]

In addition to a buildup in primary distillation capacity, Asia-Pacific refiners invested heavily in catalytic cracking, hydrocracking and petrochemical production. It is apparent that the growth in petrochemicals and the utilization of refined products will support profitability in the post-pandemic Asia-Pacific market. National oil companies in China and India are revisiting plans to expand refining capacities from earlier mandates prior to the outbreak. Conversely, Japanese refiners appear to be heading into a second round of capacity reductions.[3]

Overall, the long-term transition from fuel to petrochemicals appears to be the right direction for the market to take to remain strong. The route for middle distillate conversion to chemicals with existing technologies is challenging, and technology improvements are required to support this transition. Long-term demand and uncertainty concerning middle distillates have added to this issue. This long-term drive for petrochemicals will increase the use of catalytic cracking, resulting in increased slurry production and lost revenue if not addressed by applying the right separation technologies.

Dynamic demand on the reactors. The first commercial fluidized catalytic cracker (FCC) was introduced 70 yr ago. To keep FCC technology evolving and current, a continuous string of mechanical and catalyst improvements have been implemented to respond to factors, such as the degradation in feedstocks and the need for product quality improvement, and to other factors, including petrochemical drivers and environmental pressures. In many cases, improved catalysts have led to innovation, such as the advent of zeolites, which has also led to the implementation of riser cracking. Catalyst advances have also led to improved selec-

TABLE 1. Typical carbon black feedstock properties

CSO market	CSO clarity, ppm
Carbon black feedstock	100–500
Refinery fuel	50–150
Marine fuel	50–100
Pitch feedstock	25–100
Needle coke feedstock	25–100
Hydrotreater feedstock	10–50
Carbon fiber feedstock	5–10

tivity to allow for more and heavier feed processing in a refinery. This selectivity and the reduced demand for fuel oil have led the way to the concept of increasing the amount of residual oil entering the FCC unit (FCCU).

Catalyst coolers incorporated into FCC regenerators and highly selective catalysts with the ability to give high conversion with reduced coke are examples of technology improvements that the refiner can use to dig deeper into the crude barrel. As refiners introduce larger quantities of residual into the FCCU, slurry oil yields increase, and the quality of the slurry oil decreases due to a larger proportion of asphaltenes and heteroatoms entering the FCCU. This is relevant because the level of asphaltenes in the slurry oil becomes a factor in deciding which technology is best for removing particulate solids. Asphaltenes are the most hydrogen-deficient constituents of slurry oil. They become more active and react with one another at higher temperatures—especially in the presence of metal surfaces—to form coke. To minimize downstream processing difficulties, the removal of the contained catalyst will keep solids diluted below recommended concentration levels.

The solution right under our reactors. Slurry oil yields differ from each FCCU operation. Complex refineries can reduce slurry generation to below 4% of the FCC yield for petrochemical production. As a transportation fuel, FCC can see yields as high as 12%. Regardless of the slurry make percentage, if it is not handled properly, the result is profit loss and waste that must be disposed of properly. Generally, refineries can mix slurry into heavy fuel oil as a viscosity cutter. However, slurry oil's low API gravity limits how much can be blended.[4]

Clarified slurry oil (CSO) applications and markets. The use of slurry oil as cutter stock for heavy fuel oil blending has also historically been a major outlet for slurry oil. However, trace metals deposited on FCCU catalysts (e.g., nickel, vanadium and sodium) or adhering to catalyst particles and FCCU catalysts themselves—that contain aluminum and silicon as major components—can combine with other elements to form high-melting-point compounds that are corrosive to valve seats and exhaust valves in diesel engines. Solids contents for marine and refinery use in the range of 50 ppmw–150 ppmw are generally permissible.[5]

Beyond fuel use, CSO is also sold to make carbon black, which is used in automobile tires, belts, hoses and pigments, among others. The carbon black industry has always used slurry oil as feedstock, but this use is more prevalent in the Asia-Pacific region than in North America. Typical carbon black feedstock properties are provided in **TABLE 1.**

The global consumption of carbon black feedstock is approximately 130,000 bpd, with most of the market focused on the highly profitable low-ash specialty grades. The required density for carbon black feedstock is high, and special attention is needed to operate the FCCU fractionator at a high-enough temperature to obtain the desired density. Some refiners do not have the ability to obtain the required slurry oil density for carbon black applications. In addition, specialized separation equipment is required to meet the less than 50-ppm catalyst fines to obtain the greatest profits.

Some refiners increase slurry consumption to increase value in hydroprocessing unit process streams by feeding CSO to hydroprocessing, primarily hydrocracking or severe hydrotreating. Slurry oil solids contents should be reduced to very low levels to prevent operational disruption. Downflow packed-bed reactors will accumulate particulates near the entrance of the reactor, which will eventually bridge the hydroprocessing catalyst particles and cause plugging and premature shutdown. Reactors operating in trickle flow do not have the velocity to carry catalyst particles through the packed bed.[3]

Separating from the competition, but not from profits. Catalyst particles (ash) are a particular problem for slurry, especially for low-API and viscous oils needing long residence times to allow for catalyst settling. Obtaining low ash (< 0.05 wt%) requires special techniques such as heating, chemical additives, filters, electrostatic precipitators, centrifuges and cyclones. The selection of an attrition-resistant catalyst helps to a great extent, and a few refiners buy higher-priced hard catalysts to alleviate ash problems in slurry oil.[5]

Historically, holding tanks are used to allow solids to settle out of the slurry oil. Many refiners de-ash with chemical settling aids, which accelerates ash settling in storage. These chemicals are polymeric compounds that adhere to the catalyst surface, causing agglomeration of the fine particles to accelerate separation. In most countries, sludge from slurry oil holding tanks has been listed as a hazardous waste. Frequent and expensive cleaning of settling tanks is required. Depending on the tank size and rate of slurry oil production, cleaning costs can range from $1 MM–$4 MM per cleaning. In the absence of countermeasures, increasing residual feed to the FCCU tends to increase the rates of slurry oil production and sludge formation.[5]

The first membrane filters entered the slurry oil service market in 1990. One company's filters[a] operate at temperatures up to 315.56°C (600°F) and employ tubular porous metal elements. The solids collect on the inside of the elements, while the filtrate passes through to the outside. Another company[b] uses porous sintered woven wire mesh metal filters and operates at 204.44°C–343.33°C (400°F–650°F). A third company[c] employs 2-µm to 5-µm woven wire filter elements, recommends a light-cycle oil backwash at 176.67°C (350°F) and claims 85%–95% solids removal from the feed slurry. A fourth company[d] uses sintered porous metal filters with solids capture inside the tubes. This company claims a product with < 50-ppmw solids, and, in a departure from its competitors, uses a gas-assisted (pressure-assisted) backwash for rapid filter element cleaning.[3]

Electrostatic precipitators are routinely used to remove catalyst fines from the FCCU stack, and a similar principle is used for the removal of solids from liquids in an electrostatic slurry sepa-

rator. Electrostatic separation of FCCU catalyst fines from slurry oil has been in commercial operation for more than 30 yr. This technology has continuously been improved to offer a more robust, automatic process to remove catalyst fines from slurry oil or other hydrocarbon streams using dielectrophoresis. Only electrostatic separation can capture sub-micron catalyst fines. All other technologies are limited to the size of the particle captured (typically > 15 microns).[3]

Unique to electrostatic separation technology is the ability to backflush with raw feed or vacuum gasoil. This increases the middle distillate production and reduces loss from decreased reactor productivity. The technology is not affected by the presence of asphaltenes, making it an excellent choice for removing solids from residual FCCU-derived slurry oil and from gasoil crackers. Electrostatic separation operates efficiently and is impervious to plugging from asphaltenes and waxes, thus significantly reducing downtime and annual maintenance costs. The efficiency offered by electrostatic separation technology, coupled with reduced costs, has a direct and positive effect on a refinery's bottom line and profit margins.

The economics of making the right choice. An example of the value generated by using electrostatic separation methods in removing FCCU catalyst fines from slurry oil is illustrated in the following example.

An 80,000-bpd gasoil FCCU has a slurry oil yield of 4 vol% (3,200 bpd). Catalyst content of the slurry oil is 2,000 ppm (**FIG. 1**). This is compared against the base case in which the refinery uses a holding tank to reduce its solids. The slurry oil holding tank is assumed to require cleaning once per year for 2,000-ppm slurry solids at a cost of $1.5 MM. Increased catalyst loads will incur higher-frequency slurry holding tank cleanings and additional total costs. A portion of the FCCU feed is used to backwash the electrostatic separator, after which it and the associated catalyst are fed back to the FCCU, thus reducing fresh FCCU catalyst costs. FCCU catalyst costs are assumed to range from $2,000/t–$5,000/t. It is estimated that the average product upgrade value for this CSO can be between $2/bbl and $4/bbl. Benefits from not having to purchase chemical settling aids were not considered, even though such costs are estimated to be approximately $45,000/yr. A basic case of slurry-to-bunker fuel specifications, with a minimal uplift of $2/bbl, is presented, along with one case for recovering 4,000 ppm of catalyst with $4/bbl uplift.

Profits from the use of an electrostatic separator range from $4.5 MM/yr–$11 MM/yr. Without the proper technology installed in this process, the reality is a true loss to the refiner.[5]

An electrostatic separator removes more than 99% of the catalyst from the slurry to provide a CSO product containing < 50 ppm of FCCU catalyst. Catalyst savings might not be as valuable for a residual unit, but would still be significant. Individual cases involving deep residual cracking benefits would have to be calculated based on a thorough knowledge of the residual FCCU feed, operating conditions and catalyst characteristics, among other criteria. It is important to note that smaller catalyst particles returned to the unit have an inherently larger surface-to-volume ratio, and could have a considerably higher residual cracking activity than the larger equilibrium catalyst held in the unit. With the increased focus on petrochemical production to increase profits, a major key to survival is finding the right technology to increase the value of slurry. An improved bottom line depends on achieving greater profit from the bottom of the barrel, even in a post-pandemic reality.[3]

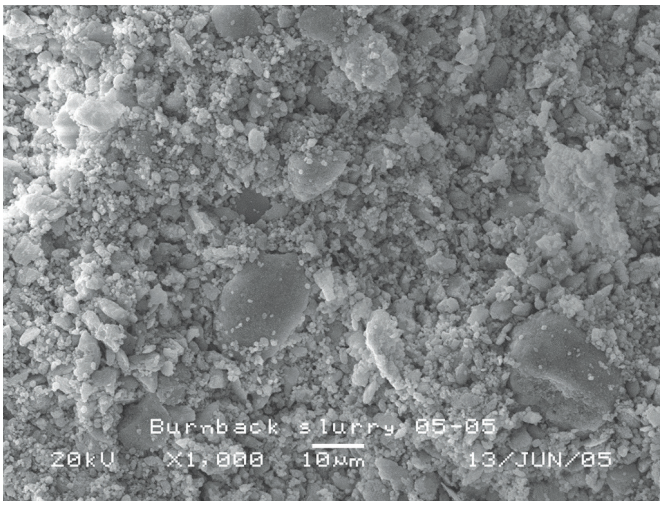

FIG. 1. View of 2,000-ppm main column bottom catalyst fines shown through a scanning electron microscope.

Post-pandemic recovery. The downstream industry must find new ways to return profits and maintain on-spec products. Whether it is providing highly valuable carbon black feedstock or meeting the new IMO 2020 mandate for marine fuels, the removal of FCCU slurry oil solids to low levels presents an opportunity for improved profitability for refiners. The ability to clarify slurry oil for use in higher-value applications—yielding more than $4/bbl or eliminating the need for the disposal of hazardous waste from a sludge in a holding tank—clearly supports the drive to stabilize and improve a refinery's bottom line.

The upheaval brought about by recent events has opened the door to new opportunities for the industry to initiate changes to weather an uncertain future. Fossil fuels are an integral part of the global economy, and these fuels still contribute strongly to the world's economies and to daily ways of life. The refining industry must continue to seek ways to innovate and evolve, and to meet the challenges in the years ahead. The first step is to invest in the right technology to increase refining capabilities and ensure a return to profitability in a post-pandemic reality. HP

NOTES

[a] Mott
[b] Pall Corp.
[c] Eaton Corp.
[d] Dahlman

LITERATURE CITED

[1] Russo, R., "Pandemic hastens threat of closure for struggling oil refineries," *Hydrocarbon Processing*, January 2021.
[2] Kelly, S. and D. K. Kumar, "A historic oil price collapse, with worries headed into 2021," Reuters, December 29, 2020, online: https://www.reuters.com/article/us-global-oil-yearend-graphic/a-historic-oil-price-collapse-with-worries-headed-into-2021-idUSKBN2930FJ
[3] Scalco, V., "The plight of the modern refinery: Racing to meet IMO 2020 regulations," *Hydrocarbon Processing*, December 2019.
[4] *Methodology and Specifications Guide—Petroleum Product & Gas Liquids: U.S. Caribbean and Latin America,* Platts, January 2012.
[5] Guercio, V. J., "U.S. producing, exporting more slurry oil," *Oil & Gas Journal,* October 2010.

A. K. COKER, A.K.C. Technology; and **A. ALSUHAIBANI,** Texas A & M University, College Station, Texas

Optimize product blending using Excel spreadsheets and LINGO software—Part 1

Linear programming (LP) is an optimization modelling technique in which a linear function is maximized or minimized when subjected to various constraints. This technique has been useful for guiding quantitative decisions in business planning in industrial engineering, refineries and chemical plants. Petroleum refining involving gasoline blending bears a different cost of manufacturing; the proper allocation for each component into its optimal disposition is of major economic importance. To address this problem, most refiners employ LP that permits the rapid selection of an optimal solution from multiple feasible alternative solutions, as each component is characterized by its gasoline blending in petroleum refining. Examples provided in this article are the solver from Microsoft Excel and LINGO software.

Product blending plays a key role in preparing refinery products for the market to satisfy product specifications and environmental regulations. The objective of product blending is to assign all available blend components to satisfy product demand and specification to minimize cost and maximize overall profit. Almost all refinery products are blended for the optimal use of all the intermediate product streams for the most efficient and profitable conversion of petroleum to marketable products. For example, typical motor gasolines may consist of straight-run naphtha from distillation, crackate [from fluidized catalytic cracking (FCC)], reformate, alkylate, isomerate and polymerate, in proportions to make the desired grades of gasoline and the specifications.

Basic intermediate streams can be blended into different finished products. For example, naphthas can be blended into gasoline or jet fuel streams, depending on the demand. On-line blending is more prevalent than batch through optimization programs. In most cases, the component blend nonlinearly for a given property (e.g., vapor pressure, octane number cetane number, viscosity, pour point) and correlations and programming are required for reliable predictions of the specified properties in the blend.

One critical economic issue for refineries is selecting the optimal combination of components for the products. Refining does not provide commercially viable products directly, but rather semi-finished products, which must be blended to meet the correct customers' specifications. Blending is an important operation within the refinery—it is a physical process in which accurately weighed quantities of two or more components are mixed thoroughly to form a homogeneous phase, which can be either similar or dissimilar in nature.

Blending specifications. Most products obtained from distillation/fractionation columns are blended with fractions obtained from other units to help minimize waste and invariably increase the quantity of the products. Almost all products—from gas to lube oil—are not only blended with fractions, but also with additives. All such blends are formulated to have the required properties conforming to the correct specifications.

Blended products include gasoline, jet fuels, heating oils and diesel fuels. The objective of product blending is to allocate the available blending components so that demands and specifications are met at the least cost and to provide products that maximize overall profit.

Gasoline blending is much more complicated than a simple mixing of the components. A typical refinery may have as many as eight to 15 hydrocarbon streams to consider as blendstocks. These may range from butane (the most volatile component) to a heavy naphtha and can include several gasoline naphthas from crude distillation, catalytic cracking and thermal processing units, in addition to alkylate, polymer and reformate. Modern gasoline may be blended to simultaneously meet 10–15 different quality specifications, including:

- Vapor pressure
- Initial, intermediate and final boiling points
- Sulfur content
- Color
- Stability
- Aromatic content
- Olefin content
- Octane measurements for several different portions of the blend
- Local governmental or market restrictions.

Since each individual component contributes uniquely in each of these quality areas and each bears a different manufacturing cost, the proper allocation of each component into its optimal disposition is of major economic importance.

Different component streams are blended into various grades of gasoline, including 83 octane (blended with an oxygenated fuel such as ethanol), regular 87 octane and premium 92 octane. The Reid vapor pressure (RVP) is set depending on the average temperature of the location the gasoline will be used (cold temperatures require higher RVP than warmer climates). These two specifications are the most significant, and they are documented with each blend to minimize the potential of octane giveaways.

If the octane specification is 87, then each 0.1 octane over

this target value incurs further costs to the refiner. For example, in the U.S., this cost calculates to approximately $1 MM per 0.1 octane giveaway per 100,000-bpd crude capacity. The RVP is slightly different, as refiners aim to blend as much low-value normal–butane (component RVP of 52 psi) into the final blend without exceeding the specification. For example, the cost of n-butane is $7/bbl that can be sold as gasoline at $25/bbl just by blending. The $18/bbl profit is significant to the refiner, making RVP economics important.

Distillate fuel blending has other specifications that must be ascertained. Distillate blending includes jet fuels, diesel fuels, kerosene and No. 1 and No. 2 fuel oils. Diesel fuels properties that are measured include:

- Cetane number (analogous to octane number for the gasoline engine)
- Flash points (relates to fire hazard in storage)
- Low-temperature properties (including cloud point)
- Pour point and sulfur content.

In blending some products, such as residual fuel oils or asphalt, viscosity is one of the specifications that must be met.

Previously, blending was performed in batch operations. However, with on-line equipment, computerization and improved techniques, blending is readily performed with greater efficiency and accuracy. Keeping inventories of the blending stocks along with cost and physical data have increased the flexibility and profits from on-line blending through optimization programs. In most cases, the components blend nonlinearly for a given property (vapor pressure, octane number, cetane number, viscosity, pour point, etc.), and correlations and programming techniques are required for reliable predictions of the specified properties in the blend.

Blends of petroleum-based gasoline with 10% ethanol (referred to as E10) account for more than 95% of the fuel consumed in motor vehicles with gasoline engines in the U.S. Ethanol-blended fuels are a pathway to compliance with elements of the federal Renewable Fuel Standard (FRS). The total volume of ethanol blended into motor fuels used in the U.S. has increased since 2010, although at a declining rate of growth; meanwhile, the use of ethanol-free gasoline (E0) by fuel consumers has declined.

FIG. 1 shows a refinery in-line blending facility.

FIG. 1. Refinery in-line blending.

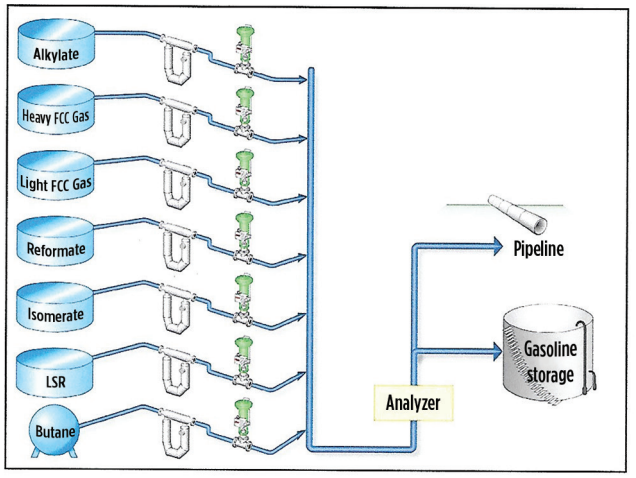

FIG. 2. Schematic diagram of a blending process.

Blending processes. Two types of blending exist: batch and continuous. Batch blending begins with mixing known amounts of components in a tank mixer using an agitator and other accessories, such as pressure gauge, liquid level indicators, etc. Agitation can also involve air where toxic materials like lead and biocides are blended. Mixing in tanks is also accompanied by heating or cooling coils.

Most refiners employ computer-controlled on-line blending for blending gasoline and distillates. All components to be blended are pumped simultaneously into a common header at rates specified as per the formulations in **FIG. 2.** The rate of flow is controlled by a valve operated by a pneumatic or electric relay system. The received signals correspond to the flowrates, and these can accurately modulate the flowrates by adjusting the valve. The long pipeline through which these proportioned components travel acts as a mixer to produce the blend. Additives can also be injected into the system.

Inventories of blending stocks, together with cost and physical property data, are maintained in a database. Many of the properties of the blending components, such as the octane number, are non-linear; therefore, estimating final blend properties from the components can be quite complex. When a certain volume of a given quality product is specified, LP models are employed, permitting the rapid selection of an optimal solution from multiple feasible alternative solutions. The LP can be used to optimize blending operations to select blending compo-

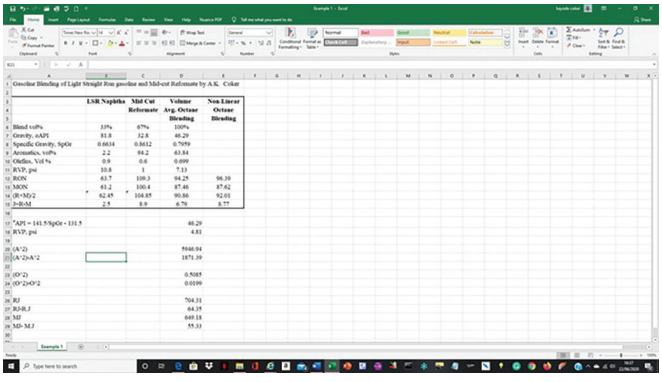

FIG. 3. Screenshot of the blending of linear straight run (LSR) naphtha and mid-cut reformate using the Ethyl model.

nents to produce the required volume of the specific product at the lowest cost. However, non-linear programming is preferred as enough data are available to define the equations because the components blend non-linearly, and values are functions of the quantities of the components and their properties.

Ensuring that the blended streams meet the desired specifications—such as boiling point, specific gravity, RVP and research and motor octane numbers—stream analyzers are installed to provide feedback control of blending streams and additives. The blending components involve an iterative process (i.e., trial-and-error) to economically achieve all critical specifications, as the large number of variables leads to several similar solutions that give the approximate equivalent total overall cost or profit. This is easily handled by a computer.

Each component is characterized by its specific properties and cost to manufacture, and each gasoline grade requirement is similarly defined by quality requirements and relative market value. The LP solution specifies the unique disposition of each component to achieve maximum operating profit. The next stage is to carefully measure the rate of addition of each component in the blend and collect it in storage tanks for final inspection before delivering it for sale.

The problem is not fully resolved until the product is delivered to the customer's tanks; frequently, last-minute changes in shipping schedules, production qualities or demand require the re-blending of the finished gasoline or the substitution of a high-quality—and therefore more costly—grade, even though it may generate less income for the refinery. Blending equations based on the various parameters—such as RVP, octane numbers, viscosity, etc.—are shown here.

Volume blending equations: specific gravity, aromatics and olefins content (vol%) are calculated using Eq. 1:

$$X_{mix} = \sum v_i X_i = \frac{\sum V_i X_i}{\sum V_i} \quad (1)$$

Mass blending equations: sulfur and nitrogen content (wt% or ppm), nickel and vanadium (ppm) and carbon residue (CCR, MCRT, etc.) are calculated using Eq. 2:

$$X_{mix} = \sum w_i X_i = \frac{\sum V_i \gamma_{oi} X_i}{\sum V_i \gamma_{oi}} \quad (2)$$

RVP is calculated using Eq. 3:

$$(RVP)^{1.25}_{mix} = \frac{\sum V_i (RVP)^{1.25}_i}{\sum V_i} \quad (3)$$

Octane numbers [research octane number (RON) and motor octane number (MON)] are calculated using Eqs. 4 and 5, respectively:

$$(RON)_{mix} = \frac{\sum V_i (RVP)^{12.5}_i}{\sum V_i} \quad (4)$$

$$(MON)_{mix} = \frac{\sum V_i (MON)_i}{\sum V_i} \quad (5)$$

Viscosity is calculated using Eq. 6:

$$\log\left[\log\left(V_{mix} + 0.7\right)\right] = \frac{\sum V_i \log\left[\log\left(V_i + 0.7\right)\right]}{\sum V_i} \quad (6)$$

Non-linear octane blending formula. The formulas for non-linear octane blending have been developed[1,2] using a set of 75 and 135 blends (**TABLE 1**) and accounting for the aromatics and olefin contents of the blendstock. The model is expressed by Eqs. 7–16:

$$R = \overline{R} + a_1\left[\overline{RJ} - \overline{R} \times \overline{J}\right] + a_2\left[\left(\overline{O^2}\right) - \overline{O^2}\right] + a_3\left[\left(\overline{A^2}\right) - \overline{A^2}\right] \quad (7)$$

$$M = \overline{M} + b_1\left[\overline{MJ} - \overline{M} \times \overline{J}\right] + b_2\left[\left(\overline{O^2}\right) - \overline{O^2}\right] + b_3\left[\frac{\left(\overline{A^2}\right) - \overline{A^2}}{100}\right]^2 \quad (8)$$

$$\text{"Road octane"} = \frac{R + M}{2} \quad (9)$$

$$\text{Sensitivity} = J = R - M \quad (10)$$

$$\text{Volume average} = \overline{X} = \frac{\sum V_i \times X_i}{\sum V_i} \quad (11)$$

$$\left(\frac{R + M}{2}\right) = (92.5)V_{nC_4} + (64)V_{LSR} + (94.1)V_{Ref} \quad (12)$$

$$(RVP)^{1.25} = (71)^{1.25} V_{nC_4} + (11.1)^{1.25} V_{LSR} + (3.2)^{1.25} V_{Ref} \quad (13)$$

$$1 = V_{nC_4} + V_{LSR} + V_{Ref} \quad (14)$$

Volume blending equations (Eq. 15):

$$X_{mix} = \sum v_i X_i = \frac{\sum V_i X_i}{\sum V_i} \rightarrow 0 = \sum V_i \left(X_i - X_{mix}\right) \quad (15)$$

Mass blending equations (Eq. 16):

$$X_{mix} = \sum w_i X_i = \frac{\sum V_i \gamma_{oi} X_i}{\sum V_i \gamma_{oi}} \rightarrow 0 = \sum V_i \left[\gamma_{oi}\left(X_i - X_{mix}\right)\right] \quad (16)$$

where the terms represent volumetric average values of given properties of components as follows[1,2]:

R = RON
M = MON
S = Sensitivity (RON – MON)
RS = RON × sensitivity

TABLE 1. Formulas for non-linear octane blending using a set of 75 and 135 blends

	75 blends	135 blends
a1	0.03224	0.03324
a2	0.00101	0.00085
a3	0	0
b1	0.0445	0.04285
b2	0.00081	0.00066
b3	-0.00645	-0.00632

TABLE 2. Typical properties of pure components and petroleum cuts that can be blended for gasoline

	Light straight-run naphtha	Mid-cut reformate	Volume average octane blending	Non-linear octane blending
Blend vol %	33	67	100	
Gravity, °API	81.8	32.8	42.29	
Specific gravity, SpGr.	0.6634	0.8612	0.7956	
Aromatics, vol.%	2.2	94.2	63.84	
Olefins, vol. %	0.9	0.6	0.699	
RVP, psi	10.8	1	7.13	
RON	63.7	109.3	94.25	96.39
MON	61.2	100.4	87.46	87.62
(R + M) / 2	62.5	104.9	90.86	92.01
J = R – M	2.5	8.9	6.79	8.77

MS = MON × sensitivity
O = Vol% olefins
A = vol% aromatics

Gasoline blending. Different gasolines (alkylates, reformates, polymerate, crackate, straight runs, etc.) are blended along with various additives to boost the performance value of gasoline. Additives include octane enhancers, metal deactivators, antioxidants, anti-knock agents, gum and rust inhibitors, and detergents, and are added during and/or after blending to provide specific properties not inherent in hydrocarbons. However, the blend should be to specifications and the two essential properties on which blends are critically constituted are vapor pressure and octane number. The vapor pressure of a mixture can be estimated by Raoult's law, but scant information on the molecular composition of a blend does not permit it; and laborious experimentation for evaluating molecular composition is unwise.

A gasoline blending example includes three blend stocks and two specifications to produce regular gasoline (87 RON) for both summer (9 psi RVP) and winter (15 psi RVP).

Non-linear programming. Non-linear blending rules can more closely match the physics of the problem. Depending on the availability of olefin and aromatic contents in the blended components, the octane number of the blend can be calculated using the linear mixing rule method with a correction factor.[1]

As an example, octane blending models using the values of coefficients a and b using the model referenced here gives Eqs. 17 and 18:

$$R = \overline{R} + 0.03324\left[\overline{RJ} - \overline{R} \times \overline{J}\right] + 0.00085\left[\left(\overline{O^2}\right) - \overline{O^2}\right] \quad (17)$$

$$M = \overline{M} + 0.04285\left[\overline{MJ} - \overline{M} \times \overline{J}\right] + 0.00066\left[\left(\overline{O^2}\right) - \overline{O^2}\right] - 6.32 \times 10^{-7}\left[\left(\overline{A^2}\right) - \overline{A^2}\right] \quad (18)$$

Product qualities are estimated through correlations that depend on the quantities and the properties of the blended components. Mixing rules and these correlations are employed to estimate the blend properties (e.g., specific gravity, RVP, viscosity, flash point, pour point, cloud point, aniline point). The octane number for gasoline is correlated with corrections based on aromatic and olefin content. The desired property of the blend is determined by Eq. 19:

$$P_{Blend} = \frac{\sum_{i=1}^{n} q_i P_i}{\sum_{i=1}^{n} q_i} \quad (19)$$

where P_i is the value of the property of component i, and q_i is the mass, volume or molar flowrate of component i contributing to the total amount of the finished product.

For example, q_i can be volume fraction x_{vi}; therefore, the denominator in Eq. 19 = 1. Eq. 19 assumes that the given property is additive (or linear). Additive properties include specific gravity, boiling point and sulfur content. However, properties such as RVP, viscosity, flash temperature, pour point, aniline point and cloud point are not additive. **TABLE 2** lists typical properties of pure components and petroleum cuts that can be blended for gasoline to meet market specifications.

The API gravity, RVP and average octane number for a 33/67 blend of light straight-run gasoline and mid-cut reformate can be determined using the Eqs. in the following section.

Since these values are vol%, they can be directly calculated as volume averages using Eqs. 20 and 21:

$$\overline{A} = (0.33)(2.2) + (0.67)(94.2) = 63.8 \quad (20)$$

$$\overline{O} = (0.33)(0.9) + (0.67)(0.6) = 0.7 \quad (21)$$

API gravity cannot be directly calculated as a volume average, but specific gravity can by using Eqs. 22 and 23:

$$\gamma_o = (0.33)(0.6634) + (0.67)(0.8612) = 0.7958 \quad (22)$$

$$°API = \frac{141.5}{SpGr} - 131.5 = \frac{141.5}{0.7958} - 131.5 = 46.3 \quad (23)$$

The volume average of the RVP is (Eqs. 24–27):

$$(RVP)^{1.25} = (0.33)(10.8)^{1.25} + (0.67)(1)^{1.25} = 7.13 \quad (24)$$

$$RVP = (7.13)^{\frac{1}{1.25}} = 4.81 \quad (25)$$

$$\overline{R} = (0.33)(63.7) + (0.67)(109.7) = 94.3 \quad (26)$$

$$\overline{M} = (0.33)(61.2) + (0.67)(100.4) = 87.5 \quad (27)$$

The Ethyl model[1,2] considers the aromatics and olefin contents of the blend stocks (Eqs. 28–31):

$$\overline{(A^2)} = (0.33)(2.2)^2 + (0.67)(94.2)^2 = 5{,}947 \quad (28)$$

$$\overline{(A^2)} - \overline{A}^2 = 5{,}947 - (63.8)^2 = 1{,}871 \quad (29)$$

$$\overline{(O^2)} = (0.33)(0.9)^2 + (0.67)(0.6)^2 = 0.509 \quad (30)$$

$$\overline{(O^2)} - \overline{O}^2 = 0.509 - (0.7)^2 = 0.02 \quad (31)$$

The Ethyl model[1,2] considers the spread between the RON and MON of the blend stocks (Eqs. 32–36):

$$\overline{J} = (0.33)(2.5) + (0.67)(8.9) = 6.79 \quad (32)$$

$$\overline{RJ} = (0.33)(63.7)(2.5) + (0.67)(109.3)(8.9) = 704.3 \quad (33)$$

$$\overline{RJ} - \overline{R} \times \overline{J} = 704.3 - (94.3)(6.79) = 64.5 \quad (34)$$

$$\overline{MJ} = (0.33)(61.2)(2.5) + (0.67)(100.4)(8.9) = 649.2 \quad (35)$$

$$\overline{MJ} - \overline{M} \times \overline{J} = 649.2 - (87.5)(6.79) = 55.5 \quad (36)$$

Using the Ethyl model based on 135 blends, the RON and MON are (Eqs. 37 and 38):

$$R = 94.25 + (0.03324)(64.5) + (0.00085)(0.020) = 96.4 \quad (37)$$

$$M = 87.5 + (0.04285)(55.5) + (0.00066)(0.020) - (0.00632)\left(\frac{1{,}871}{100}\right)^2 = 87.6 \quad (38)$$

Average of R and $M = (96.4 + 87.6)/2 = 92.0$

Severity, $J = 96.4 - 87.6 = 8.8$

The model shows that the gasoline will meet the premium octane specification, and the Excel spreadsheet shows the calculations of the Ethyl model. **FIG. 3** shows a screenshot of the Excel program. **FIG. 4** shows the relationship between octane number vs. fraction of light straight-run naphtha for an Ethyl 135 blend model.

Takeaway. Petroleum blending of refinery products is a rather complex mixture of hydrocarbons with components that frequently vary widely in properties. The final blended products must meet certain specifications, and optimization techniques can be employed to achieve the desired parameters; otherwise, a trial-and-error procedure can prove costly in time and materials.

Furthermore, due to the complexity of the blending problem, many blends can be used to meet the required specifications. Such a problem becomes more complicated as refiners resort to a linear program to optimize their blends, especially in the case of gasoline.

Refiners still blend products batch-wise; however, most facilities apply continuous or inline blending with much-improved analyzers for octane and volatility by applying optimization techniques. Refiners can confidently blend directly to tankers and pipelines at considerable savings over batch blending.

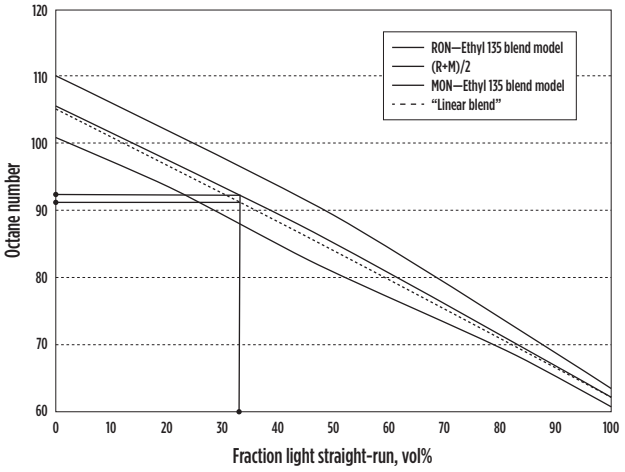

FIG. 4. Octane number vs. fraction light straight-run gasoline for Ethyl 135 blend model.

Part 2 of this article will appear in the July issue and further explores the optimization technique in Microsoft Excel and the LINGO program with the application of a case study. HP

LITERATURE CITED

[1] Maples, R. E., *Petroleum refinery process economics,* 2nd Ed., PennWell Corp., January 2000.

[2] Healy Jr., W. C., C. W. Maasen and R. T. Peterson, "Predicting octane numbers of multi-component blends," Report number RT-70, Ethyl Corp., Detroit, Michigan, April 1959.

A. KAYODE COKER is an Engineering Consultant for AKC Technology and has been a chartered chemical engineer for more than 30 yr. Dr. Coker is an Honorary Research Fellow at the University of Wolverhampton, U.K., a former Engineering Coordinator at Saudi Aramco Shell Refinery Company (SASREF) and Chairman of the department of Chemical Engineering Technology at Jubail Industrial College, Saudi Arabia. He is a Fellow of the Institution of Chemical Engineers, U.K. (C. Eng., FIChemE), and a senior member of the American Institute of Chemical Engineers (AIChE). He holds a BS (honors) degree in chemical engineering, an MS degree in process analysis and development and a PhD in chemical engineering, all from Aston University, Birmingham, U.K., as well as a Teacher's Certificate in education at the University of London, U.K. He has directed and conducted short courses extensively throughout the world and has been a lecturer at the university level. His articles have been published in several international journals. Dr. Coker is an author of six books in chemical engineering, a contributor to the *Encyclopedia of Chemical Processing and Design,* Vol. 61, and a certified trainer and mentor. He is a Technical Report Assessor and Interviewer for Chartered Chemical Engineers (IChemE) in the U.K. as well as a member of the International Biographical Centre in Cambridge, U.K. (IBC) as "Leading Engineers of the World" for 2008.

ABDULRAHMAN S. ALSUHAIBANI is a PhD candidate in the Chemical Engineering Department at Texas A&M University. His research is in sustainable design of industrial systems with a specific focus on developing a novel collaborative approach between process systems engineering and catalysis to efficiently accelerate the development of process design and optimization. He has focused his research applications on important contemporary issues for sustainability, including CO2 utilization and hydrogen economy. Prior to pursuing his PhD, Mr. Alsuhaibani worked for Saudi Aramco R&DC.

S. DANBAY, E. SULEIMENOV, A. SHOSHANBASOV, O. SMARKIN and **D. MAKEEV,** KazMunaiGas (KMG) Atyrau Refinery; **A. POPOV, R. GONZÁLEZ** and **V. JEGOROV,** Grace GmbH; and **N. LAMBERT** and **J-M. BESNAULT,** Axens

Maximize refinery profitability with novel RFCC technologies

The Atyrau Oil Refinery (AOR), the oldest refinery in Kazakhstan, was built in 1945. It is located in Atyrau, the capital of the Atyrau Region, at the mouth of the Ural River on the Caspian Sea, and is a base for modern oil and gas industries. AOR is operated by the state-owned KazMunayGas (KMG) and has successfully completed modernization, adding a deep oil conversion refining complex that has increased crude oil refining capacity up to 5.5 MMtpy and converted the site to one of the key refining complexes in the region.

AOR's target is to produce an optimized combination between high-value clean transportation fuels and specialty precursors for chemicals production, such as benzene or paraxylene. AOR is very complex (the Nelson Index is 13.8) and includes a number of conversion units, such as a proprietary resid fluid catalytic cracking unit[a] (RFCCU); proprietary catalyst[b] for selective AMPD/butadiene hydrogenation; and various hydrotreatments, including a proprietary catalytic process[c] for FCC gasoline, etherification (TAME), an extractive sulfur removal process[d] for liquefied petroleum gas (LPG) sweetening and indirect alkylation process[e] oligomerization, among others. AOR is continuously upgrading its process units (FIG. 1) with state-of-the-art technologies; for example, the refinery is working to modernize its TAME unit and adapt its product slate to IMO 2020 and use a proprietary digital service platform[f] for remote monitoring.

The FCCU is the primary hydrocarbon conversion unit in the modern petroleum refinery. It utilizes heat and catalyst to convert a variety of high molecular-weight feed types (e.g., gasoils and at-

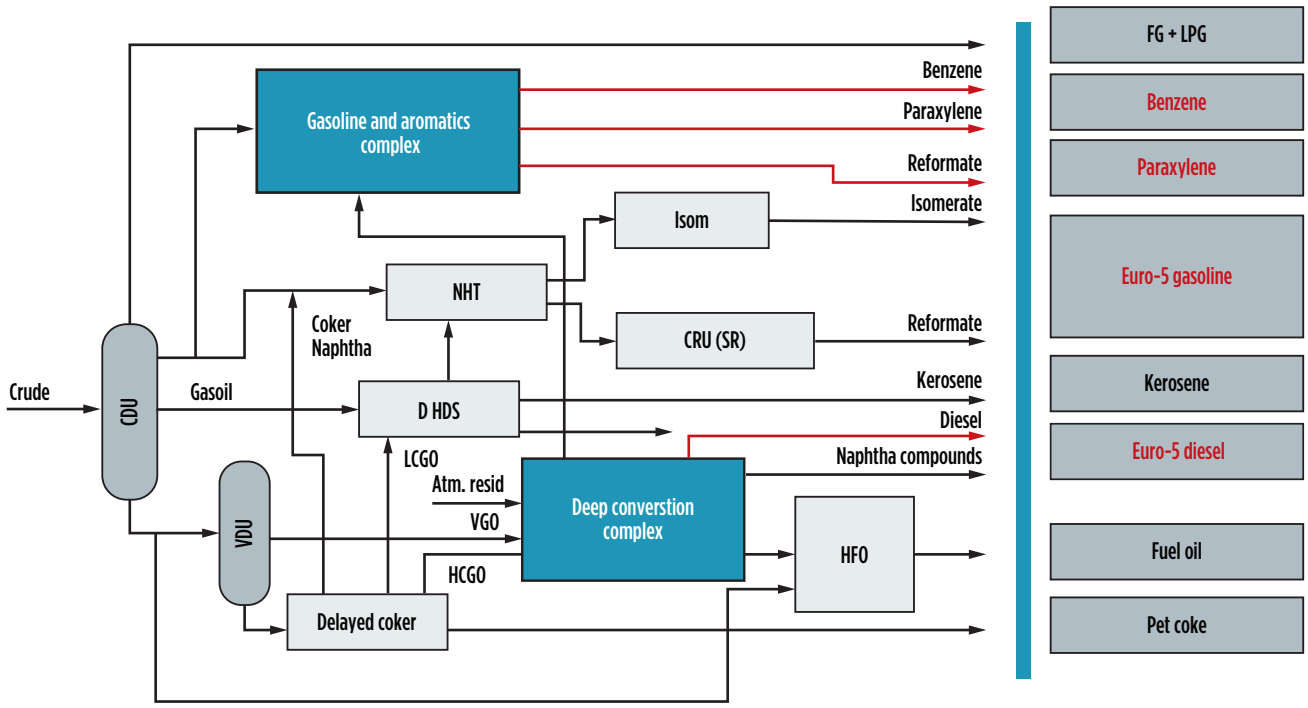

FIG. 1. Final configuration of modernization of Atyrau refinery.

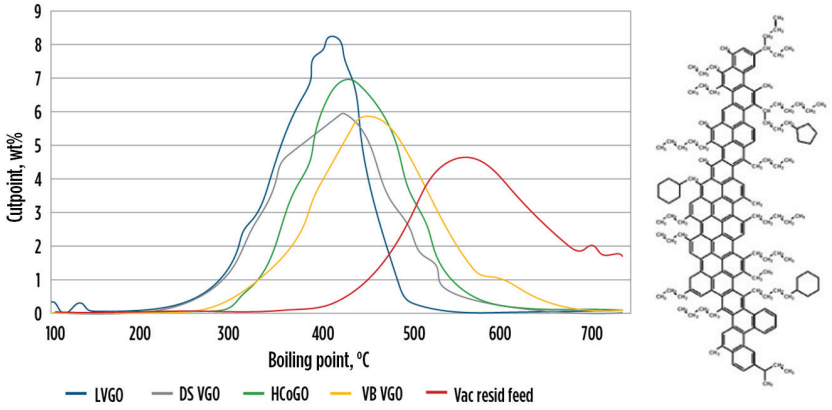

FIG. 2. Boiling point distribution of residue vs. typical FCC gasoils (left), and an asphaltene molecule (right).

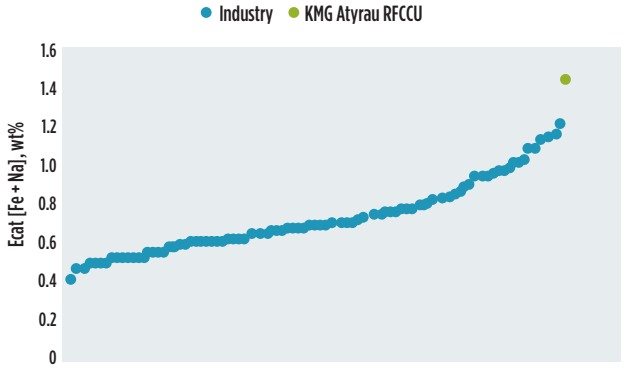

FIG. 3. Industry Ecat benchmark of [Fe+Na] (wt%) content.

TABLE 1. Atyrau RFCCU feedstock typical properties

Property	VGO	Atm residue	Coker gasoil
Content in feed, wt% FF	<35	>53	~5
V, mg/kg	0.1	11	<0.03
Ni, mg/kg	0.18	20	<0.04
Fe, mg/kg	22	95	0.13
Na, mg/kg	4.1	28	<0.17
Ca, mg/kg	0.87	9.37	<0.25
Feed S. G.	0.86	0.92	0.89
Feed concarbon, wt%	0.1	5.5	0.11
Distillation 10%, °C	319	394	350
Distillation 30%, °C	371	481	387
Distillation 90%, °C	474		463

mospheric/vacuum residues) into lighter, more valuable products such as transportation fuels and petrochemical feedstocks.[1] Almost every option under consideration involves upgrading residue type feedstock through an FCCU to compete under current market conditions. Considering future demand for refined products, slow-to-flat growth is projected for transportation fuels over the next decade, developing in parallel with the high-margins opportunities available in the petrochemicals market.

To be successful in such a challenging environment, it is of paramount importance to develop strong partnerships between refiners and technology suppliers to ensure maximum conversion, product slate flexibility and unit availability, driving to the most profitable operations needed to stay competitive. This article describes a successful case of how a robust combination of operating expertise, state-of-the-art hardware and novel catalyst technologies have enabled AOR's RFCCU to achieve the facility's ambitious conversion objectives while processing one of the most challenging feedstocks found worldwide.

Residue conversion challenges. Residual streams from atmospheric or vacuum distillation fractionators are characterized as having a heavier nature than traditional gasoils used in FCCUs due to the presence of high molecular-weight polynuclear aromatic rings—such as resins or asphaltenes—which then result in a higher boiling point distribution, between 500°C–700°C (FIG. 2).

Residue streams possess high density and aromaticity, in addition to much higher Conradson carbon residue, as compared to vacuum gasoil (VGO). It is commonly accepted that the conditions in the FCCU do not allow the ring-opening cracking of aromatic rings; therefore, increasing density and/or aromaticity directly results in loss of feed conversion. The high CCR presence is believed to convert to coke within 30%–90%, depending on the feed nature, which heavily impacts the heat balance in FCC operations, as seen with higher regenerator temperature, lower cat/oil (C/O) ratio and reduced conversion.

Residue feeds also contain high levels of contaminants. The high metal "complexes" typical of residues like nickel (Ni) or vanadium (V) accelerate poisoning of conventional catalysts. Ni deposits on the catalyst surface present a strong dehydrogenation activity to form undesired hydrogen and coke precursors if not inhibited properly. Unlike Ni, the V complexes destroy the zeolite Y portion in the cracking catalyst and lower activity due to the formation of vanadic acid. Further, its mobility characteristics allow it to move from one catalyst particle to another catalyst particle, extending its destructive impact to multiple catalyst particles. V is most detrimental when the FCCU is operated in full burn mode.[2] Therefore, an effective V trap dramatically reduces the FCCU's ability to destroy the active components of FCC catalyst and, therefore, maintain high inherent cracking activity.

In addition, other metals can be present, such as iron (Fe) or sodium (Na), which remarkably enhance the detrimental impact of V on the catalyst activity when processing heavy residue feedstock. Fe and Na tolerances are crucial factors for Atyrau's FCCU, as it presents the highest Ecat [Fe+Na] among 81 FCCUs benchmarked in the industry (FIG. 3).

Typical feedstock properties of AOR's RFCCU are shown in TABLE 1. Besides the mentioned extreme [Fe+Na] levels, the residue fraction has very high Ni, V and calcium (Ca) levels, along with a Conradson carbon content exceeding 5.5 wt% and a 30% distillation point > 480°C. This very challenging residual stream is fed into the unit well above 50 wt% of the

total feed, making the FCC processing in the AOR one of the most challenging worldwide.

The feed characteristics in TABLE 1 from residual streams may lead to the following FCCU limitations:

- Main air blower (MAB) or wet gas compressor (WGC) capacities may be exceeded—in many FCC operations, the Ni content of Ecat systematically grows, making it necessary to use catalysts with improved Ni trapping to avoid running into WGC constraints, as Ni is known to produce hydrogen.
- Upper limits for regenerator temperature and stripping efficiencies create bottlenecks and are strongly interrelated with the coke remaining on the spent catalyst. If the hardware in the regenerator or regenerator design cannot cope with the temperature increase or afterburn, this will also be a limiting factor.
- Bottom-of-the-barrel products (e.g., FCCU bottoms product) have a limited market, either for sale to a coking refinery or as one of a few different grades for coking.

RFCCU. AOR uses a proprietary RFCCU[a] technology to convert heavy, high molecular-weight and metals content feedstock into higher value streams. This technology was originally developed as a cost-effective, flexible and reliable means to profit from market opportunities at times when it was crucial to leverage the intrinsic potential of residuum feedstocks. Various challenges posed by such feeds have been overcome as detailed here, and innovations have been kept up-to-date. In particular, the Atyrau proprietary RFCCU[a] is equipped with:

- A leading resid feed injector technology[c] that ensures appropriate feed distribution to promote vapor-phase cracking, resulting in low coke and dry gas make and superior liquid selectivity that limits the burden on the WGC
- Mix temperature control (MTC) that ensures riser temperature control through quench to increase the C/O ratio and displace the equilibrium between catalytic and thermal cracking to achieve better selectivities
- A riser termination device[g] offering high gas containment to limit products degradation to light ends, while being highly resilient to transient phases
- Superior catalyst stripping with structured packing to preserve the valuable hydrocarbon material and reduce the regeneration temperature at low stripping steam rates.

More importantly, the RFCCU configuration incorporates a two-stage catalyst regeneration (FIG. 4) that minimizes catalyst deactivation in the presence of metals to maintain higher activity with more metals on the catalyst, thereby reducing catalyst replacement costs.

The first regeneration stage operates in partial burn mode. High hydrogen content molecules are burned in this stage, yielding water. The extent of the regeneration is controlled to limit the temperature elevation in the presence of water, which would otherwise cause high hydrothermal deactivation of the catalyst. Moreover, in the absence of excess oxygen, V oxidation cannot occur. This is the first step in the mobility cycle of this molecule, which ultimately leads to the collapse of the catalyst structure and drastic reduction of its ability to convert the longer molecules inherently present in FCC feeds.

The second regeneration stage operates in full burn mode to restore the full catalyst potential. In this stage, the temperature is further elevated, which is less detrimental to catalyst activity than other solutions because water was removed with flue gas in the first stage. Furthermore, in the absence of water, the transformation of vanadium oxide to vanadic oxide is largely impaired—once more this limits the V mobility, thus inhibiting the noxious effects of this contaminant on catalyst.

It is worth noting that the two-stage scheme also rejects a substantial portion of the regeneration heat as carbon monoxide (CO) in the first stage, thus removing the necessity to install a catalyst cooler at Atyrau despite the high concarbon feedstock. This has a direct and positive impact on unit costs and complexity of operation, as well as removing a burden for maintenance. CO is subsequently oxidized to CO_2 and noxious components are captured or neutralized to ensure full compliance with environmental norms. The expertise of various partnerships are leveraged to systematically develop tailor-made, highly energy efficient FCC flue gas treatments abiding with the most stringent regulations worldwide. In the case of AOR, an SCR DeNO$_x$, followed by a flue gas scrubber, was retained.

Additionally, state-of-the-art thermal integration was developed specifically to accommodate changes in feed composition, as well as the different seasonal modes of operation required by KMG, while maintaining a high energy efficiency throughout all those cases.

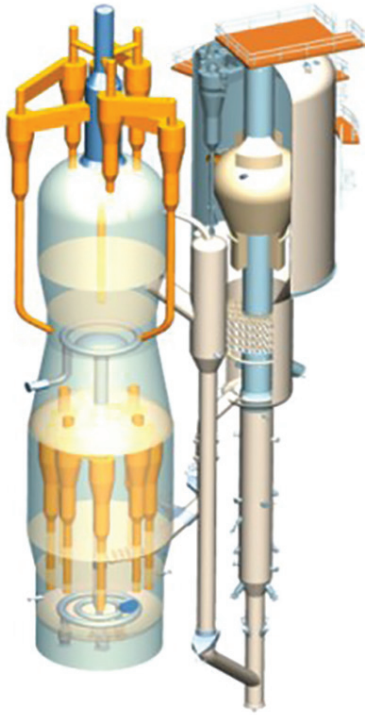

FIG. 4. Typical RFCCU[a] arrangement with dual-regeneration system.

For these reasons and owing to a strong experience due to more than 40 designs performed on feedstocks with concarbon higher than 3 wt%, the RFCCU[a] process provides yields and performances with the flexibility to process a wide range of feedstocks—from gasoil through residue—in the same unit to meet multiple product scenarios (max distillate, max gasoline or max light olefins).

Finally, thanks to a robust design in conjunction with a dedicated catalyst design, AOR's FCCU succeeds in ensuring catalyst circulation and is delivering expected performances while processing high Fe content feeds.

RFCC catalyst design. For a given residue-containing feedstock to be processed in an FCCU, there is an optimized set of operating conditions to maximize unit conversion for a given FCC hardware design. The mastery of such operating variables handling, as well as continuous improve-

ments in hardware technology, enable refiners to push profitability up to the FCCU or to downstream process constraints.

Nevertheless, another variable exists that can significantly improve unit profitability and reliability, resulting in substantial economic benefits: the FCC catalyst technology. The main advantages of catalyst technologies are:

- Wide flexibility to change design to adapt performance to objectives
- No need to stop the unit as with major hardware revamps, which enables changes between planned mean-time to application recovery (MTAR) dates
- Minor costs only involved and no CAPEX needed compared to high CAPEX investments
- Significant value creation for a refinery with optimized catalyst system selection.

A commercially well-proven catalyst[h] specifically tailored for the very adverse conditions of AOR's process was proposed. The main characteristics of this catalyst are:

1. **High-stability zeolite technology** that yields superior activity retention and hydrothermal stability while exhibiting low hydrogen-transfer selectivity to minimize undesired bimolecular reactions, as well as increased low-value LPG and gasoline linear paraffins.
2. **Integration of proprietary metals traps,** including an alumina-based matrix Ni passivator[i] and the rare earth-based vanadium trap (IVT). Research has been conducted using x-ray diffraction (XRD) to demonstrate the interaction between γ-Al_2O_3 and Ni. As can be seen in FIG. 5, this interaction is stronger with increasing Ni concentration. An IVT trap technology[j] was also used to reduce the harmful effects of V. This well-established technology has shown excellent V inhibition, as can be seen using a cross-section SEM-EDX microscopy technique (FIG. 6) in contaminated Ecat samples, which demonstrates the co-existence of hot-spots of rare earth RE and V, thus trapping the V and preserving the zeolite integrity.
3. **Intracrystalline pore architecture** is optimized to enable large molecules often encountered in a residual feedstock stream to enter the catalyst system and therefore be cracked into smaller, higher value molecules. This open pore volume is a characteristic signature of a proprietary catalyst system series[k], and it improves molecular diffusivity and pre-cracking of heavy molecules that otherwise would interact only on the surface of the zeolitic part of the catalyst and, in that case, hinder both the extent and selectivity of the monomolecular cracking aimed at the zeolite section properly designed for residue cracking.[3] This is clearly observed when comparing the pore size distribution (PoSD) of different commercially available catalysts (FIG. 7). The PoSD of the catalyst[k] exhibits a wide peak between 300 Å and 1,000 Å, where molecular diffusion is much faster and in line with typical heavy molecular size contained in resid fractions.

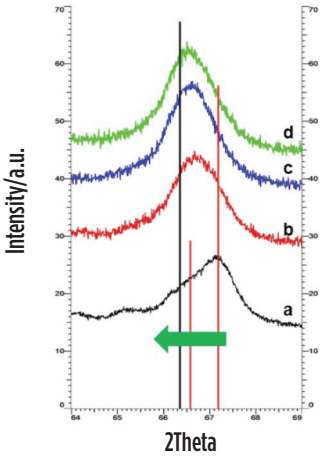

FIG. 5. XRD diffraction patterns of γ-Al_2O_3 with Ni, from containing no Ni (black) up to maximum Ni content (green).

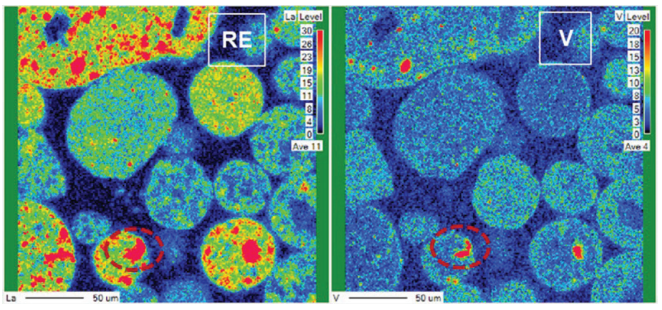

FIG. 6. SEM mapping for rare earth (RE) and vanadium (V) of a contaminated Ecat containing proprietary IVT technology[i].

KMG FCCU industry benchmarking. Thanks to the combination of state-of-the art hardware and catalyst technologies, AOR's RFCCU is showing outstanding conversion results that position it among the top refiners in the industry processing heavy feeds. Typical yields achieved in the refinery's RFCCU are indicated in TABLE 2.

These yields and conversion levels, when compared to EMEA refineries in general at normalized yields, further sup-

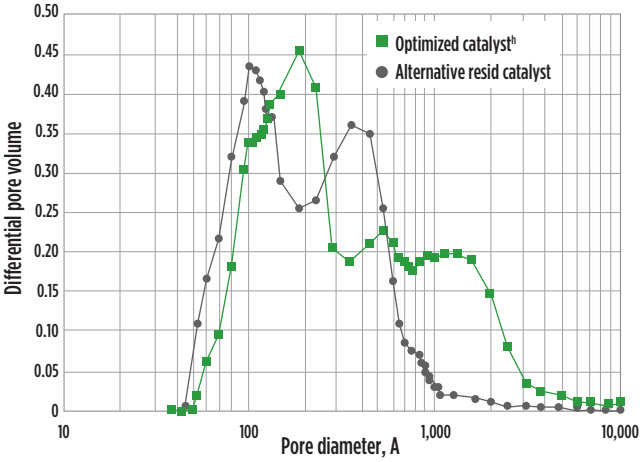

FIG. 7. Pore size distribution (Å) of optimized resid catalyst[k] and alternative resid catalyst in the market.

port the outstanding performance of the AOR RFCCU. As can be seen in FIGS. 8–13, Atyrau's RFCCU shows very high conversion and superb gasoline yield, while excelling at bottoms cracking. This is enabled by an excellent coke and gas selectivity, as observed in the EMEA Ecat benchmarking monitored by pilot plant laboratories[l] to Ecat samples of all FCCUs in the region.

Value creation through partnership. The coordinated efforts between the KMG's refinery operating excellence and additional expertise from partners like the authors' companies are reflected in faster, more efficient problem-solving that ultimately significantly increases the unit availability and reliability. As an example, in the beginning of 2019, the Atyrau FCCU faced a catalyst loss issue. Catalyst particles were observed both in the regenerator flue gas scrubber and the main fractionator bottoms line. A team analyzed pertinent catalyst fines samples and reviewed the unit's operating mode to identify changes that may lead to the root cause. A proprietary advanced microscopy technique[m] revealed that catalyst particle fracture was occurring in the unit (FIG. 14).

FIG. 8. Conversion (wt% FF) vs. cat/oil (wt/wt) industry benchmarking.

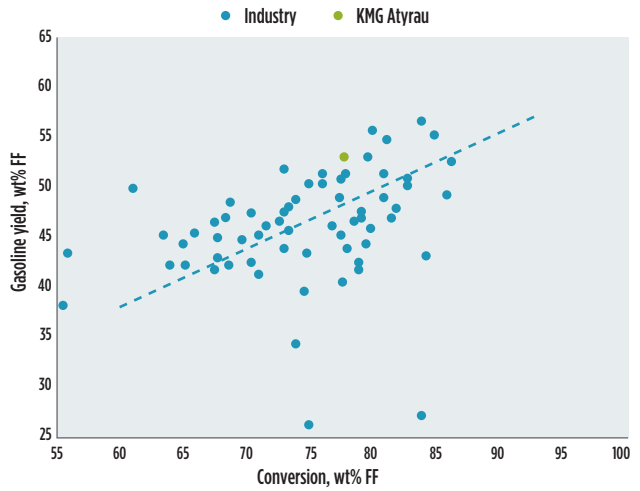

FIG. 9. Gasoline (wt% FF) vs. conversion (wt% FF) industry benchmarking.

After extensive joint brainstorming to target potential causes, a battery of actions was developed that included checking each air and steam injection point. It appeared that the steam values to the feed distribution nozzles were far above the recommendation. Through a comprehensive set of experiments, the team discovered that one of the seven feed nozzles received four times more steam than expected, well beyond the unit's recommended range of operation. While this did

TABLE 2. Atyrau RFCC typical yields

Parameters	Yields
Conversion, wt%	77.6
LPG, wt%	16.2
Gasoline (C5-215°C), wt%	52.4
Distillates (LCO+HCO), wt%	14.9
Slurry, wt%	7.5
Gasoline RON	92

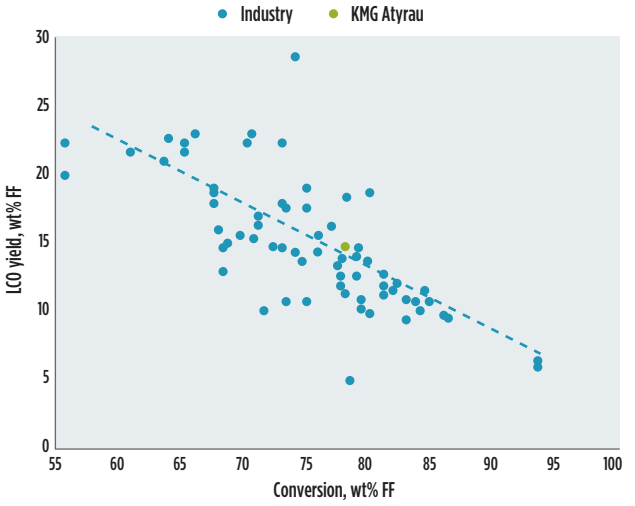

FIG. 10. LCO (wt% FF) vs. conversion (wt% FF) industry benchmarking.

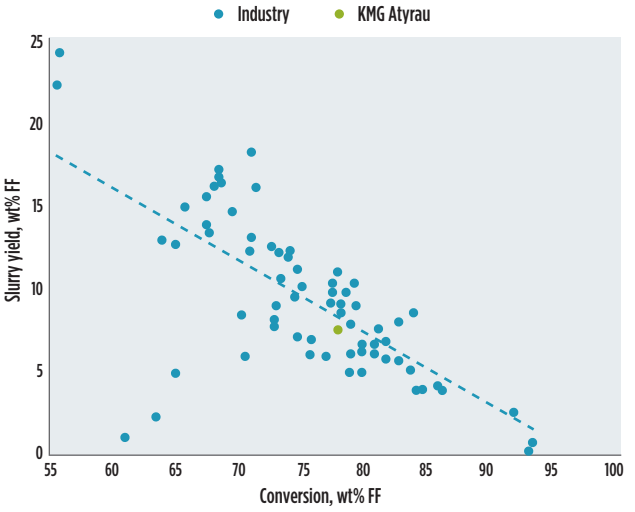

FIG. 11. FCC slurry (wt% FF) vs. conversion (wt% FF) industry benchmarking.

not severely impair the yield pattern due to a robust feed injector design, this was confirmed as being the root cause of the catalyst particles fracture episode.

In this way, a double benefit solution was achieved: the steam-to-nozzles amount was optimized with the corresponding savings, and a more evenly distributed steam injection resulted in a smoother mixing without damaging the quality of the catalyst circulating inventory. The improved circulation with reduced particulate losses delivered savings estimated at $1.3 MM/yr. The three-party cooperation delivered value by means of significant cost savings and much improved unit performance at Atyrau's FCCU and is expected to continue to provide benefits in the future.

Takeaway. A combination of technologies using a three-pronged approach—AOR's expertise and operations management, tailored FCC catalyst technology and the advanced hardware technology—enabled AOR to extract the maximum profitability from the very challenging operation at its RFCCU. Thanks to the close partnership between different parties, including the unit licensor and the catalyst supplier, it has been demonstrated that multidisciplinary teams can achieve excellent results and drive value for the refinery. The combination of the RFCCU[a] with the proprietary catalyst[h] delivered best-in-class bottoms cracking functionality, while preserving superior metals tolerance, which is crucial to keep the maximum number of residual streams in the feedstock diet. HP

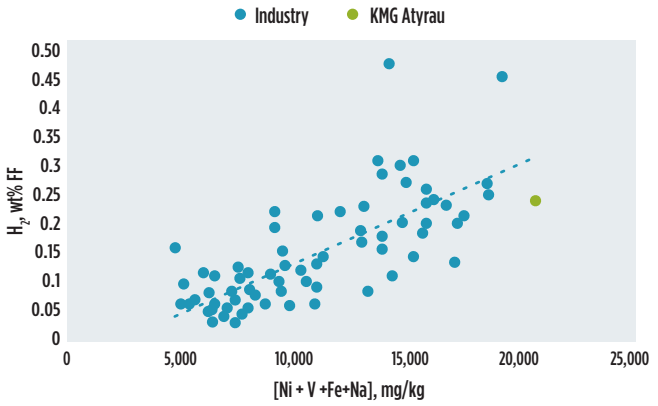

FIG. 12. Ecat[l] H_2 yield vs. metals industry benchmarking.

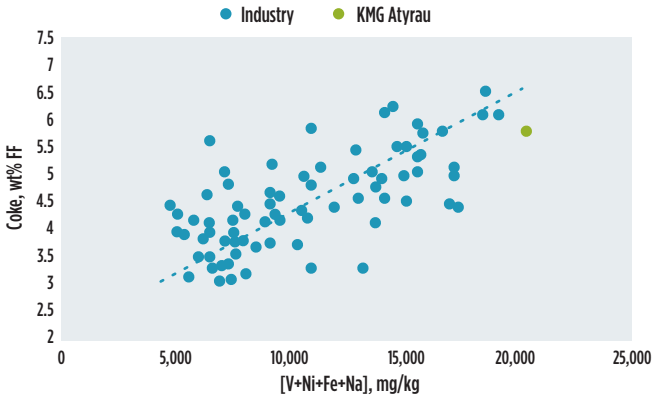

FIG. 13. Ecat[l] coke yield vs. metals industry benchmarking.

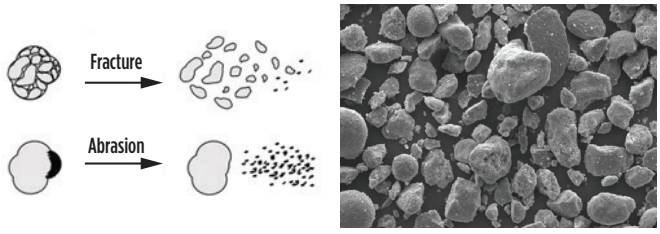

FIG. 14. Ecat[m] analysis revealing particulate fracture.

NOTES

[a] R2R™ resid fluid catalytic cracking unit by Atyrau Oil
[b] IFP Energies Nouvelles' Alkyfining®
[c] Axens' Prime-G+®
[d] IFP Energies Nouvelles' SULFREX®
[e] Axens' Polynaphtha®
[f] Axens' Connect'In®
[g] Axens' RS2™
[h] W. R. Grace & Co.'s MIDAS®-350
[i] W. R. Grace & Co.'s alumina-based matrix Ni passivator
[j] W. R. Grace & Co.'s IVT trap technology
[k] W. R. Grace & Co.'s MIDAS® series
[l] W. R. Grace & Co.'s Grace's ACE™
[m] W. R. Grace & Co.'s SEM/EDX

LITERATURE CITED

[1] Bryden, K., U. Singh, M. Berg, S. Brandt, R. Schiller and W.-C. Cheng, "Fluid catalytic cracking: Catalysts and additives," *Encyclopedia of Chemical Technology,* June 2015.
[2] "Grace guide to fluid catalytic cracking," 2nd Ed., W. R. Grace & Co, 2020.
[3] Zhao, X., W. Cheng and J. Rudesill, "FCC bottoms cracking mechanisms and implications for catalyst design for resid applications," National Petrochemical & Refiners Association (NPRA), 2002.

SHUKHRAT ABDURASHITOVICH DANBAY is the Chairman of the managing board for Atyrau Refinery LLP. Throughout his career, he has headed large commercial structures for the supply and refining of oil: he previously served as General Director of Gelios LLP; General Director of the Fuel Energy Complex of Kazakhstan LLP; Deputy General Director of Pavlodar Petrochemical Plant LLP for economics and finance; Executive Director of the oil refining and petrochemicals unit of NC JSC KazMunayGas; General Director of Pavlodar Oil Chemistry Refinery LLP; and Managing Director for oil refining of JSC NC KazMunayGas. Mr. Danbay graduated from Kainar University with a degree in international economic relations and from the Russian Academy of National Economy and Public Administration with a degree in business administration. He also received an Executive Master of Business Administration Energy Leadership from the Russian State University of Oil and Gas.

ERKIN BORISOVICH SULEIMENOV serves as the First Deputy General Director for production—Chief Engineer of Atyrau Refinery LLP, and is also a Member of the managing board. He began his career as an operator of a technological unit at the Atyrau Refinery LLP, and has held various positions, including Head of plant installations, Deputy Head of a workshop, Head of a technical department, Chief Technologist-Head of a technical department, Director of an oil refining department, Deputy Chief Engineer for technology and production, Deputy Chief Engineer for technology, Director of the department for reliability and mechanical integrity of production assets, Managing Director for technology, and First Deputy General Director for production. In August 2019, he was appointed First Deputy General Director for Production–Chief Engineer of Atyrau Refinery LLP. Mr. Suleimenov graduated from the Atyrau Institute of Oil and Gas with a degree as an Engineer Chemist-Technologist and received an MBA from the non-governmental educational institution Almaty Management University.

ADILET SHOSHANBASOV is the Chief Technologist for Atyrau Refinery LLP. He has worked at the Atyrau Refinery since 2003, and spent 4 yr in the oil refining department of JSC KazMunayGas. He took part in the reconstruction and modernization of the Atyrau refinery in 2003–2006, as well as in the

construction of the complex for the production of aromatic hydrocarbons and the complex for deep oil refining. Mr. Shoshanbasov graduated from the Kazakh National Technical University.

OLEG SAMARKIN is the Managing Director for commodity production and internal logistics for Atyrau Refinery LLP. He has worked at the Atau Refinery since 2005, and took part in the reconstruction and modernization of the Atyrau Refinery, as well as the startup and adjustment of the catalytic cracking unit (FCCU) and deep conversion complex. Mr. Samarkin graduated from South Kazakhstan State University in Shymkent.

DMITRY MAKEEV is Director of the technical development department for KazMunaiGas. He began his career at the Atyrau Refinery in 2005 as a Process Unit Operator. Later, he held various positions, including: Senior Operator, Shift Supervisor, Head of the technological unit, and Head of the project and development center. From 2010–2012, Mr. Makeev worked at the Petromidia Refinery (Romania, near Constanta) as Deputy Manager of the procces enginering department. He returned to the Atyrau Refinery as the Chief Technical Manager in the construction and startup of the aromatics production complex and the deep oil refining complex, and was then appointed Director of the production department of the Atyrau Refinery. Mr. Makeev graduated with honors from the South Kazakhstan State University with a degree in chemical technology of organic substances and materials, with a specialization in oil and gas refining, and earned an MBA degree. He is the author of several articles and has made presentations at numerous professional conferences.

ALEKSEY POPOV is the Technical Service and Sales Manager, Russia and CIS, for Grace. He began his career in the refining industry in JSC "Slavneft YANOS," where he served in various positions in the FCC unit, including as Chief Deputy and within the operative planning department. In 2014, he joined Grace as a Technical Service Engineer and moved to Technical Sales Manager in 2018, where he is responsible for providing FCC units technical service and sales in Russia and CIS countries. Mr. Popov is the co-author of several publications in the FCC industry and earned a BS degree in economics and an MS degree in oil chemistry.

RAFAEL GONZÁLEZ SÁNCHEZ is Regional Marketing Manager EMEA for Grace Refining Technologies. He joined Grace as an R&D researcher leading new FCC catalyst and additives developments before moving to Regional Technical Sales Manager to provide FCC technical service to refineries prior to current position. Dr. González has more than 14 yr of extensive multidisciplinary experience in catalyst design and development, as well as FCCU technical service. He earned an MS degree in chemical engineering and a PhD in engineering and advanced technologies from Barcelona University, Spain. His thesis topic was heterogeneous catalysis developments for the refining industry. Dr. González is the co-author of several publications in the FCC industry field.

VLADIMIR JEGOROV is the Sales and Technical Service Director for CIS accounts for Grace. He joined GRACE GmbH & Co.KG, Refining Technologies Europe, in 1996 as Regional Technical Service Engineer in the Moscow office. Prior to joining GRACE GmbH & Co.KG, Refining Technologies Europe, Jegorov worked in FCC units as a Process Engineer and Chief Technologist Deputy at the Mazheikiai refinery. He graduated from the Novopolotsk Polytechnical Institute, specializing in refining and gas processing.

NICOLAS LAMBERT manages the team of technologists in charge of fluidized catalytic cracking, residue hydrotreatment and sweetening technologies in Axens' Middle Distillates & Conversion Business Line. He joined Axens in 2002 as Process Engineer and has successively served as Project Manager for aromatics, reforming and FCC technologies, then as an FCC Technologist before attaining his current position in 2017. Mr. Lambert is an engineering graduate from Arts & Métiers ParisTech (ENSAM).

JEAN-MICHEL BESNAULT is a Technologist for fluidized catalytic cracking and sweetening technologies for Axens. He started his career at TOTAL Feyzin Refinery as an FCCU, VDU and Claus units Process Engineer in 2011. He moved to IFPEN in 2013, where he was involved in FCCU R&D projects before joining Axens in 2014 as a Technologist. Mr. Besnault is an engineering graduate from Ecole Nationale Supérieure des Ingénieurs en Arts Chimiques et Technologiques (ENSIACET).

G. LIU, Tianjin Dagu Chemical Co., Ltd., Tianjin, China; **R. SUNDARARAMAN,** ExxonMobil Chemical Co., Spring, Texas; and **J. CAO,** ExxonMobil Catalysts and Licensing, Spring, Texas

Ethylbenzene plant debottleneck with a high-activity transalkylation catalyst

Modern commercial ethylbenzene (EB) plants use liquid-phase alkylation processes with zeolite catalysts to achieve high product yields. The desired primary reaction is the alkylation of benzene with ethylene. However, successive undesired reactions also occur in the alkylator, producing polyalkylated compounds such as diethylbenzene (DEB) and triethylbenzene (TEB). To maximize EB yield, these polyethylbenzenes (PEBs) are separated in the fractionation section and recycled into a transalkylation reactor in which the ethyl groups are transferred onto the benzene ring to produce additional ethylbenzene. FIG. 1 shows the schematic of the alkylation reactions and the transalkylation reactions in EB production.

At the heart of the technology is the shape-selective MWW family of zeolite catalysts that enables EB production in high purity and yields. The MCM family of alkylation zeolite catalysts revolutionized EB production. Tailored to the molecular diffusion rate of the different reactants, the MWW family zeolite pocket structure is designed to achieve high selectivity to EB. This high-activity catalyst enables the process to be operated in liquid phase at low temperatures, which dramatically lowers capital expenditures and operational expenditures (OPEX). This proprietary EB alkylation process[a] was first commercialized at the Chiba Styrene Monomer Co., Chiba, Japan, in 1995.[1-3]

The MCM family of zeolite catalysts is more EB or monoalkylate selective than large-pore zeolites, including zeolites beta and Y.[3] This enables the process to use low feed ratios of benzene to ethylene. The lower benzene-to-ethylene (B/E) ratio reduces the benzene circulation rate, which, in turn, improves operational efficiency and reduces the throughput to the benzene recovery column.[4] The monoalkylating selectivity to EB is measured by the once-through production rate of PEB, which decreases with the increase of the B/E ratio (FIG. 2).

The transalkylation reactor in the proprietary EB alkylation process is designed to match the alkylation reactor performance. Because of the high monoselectivity of the alkylation catalyst, the production rate of PEB in the alkylator is small. Therefore, the size of a transalkylator in the EB alkylation process tends to be small. At a constant EB production rate, the amount of activity of transalkylation catalyst required to maximize the PEB conversion, while minimizing the low-value heavy residue purge, is determined by the amount of PEB pro-

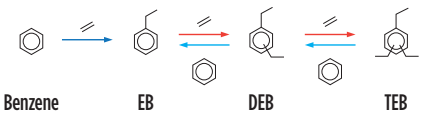

FIG. 1. EB production via alkylation and transalkylation reactions.

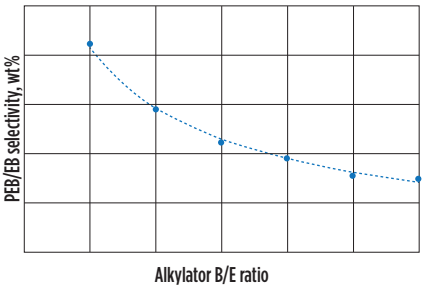

FIG. 2. Impact of B/E ratio on catalyst selectivity.

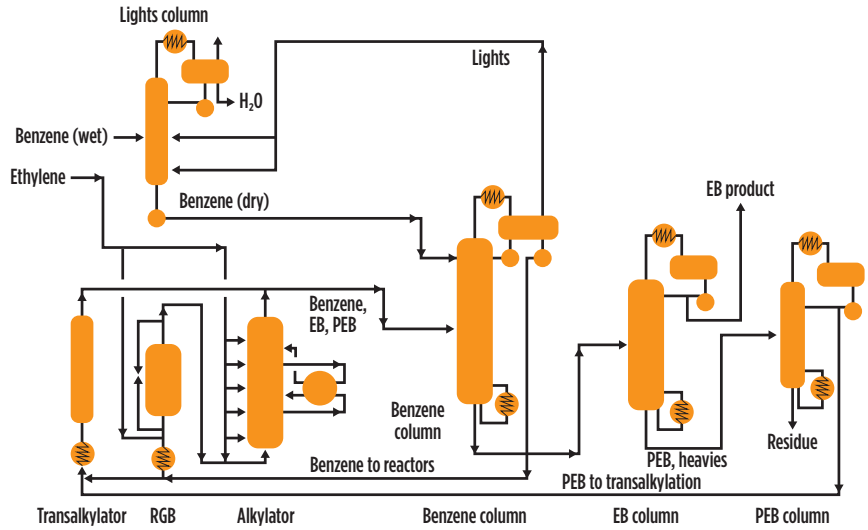

FIG. 3. Process flow scheme of the proprietary EB alkylation process[a] at TDCC's facility.

duced in the alkylator. Increasing the EB production rate will directionally lead to high PEB production, which increases the weight hourly space velocity (WHSV) of the transalkylator. To maintain constant conversion to reduce PEB recycle, the reactor temperature must be increased. However, high-temperature operation results in higher heavies yield and fast catalyst deactivation.

The other mitigation steps include increasing the B/E ratio in the alkylator operation. As shown in FIG. 2, the selectivity to PEB decreases with the increase of B/E. However, high B/E operation increases benzene recycle and results in high energy consumption. In such a case when the operation flexibility in the alkylation section is limited, the transalkylator becomes a bottleneck in the EB process unit. Therefore, a higher-activity transalkylation catalyst is required to convert more PEB at increased EB production rates, while minimizing residue production.

Overview of Tianjin Dagu Chemical Co.'s EB alkylation operation and constraints. Tianjin Dagu Chemical Co.'s (TDCC's) EB alkylation[a] unit was first commissioned in January 2010 with a production rate of 500,000 metric tpy of styrene monomer. The unit was originally designed to use a proprietary catalyst[b] in the reactor guard bed (RGB) and six-bed alkylator, along with a proprietary transalkyation catalyst[c] in the transalkylator. FIG. 3 shows the process flow scheme of the proprietary EB alkylation process at TDCC's facility.

During the booming period of the styrene market, TDCC's primary objective was to increase the plant's capacity. TDCC and the co-authors' companies' technical teams collaborated for months to evaluate the proprietary EB alkylation performance and identify the bottleneck in the transalkylation section at increased capacity. It was found that the unit was unable to maintain the designed PEB conversion at design temperature and WHSV when higher PEB was made in the alkylator; therefore, the operation needed to increase the reactor temperature, which inevitably led to high heavies yield and catalyst aging.

Plant operation optimization was attempted to achieve a high EB production rate while minimizing residue purge. While the results showed improvement, they did not meet TDCC's operational expectations (i.e., high production rate and low residue make at low OPEX). Measures were then taken that included increasing the alkylation section's B/E ratio. The increased B/E ratio did reduce PEB yield, but resulted in high OPEX due to high benzene recirculation. As a second option, TDCC reluctantly shut down the unit temporarily to load additional proprietary transalkylation catalyst[c] in the remaining limited space of the reactor. Unfortunately, the additional catalyst was still unable to bring adequate activity for the required PEB conversion. Eventually, there were essentially two remaining options:

1. Invest in a new larger reactor to load more catalyst
2. Deploy a higher-activity transalkylation catalyst.

Option 1 was not economical in terms of capital and schedule. To support TDCC's objective to increase EB production, and to enable increased plant capacity and address the transalkylation section bottleneck, the technical teams started an accelerated catalyst development program to identify a higher-activity transalkylation catalyst for potential deployment at TDCC.

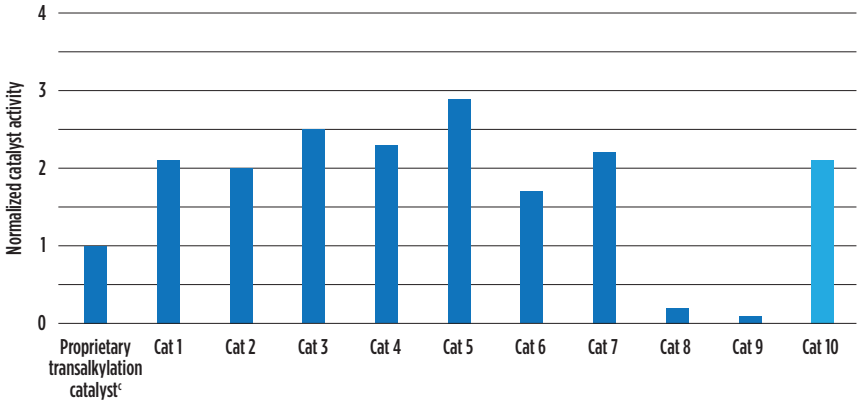

FIG. 4. Catalyst screening for a higher-activity transalkylation catalyst.

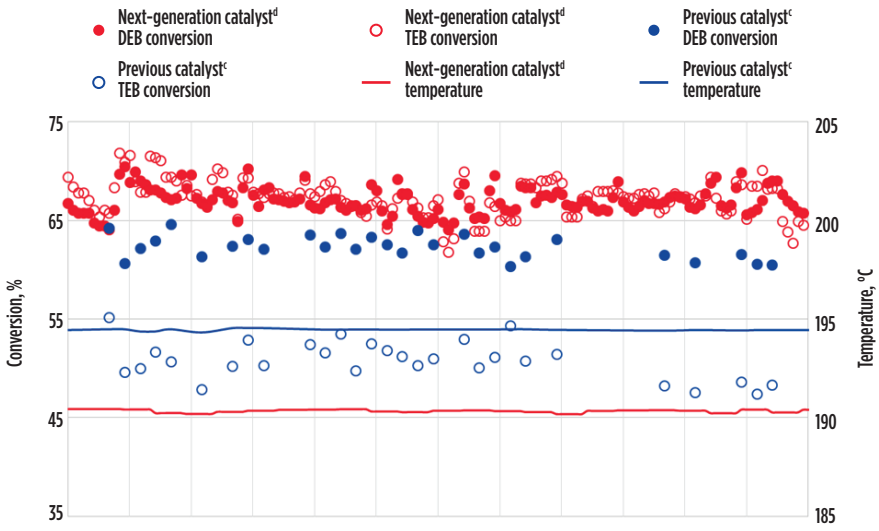

FIG. 5. Next-generation transalkyation catalyst[d] (2017 cycle) vs. the previous catalyst[c] (2013 cycle) at a PEB WHSV of 1.2 h^{-1}.

High-activity transalkylation catalyst development: Pilot plant experience.

With an extensive catalog of active materials, the technical teams quickly identified 10 catalysts with varying zeolite types, compositions and treatment methods to address TDCC's constraints. These materials were screened in a lab-scale batch reactor with commercially representative feed specifications and conditions. A normalized catalyst activity plot from this testing (FIG. 4) illustrates that six out of the 10 catalysts tested showed two times the activity vs. the proprietary transalkyation

catalyst[c]. In addition to being two times more active than the proprietary transalkylation catalyst, Cat 10 was selected for further testing and qualification, since it had the shortest lead time for commercial manufacturing, which would enable faster deployment to TDCC.

The selected catalyst from this lab testing was designated as the next-generation, higher-activity transalkylation catalyst[d]. For detailed product yields, pilot plant testing of the next-generation transalkylation catalyst[d] and its predecessor[c] were conducted using a commercial PEB recycle feed and conditions that would best simulate TDCC conditions. Data obtained showed the next-generation transalkylation catalyst to be 15°C more active vs. its predecessor under similar DEB conversion. If operated at the same temperature, the next-generation transalkylation catalyst showed significantly higher DEB conversion vs. its predecessor. The results of the pilot plant testing are shown in **TABLE 1.**

The combination of lab and pilot plant testing data showed that the next-generation transalkylation catalyst could overcome TDCC bottlenecks in the transalkylation section.

High-activity transalkylation catalyst deployment: Commercial experience.

TDCC technical and management teams and the co-authors' company evaluated the impact of the drop-in, next-generation transalkylation catalyst upgrade on the proprietary EB alkylation process[a] unit's performance and associated risks. Based on lab and pilot plant data, risk matrix and mitigation steps were developed. The new catalyst was fully compatible with TDCC's existing EB alkylation facilities. No issues were identified with respect to operating constraints or feed specifications.

TDCC eventually became the first adopter of the novel, high-activity transalkylation catalyst. Catalyst loading took place in May 2017, and alignment between technical teams on startup and initial operating procedures was gained prior to oil-in. The plots in **FIG. 5** show the start of cycle performance of the next-generation transalkylation catalyst (2017 cycle) and its predecessor (2013 cycle) under similar PEB WHSV of 1.2 h^{-1} for both cycles.

The performance of the next-generation catalyst for transalkylation to EB showed significantly better performance over the previously used catalyst under similar conditions at TDCC. As shown in **FIG. 5,** the next-generation transalkylation catalyst had a 3°C lower reactor temperature vs. the previously used catalyst. The next-generation catalyst also had a higher average DEB conversion of 67% vs. 62%. At the start of cycle-fresh catalyst conditions, TEB conversion averaged 67% for the new catalyst vs. 51% for the previously used one. This start-of-run benefit of lower cycle temperature and higher conversion is consistent with the pilot plant data shown in **TABLE 1,** demonstrating the higher activity of the next-generation transalkylation catalyst. More importantly, with the change in transalkylator catalyst to the higher-activity catalyst, TDCC did not see additional residue make from the plant.

TDCC's primary objective was to increase plant capacity to capture the booming styrene market. The higher activity of the next-generation transalkyl-

TABLE 1. Pilot plant testing of the next-generation transalkylation catalyst vs. its predecessor

	Target DEB conversion		Target temperature	
Catalyst	Transalkylation catalyst[c]	Next-generation transalkylation catalyst[d]	Transalkylation catalyst[c]	Next-generation transalkylation catalyst[d]
Bz/PEB wt ratio	2	2	2	2
PEB WHSV, h^{-1}	1.1	1.1	1.1	1.1
Temperature, °C	194	177	190	190
DEB conversion	65%	65%	60%	72%
TEB conversion	56%	60%	42%	83%
Heavies/EB, wt/wt	0.59%	0.62%	0.63%	0.85%

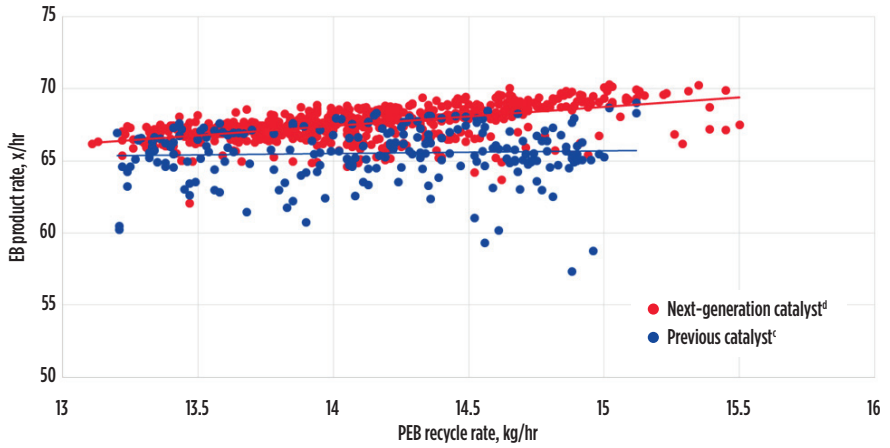

FIG. 6. EB production rate vs. PEB recycle rate: Next-generation transalklyation catalyst[d] and the previously used catalyst[c].

ation catalyst enabled TDCC to meet this objective. As shown in **FIG. 6,** higher PEB conversion with the new catalyst cycle enabled TDCC to overcome the bottleneck in the transalkylation section, resulting in up to a 9% increase in EB production vs. the previous cycle. At the time of the publication of this article, the next-generation transalkylation catalyst load has been on stream for nearly 4 yr. The new catalyst has shown exceptional stability, with a very low aging rate, and it continues to meet TDCC's expectations.

Takeaway. Rapid deployment of a next-generation, high-activity transalkylation catalyst[d] has provided TDCC a fit-for-purpose technology solution for debottlenecking its EB transalkylation plant. The site was able to achieve 109% of design capacity to allow market value capture of $5.5 MM/yr. The novel transalkylation catalyst presents higher activity than its prior version. With the same load size, higher single-pass PEB conversion was achieved at a lower reactor temperature. The next-generation transalkylation catalyst has been in stable operation—with negligible aging—at TDCC's facility since May 2017.

Overall, the high-activity transalkylation catalyst provides operating flexibility to achieve the following benefits:

- Debottleneck a transalkylation/PEB loop to achieve higher overall unit capacity
- Lower PEB recycle to save PEB loop energy consumption
- Lower start-of-run temperature slows catalyst aging rate, providing a larger operating temperature window and increasing the cycle length
- Low-temperature operation reduces heavies production to minimize fuel value downgrading
- Lower initial catalyst fill cost, with reduced load size for constant unit capacity. HP

NOTES

[a] Badger Licensing's EBMax[SM] technology
[b] ExxonMobil's EM-3300 catalyst
[c] ExxonMobil's EM-3700 transalkylation catalyst
[d] ExxonMobil's EM-3750 transalkylation catalyst

LITERATURE CITED

[1] Maerz, B. R., C. R. Venkat, S. S. Chen and D. N. Mazzone, "EBMax[SM]: Leading-edge ethylbenzene technology from Mobil/Badger," DeWitt & Co. Inc.'s 1996 Petrochemical Review, Houston, Texas, March 1996.
[2] Mazzone, D. N., P. J. Lewis, C. R. Venkat and B. R. Maerz, "Mobil/Badger into the future," *Hydrocarbon Asia,* April 1997.
[3] Cheng, J. C., T. F. Degnan, J. S. Beck, Y. Y. Huang, M. Kalyanaraman, J. A. Kowalski, C. A. Loehr and D. N. Mazzone, "A comparison of zeolites MCM-22, beta, and usy for liquid phase alkylation of benzene with ethylene," *Studies in Surface Science and Catalysis,* Volume 121, 1999.
[4] Degnan Jr., T. F., C. M. Smith and C. R. Venkat, "Alkylation of aromatics with ethylene and propylene: Recent developments in commercial processes," *Applied Catalysis A: General,* November 2001.
[5] ExxonMobil Catalysts and Licensing LLC, Fact Sheet: "Cutting-edge catalysts for ethylbenzene production ExxonMobil zeolite catalysts: Producing the majority of the world's ethylbenzene."

GEHONG LIU is the General Manager of Tianjin Dagu Chemical Co. Ltd. He has been working in chemicals manufacturing for 18 yr and has extensive management experience in chloralkali chemicals and the petrochemical industry. Mr. Liu holds six patents and has published 12 peer-reviewed technical papers. He graduated from the Wuhan Institute of Technology with a degree in chemical engineering. He obtained a post-graduate degree from Tianjin University.

RAM SUNDARARAMAN is a Staff Engineer with ExxonMobil Chemical Co. Dr. Sundararaman has 15 yr of experience in catalyst and refining technology development and holds several U.S. patents. He earned a PhD in fuel science from Penn State.

JAMES CAO is the Senior Technical Sales Manager for aromatics licensing with ExxonMobil Catalysts and Licensing LLC. He has more than 25 yr of experience in heterogeneous catalysis and its commercial applications and holds 25 U.S. patents and various international filings. Dr. Cao has been responsible for technology licensing and catalyst sales of xylenes, EB and cumene processes. He earned his MS and BS degrees in chemical engineering from Tsinghua University, and his PhD in chemical engineering from the City University of New York.

S. RIVA, BASF, Italy; and S. CHALLIS, Chalcat Consulting, UK

Understanding HCN in FCC: Formation, effects and mitigating options

In these challenging times, fluidized catalytic cracking units (FCCUs) aim to improve margins by processing poorer- or different-quality feeds, while maintaining good yield performance. These feeds may produce more coke and have elevated nitrogen levels, which can then increase the potential for higher cyanides and associated equipment damage in wet hydrogen sulfide (H_2S) service.

A general overview of cyanide formation and associated corrosion problems in the catalytic fractionator and gas plant is provided to help explain the nature of the problem and what mitigating actions can be taken. Many FCCUs have no history of cyanide-related problems, as potential cyanide effects are adequately controlled by water washing and by using chemical additives.

In addition, unit operating parameters can be adjusted to help control cyanide production. Application of this approach is discussed for a unit that observed higher cyanides in the catalytic fractionator overhead water following increased processing of heavier feeds enabled by a catalyst change. An in-depth investigation showed that the amount of cyanides was increasing with the heaviness of the feed. This unit subsequently found no cyanide-related problems during a unit turnaround inspection.

Wet H_2S equipment damage mechanism. In wet H_2S service, H° is formed in the steel corrosion reaction, as indicated in **FIG. 1.** The presence of H_2S in water inhibits the recombination of the H°, and potentially enables these atoms to penetrate into and diffuse through the equipment steel.

The H° can combine inside the steel to form molecular H_2, which causes these larger structures to be trapped and unable to diffuse back out. The H_2 can then cause damage to the steel in the form of blistering, sulfide cracking, H_2-induced cracking and stress-oriented H_2-induced cracking. However, under normal circumstances, the iron sulfide (FeS) scale formed on the steel surface in a wet H_2S environment provides a barrier to the H° produced, thereby generally mitigating the issue.

HCN and potential for wet H_2S damage. Hydrogen cyanide (HCN) and ammonia (NH_3) from the FCC reactor leave in the catalytic fractionator overhead product, and free cyanide ions (CN^-) are formed in water by the reaction HCN (aq) + NH_3 (aq) $\leftrightarrow NH_4^+$ (aq) + CN^- (aq). The CN^- tends to remove the FeS scale on steel surfaces by forming a ferrocyanide complex, which is soluble in water by the reaction $FeS + 6CN^- \rightarrow Fe(CN)_6^{4-} + S^{2-}$. Removal of the scale then allows H° to diffuse into the steel, leading to wet H_2S damage, as previously described.

Experience shows that hydrocyanic acid in the overhead water does not cause significant metal loss, as NH_3 absorbed with the HCN acts as a buffer, typically keeping the water pH above 8.

Locations prone to cyanide corrosion. A typical catalytic fractionator overhead system with water wash injection used as a corrosion mitigation measure is shown in **FIG. 2.** Locations most prone to cyanide corrosion problems are circled.

Industry experience shows that if wet H_2S damage occurs, it is most frequently observed in the vicinity of the compressor coolers and absorber tower due to high HCN in the gas streams vs. hydrocarbon liquids and in the deethanizer tower. Reported problems have been related to changes in feed quality (e.g., high nitrogen, low sulfur), which required adjustment to corrosion control measures, inadequate water wash rates, poor distribution of water upstream of coolers, and poor separation of hydrocarbons and water.

HCN limits and measurement of free cyanides. A typical guideline is to maintain free cyanides (HCN and CN^-) in sour water below 20 ppm (mg/l) for corrosion control. However, it is relatively difficult to accurately measure free cyanides due to a number of potential interferences. Measuring total cyanides includes both free cyanide plus stable cyanide compounds, which

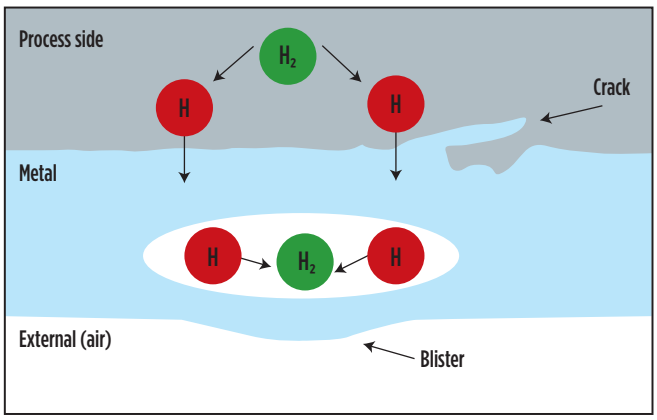

$Fe + H_2S \leftrightarrow FeS + 2H°$ (atomic)
$2H°$ (atomic) $\leftrightarrow H_2$ (molecular)

FIG. 1. Steel corrosion reaction and damage caused by H_2.

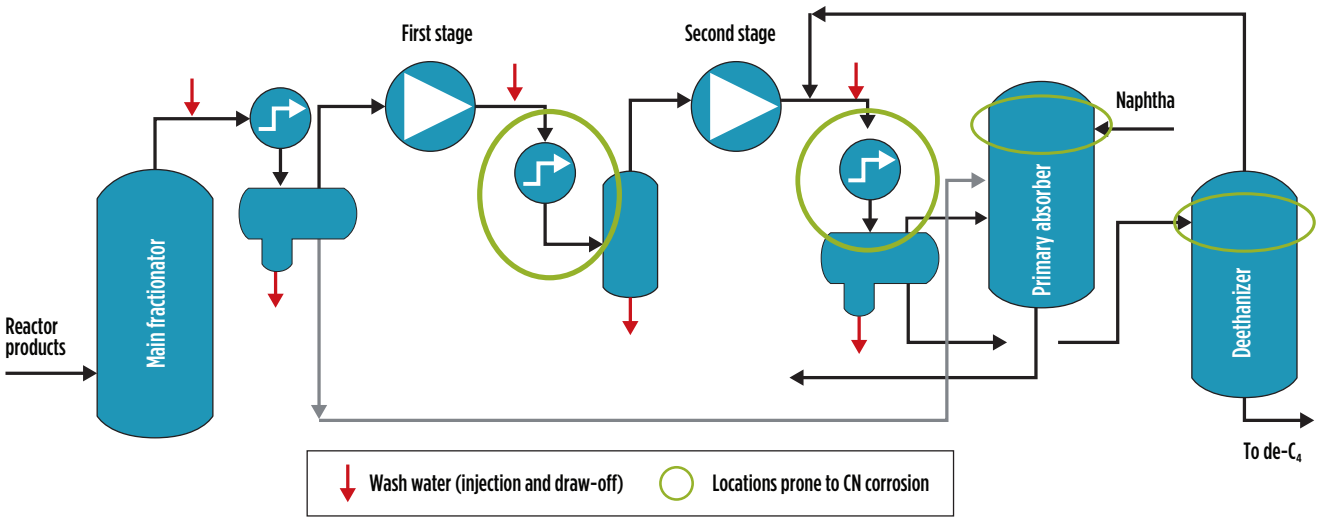

FIG. 2. Locations prone to cyanide corrosion damage.

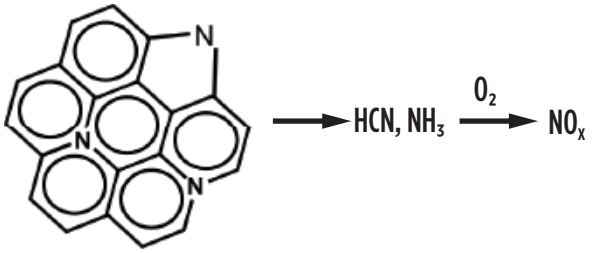

FIG. 3. HCN formation.

do not form a weak acid and do not "complex" FeS scale. Total cyanides measurement would be expected to over-estimate free cyanides and the related concern for wet H_2S damage.

Some FCCUs have reported elevated total cyanides close to 100 ppm, and no cyanide-related problems have been experienced. Polysulfide has been successfully used for many years to control high cyanide levels.

HCN formation chemistry. Various organic nitrogen (N) compounds are present in FCC feed. Some HCN may form in the FCC riser due to reactions such as $NH_3 + CO \rightarrow HCN + H_2O$, for example. However, a significant amount of the HCN is also being entrained with the catalyst circulated back to the riser from the regenerator. Coked catalyst from the reactor, containing C, H, S and N, is sent to the regenerator, where the coke is burned off. Here, HCN and NH_3 are formed as intermediate products from coke N reactions and are oxidized to N_2 and NO_x products given adequate time, temperature and O_2 availability (**FIG. 3**).

FCC coke consists of coke from four main sources:

1. Catalytic reactions
2. Metal dehydrogenation reactions
3. Hydrocarbons adsorbed/entrained in the catalyst pores from the stripper (strippable)
4. Feed additive (Conradson carbon residue, or concarbon, is a measure).

"Hard" coke formed by catalytic reactions would tend to be highly stable aromatic hydrocarbons formed deep within catalyst pores. This type of coke would be more difficult to burn off in the regenerator vs. other sources of coke. It suggests that the amount of HCN formed will depend on the source of the FCC coke, as well as the type of N compound in the feed and operating conditions.

HCN in fractionator overheads. Feed quality and reactor operating conditions influence the amount of N in coke and coke burned and, therefore, the potential for increased HCN. The amount of HCN entrained from the regenerator to the riser depends on the catalyst circulation rate, the gas volume entrained, and the regenerator operating conditions leading to HCN formation.

All these factors will be discussed in more detail by reference to a case study for Refiner A that experienced increased HCN in the catalytic fractionator overhead system following a catalyst technology switch. Improved delta coke enabled a significant increase in heavier feed (as measured by feed concarbon) and catalyst/oil ratio, which resulted in higher HCN, as shown in **FIG. 4.** "CN control" shows data after actions were taken by the refinery to maintain total cyanides below a limit set for the unit.

Feed quality and HCN formation. Typically, 50%–75% of feed concarbon goes to coke and increases the potential for HCN production due to an increase in coke burning.

FCC feed total N typically ranges from 500 ppm–2,000 ppm (basic N comprises approximately one-third of the total). As shown in **FIG. 5,** feed total N correlated with feed concarbon for this unit.

Feed N is distributed throughout the FCC reactor products, with approximately 40%–50% of the N ending up in coke. The distribution depends on the types of N compounds present in the feed and on the operating conditions. For example, concarbon coke may contain more N compounds that can form HCN under regenerator conditions than catalytic coke.

Regenerator operating conditions. Refiner A operates a partial CO burn regenerator. Partial CO burn regenerators typically operate with 4%–7% CO in the flue gas, and lower O_2 concentration in part of the bed would be expected to reduce con-

version of HCN to NO_x. HCN levels tend to be very low when the regenerator is operating in full CO burn; i.e., there is an excess of flue gas O_2, and HCN can be fully oxidized in this mode.

FIG. 6 shows total cyanides in overhead drum water vs. some regenerator operating variables for Refiner A's FCCU. Three data sets are shown:

1. "Other supplier" period represents the baseline when a non BASF catalyst was in use
2. "All" period documents the effects of the change to a low-delta-coke catalyst[a], which allowed Refiner A to expand the envelope of its operations to feed concarbon above the historical maximum of 4 wt%, while increasing the catalyst circulation rate
3. "CN control" period shows how Refiner A was able to mitigate the CN level while maintaining the advantages offered by the low-delta-coke catalyst[a].

Process variables interact on an FCCU, making it sometimes difficult to isolate the effects of one variable. For example, higher feed concarbon tends to increase regenerator bed temperature at constant feed preheat and lead to a reduction in catalytic circulation rate, as shown in FIG. 6. Although higher regenerator bed temperature and lower catalytic circulation rate might be expected to reduce HCN, the percentage of CO in flue gas was the dominating variable for controlling HCN production. **Note:** Wash water rates were maintained within the normal operating range.

This unit has some regenerator design shortcomings due to expanding capacity over the years, emphasized by the high feed concarbon intake with insufficient residence time to complete HCN conversion, inefficient catalyst/air distribution leading to localized regions of O_2 deficiency/low bed temperatures, potential short-circuiting of catalyst high in HCN directly to the outlet, etc. At the same time, these issues highlighted the potential to further optimize the unit design to enable the full concarbon intake offered by the catalyst[a].

Measures to reduce HCN production. Other operational changes that may be considered for reducing HCN are to increase O_2 partial pressure and gas/catalyst residence time by raising regenerator pressure and catalyst bed level. Use of additives to promote the conversion of C to CO_2 is also known to increase NO_x emissions.

Some experimental work indicates that use of a CO promoter will reduce HCN as it is converted to N_2 or NO_x. The CO promoter would be expected to be more effective for reducing HCN in a full CO burn environment.

Changes to the regenerator design can also be considered to reduce HCN by increasing conversion. Some examples are providing more air near the spent catalyst inlet to increase O_2 availability and regenerator bed temperature in this zone where HCN is initially formed, and improving the distribution of catalyst to achieve optimal contacting and minimize localized zones of high CO.

Corrosion control and monitoring for wet H_2S damage. As previously indicated, wash water is commonly injected into the overhead gas streams to reduce cyanide and ammonium levels. In addition, many North American FCCUs processing high-N feeds supplement water washing with ammonium polysulfide (APS) injection, which has enabled satisfactory operation with

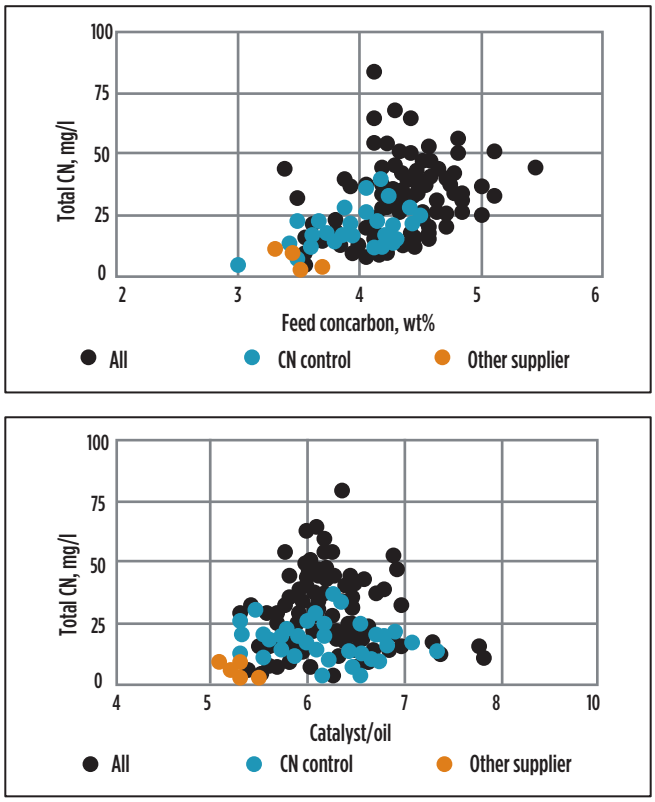

FIG. 4. Processing heavier feed with increased cyanides.

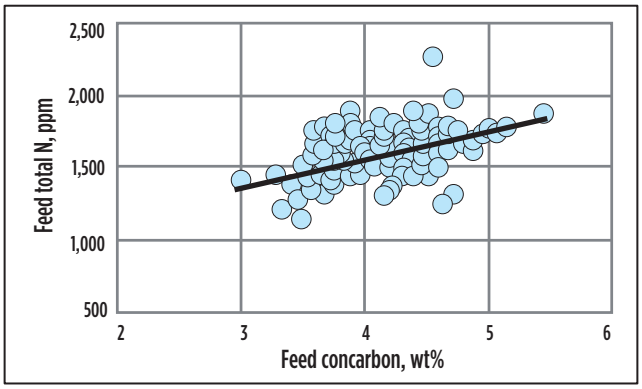

FIG. 5. Feed total N vs. feed.

very high cyanide levels above 100 ppm in water. Some FCCUs also use filming inhibitors for corrosion control.

Various water wash schemes are used. Condensate is commonly injected upstream of the first-and second-stage compressor coolers. Some FCCUs also inject wash water upstream of the catalytic fractionator overhead condensers to supplement condensed reactor steam and water that may be recycled from the overhead drum back to the condensers. To achieve optimal water/gas contacting for maximum HCN removal, it is important to provide suitable water spray nozzles and efficient water distribution systems across multiple exchanger banks (if present).

Cyanides are more soluble in water at higher pressures; therefore, injecting water upstream of the compressor coolers is the best location to maximize HCN removal from gas. It also pro-

motes mixing of the water and gas in the cooler itself. FCC wash water rates are typically in the range of 1 gal/min–2 gal/min of water/1,000 bpd feed (0.034 m^3/m^3 feed–0.068 m^3/m^3 feed) to maintain an acceptable concentration of free cyanides in water. The preferred scheme is to send water collected from the higher-pressure drums directly to the sour water stripper, as sending water back to the catalytic fractionator drum can set up an HCN recycle in the gas due to flashing off at the lower drum pressure.

APS appears to react with the FeS scale to help form iron bisulfide (FeS_2), which is more resistant to complexing with HCN. APS is typically added to the wash water to maintain a low excess ppm level and to ensure that the water samples have an amber color. If the FeS scale no longer provides protection due to high cyanides and insufficient APS dosage, then Prussian blue deposits (indicative of ferrocyanides) are observed in the water samples.

Filming inhibitors minimize the impact of corrosion by providing a thin barrier on surface equipment and reducing the formation of H° atoms through the use of specially designed filming inhibitor chemistries. The filming inhibitor must effectively cover all equipment surfaces by using efficient dispersion systems as for water washing and APS.

Many FCCUs have no history of cyanide-related problems. However, closer monitoring may be warranted if significant changes in feed quality (e.g., higher concarbon/N and/or operating conditions) are observed. Several options for monitoring the likelihood of wet H_2S damage occurring can be considered. Water can be analyzed for total and free cyanides in water and the water color can be checked, as a Prussian blue color would indicate that the HCN has removed some FeS scale. Routine onstream ultrasonic thickness measurement (UTM) from the outside of susceptible equipment can be performed, and H_2 patch probes can be used to detect an increase in H_2 flux through metal walls.

Takeaway. A change to a low delta coke catalyst[a] at Refiner A demonstrated that FCC profitability can be improved by increasing heavier feed processing while expanding the envelope of the operating parameters, even if poorer feed quality gives rise to increased cyanide production and potential risk of wet H_2S damage. A combination of monitoring, cyanide corrosion control and adjustment of operating parameters is available to mitigate the risk, instead of giving up on improved economics, while unveiling the potential for further FCC regenerator design optimizations. HP

NOTE

[a] BASF catalyst

STEFANO RIVA is BASF's Europe/Middle East/Africa (EMEA) Technical Service Manager. He has 30 yr of experience in the refining industry. After graduating in chemical engineering at the Polytechnic University of Milan, he joined ExxonMobil, where he served for 8 yr in the FCC area. In 2002 he joined BASF, where he gained further FCC catalyst experience and now supports customers with FCC optimization and troubleshooting.

STEVE CHALLIS is a UK-based consultant at Chalcat Consulting Ltd. with more than 30 yr of FCC process experience, including unit design, operations optimization, troubleshooting, incident investigation, turnaround and startup support, and engineer/operator training. Mr. Challis worked with ExxonMobil for more than 20 yr as a process specialist. Since 2009, he has acted as an independent FCC Process Consultant. Mr. Challis graduated from the Imperial College of London with an MSc degree in advanced chemical engineering.

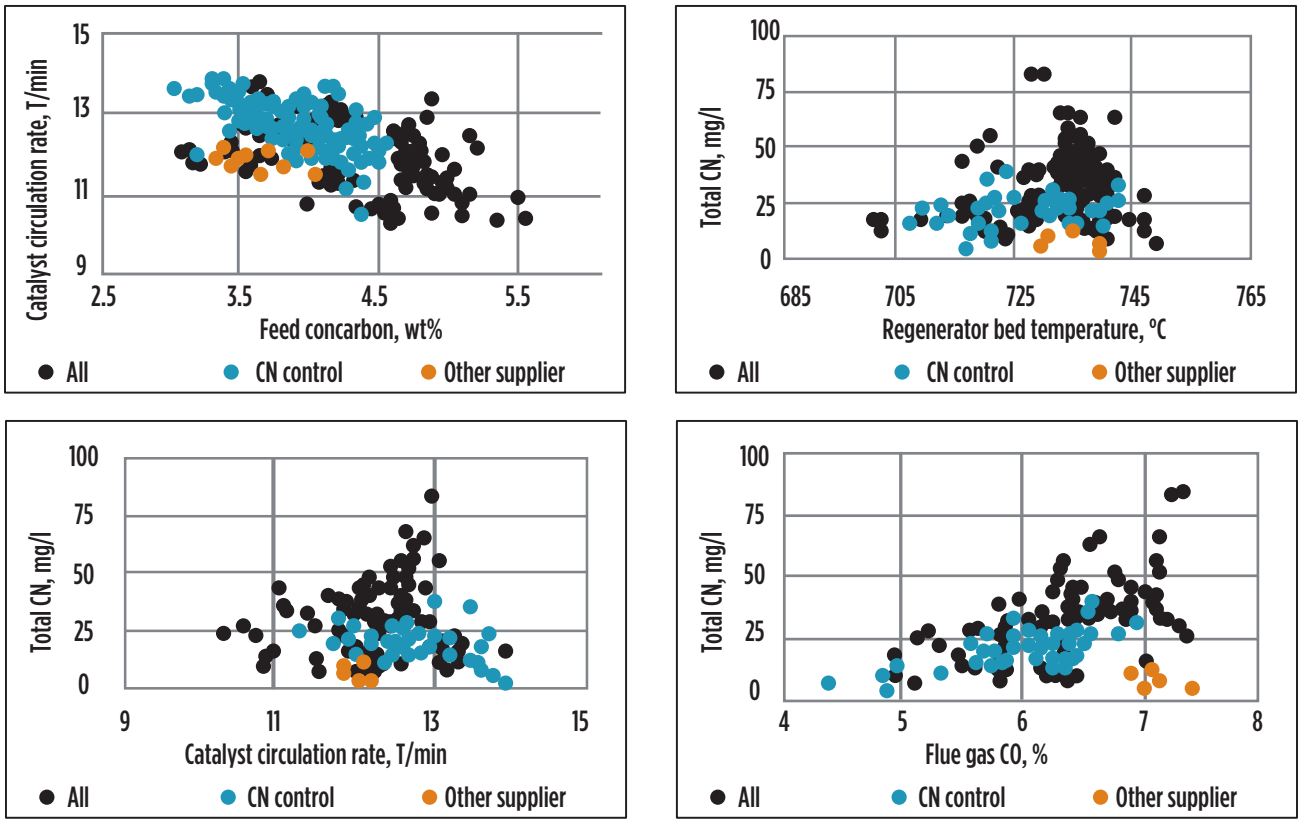

FIG. 6. Regenerator operating parameters.

A. JHA, V. RAVURU, M. YADAV, S. MANDAL and A. K. DAS, Reliance Industries Ltd., Jamnagar, Gujarat, India

A critical analysis of CO_2 capture technologies

The use of fossil fuels as a source of energy continues to add carbon dioxide (CO_2) to the atmosphere, causing detrimental effects to the environment. Scientists around the world are working to reduce the effects of CO_2 emissions, and many research efforts are ongoing at both academic and industrial levels.

Among the available CO_2 capture technologies, solvent-based technologies are commercially proven and practiced in many industries. Despite the commercialization of solvent-based technologies, research on CO_2 capture processes is still vigorously being pursued to significantly minimize capital and operating costs per ton of CO_2 capture, while improving operational reliability.

In the last decade, solid sorbents have been recognized as a very promising technology for CO_2 capture, with the potential to overcome the existing limitations of solvent-based technologies. This article highlights the recent developments in commercial solvent-based technologies and compares their economics with a proprietary hydrated sorbent process[a] for CO_2 capture recently developed by the authors' company.

Contributing to global warming and environmental damage. Rapid industrial growth globally has increased CO_2 emissions from pre-industrial levels of 280 ppm to 407.4 ppm in 2018—up 2.4 ppm since 2017—and is growing rapidly at approximately 1.5 ppm/yr–2.5 ppm/yr.[1] Coal is the second-largest source of primary energy: China, India and the U.S. have accounted for 85% of the net increase in CO_2 emissions. Fossil fuel combustion supplies more than 85% of energy for industrial activities and is the major contributor of CO_2 emissions.[2] Moreover, fossil fuels will remain the major sources of energy for the next several decades.

The process of carbon capture and storage (CCS) has the potential to reduce future world emissions from energy by 20%.[3] According to the Global CCS Institute CO_2RE database, in 2018, 23 large-scale CCS facilities were in operation or under construction, capturing ~40 MMtpy of CO_2.[4] The separation of CO_2 from the source consumes approximately 75% of the total cost of the CCS system, which impacts system implementation.[5] Therefore, it is necessary to employ a cost-effective technology for CO_2 separation from flue gas.

Three main techniques are commercially used for CO_2 capture:

- A post-combustion capture process, which involves CO_2 capture from flue gas after the complete combustion of fuel
- A pre-combustion capture process in which fuel is placed in the furnace by first converting coal into a clean-burning gas and stripping out the CO_2 released by the process
- An oxyfuel process, which burns the coal in the pure oxygen-rich atmosphere, resulting in an exhaust gas with almost pure CO_2.[6]

Among these technologies, the post-combustion capture technique involves a higher cost of capture per ton of CO_2, as it involves the diluted concentration of flue gas (i.e., < 15%).[7] Based on the technological readiness level (TRL), the available post-combustion capture technologies can be classified at various stages of development.

Abanades, *et al.,* reviewed various CO_2 capture technologies in the context of post-combustion capture, including calcium looping, chemical looping, post-combustion capture using adsorbent, solvent and membrane, and concluded that post-combustion capture is the most mature and successful technique for CO_2 capture using solvent.[8] In recent years, the solid sorbent route is garnering the most attention for use in the post-combustion capture process due to its inherent advantage of wider temperature range application from ambient temperature to 700°C, less waste formation during cycling, and the safe disposal of spent solid sorbent without undue environmental precautions.[7]

Published literature on CO_2 capture by the adsorption technique using porous organic frameworks, supported alkali metal carbonate and membranes has shown considerable CO_2 capture capacity. However, the high temperature and resource requirements to regenerate the solid sorbent negatively influences the overall cost and time efficiency of the process.[9]

In this article, the most recent and promising developments in post-combustion capture technologies that are at pilot and commercial scale are reviewed critically. Further, the proprietary hydrated CO_2 sorbent process[a] is discussed and compared, as well as its economic and energy estimates vs. the conventional and hindered amine process.

Post-combustion CO_2 capture technologies. The two major technologies for post-combustion capture are based on solvents and solid sorbents. These two technologies differ, particularly in terms of reaction rate, CO_2 capture capacity, absorption/regeneration temperature, capital cost, corrosivity, mass and heat transfer and stability (thermal, oxidative and chemical, where chemical stability denotes reactivity against the impurities present in the flue gas).[9]

SOLVENT TECHNOLOGIES

The solvent route is based on chemical absorption of CO_2 from the source, such as a coal-fired power plant. The develop-

ment of a CO_2 capture technology depends on parameters that include energy demand, cyclic capacity, solvent stability, reactivity, volatility, environmental sustainability and availability.[10] Solvent-based technologies are categorized based on the solvent used in the CO_2 capture process.

Conventional amine absorption process (CAAP). A conventional amine absorption process applied to the flue gas (10 kPa CO_2–15 kPa CO_2) for CO_2 capture using monoethanolamine (MEA) as a solvent involves absorption at 40°C–45°C and desorption at 115°C–120°C. An aqueous MEA solution (20 wt%–30 wt%) can achieve a high level of CO_2 capture (90% or more) due to the fast kinetics and strong chemical reaction. The typical minimum stripper reboiler duties for CAAP are ~3.6 GJ/metric t–4 GJ/metric t of CO_2 captured.[11,12] In the solvent-based process, gas and liquid streams are contacted in a counter-current fashion. A simplified flow diagram of this process is given in FIG. 1.

One commercial example of a CAAP is Econamine FGSM (EFG), a Fluor proprietary conventional amine-based technology used for large-scale, post-combustion CO_2 capture. The EFG technology is the first and most widely applied process that has extensive proven operating experience in the removal of CO_2 from high-oxygen content flue gases. The Econamine FGSM technology uses a 30 wt% MEA as the absorption solvent, with chemical inhibitors to counter the effects of corrosion caused by oxygen in the flue gas. This process is best operated at low levels of sulfur dioxide (SO_2) (< 10 ppmv) and nitrogen oxide (NO_x) (< 20 ppmv) to avoid excessive solvent degradation.[13]

MEA has good rates of CO_2 mass transfer, is low in cost and readily biodegradable but suffers from moderate rates of oxidative, thermal degradation and moderate levels of toxicity. It is also corrosive when used at higher concentrations and is particularly suited to low-CO_2, partial-pressure applications.[14] The major drawback of such a process is its high energy consumption of 3.6 GJ/metric t–4 GJ/metric t of CO_2 capture and, therefore, high operating cost. The capital cost is also quite high with very tall absorption and desorption towers required for a high percentage of CO_2 capture. Another major difficulty is high solvent degradation in the presence of oxygen in flue gas, as well as an excess corrosion rate demanding high metallurgy for both the absorber and desorber columns.

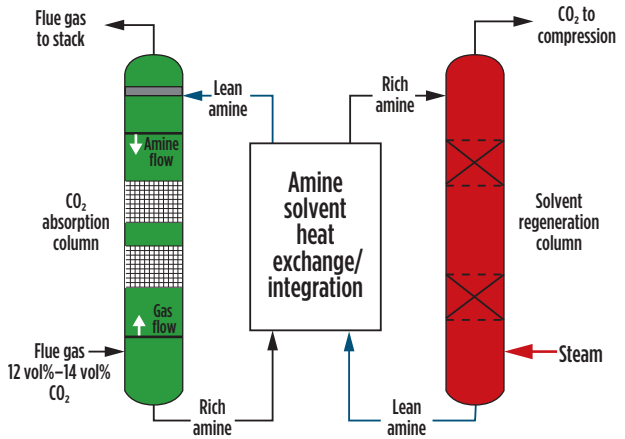

FIG. 1. Schematic of amine-based post-combustion CO_2 capture process.[12]

Hindered amine absorption process. With the potential of large-scale power plant CO_2 mitigation, technology developers—such as Mitsubishi Heavy Industries (KM-CDR process), Linde-BASF (OASE blue process) and Carbon Clean Solution Ltd. (CDRMax™ process)—have begun to optimize chemical absorbing technologies to reduce the overall operating and capital costs of CO_2 capture. The modifications focused are primarily on thermal integration of the CO_2 capture system with the power plant and development of improved solvent formulations with lower stripping steam demand, lower solvent circulation rates than CAAP, and reduced solvent degradation. These process improvements have the potential to reduce the cost and energy intensity of post-combustion CO_2 capture by an estimated 30% compared to a conventional amine route.

Recent commercial solvent technologies for CO_2 capture are based on the use of hindered amine solvent or blends of amines with additives to reduce problems related to equipment corrosion, amine degradation and high energy consumption. Hindered amine solvents are basically derivative of tertiary amine, which has greater absorption capacity but lower CO_2 mass transfer rates than sterically unhindered primary and secondary amines. Blending of hindered amine solvent with additives can help to overcome the mass transfer problem.

MHI's CO_2 capture technology. To overcome the issues of CAAP, Mitsubishi Heavy Industries (MHI) has developed a post-combustion CO_2 capture technology called the KM-CDR™ (Kansai Mitsubishi Carbon Dioxide Recovery) process. It uses KS-1™ solvent, which has low energy consumption, minimal solvent loss and low corrosivity.[15] The KM-CDR process can capture more than 90% of the CO_2 from a flue gas stream and the produced CO_2 is more than 99.9% pure. The use of steam in MHI's KM-CDR technology (0.98 metric t/metric t–1.48 metric t/metric t of CO_2) is lower than CAAP. So far, MHI has commercialized 13 CO_2 capture plants to produce fertilizer, methanol and oil.[16] The world's largest CO_2 capture plant (4,776 metric tpd) on a coal-fired power plant to Petra Nova Parish Holdings LLC was delivered by MHI in 2016. Details of the plant are provided in TABLE 1.

MHI improved its CO_2 capture technology by implementing a new system into the KM-CDR process. Three of the major improvements are:

1. A load adjustment control system that helps maintain smooth operation for the dynamic flue gas changes in the host coal-fired plant. This allows the desired CO_2

TABLE 1. Outline of CO_2 capture plant for EOR project in Texas, U.S.[18]

Item	Description
Gas Source	NRG WA Parish power generation plant, 610-MW (net) coal-fired power generation facility
Process	KM CDR Process™
Absorption liquid	KS-1™ solvent
Plant scale	Corresponding to 240 MW
CO_2 recovery rate	90%
CO_2 capture amount	4,776 metric tpd (1.4 MM metric tpy)
CO_2 concentration	11.5 mol%-wet

recovery ratio, capture amount and steam consumption rate to be maintained, even if the CO_2 concentration in the flue gas changes significantly.
2. An improved amine emissions reduction system that reduces the loss of solvent. The improved system reduces amine emissions by more than 90% compared to the conventional system.
3. The recently improved energy saving system improves energy efficiency by reducing steam consumption by 5%.

However, such hindered amine-based processes are generally very sensitive to SO_2 and (in particular) sulfur trioxide (SO_3) impurities; therefore, they require additional, deeper desulfurization of the flue gas—implying increased CAPEX compared to the CAAP route.

OASE Blue Technology for CO_2 capture. Linde and BASF Group are jointly developing a post-combustion capture technology using BASF's novel amine blended solvent comprising aqueous solutions of the tertiary amine methyl diethanolamine (MDEA) and 10 wt% of additive cyclic diamine (piperazine).[17] This technology offers significant benefits for CO_2 capture as it saves 20% on energy input over CAAP and has superior oxygen stability, significantly reducing solvent consumption. This collaboration completed a pilot-sale demonstration at the National Carbon Capture Center (NCCC) on a coal-fired power plant flue gas in 2014, and final commissioning was completed in January 2015. The design capacity of the operation was 1 MWe–1.5 MWe and it requires less regeneration energy (2.8 GJ/metric t of CO_2) than the conventional amine process at regenerator pressure of 3.4 bar absolute. The pilot plant captures up to 30 tpd of CO_2 at more than 90% capture rate, and CO_2 purity was > 99.9%. BASF and The Linde Group's Engineering Division have agreed to further develop the process with demonstrations at other facilities.

Carbon Clean Solution Ltd. (CCSL) technology for CO_2 capture. CCSL has developed a process, CDRMax™, that operates at near atmospheric pressure, enabling 95% CO_2 recovery and > 99% purity that can be used to produce fuels and chemicals.[18] The salient features of the technology are:

- Reduction in energy consumption of 27%
- Loss of amine solvent reduced by eight times
- Reduction in equipment corrosion by seven times
- Reduction in amine emissions by five times.

CCSL can capture CO_2 at the cost of $30/metric t, while other available technologies achieve $45/metric t–$60/metric t. The company's first plant, with a capacity of 60,000 metric tpy, came online in 2016 in partnership with Tuticorin Alkali Chemicals and Fertilizers in India; the plant converts recovered CO_2 from its coal-fired boiler into soda ash. The technology uses a solvent called amine promoted buffer salt (APBS), which causes less corrosion. The APBS is a mixture of hindered amine (2-amino-2-methyl-1, 3-propandiol), potassium salt of amino carboxylic acid or amino sulfonic acids and about 75 wt% of water. The CCSL solvent has significantly higher CO_2 loading

capacity compared to the commercially used solvents MDEA and dimethyl ether of polyethylene glycol (DEPG). Heat of reaction for the CCSL solvent is 39.2 kJ/mol CO_2, which is 20% lower than that of MDEA (48.9 kJ/mol CO_2). This solvent can handle 80 times more CO_2 than other amine-based solvents. The absorption temperature of the CDRMax™ process is between 50°C–70°C and the stripper temperature is at 80°C–120°C. CCSL claims 40% lower OPEX and 30% lower CAPEX than a conventional CO_2 capture technology.

Drawbacks of solvent-based technologies. Solvent-based technologies have the inherent advantage of being ''end-of-pipe'' technologies, like existing technologies for the mitigation of sulfur oxide (SO_x), NO_x and hydrogen sulfide (H_2S) emissions. Moreover, their addition to power plants, either as a retrofit or as new build, will not unduly affect the flexibility of operations demanded of these facilities.[3] However, solvent-based technologies have major disadvantages, including:

- Large equipment size
- Large volumes of solvents required
- Amine-based solvents are corrosive in nature
- Susceptible to degradation, even by trace amounts of flue gas impurities (particularly SO_x and O_2)
- Produces toxic byproducts on heating
- Emissions of solvents from recovery columns must be scrubbed and eliminated
- High amount of steam requirement
- Disposal of expired solvents is problematic
- Energy and CAPEX-intensive process.

Shortcomings in existing solvent-based technologies have driven research to develop solid adsorbent-based technologies for CO_2 capture. Adsorption processes using solid regenerable sorbents capable of capturing CO_2 from flue gas streams have many potential advantages compared to conventional amine-based absorption process, such as reduced energy for regeneration, greater adsorption capacity, selectivity and ease of handling.

Solid sorbent technology. The CO_2 capture process was also studied over various solid sorbents, such as zeolites 13X, metal organic framework (MOF), activated carbon, supported alkali metal carbonate, etc. Among these sorbents, supported alkali metal carbonate are widely studied as a capture media for CO_2 from a diluted gas stream using a thermal swing adsorption process.[19] Alkali metal carbonate can capture CO_2 within the temperature range of 50°C–100°C, with regeneration at 120°C–200°C, which makes it a potential sorbent to capture CO_2 from coal-fired power plants with wet flue gas desulfurization (FGD). The main drawbacks of alkali metal carbonate sorbents are the requirement of higher regeneration temperature and handling of solid phase.[7]

The developed proprietary hydrated sorbent process[a] for CO_2 capture (HSC) provides the desired characteristics required for the commercial plant. The developed sorbent shows high adsorption capacity, fast adsorption/desorption kinetics and multi-cycle stability. The process utilizes potassium carbonate supported on solid support as a sorbent. The salient features of the solid sorbents are:

- Higher surface area (35 m^2/g) and pore volume (0.15 cm^3/g) despite high loading of active species

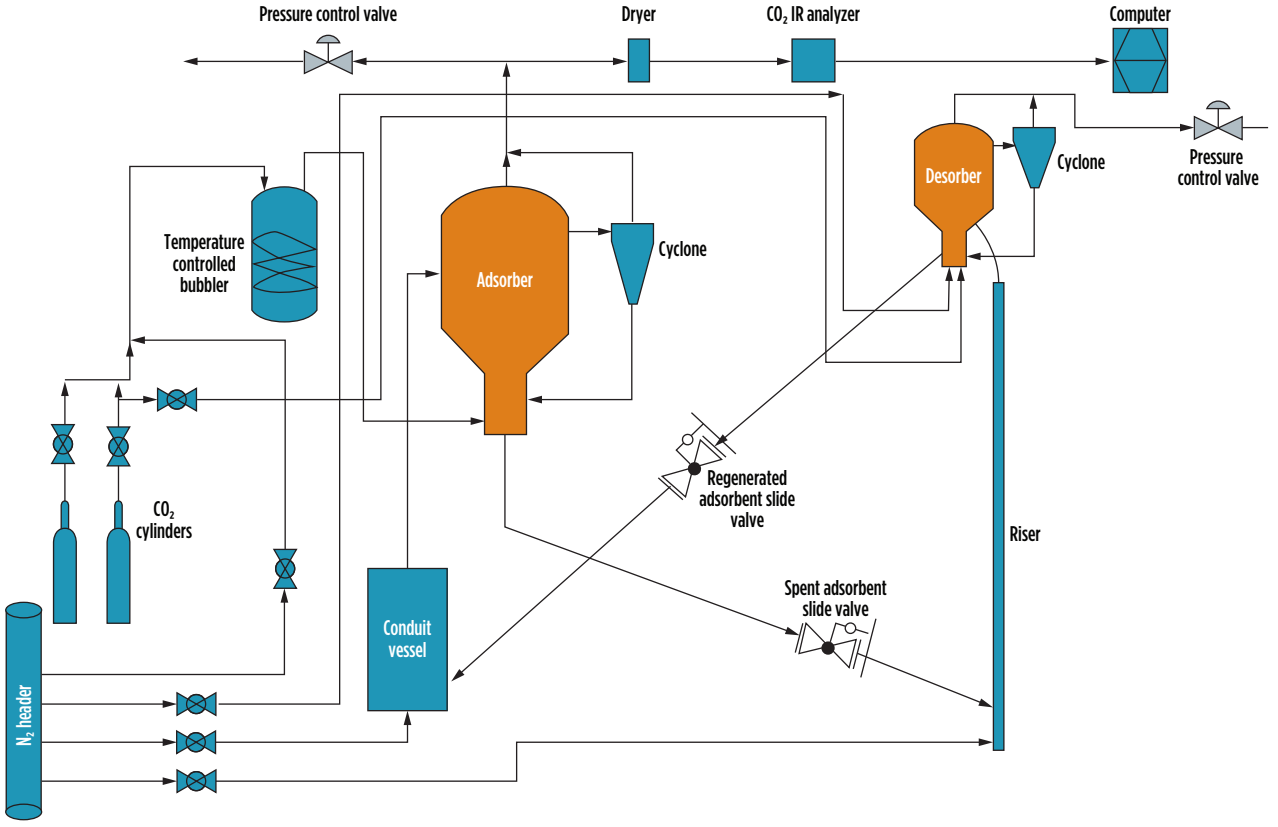

FIG. 2. Schematic view of the pilot plant used for the proprietary CO_2 capture process.

- Higher adsorption capacity (3.2 mmol/g)
- Multi-cycle stability
- Lower regeneration temperature (120°C–130°C)
- Stability with flue gas impurities (SO_x, NO_x, O_2, etc.)
- Minimal reliability issues.

The hydrated sorbent process follows carbonate-bicarbonate chemistry according to the following reaction schemes:

Pre-treatment: $K_2CO_3 + 1.5H_2O \rightarrow K_2CO_3.\ 1.5H_2O$
$\Delta H = -40$ kJ/mol

Adsorption: $K_2CO_3.\ 1.5H_2O + CO_2 \leftrightarrow 2KHCO_3 + 0.5H_2O$
$\Delta H = -101$ kJ/mol

Partial regeneration: $2KHCO_3 + 0.5H_2O \leftrightarrow K_2CO_3.\ 1.5H_2O + CO_2$
$\Delta H = 40$ kJ/mol

Full regeneration: $2KHCO_3 \leftrightarrow K_2CO_3 + CO_2 + H_2O$
$\Delta H = 141$ kJ/mol

The supported alkali carbonate sorbents in the presence of H_2O form hydrated species, which in turn can capture CO_2 to form bicarbonate species at temperatures 70°C–90°C. By performing a moderate temperature swing of 120°C–130°C, the bicarbonate decomposes and releases a CO_2/H_2O mixture that can be converted into a "sequestration-ready" CO_2 stream by steam condensation.

Unlike amine-based absorption, there is no heat demand for vaporization of water or corrosion/solvent degradation issues. The important feature of the proprietary process is the ability of the sorbent to adsorb at higher temperatures of 70°C–90°C, and regenerate at 120°C–130°C; therefore, the temperature difference between adsorption and regeneration is only 40°C–50°C, which is suitably utilized for the heat pump to further minimize heat demand.

The lower temperature differential between adsorption and regeneration is helpful in an effective temperature approach for heating and cooling of adsorbent in addition to its thermal stability. The proprietary hydrated sorbent process can be used for:

- Natural gas-fired power plant flue gas with nominal make-up quantity (0.5 kg/metric t of CO_2)
- Coal-fired power plant flue gas incorporating wet FGD (for SO_x levels < 20 ppm).

Conversely, NO_x tolerance for the proprietary sorbent[a] is expected to be much better than amine systems due to its inertness towards NO_x. It is important to note that there is no concern for oxygen presence in the flue gas for this technology, unlike a conventional amine system.

The innovations in sorbent and process were instrumental in achieving minimum OPEX in the HSC process. The overall heat demand in the HSC process is significantly lowered by partial regeneration of sorbent in accordance with hydration chemistry, as discussed here. As a result, a significant reduction is seen in regeneration heat demand from 141 kJ/mol CO_2 (non-hydrated) to 70 kJ/mol CO_2 (hydrated). In addition to no heat loss due to water evaporation in the solid sorbent, this results in an overall 60%–70% lower energy demand per ton of CO_2 capture vs. a conventional amine process for rich and lean concentrations of

CO_2 in flue gas from a coal-fired power plant/FCC flue gas and natural gas-fired power plant, respectively.

Unlike in a conventional amine absorption system—where it is not possible to minimize energy demand beyond a point since the heat loss due to evaporation of water is unavoidable—the proprietary hydrated sorbent process for CO_2 capture works on the principle of circulating fluidized bed reactors with solid hydrated sorbent circulating between the adsorber and regenerator, as shown in FIG. 2.

Furthermore, the closer ΔT between adsorption and desorption allows the heat pump concept to extract and utilize low-temperature (120°C–180°C) streams available in a refinery or power plant. This reduces the energy consumption close to 80%–90% of CAAP, when heat integration is done with a low-temperature (120°C–180°C) process stream in a refinery and power plant.

A recent circulating fluidized bed pilot plant study with high-capacity HSC sorbent has demonstrated 93% CO_2 removal on a continuous basis at steady state. The sorbent has also shown excellent stability. The high-capacity HSC sorbent has shown 3.2 mmol/g of CO_2 capture capacity, which is one of the highest values among published research, including all amines and solid sorbents.

The circulating fluidized bed in the HSC process exhibits a very good heat transfer rate, as in the case of a liquid amine system. The sorbent is thermally stable, attrition resistant, non-corrosive, non-sticky/free-flowing in the operating regime and demonstrates excellent heat transfer and fluidization properties of Geldart-A particles. The comparison of key parameters for the proprietary process vs. a conventional amine process for rich flue gas case is summarized in TABLE 2.

TABLE 2 clearly shows the advantage of the hydrated sorbent process[a] for CO_2 capture over solvent-based commercial technologies. The net energy demand for per mol of CO_2 capture in the hydrated sorbent process is ~ 40% of the conventional amine process and less than the hindered amine process. The hydrated sorbent process creates significant savings in per metric t cost of a CO_2 capture plant by driving down the operating and capital costs by 70% and 40%, respectively, over the CAAP route.

Takeaway. Solvent-based technologies based on hindered amine have shown potential progress to develop CO_2 capture technology and reduce CAPEX and OPEX by process heat integration, use of amine blend solvent and additive, etc. However, recent developments in hydrated solid sorbent have shown potential to substitute a solvent-based technology for CO_2 capture. Unlike gas-liquid contacting for amine—where the absorber vessels' heights are very large and tall to satisfy the flooding and mass transfer requirement—the circulating bed system used for CO_2 capture is very compact in height and can provide much higher capacity in a single unit compared to an amine absorption system.

The overall operating cost of the proprietary process is 70% lower, whereas the CAPEX cost is 40% lower than a conventional amine process (due to the vessel size with no exotic metallurgy, unlike amine). The hydrated sorbent process is well demonstrated for continuous sorbent circulating mode in a pilot plant with 35 kg inventory. The effects of various parameters were studied and resulted in CO_2 removal efficiency of > 90% and purity above 99%. The pilot trial provided definite indications towards the efficacy and scalability of the hydrated sorbent process for capturing CO_2 from stationary point sources in a power plant, refinery or petrochemicals facility. HP

ACKNOWLEDGEMENTS

The authors thank Reliance Industries Ltd. (RIL) for its cooperation in executing all the experiments discussed here.

NOTES

[a] Reliance Industries Ltd.'s KM-CDR™ (Kansai Mitsubishi Carbon Dioxide Recovery) process.

LITERATURE CITED

[1] International Energy Agency (EIA), "Global energy and CO_2 status report 2018," March 2018.
[2] Oschatz, M. and M. Antonietti, "A search for selectivity to enable CO_2 capture with porous adsorbents," *Energy & Environmental Science,* Iss. 1, 2018.
[3] Haszeldine, R. S., "Carbon capture and storage: How green can black be?" *Science,* September 2009.
[4] *Carbon Capture Journal,* Iss. 67, January/February 2019.
[5] Nie, L., Y. Mu, J. Jin, J. Chen and J. Mi, "Recent developments and consideration issues in solid adsorbents for CO_2 capture from flue gas," *Chinese Journal of Chemical Engineering,* Vol. 26, Iss. 11, November 2018.
[6] MacDowell, N., N. Florin, A. Buchard, J. Hallett, A. Galindo, G. Jackson, C. S. Adjiman, C. K. Williams, N. Shah and P. Fennell, "An overview of CO_2 capture technologies," *Energy & Environmental Science,* Iss. 11, 2010.
[7] Wang, J., L. Huang, R. Yang, Z. Zhang, J. Wu, Y. Gao, Q. Wang, D. O'Hare and Z. Zhong, "Recent advances in solid sorbents for CO_2 capture and new development trends," *Energy & Environmental Science,* Iss. 11, 2014.
[8] Abanades, J. C., B. Arias, A. Lyngfelt, T. Mattisson, D. E. Wiley and H. Li, "Emerging CO_2 capture systems," *International Journal of Greenhouse Gas Control, 2015.*
[9] Amte, V., A. K. Das, S. Sengupta, M. Yadav, S. Mandal, A. Pal, A. Gupta, R. Bhujade, S. R. Akuri and R. Dongara, "Single compression system and process for capturing carbon dioxide," Patent #: US10166502B2.
[10] Bhattacharyya, D. and D. C. Miller, "Post-combustion CO_2 capture technolo-

TABLE 2. Performance comparison between the proprietary hydrated sorbent process[a] with other capture technologies

Key parameters	CAAP	Hindered amine process	Proprietary HSC process[a]
Solvent/Sorbent	MEA	Sterically hindered amne + promoter	K_2CO_3 solid support
Absorption/Regeneration temp, °C	35–40/110	35–45/110	70–90/120–130
Reaction enthalpy, kJ/mol	72	58	60
Net energy demand, kJ/mol CO_2	198	97–141	87
Steam (@ 3 bar) required, t/t CO_2	2.1	0.98–1.48	0–0.7
Electricity, k Wh/t CO_2	70	110	85
Cooling water, ton/ton CO_2	70–105	160–175	40–55
Oxidative degradation (mg/Nm^3)	100	0.2–1.5	stable
OPEX, $/t-$CO_2$	Base	–	0.3 of base

gies—a review of processes for solvent-based and sorbent-based CO_2 capture," *Current Opinion in Chemical Engineering*, Vol. 17, August 2017.
[11] Creamer, A. E. and B. Gao, "Carbon-based adsorbents for post-combustion CO_2 capture: A critical review," *Environmental Science & Technology,* June 2016.
[12] U.S. Department of Energy (DOE)/NETL Carbon capture program, "Carbon dioxide capture handbook," August 2015.
[13] Reddy, S., J. Yonkoski, H. Rode, R. Irons and W. Albrecht, "Fluor's Econamine FG Plus℠ completes test program at Uniper's Wilhelmshaven coal power plant" *Energy Procedia,* Vol. 114, July 2017.
[14] Wang, M., A. S. Joel, C. Ramshaw, D. Eimer and N. M. Musa, "Process intensification for post-combustion CO_2 capture with chemical absorption: A critical review," *Applied Energy,* Vol. 158, November 2015.
[15] Hirata, T., H. Nagayasu, T. Yonekawa, M. Inui, T. Kamijo, Y. Kubota, T. Tsujiuchi, D. Shimada, T. Wall and J. Thomas, "Current status of MHI CO_2 capture plant technology, 500-tpd CCS demonstration of test results and reliable technologies applied to coal fired flue gas," *Energy Procedia,* December 2014.
[16] Hirata, T., S. Kishimoto, M. Inui, T. Tsujiuchi, D. Shimada and S. Kawasaki, "MHI's commercial experiences with CO_2 capture and recent R&D activities," *Mitsubishi Heavy Industries Technical Review,* Vol. 55, March 2018.
[17] Online: https://www.basf.com/global/en/media/news-releases/2016/07/p-IR-160719.html
[18] Patkar, A. and P. Bumb, "Carbon capture technology for flue gas applications," CMTC conference, Houston, Texas, July 17–20, 2017.
[19] Sengupta, S., V. Amte, R. Dongara, A. K. Das, H. Bhunia and P. K. Bajpai, "Effects of the adsorbent preparation method for CO_2 capture from flue gas using K_2CO_3/Al_2O_3 adsorbents," *Energy Fuels,* December 2014.

AJAY JHA completed a PhD in chemical science from CSIR-National Chemical Laboratory, Pune, India, followed by a postdoctoral from Yonsei University, South Korea. Dr. Jha serves as a Senior Research Scientist in the refining R&D division of Reliance Industries Ltd. in Jamnagar, India. His current research focuses on the development of sustainable processes for CO_2 capture and utilization (CCU).

VENKAT RAVURU is a Research Scientist in the refining R&D division of Reliance Industries Ltd. in Jamnagar, India. He earned a PhD in chemical engineering from the Indian Institute of Technology (IIT) Bombay. Dr. Ravuru's experience includes modeling and simulation of chemical processes, development of multi-scale models, kinetic models and parameter predictions.

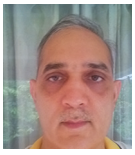

MANOJ YADAV is an Assistant VP, working in fluidized catalytic cracking process engineering at the refining R&D division of Reliance Industries Ltd. in Jamnagar, India. He holds an MTech degree in chemical engineering from IIT Delhi and a BS degree in chemical engineering from Punjab University, Chandigarh. Mr. Yadav's experience includes process optimization and troubleshooting in various refinery processes, process development in separation and fluidized catalytic cracking.

SUKUMAR MANDAL is a Vice President and leads the FCC, coker and gasification research groups in the refining R&D division of Reliance Industries Ltd. in Jamnagar, India. He has 29 yr of research experience in refining processes and petrochemicals with several patents and publications to his credit. Mr. Mandal holds degrees in chemical engineering (MTech) from IIT, Kanpur.

ASIT K. DAS is the Head of Refinery R&D and Process Development of Reliance Industries Ltd. in Jamnagar, India. He has more than 33 yr of research experience in refining and petrochemical segments. He has developed and commercialized many processes and has more than 80 patents, 70 publications and five book chapters to his credit. He has guided several PhD and MTech theses and board members in advisory council for several academic institutions. He is also the current President of the Engineering Science section to organize the Indian Science Congress 2020.

A. YAMAGUCHI and Y. IKEGAYA,
Yokogawa, Tokyo, Japan

Process control reimagined

Imagine visiting the control room of a typical process unit at a refinery. Everything is running well under the watchful eyes of experienced operators. Looking at the unit's final output flow, you ask a simple question: "Why are you operating at this production rate?"

A variety of answers can exist, with perhaps as many thoughts as the number of individuals working the unit. Possibilities could include something about maximizing output, product quality or overall efficiency.

However, a better answer and one that is likely to become more common is: This is exactly where we need to be to fulfill corporate goals, including profitability, while matching demand for our output. This more-complete answer has two parts that will need to be detailed individually.

First, fulfillment of corporate goals can include many factors. Profitability is always one of them, but it is part of a complex picture. There can be additional aspects relating to efficiency, emissions, feedstock utilization, carbon footprint and other considerations. Whatever the case, the company will have specific goals and expect operators to be aware of these directives. If markets are favorable and the company is sold out due to high customer demand for a particular product, the direction may simply call for maximizing production.

Second, matching output to demand may also be a complex picture if the product is an intermediate planned for use in another process unit. If the output of Unit A becomes a feedstock for Unit B and is sent there directly, the volumes need to match. Both units are under corporate direction and they must work together to achieve mutual goals without creating a surplus or starving the second unit. Things get even more complicated when multiple units are involved. More on this point later.

All these possible scenarios exist in the real world of process manufacturing (FIG. 1), which means companies and operators must deal with variability of raw materials and feedstocks, tighter and more complex regulations, and changing markets. Maintaining a stable and profitable operation is a major challenge for these and other reasons.

Despite these challenges, there are also new software tools and control techniques to help address these and other issues by optimizing production based on any one of several desired outcomes.

Digital transformation supports production optimization. How do these new tools and techniques work, and why are they better than traditional regulatory control? First, corporate and plant managers must determine their most critical objectives. The obvious answer is usually maximum output, but this is not necessarily always at the top of the list. Other factors may be more important, such as a specified output below maximum.

If another element is critical, such as carbon footprint, product purity or overall efficiency, the ultimate variable might not be measured in real time by any single type of instrument. This presents a particularly complex situation, as illustrated by the four phases in FIG. 2. These phases need additional explanation.

If there is no instrument measuring the critical variable in real time (Phase 1 on the left side of FIG. 2), unit operators must make their best guess and then adjust setpoints based on analysis after the fact. If the attribute is a product characteristic, it may depend on data from lab analysis. If it is something like plant efficiency, it may be necessary to wait for operational reports to be generated. In any case, achieving the goal is often

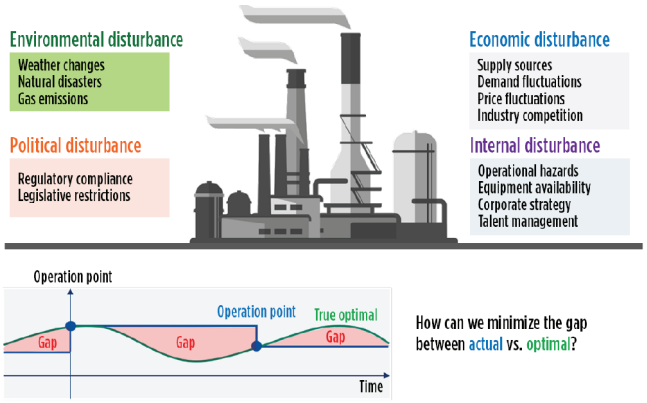

FIG. 1. In addition to feedstock variabilty, there are many possible sources for disturbances in processing plants.

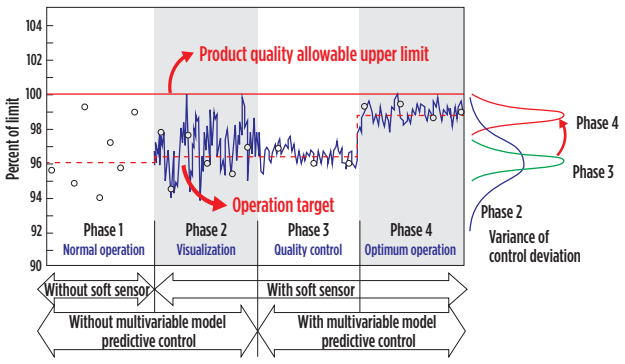

FIG. 2. This diagram illustrates four phases of improving production control by adding new approaches.

hit-or-miss. This can be tolerable if the results are generated quickly, but there is always a time lag.

Improvements can be provided by creating a software sensor. With sophisticated analysis of the process from historical data (Phase 2), it is possible to build a picture of what the process looks like when it is operating. This provides ranges for the variables that are possible to measure through conventional instrumentation. By applying the soft sensor, all those critical variables can be monitored as a continuous value like temperature, flowrate and pressure, helping to determine if the process is running as it should. This provides a better handle on what the process is doing, but frequently leaves it running with too wide a deviation from the target.

The next level of sophistication is applying multivariable model predictive control (MMPC). With this approach (Phase 3), the controller has a model capable of expressing dynamic characteristics of the process. Control is now based on prediction by the model, which can make operation far more stable than is possible with regulatory control built on multiple proportional, integral and derivative (PID) loops. Variability common to the previous control approach can be tightened up, keeping the critical attribute within a much narrower range. The result is operation closer to the desired goal, regardless of its nature.

It is now possible to determine exactly where to place the operating level, whether it is closer to an upper limit (Phase 4) or somewhere else dictated by big-picture corporate objectives.

Capabilities of a digital twin. The kind of analysis used to build a software sensor can be extended to support a digital twin, which provides a simulation designed to respond to changes in the same way as the actual plant. If a setpoint is changed, the digital twin responds in a similar manner to the actual process plant.

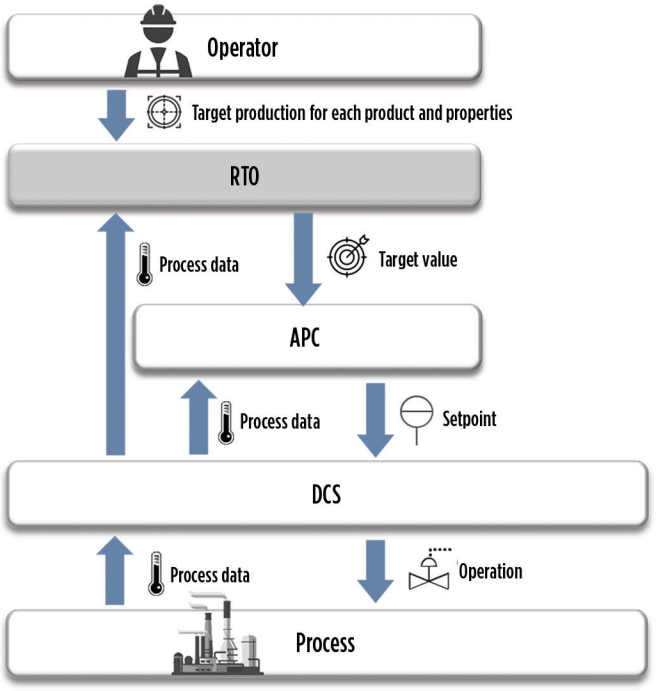

FIG. 3. New platforms placed on top of the DCS use improved control methodologies as compared to conventional regulatory practices.

This allows operators to test setpoint changes and other process adjustments to determine if they will have the desired effect.

This capability is especially valuable since parameters change, which can make achieving optimal operation a moving target. For example, the crude oil coming into a crude distillation unit could easily be from a different source than the crude running yesterday. Will the new crude allow the same draw rates of desired products today as yesterday?

Rather than experimenting with the actual distillation tower, operators can program the digital twin with the new crude attributes and let the simulation do its analysis. Likely, the analysis will call for setpoint and constraint adjustments to achieve the desired product distribution. These adjustments can be implemented automatically, or they can be provided as advice to operators.

Assembling the pieces. The parts just described can be combined so they build on each other, so it soon becomes possible to implement a largely self-functioning process control mechanism able to move into a new level of total plant productivity with real-time optimization (RTO). This type of mechanism uses an advanced process control (APC) technique, such as MMPC, to help analyze all the trade-offs that occur when making individual unit optimizations. Simulation can be used to find optimum operating points for multiple process units by using current process data.

Greater detail is needed on how these elements interact (**FIG. 3**). At the top are the operators, but this level goes beyond the control room as it involves corporate management and company-wide production scheduling as much as the individuals in vests and hardhats.

People in the control room now understand how their efforts fit into the bigger picture and exactly what is expected of the specific unit and overall facility. Their tasks are simplified because the control systems can automatically implement all the constant tweaking and loop adjustments connected with traditional regulatory control.

At the bottom of the diagram is the process itself, still controlled by the distributed control system (DCS). This remains as it always has been because it is still the mechanism that collects data from instrumentation and sends instructions to actuators. With traditional systems, the DCS would be controlled by the operators directly, but now the APC system monitors the DCS and supplements the efforts of operators. Setpoints in the DCS can now be tweaked, as needed, automatically to maintain target values.

The APC system is under the control of the RTO system, which is programmed with economic targets. In a perfect world where nothing changes, this would be enough, but nothing is perfect. As mentioned earlier, feedstocks change, and with something as complex as crude oil, the variability can be subtle or drastic.

This is where the digital twin comes into play. It functions as a steady-state simulator representing the actual process. The simulator has a library of information on specialized feedstock characteristics, so it can determine exactly how the optimizer must adjust the process to accommodate changes in feedstock characteristics. This avoids any trial-and-error hunting for setpoints. The process remains stable and within desired operational parameters, even with these types of changes, as well as others.

Changes are not only connected with feedstocks. Fuels and chemical additives can affect the process, as well. For example, fired heaters may change to a different grade of fuel oil to take advantage of a price break, resulting in a change of Btu content. This could affect both the fuel consumption rate and emissions.

For this kind of system to operate reliably, there must be a constant flow of data and information in all directions. In some areas, such as between the process and the DCS, updates happen every second or even faster. For APC, it may be once per minute. For RTO, it may be once per couple of hours. The key is to ensure information exchange is suitable to support this environment of more advanced decision making, where the process effectively runs itself automatically. The need for constant human monitoring and tweaking is eliminated, leaving operators to handle higher value-added responsibilities.

Extending across multiple units. Sometimes, the optimizer really needs to control multiple units when they are working in concert (e.g., when producing intermediates that get sent from one unit to another). The ultimate final product has its practical limits for production or under market constraints, so it must be the starting point. From there, it is necessary to move up the stream, back to where the other units are creating their output. Optimization for one unit now reflects the amount needed for the next, but it is still important to maximize profitability at each unit.

The same concepts apply as with a single unit, but the local RTO gets its orders from higher up the chain of command based on demand.

Technologies together. The authors' company is innovating RTO strategies designed to work in cooperation with digital twin technology. These advances are now possible thanks to expanding digital capabilities and are capable of increasing profits by improving all operational elements of a unit, plant and a company. This is achieved through visualization and simulation in ways that are only now possible.

Therefore, companies can achieve seamless optimized production through the combination of simulation technology and control technology, reflecting the plant model in the production plan. By repeating this cycle across all units and locations, total plant productivity can be increased throughout all plant lifecycles. HP

AKIO YAMAGUCHI manages the APC and Optimization business and portfolio at Yokogawa. He has 11 yr of comprehensive experience in APC engineering, as well as an additional 10 yr of professional experience in software development, programming and project management. He leads the development of APC and Optimization business to achieve Yokogawa's Industry Automation to Industry Autonomy (IA2IA) vision.

YOSHIHIRO IKEGAYA is the Product Manager for APC products at Yokogawa. He has developed Yokogawa's APC products for 15 yr, as well as an additional 6 y of product planning, marketing and technical support.

A. RIVERO, Rajant Corp., Houston, Texas

Taking on petrochemical plant hurdles with networking smarts

The petrochemical industry is facing one of the most significant challenges in its history. The COVID-19 pandemic has shrunk demand for a variety of end products that rely on petrochemicals, polymers and specialty polymers. The petrochemicals market has witnessed instability in pricing for naphtha, ethylene and heavy paralysis oil, among others. These factors combined are byproducts of the fact that our usual energy-consuming activities have been halted. The situation is hitting the industry hard as fewer vehicles take to the road.

The volatility in the chemicals space has triggered a chain of events in the energy markets that will inevitably impact the industry for years to come. As a competitive industry in standard times, the pressure on companies to economize has been made even more significant.

To remain competitive and profitable in a time of economic uncertainty, one way for petrochemical operations to prosper is by embracing new and innovative technologies to improve safety and optimize production at their plants. For these advanced applications to realize their full potential, they need full Industrial Internet of Things (IIoT) connectivity in petrochemical plants. To interact with and manage this network, companies need a network infrastructure that is fully mobile and provides optimal broadband connectivity across the entire organization. Reliance on IIoT and machine-to-machine (M2M) connectivity to improve productivity, streamline operations and control costs have created a demand for private wireless mesh networks.

Embracing Industry 4.0. Embracing Industry 4.0 and IIoT are some of the elements to future proof your environment. Industry 4.0 is the move from traditional manufacturing and industrial practices in combination with the latest smart technology. This evolution represents a step towards higher productivity. However, deploying a network to support the levels of connectivity required in a dynamic and potentially hazardous environment can be extremely difficult. Ensuring an equilibrium between facility and production growth with employee safety standards is imperative.

Many petrochemical plants operate multiple networks to accomplish separate communication needs for their employees. This often outweighs the burden of maintaining a WiFi network for data and a two-way radio WAN for voice, which can generate high costs and can be a notable drain on resource demands for daily operations.

The explosive and flammable gases—such as ethylene, propylene, butadiene and other potential vapors—found in petrochemical plants make maintaining safety in danger zones a top priority. This process is even more complicated. To prevent equipment from sparking and starting a fire, networking infrastructure must be kept in an explosion-proof enclosure (e.g., ATEX 1, ATEX-2/C1D1 and C1D2 requirements).

From the initial deployment to complex day-to-day plant operations, constant connectivity is required for the mission-critical operations carried out in petrochemical plants. Signal loss often equates to productivity loss and—in a worst-case scenario—can put plant workers' safety at risk. With petrochemical plants undergoing significant expansion, choosing the wrong industrial network solution could mean a plant's investment is wasted due to an unsuitable solution for connecting its operations.

A new way to enable petrochemical prosperity. A new type of networking is necessary for petrochemical plants to embrace Industry 4.0. An IIoT-enabling network, more dynamic than WiFi networks or two-way radio WAN, can provide the petrochemical industry the prerogative to take advantage of the innovative technologies that can maximize productivity, improve safety and help organizations survive amid increased petrochemical competition.

A solution for petrochemical plants is to implement a mesh network topology—a resilient architecture constructed of nodes that allows a multitude of devices to connect wirelessly. The result is a node network that can communicate data across the network until it reaches its target destination. Interest in this technology is peaking due to its capability to handle the wave of data expected because of the proliferation of IIoT-connected devices. A mesh network can provide real-time, site-wide communications for the varying personnel and assets crucial to the running of a petrochemical plant, including video cameras, smart meters, sensors, laptops and smartphones.

However, some mesh networks can be too complex or unfeasible to install. Some need continuous, labor-intensive maintenance. Plants need mobile wireless broadband connectivity that can meet their demands and is simple, instantaneous and robust in any application—a kind of autonomous network.

Critical connectivity. Critical connectivity is possible through a combination of wireless network nodes and networking software that utilizes any-node to any-node capabilities. This type of network can continuously route data via the best available traffic path and frequency for several nodes with extremely low overhead. More advanced mesh networks can connect with any WiFi or Ethernet-connected device to deliver low-latency,

high-throughput data, voice and video applications.

An effective mesh network can reduce the total cost of ownership and simplify the work demands of employees by allowing them to centralize their communications to a single device. This is because, as a secure and converged solution for plants, the right mesh network can reduce the need to maintain multiple networks by supporting data, voice and video. Furthermore, depending on the mesh network provider, certain nodes can be deployed in any corner of a petrochemical plant without the need for mounting in explosion boxes.

Wireless network nodes can be attached to both fixed and mobile assets, including equipment, vehicles and facility infrastructure. They can maintain multiple immediate connections between peers while sending and receiving data on multiple frequency bands. They need never break connections to form new ones, meaning the connections are maintained until they are no longer required. With high-bandwidth speeds across multiple mesh node hops, a mesh network offers extremely low-latency for real-time, plant-wide connectivity, even at the network edge, making it the perfect solution for mission-critical operations that require ubiquitous connectivity.

Mesh networking software can direct traffic by dynamically load-balancing and routing data around signal blockages from moving assets and potential interferences. This ensures that data packets get to their destination via the fastest path available. It also eliminates the need for a controller node, meaning that the network will have no single point of failure.

As petrochemical plants are spread out over vast areas, they are forced to add new bandwidth-intensive applications to support continued growth. A superior mesh network topology can rapidly evolve as the plant does. As more nodes are added, more paths to direct mission-critical data are naturally formed. With more paths, the network becomes more resilient.

A mesh network can also protect plants, which are potential targets for high-risk network security attacks. The multi-layered, military-grade security for network traffic of a mesh network makes it incredibly difficult to penetrate. It boasts multiple cryptographic options, configurable data and MAC-address encryption, and configurable per-hop, per-packet authentication between nodes.

A trail to operational enhancement. Novel proprietary wireless network nodes[a] are built for hazardous locations where ignitable concentrations of flammable gases, vapors or liquids can exist all or some of the time under normal operating conditions. The author's company enables plants to deploy these nodes on fixed- and mobile-plant infrastructure and equipment to enable the maintaining of multiple immediate connections between peers while sending and receiving data on multiple frequency bands.

The author's company's kinetic mesh networks[b], built with proprietary wireless network nodes, can dynamically connect the people, assets and devices that comprise every aspect of a plant's current and future operations. The network offers benefits, which include reducing the total cost of ownership and simplifying the work demands of employees by allowing them to centralize their communications to a single device.

These self-healing, peer-to-peer industrial wireless networks give petrochemical plant operators the communication flexibility, reliability, high performance and scalability they need to maximize productivity and innovation. In turn, risk is minimized, downtime and costs are decreased, and security is increased to keep them ahead of the competition.

The way forward for petrochemical plants. To tackle competitiveness and move with the changing digital environment, utilizing mesh-based, IIoT networks is essential. With more significant pressure on the industry, ensuring cost-effectiveness and safety is even more vital. These networks can provide plant-wide connectivity to manage, monitor and optimize assets critical to efficient, safe and competitive petrochemical operations. In addition, a complete IIoT solution can be deployed in a matter of days or weeks as opposed to months. This means petrochemical plants can quickly maximize this sector of industrialization. HP

NOTES

[a] Rajant Corp.'s BreadCrumbs® wireless network nodes
[b] Rajant Corp.'s Kinetic Mesh® networks

AL J. RIVERO is Vice President of Global Energy at Rajant and is responsible for working and engaging with clients who seek to implement a secure, reliable IIoT and mobility strategy for their oil and gas operations. He works closely with clients to develop a strategic technology transition plan that ensures a reliable and secure migration of technologies. Mr. Rivero has more than 30 yr of experience in various roles, ranging from staff engineer and project manager to operations management and technology management within Chevron companies. He also has extensive IT/OT integration project experience having worked with SAP, JDE, ESRI and a variety of automation and SCADA/DCS solutions within the upstream, midstream, refining and petrochemical segments.

F. MONTEMURRO, Voovio Technologies, Richmond, Virginia

Achieve zero execution errors through procedure clarity

It is well-documented that many unplanned manufacturing events could have been prevented if procedures were executed properly. Ensuing investigations cite "failure to follow procedure" as the event root cause, resulting in next step recommendations that include additional operator training and discipline.

However, a more systemic failure could be at the root of these unplanned events. When an operational execution error occurs during a process or equipment startup, shutdown, changeover, process loss out of primary containment or other event, how often is "procedure clarity" considered the root cause? This can be considered a major source of error that is overlooked by the industry.

Operating procedures originate during capital project installation and are developed using the technical process design basis. Procedures include safety warnings, specific instructions and details required to complete the desired outcome. Following a project startup, the initial operating procedures are redlined, updated and institutionalized as part of the site's management of change (MOC) process.

Two major reasons for suboptimal procedure clarity have been identified:

Procedure does not reflect operator practice. The author's company analyzed 300 customer procedures, the majority of which were startup and shutdown procedures. The data shows a significant number of procedures do not match operator practice, a foundational element for operational discipline. When surveying manufacturing subject matter experts (SMEs), the written procedures vary from the unit's established practices, with some practices varying from shift to shift. The Ron Moore Group found this causes up to 23% of manufacturing downtime losses (FIG. 1).

Ambiguities and generalizations. Using procedures, manufacturing operators train on how to operate the process, unit or plant safely and effectively. Operators are challenged to learn and qualify on hundreds of pages across a range of procedures. Often, these procedures are written with a large amount of technical content, generalizations and ambiguities that assume clear understanding by the operator. Procedures are typically written by engineers or SMEs that are very familiar with the process—these engineers or SMEs can overlook basic details of execution, believing those details are largely understood.

Example: Procedure line with additional peripheral information and options on how to execute the procedure:

> "Level indicator transmitters (ABC-111 and DEF-222 at A-C-9 and GHI-871 and GHI-872 at A-C-8) provide an initial inventory in these vessels. To provide initial inventory in A-C-7 and A-C-6, 30-psig condensate control valve (FV-4447) can be manually opened or put in automatic at 30%. The steam regulator for A-C-6 is located beside the CO_2 plant."

The first and third sentences are unnecessary for procedure execution and may add uncertainty for the operator. The second sentence gives the operator options, leaving to question the preferred best methodology to inventory the system.

Examples: General, ambiguous information in procedures:

- "Close all bleeders and open-ended lines"
- "Blow product return lines and control valve loop with blend gas from A-123 take-off manifold to ensure lines are clear, then isolate from all equipment"
- "Outside operator will verify manual valves on feed system are lined up"
- "Ensure cooling water is lined up to all coolers and exchangers that require cooling water"
- "Manually close all condensate controllers outside."

An operator is expected to follow the above procedural statements and remember where "all" components are located while executing the one procedure line item. In the 1990s and early 2000s, this problem was masked by workforce experience; shift teams had many individuals with more than 20 yr of operating experience, so procedure clarity was unimportant. With the present gap in experience, the lack of procedure clarity, and few operator aids to ensure execution accuracy, incidents and unplanned events will continue to occur.

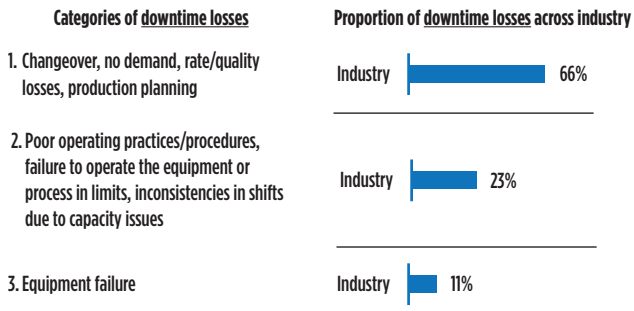

FIG. 1. Unleashing the hidden plant. Source: Ron Moore Group.

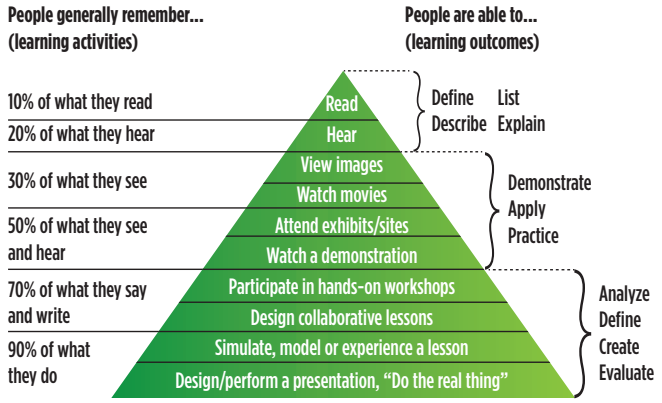

FIG. 2. The learning pyramid or cone of learning.

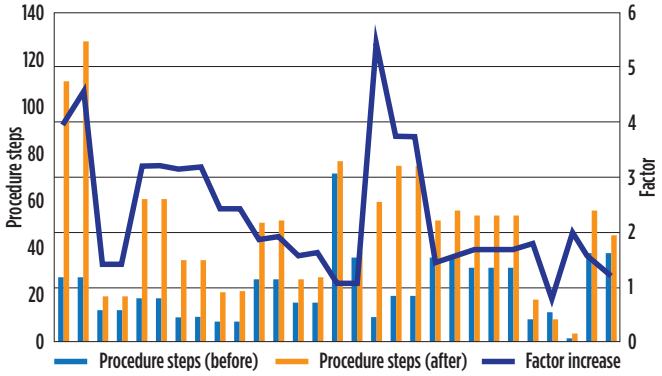

FIG. 3. Improved procedure clarity of past projects.

Impact of procedures during operator training. Once an operator reads a procedure, shadows an experienced operator and completes an assessment, they are "signed off as qualified." Industry data indicates that operators may only have experienced 40% of their procedures because equipment is always running and other priorities. Following qualification, the operator is released to perform the work. Therefore, procedure quality and specificity are the building blocks for developing operator competency.

Procedure formats and templates vary from company to company, even from site to site. Some companies have implemented digital procedure solutions, requiring many plant resources and subsequent procedure conversions. Other companies maintain procedures manually with internal document control systems. Whether operators need to print procedures or take a tablet out in the field and sign off steps as they are completed, both formats require operators to read procedures for understanding.

It is well-documented that individuals learn and retain ~90% using simulation and doing vs. ~10% when reading procedures (FIG. 2). The industry challenge is to move operator training—proactive development—down the pyramid[1] to increase individual retention and reduce an operator's time to full competency.

Ultimately, to see a step-change improvement in operational discipline, procedures must be developed, implemented and maintained based on successful execution by the end user—the operator—and they should be clear, concise and action-based.

Employing best practices. The author's company employs two best practices to ensure accurate procedures and standard operator execution. First, a line walk is performed for procedures with the resident SME to accurately document procedure execution using photographs, and an action-based checklist is created. This visual walkthrough identifies gaps in the written procedure and the actual operating practice.

All deviations from the documented procedure are reviewed and approved using the site MOC process. Using the author's company's patented technology, users can perform the newly documented procedure in an immersive photo-based environment (called the digital replica) where they can interact and perform the procedure. This simulation allows operators, engineers, production specialists and others the chance to visually verify procedure accuracy.

The second best practice is the addition of action steps, better known as a checklist. This practice has significantly improved safety performance in air travel, medical procedures and other sectors. During the line walk with the SME, each action the operator is expected to complete is confirmed and photographed. Multiple actions are regularly discovered within a single procedure line. Below are two examples:

- The procedure line item, "Close all bleeders and open-ended lines," resulted in 12 action steps—12 bleeders and open-ended valves required closing to ensure that no contents left primary containment and/or caused an environmental incident.
- The procedure line item, "Manually close all condensate controllers outside," resulted in 20 action steps to close 16 valves.

On average, the author's company's process eliminates procedure generalities and ambiguities and results in 2.4 times more procedure steps that are clear and concise, action-focused steps with visual clarity. A summary of past projects is depicted in FIG. 3.

Takeaway. Operational discipline and speed to operator competency are and will remain competitive advantages due to the current and projected attrition slated for plant sites. Clear and concise procedures, standardized on plant operation that have objective assessments, are foundational building blocks to ensure operator competency. Manufacturing plants can build operator competency and deliver business results safely and successfully by using the established best practices detailed here, combined with the visual clarity that simulation provides. HP

LITERATURE CITED

[1] Dale, E., "The learning pyramid," online: https://en.wikipedia.org/wiki/Learning_pyramid

FRAN MONTEMURRO, Director of Operations at Voovio, is an operations leader with more than 30 yr of experience in manufacturing. Over his career, Mr. Montemurro has been a plant manager at multiple DuPont sites, including highly hazardous PSM and EPA/RMP operations, as well as discrete manufacturing facilities. His teams were awarded both the E.I. DuPont Safety Excellence Medal and E.I. DuPont Engineering Excellence Award.

C. OBERLE and **T. BONKAT,** Emerson Automation Solutions, Shakopee, Minnesota

Key instrumentation technologies to tackle the toughest measurement challenges

Just as some people seek out extreme sports, process manufacturing has its extreme applications, and engineers who design for these environments must find ways to safely contain and monitor all manner of dangerous reactions and products. Consider a process where two feedstocks come together, generating a powerful exothermic reaction. The equipment must withstand what is, in effect, a continuous explosion capable of generating enormous amounts of heat and pressure, while ensuring safety for products that may be both highly corrosive and toxic.

Such situations are well beyond the capabilities of garden-variety equipment, including instrumentation. The need for accurate and reliable measurements is crucial to control critical processes and avoid serious safety incidents. If the continuous explosion cannot be monitored effectively, it could break out of its constraints, causing serious damage.

Extreme applications take many forms, some potentially violent, flammable and toxic, while others have more subtle hazards, but all these still have the potential to damage or shorten the service life of conventional process instruments. In this article, the authors will examine five types of difficult conditions. These include:

- Excessive vibration
- Difficult flows
- Demanding process fluids
- Extreme temperatures
- Severe pressures.

For each condition, the authors will consider what makes the process extreme, and then look at pressure and temperature instruments and associated tools designed to tame them. Most of the solutions involve specialized materials, physical design modifications and sensor signal processing, supported by software able to analyze the situation and offer practical alternatives.

PART 1: VIBRATION

In a refinery or chemical plant, there are few, if any, situations where vibration is desirable, so maintenance teams go to great lengths to minimize it. With rotating equipment (e.g., motors and pumps), excessive vibration indicates misalignment, failing bearings or other problems. If excessive vibration is transferred from a pump to adjacent piping, it can cause fittings and flange bolts to loosen, creating leaks.

FIG. 1. A proprietary wireless pressure gauge[a] does the same job as the mechanical version but with multiple advantages.

Such vibration is tough on mechanical instruments, especially pressure gauges, which operate using a delicate mechanism with springs and gears, making them vulnerable to shock and damage.

Most operators have seen typical results of vibration: leaking bourdon tubes, bent indicator needles or stuck needles from broken gears. Some models are armored with rubber covers and use beefed-up mechanisms, but these options add cost and have limited effectiveness.

Many users like the functionality of a traditional pressure gauge, but not its finicky mechanism and instability. Electronic gauges (**FIG. 1**) use an electronic sensor to provide the capabilities of a full process transmitter. Some include device diagnostic functions and *Wireless*HART connectivity, but in an analog gauge form factor with a traditional needle display. This approach checks the boxes for most-wanted features, without the problems of traditional pressure gauges.

Fluid-induced vibration. Vibrations can be created by flowing fluids in the piping configuration, causing wake shedding and peculiar eddy currents. This situation is very common where a thermowell is inserted into the fluid stream—perpendicular to the flow—to provide a temperature reading. Vortices form on both sides of the thermowell and create high- and low-pressure areas capable of inducing vibration (**FIG. 2**).

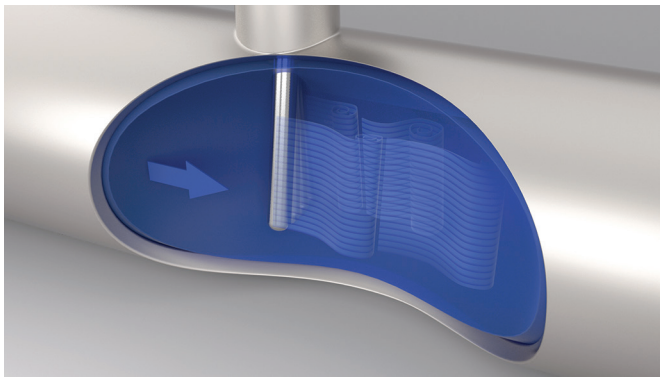

FIG. 2. Liquid flow around a thermowell can create vibrations sufficient to cause fatigue-induced failure.

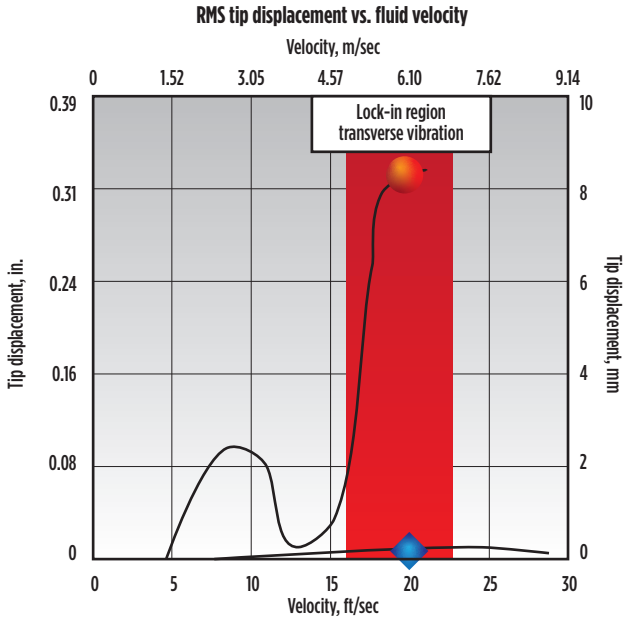

FIG. 3. When the frequency of the wake shedding matches the resonant frequency of the thermowell, the resulting vibration can be violent.

Sometimes, this vortex-induced vibration (VIV) is tolerable, but when severe, it can lead to two problems: sensor failure causing a lost reading or fatigue-induced failure of the thermowell itself. In this situation, the thermowell eventually bends or cracks, which can lead to process containment loss.

Wire fatigue and breakage. If vibration cannot be eliminated, one mitigation technique is using redundant sensors. Some temperature transmitters can process signals from two sensors, either from separately mounted sensors or from dual sensors built into a single sheath. If the values differ, transmitter diagnostics can trigger an alert. Similarly, if one sensor fails, the transmitter can switch immediately from the primary to the backup sensor without losing the reading.

The greatest reduction in risk is achieved with two independent sensors; however, this requires additional process penetrations. Two independent sensors—even if they are feeding one transmitter—can reduce the probability of losing the reading by 80%.

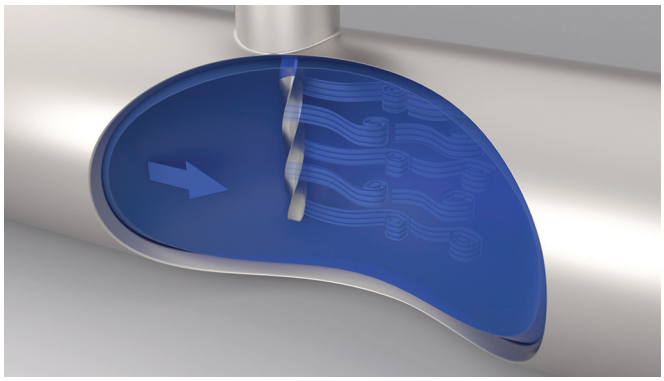

FIG. 4. Helical square designed thermowells[c] break up wake-shedding effects, reducing vibration by up to 90%.

Thermowell durability. When VIV is an issue, the conventional solution is simply using a massively thick and/or very short thermowell that can stand up to the vibration. This is a problem for several reasons, including:

- A heavy cross-section causes significant time lag for the sensor to respond to changes in temperature
- Large diameter thermowells can be difficult to mount and can cause increased internal pipe blockage
- A short thermowell may not extend far enough into the process media stream to deliver an accurate temperature reading.

This leaves designers trying to determine how thin and long a thermowell can be and still withstand the VIV. For a given thermowell installed in each pipe, vibration will change with fluid velocity, but the two do not have a linear correlation. A certain fluid velocity will cause the VIV frequency to match the natural frequency of the thermowell, which can cause the amplitude to increase significantly (FIG. 3), with accelerated metal fatigue as the result.

These critical relationships can be analyzed mathematically using formulas outlined by ASME in its PTC 19.3 TW-2016 Standard. This calculation method has been built into free online thermowell calculation tools[b] that guide a design engineer through the sizing process by analyzing the likelihood of vibration problems for a specific thermowell shape in a specific installation. Each calculation involves about 20 variables for the dimensions and operating characteristics, so it is difficult to process manually. It must also be repeated for each set of operating characteristics, another reason to use automated online software.

Process data for various operational levels can be entered manually or uploaded using a template, so a designer can test multiple thermowell tags at once. The system performs calculations in the usual way, but also permits users to test what-if scenarios to see if a thinner thermowell might work or if a stock size already in use in the plant can do the job. These alternatives are offered as possibilities, providing designers with the flexibility to make the final call.

Avoiding fluid-induced vibration. Suppressing vibration at its source generally involves using a thermowell profile designed to avoid normal wake-shedding problems. Helical square designs (FIG. 4) disrupt the formation of long vortices, resulting in far less vibration—up to a 90% reduction in some cases.

Helical geometries have been used successfully with wind

stacks and deep-sea risers to solve similar problems. This type of thermowell does not depend on a specific orientation when inserted and reduces the need for excessively-thick thermowells and large-diameter process penetrations.

PART 2: CHALLENGING FLOWS

Applications can become extreme based on fluid flow characteristics, with these three areas posing challenges for instrumentation: high-velocity flows, wide flow-turndown range and large line sizes.

High velocity. Historically, piping guidelines called for liquid velocities below 7 ft/sec to avoid excessive pressure loss, pipe wear and high pumping costs. Much of this practice has been abandoned as too expensive, with engineers increasing flowrates and/or using smaller pipes to save initial costs, resulting in higher velocities. The following are some ways velocity-related problems can be avoided or mitigated.

High-fluid velocities are particularly problematic for flow measurement. Many plants that routinely use differential pressure (dP) methods experience this directly. For those situations, there are straightforward cures. First, it is important to minimize the pressure drop across the primary element. Second, velocity gradients within the pipe increase with velocity, so an averaging reading across the full cross-section must be taken to ensure an accurate measurement, especially with large line sizes.

One way to solve both problems is to use a specific type of primary element design instead of a conventional single orifice. An averaging pitot tube sensor is minimally intrusive in the pipe, can work symmetrically for bi-directional flow and self-averages velocity gradients for high accuracy. It is suitable for liquid, gas and steam with velocities up to 300 ft/sec, and determines volumetric flow—which can be combined with a temperature measurement and known fluid density characteristics—to calculate mass flow.

Widely variable flow range. Most process units are designed to operate within a relatively narrow production range. With that knowledge, engineers can size instruments to fall in the measuring sweet spot during normal operation, but applications with a wide flow range can still create challenges. Coriolis flowmeters have an especially wide flow range but are not suitable for every application.

When conventional dP flow measurement techniques are used, some users resort to an outdated practice of double-stacking two dP transmitters with different measuring ranges on the same primary element. This works but is cumbersome for installation, maintenance and signal processing.

Today's dP transmitters are available with electronics that extend the measuring range to keep the percentage error range far more uniform. This avoids the problem of reduced accuracy at the low end of the range due to percentage-of-span accuracy characteristics.

Large line sizes. While many flowmeter types are highly scalable, creating versions for large pipe sizes can get expensive. An averaging pitot tube sensor is very well suited to large line sizes since it can be built for cross-sections up to 96 in.

Temperature measurements have different complications. Large line sizes call for long thermowells able to reach to the pipe center, but these are especially vulnerable to VIV. Again, using square helical thermowells verified by suitability calculations makes these difficult applications far easier to implement.

Help with dP flowmeter selection. DP meters have long been the most widely used technology for flow measurements thanks to their range of configurations and adaptability, but they can present challenges for a novice instrumentation engineer trying to choose from the variety of primary elements. Which best suits the application? Fortunately, any instrumentation engineer trying to make the best selection can use new online software tools[d] to simplify the choice. These tools streamline product sizing and configuration by generating flow calculations faster and with high accuracy.

Once the initial operating scope parameters are settled and the specific application is identified (instrument location, tag number, etc.), a flowmeter or primary element selection must begin with a detailed understanding of the application conditions, including piping size, process fluid and normal operating parameters.

Once these variables have been characterized, more subjective elements come into play. Questions to ask include:

- What degree of accuracy and turn-down range is expected?
- How much pressure loss can be tolerated?
- How easy is it to install a given type of primary element?
- How much straight pipe run is available and practical to deliver accurate readings?

These tools augment the limited experience of younger engineers, while expediting the selection process for their more experienced counterparts. The final presentation includes a table of data illustrating the operating characteristics in the application context. When the process is complete, the designer will receive a full configuration description and part number based on vendor catalog data.

PART 3: DEMANDING PROCESS FLUIDS

When considering instrumentation, it is important to look at what is flowing through the pipes—the process fluid itself—liquid, gas or steam. Characteristics that make a fluid extreme include some mix of abrasiveness, usually due to fine particulates or corrosiveness, due to highly acidic or caustic process media, or one containing aggressive chemicals, such as chlorine.

Some products can be highly toxic, flammable or environmentally dangerous, but these characteristics do not necessarily attack instruments and equipment. This section will concentrate on elements able to affect instruments and equipment directly.

The damage caused by these fluids is loss of metal, either eaten away chemically, worn away by abrasiveness or both. Solutions call for materials that are chemically inert relative to the fluid and/or hard enough to withstand the constant scraping action. When materials reach their limits, the solution may call for ways to live with a shorter service life.

For corrosiveness, the solution often requires wetted parts in a specialized alloy designed to withstand the service, including a large family of stainless-steels with high nickel (Ni), molybdenum and chromium content. However, the answer is not always so simple. Pressure instruments are particularly vulnerable to attack, so this calls for a closer look.

With severe fluids, containment is very critical, so engineers often use remote seals to eliminate the possibility of process

fluid getting into impulse lines or the pressure instrument itself. These thin diaphragms have unique flexing characteristics to provide the necessary measuring sensitivity and accuracy. Fortunately, diaphragms can be manufactured from a variety of materials, including stainless-steels, tantalum and Ni-based alloys such as alloy C-276 or alloy 400.

All diaphragm materials have their limits for protection against abrasive fluids. The durability of these diaphragms can be increased with coatings of hard-carbon nanostructured material. The micro-thin coating withstands abrasion, extending service life up to 10 times compared to a standard 316 stainless-steel diaphragm in abrasive service but does not impact remote seal accuracy or sensitivity. The range of coating options also includes a variety of metallic and polymer materials.

Another problem is a seal's permeability to atomic hydrogen if present in the process fluid. Hydrogen atoms can migrate through the diaphragm and once in the fill fluid, form molecular hydrogen. Because molecular hydrogen is too large to permeate back through the diaphragm, it gets trapped and forms hydrogen bubbles in the fill fluid. These bubbles can severely affect transmitter performance. Depositing a 5-micron thick layer of gold to a stainless-steel diaphragm provides protection against hydrogen permeation.

Avoiding wetted parts. Where conditions make adding a conventional thermowell impractical, some users clamp a temperature sensor to the pipe. This provides a reading, but heat dissipation keeps the external temperature from fully reaching the internal value. Adding insulation can help, but the reading will likely never reach the degree of accuracy needed and changing external conditions will cause unpredictable fluctuations.

Specially designed temperature transmitters[e] make measurements outside of the pipe while solving the normal problems by using a different methodology to correct for heat loss (**FIG. 5**). These transmitters use an algorithm to compensate for heat transmission and external conditions. The user enters factors for the pipe material and thickness, and the instrument provides a process temperature measurement, often as accurate as a traditional thermowell installation.

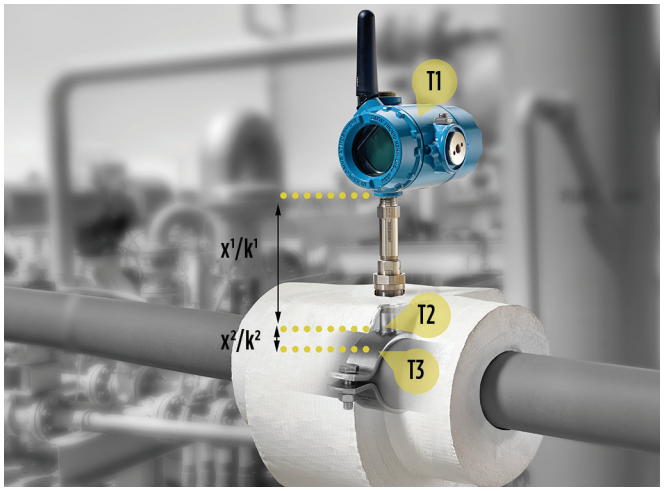

FIG. 5. A specially designed temperature transmitter[e] provides a highly accurate process temperature reading through a pipe wall without a penetration.

When clamped on a pipe, the bracket holds a resistance temperature device (RTD) in contact with the pipe surface to ensure consistent heat transfer. Once insulated and operating, an algorithm compares the reading from the pipe's RTD to a second RTD in the transmitter. These two readings are continuously compared to precisely calculate the temperature inside the pipe, even when ambient and other conditions change significantly. The result is a highly-accurate temperature reading without the need for a process penetration.

Designed for durability. Flammable or dangerous fluids require equipment designed with features that ensure reliable and safe operation in these environments. This often calls for construction using industrial strength proportions able to take the punishment, while allowing for changing out parts when necessary, with minimal disruption. Since dP flowmeters are frequently used in tough refinery service, this technology has been beefed-up to withstand the abuse.

This flowmeter is built upon a fully welded spool section with built-in isolation valves and temperature input. It comes fully assembled to the dP transmitter and is leak tested at the factory, and it uses a multi-orifice primary element to minimize the need for upstream and downstream straight pipe run. The impulse lines are short, and the dP transmitter is close-coupled to minimize the potential for plugging. The impulse lines also have gate-type isolation valves and clean-out ports so they can be rodded out while the unit is in operation. The entire dP transmitter can be removed and replaced without a process shutdown.

The assembly can include an integral temperature sensor that sends its information to the main dP transmitter, which can report the value to the automation host system. When the fluid temperature is combined with the dP volumetric flowrate and a known fluid density, the transmitter can provide a mass flow measurement.

The dP transmitter can also provide static line pressure values to enhance the mass flow measurement without the need for an additional pipe penetration. A setup such as this can typically handle fluids up to 315°C (600°F) or higher, depending on the application and installation.

PART 4: EXTREME TEMPERATURES

When considering difficult temperatures, hot usually comes first, but cold also presents challenges, particularly in cryogenic ranges. With either extreme, the first step is protecting electronics since circuit boards and components have limited temperature operating ranges.

As for instrument configurations, many of the same techniques used to protect from aggressive fluids protect from cold and hot temperatures, although there are some specialized variations. The following will detail how these solutions work together.

Low environmental temperatures. The cold end of the temperature range is doubly problematic because it can reflect not only the process fluid, but also the environment. Some oil production areas in Canada and Russia routinely experience winter temperatures of –40°C (–40°F), which affect equipment as well as people.

Many electrical devices work better in mildly colder weather. However, problems begin to develop when sophisticated

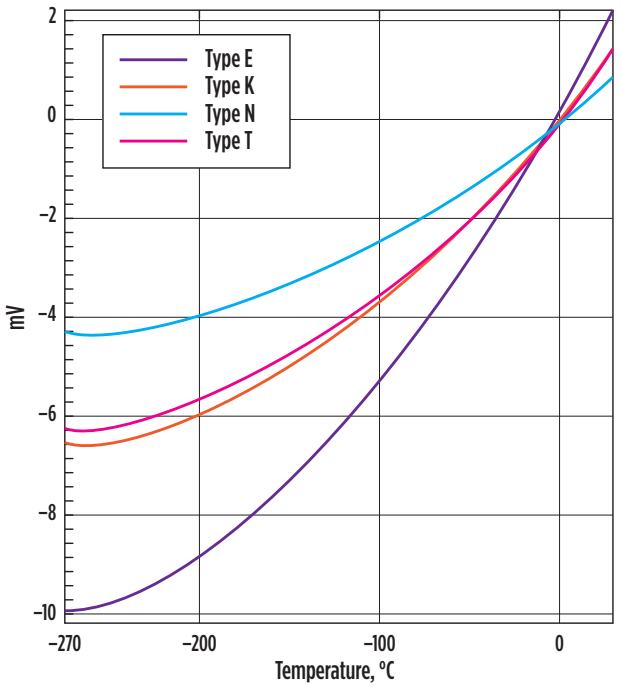

FIG. 6. Thermocouples are better than RTDs for low temperature, but it is critical to compensate for changes in linearity.

devices—such as the A/D converters and other elements of field device transmitters—move out of a moderate range. Fortunately, many transmitters have more robust circuits, and the internal components are less affected by colder temperatures.

Many transmitters can operate at temperatures down to –40°C (–40°F), but this limit can be extended to guarantee startup down to –60°C (–76°F). However, the transmitter may not deliver full accuracy if the temperature remains below –40°C (–40°F).

In these environments, more extreme measures are often used, including the liberal use of heat tracing and heated instrumentation cabinets. Fortunately, specialized instruments are available to handle the most extreme cold temperature ranges without the need for extra protection.

Measuring cryogenic temperatures. Conventional temperature sensors can often be used even at the low end of the spectrum; however, there are limitations. Whereas RTDs are often a first choice for many normal applications, when reading below –50°C (–58°F), it is critical to know the sensor's rating. Different classes of RTDs have different low limits, ranging from –50°C to –200°C (–58°F to –328°F). Thermocouples are better adapted to handling low temperatures, provided an appropriate type is selected. Some—such as type B—simply are not suitable for low temperatures. Types E, K, N and T have ranges down to –270°C (–450°F), with Type T especially popular in cryogenic applications.

Once below –100°C (–150°F), most thermocouples begin to lose linearity (**FIG. 6**). This is not necessarily a problem since it is a known characteristic and can be corrected in the transmitter. However, not all temperature transmitters or controllers are set up to work at the low end, so users must ensure any device intended for these applications has the required capabilities.

FIG. 7. DP flowmeters can be used with LNG and other cryogenic liquids, but the transmitter should be placed above the pipe.

DP flowmeters for low temperatures. Out of the many potential flowmeter technology choices, dP flowmeters using appropriate dP transmitters are well suited for cryogenic liquids, such as LNG. Users must pay particular attention to the placement of the various devices and the material selection for components.

For dP flowmeters in conventional liquid applications, the typical mounting position places the transmitter and impulse lines below the pipe to prevent air and gas entrapment. LNG applications reverse this, positioning the transmitter above the primary element (**FIG. 7**) so there is an insulating gas barrier preventing contact of the cold liquid directly with the transmitter diaphragm. Brief direct contact should not cause the instrument to fail, but it will slow responsiveness.

The transmitter has a stainless-steel body that can handle the cold, but it is important to look at other parts, such as the impulse lines. Designers must ensure gaskets, O-rings and bolts are also compatible with these low temperatures, as the wrong materials can become brittle and lead to leakage. DP flowmeters equipped with welded impulse lines reduce the potential for sealing material embrittlement by moving gaskets away from the frost line. Impulse tubing should have a small diameter—typically 0.25 in. (6 mm)—to help maintain the gas barrier.

Isolating the transmitter. Treatment of high- and low-temperature applications uses similar techniques as those employed for handling aggressive fluids. A diaphragm seal can be used for pressure or level measurements, but extreme temperatures call for specialized fill fluids designed to retain their fluidity at the operating temperature without freezing or boiling. In cases

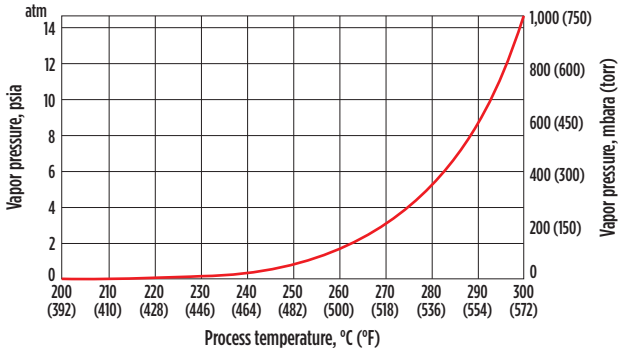

FIG. 8. Pressure and temperature figure into selection of a fill fluid in a high-vacuum application.

where the length of the capillary lines allows the fill fluid to come to ambient temperature, it can slow response or cut it off entirely.

Some stand-off mounts use two fill fluids, one optimized for the process temperature and the other for the ambient temperature. Each fill fluid is tailored to the application and environment, eliminating the need for heat tracing or other protection methods. With appropriate fill fluids, dual-fluid mounts can be used for temperatures up to 410°C (770°F) or down to –105°C (–157°F).

PART 5: SEVERE PRESSURES

Like temperatures, extreme pressures can be high or low, and both ends of the spectrum present their unique challenges. A pressure gauge or transmitter must be able to operate continuously—potentially for 1 yr—within its expected operating range, and it should also withstand pressure spikes. Countless mechanical gauges have suffered damage in this way due to their delicate internal mechanisms. A bourdon tube pushed past its limits will not return to the correct shape or may simply burst. Fortunately, electronic transmitters provide more robust construction, allowing them to absorb severe increases in process pressure and return to normal operation as if nothing happened.

Most general process instrumentation providers max out at 20,000 psi (1,379 bar), since applications beyond this are rare and highly specialized. A proprietary electronic pressure gauge[a] does not have a conventional mechanical mechanism. Instead, it uses the same sensor technology as electronic transmitters, thus avoiding common traditional gauge failures. This pressure gauge can measure up to 10,000 psi (690 bar), with overpressure protection up to 1.5 times its range.

When a more conventional pressure transmitter is needed, in-line pressure transmitters cover a variety of ranges—up to 20,000 psi (1,379 bar) gage pressure or absolute pressure. Many are SIL 2/3 certified for use in the most safety critical applications. In addition, many include basic and advanced device diagnostic capabilities.

Panel-mounted transmitters can also handle up to 20,000 psi (1,379 bar) gage pressure or absolute pressure. These devices are compact, lightweight and can come with all-welded, stainless-steel construction, providing a stable and robust solution for harsh environments.

Tough dP flow measurement. Consider the challenge of measuring flow of a high-pressure line—e.g., 5,000 psi (345 bar)—using a dP transmitter and conventional primary element. There will be a pressure drop across the primary element, but if the application is engineered well, it should only be around 30 psi (2 bar) at normal operating range. This presents a serious challenge for the transmitter to produce a precise reading of a very small pressure differential in an environment where the static pressure can easily be hundreds of times more than the differential.

Some dP transmitters[f] are designed exactly for this scenario. They have a modest measuring range up to 150 psi (10.3 bar) but can withstand static line pressures up to 15,000 psi (1,034 bar). Their construction can resist overpressure and line pressure effects to maintain high accuracy and stability, even in harsh environments.

Working in a vacuum. Low pressures are anything below atmospheric: 14.7 psi (1 bar) absolute. Measurements made in these conditions still use the same instruments and associated equipment, including diaphragm seals, but special consideration must be given to the fill fluid. When enough vacuum is applied to a liquid, it can reach its boiling point and vaporize. If this happens to the fill fluid, it can cause the whole system to fail. These issues are exacerbated when ambient or process temperatures are high.

When the process is under vacuum conditions, the fill fluid will vaporize under a lower temperature than when it is operating under normal atmospheric or greater pressure. Fortunately, there are a variety of fill fluids for remote seal systems, each with a specific vapor-pressure curve (**FIG. 8**) indicating the pressure and temperature relationship where a fluid remains in a liquid state. When a diaphragm seal is used in a vacuum application, all-welded construction avoids drawing air into the capillary system.

The right tools. Any reasonable person participating in extreme activities, whether for pleasure or work, will want to have the right protective equipment because it is critical to success and even survival. In a similar manner, products for extreme applications are designed to ensure reliable performance and safety in the most challenging applications. The technologies and practices suggested here are designed to improve instrumentation performance, increase reliability and reduce maintenance. None require major capital projects, nor do they have to be executed on a grand scale. Each improvement can be implemented one-by-one to deliver incremental gains and a quick return on investment, eliminating obstacles to effectiveness and profitability. HP

NOTES

[a] Rosemount™ wireless pressure gauge
[b] Emerson's Thermowell Design Accelerator
[c] Rosemount Twisted Square™ thermowells
[d] Emerson's dP Flow Sizing and Selection Tool
[e] Rosemount X-well™ technology
[f] Rosemount 3051S High-Static DP Transmitter

CONNOR OBERLE is a Global Pressure Product Manager for Emerson's Automation Solutions business in Shakopee, Minnesota, with responsibility for Rosemount pressure transmitters. He earned a BS degree in mechanical engineering from the University of North Dakota.

TIMCHAN BONKAT is a Global Temperature Product Manager for Emerson's Automation Solutions business in Shakopee, Minnesota, with responsibility for Rosemount sensors and thermowells. He earned a BS degree in electrical engineering from St. Cloud State University.

T. ZOU, Houston, Texas, T.A. Cook

Risk mitigation procedure following criticality assessment and FMEA

In asset performance management (APM), criticality assessment and failure mode and effects analysis (FMEA) are powerful tools that enable the identification of opportunities to minimize asset lifecycle costs during the development of equipment strategies.

Here, the author proposes a risk mitigation procedure that prioritizes tasks based on the criticality assessment and FMEA results, considers multiple aspects of failure effects and aims to provide data-driven solutions to maximize the risk mitigation benefit and return on investment (ROI).

Criticality assessment and FMEA. A criticality assessment is used to chart the probability of a failure against the severity of its consequences with regard to organizational impacts, such as safety, environmental or production consequences. When performed at the functional location level (in most cases, an individual component), a criticality assessment identifies the worst combination of severity and occurrence against a predetermined risk matrix. The results highlight one or several groups of "critical" components, allowing remedial efforts to be directed to mitigate the most prominent risks.

FMEA is a bottom-up, inductive analytical method that is typically performed at the failure mode level. When previously assessed criticality results are available, the information can be used as a reference to speed up FMEA development. Adding the failure mode detection rankings to the criticality results yields a risk priority number (RPN). RPNs can be calculated before and after risk mitigation for a specific failure mode.

In general, multiple failure modes (around 10, on average) are associated with a given component, and the risk mitigation tasks identified by the FMEA are usually a much longer list at a more detailed level, compared to those from the criticality assessment.

Risk mitigation benefit realization. Depending on the findings of the criticality assessment and the FMEA, one or several risk mitigation strategies can be applied to each risk item:

- **Root cause analysis (RCA):** This strategy applies to failures associated with very high impact, where the root causes are unknown. Only with the completion of the RCA can mitigation strategies be developed for certain risk items.
- **Preventive maintenance (PM):** This strategy brings the most benefit to certain wear-out failure modes where it is difficult to effectively monitor damage conditions.
- **Predictive maintenance (PdM):** These typically nondestructive inspections can predict an upcoming failure (with a probability) and trigger a preventive maintenance action. Some examples are periodic vibration analysis and/or oil sample analysis for rotating equipment.
- **Operators' rounds:** These inspections are conducted by equipment operators, sometimes referred to as operator-driven reliability. Compared to PdM, these tasks are conducted more frequently and involve more visual and auditory observation and less technology.
- **Spare part strategy:** Having critical spare parts available may significantly reduce the mean time to repair (MTTR) upon an equipment failure, thereby lowering the severity of the failure. This is especially important for parts with long lead times.
- **Redesign:** When the risk cannot be effectively or economically mitigated by any of the prior strategies, a redesign may be the last resort. An example is adding a standby pump to form a redundant pump system at a process-critical location.
- **Risk acceptance:** If no risk mitigation strategy, including redesign, is able to address the risk item effectively, then the best option is to accept the risk. This is sometimes referred to as "run to failure." Risk acceptance often applies to components with lower criticality and should be assessed on a case-by-case basis.

Each of the outlined strategies (except for risk acceptance) has a potential benefit, either financially or with respect to environment, health and safety (EHS) risk. However, the benefit is not realized until the risk mitigation tasks are implemented. In a typical plant-level APM project, a large number of failure modes may be identified as candidates for risk mitigation. Most clients face the challenge of limited human resources, including engineers, technicians and planners, as well as limited budget for capital projects and spare parts. To best utilize limited resources, it is important to develop and follow a procedure that helps prioritize risk mitigation tasks.

Procedure to prioritize risk mitigation tasks. The following proposed procedure starts after the completion of the criticality assessment and the FMEA and ends with a list of recommended tasks for implementation:

TABLE 1. Information for risk mitigation

Information category	Location in criticality assessment and/or FMEA	Required information	Desired information
Failure effects	Severity ranking	• Production impact • Repair duration (MTTR) and cost (labor, tools, material)	• Logistic delay • Rental and backup cost • Repair effectiveness
Failure characteristics	Occurrence ranking	• Failure mechanism • MTBF	• Failure history • Age • Expected end of life
PM	Corrective action (FMEA only)	• PM duration and cost (labor, tools, material)	• Existing PM • Maintenance history • PM frequency • Shutdown schedule • PM effectiveness
PdM	Detectability ranking (FMEA only)	• Labor and tools cost • Probability of detection	• Existing PdM • P-F interval[1]
Spare part	Recommendation	• Spare cost • Lead time • Logistical delay	• Storage cost • Part shelf life
Redesign	Recommendation	• Cost of redesign • Redesign effectiveness	• Post redesign RPN

TABLE 2. Risk mitigation implementation cost

Strategy	Risk mitigation implementation cost
RCA	• Engineering hours for RCA • Implementation cost (strategy-dependent)
PM/PdM	• PM/PdM development • PM/PdM training, labor, materials and tools • Lost production opportunity if shutdown is required
Operators' rounds	• Operators' training and labor • Development of operators' checklist • Development of DCS parameters for condition monitoring
Spare part	• Spare part purchase and storage • Spare part obsolescence
Redesign	• Redesign engineering hours • Initial investment

1. Perform failure mode pre-screening
2. Collect information for prioritization
3. Quantify risk mitigation benefits for top-failure modes
4. Perform resource allocation optimization
5. Summarize results and make recommendations.

Failure mode pre-screening. A pre-screening helps narrow down the risk mitigation candidates efficiently. In general, failure modes satisfying the following conditions should be selected for the next step (prioritization):

- Associated with components with high or medium criticality ranking
- Relatively high RPN scores prior to risk mitigation (identify a cutoff value based on overall RPN distribution)
- Post vs. prior risk mitigation RPN scores have the largest percentage reduction.

In addition, consider failure modes that map to a large number of components (functional locations) in the plant. In this case, the risk mitigation benefit on one component may have a large multiplier effect.

Information collection for prioritization. Provided that the criticality assessment and the FMEA are performed thoroughly, the majority of the information required for risk mitigation prioritization is already available. TABLE 1 summarizes the required and desirable information to be collected for the failure modes selected.

In TABLE 1, the required information is typically included in the standard output of the criticality assessment and the FMEA. By referring to the criticality assessment or FMEA ranking matrix, the approximate values of the financial loss (severity), the probability of occurrence or the detectability can be obtained for a given component or failure mode. To allow easy and accurate decision-making, the information should be as specific as possible. For example, a loss of $100,000/occurrence is preferable to a loss of $50,000/occurrence–$250,000/occurrence, although the latter can be estimated statistically.

Depending on the level of detail of the criticality assessment and FMEA results, the desired information may take extra effort to obtain. However, including that information in the calculation would increase the confidence level of the prioritization.

Risk mitigation benefit quantification. Depending on the type of information listed in TABLE 1 that can be collected, the amount of risk mitigation for a failure mode can be estimated accordingly. For each type of risk mitigation strategy, the benefit can be calculated by the difference between the lifecycle cost (LCC) prior to the risk mitigation and the LCC after the risk mitigation, plus the cost of implementation of the strategy, as shown in Eq. 1:

$$\text{Benefit} = \text{LCC}_{\text{Prior}} - (\text{LCC}_{\text{Post}} + \text{Implementation cost}) \quad (1)$$

For failure modes with a constant failure rate (i.e., random failure), the calculation of LCC is straightforward. Otherwise, a software capable of performing random lifecycle simulation can be used. Other advantages of using this type of software include its capability to handle random input parameters and address imperfect repairs or failure detection.

TABLE 3. Risk mitigation example

Failure mode	Strategy name	Annual labor	Investment	Annualized benefit[a]	5-yr ROI[b]
1	3-yr compressor major overhaul	240 hr	N/A	$96,000	4[c]
2	Annual compressor inspection	72 hr	N/A	$36,000	5[c]
3	Spare blower	N/A	$10,000	$6,000	3
4	Redesign pump system	N/A	$25,000	$10,000	2

[a] This benefit needs to be calculated following risk mitigation benefit quantification
[b] Assume the labor hours are the same every year and the investment is a one-time spend
[c] Labor rate is assumed to be $100/hr

TABLE 2 lists the implementation costs that must be considered for each of the risk mitigation strategies. The accuracy of the benefit estimate depends on the quality of the input parameters. Ideally, most input parameters should be determined in a data-driven approach, with a combination of data sources including FMEA, computerized maintenance management system data and inputs from maintenance and operations personnel. Commonly, some data is unavailable, in which case necessary assumptions can be made using industry averages, adjusted by the client's operating environment and equipment conditions.

When the failure consequence is related to EHS, it is difficult to calculate the benefit in terms of dollar value. In these cases, decisions on risk mitigation should follow the EHS guidelines of the company and site.

Resource allocation optimization. In general, each risk mitigation category is subject to one type of constraint. For example, PM and PdM are usually labor-intensive and subject to labor availability, while spare part and redesign both require an initial investment and must stay below the financial budget.

Both the labor and financial constraint categories can be further divided into sub-categories, each with their own constraints. For example, labor resources may include engineers, technicians (mechanical, instrumentation and electrical, boilermaker, contractors, etc.) and planners, while the financial budget may include maintenance and capital.

Both labor and budget constraints are time-sensitive. When prioritizing risk mitigation tasks, it is important to keep the timeline of risk mitigation tasks aligned with the foreseeable constraints.

The optimization of prioritization is demonstrated with a simple example (TABLE 3). Consider four risk mitigation tasks, each associated with a different failure mode. The first two tasks are PM and PdM, respectively, and are subject to the labor constraint. The last two tasks are spare and redesign, respectively, and are subject to the budget constraint.

Consider a labor constraint of 300 hr/yr and a budget constraint of $30,000. Only one of tasks 1 and 2, plus one of tasks 3 and 4, can be implemented. If the goal is to maximize the total amount of benefit, then tasks 1 and 4 will be chosen; however, if the goal is to maximize ROI, then tasks 2 and 3 will be chosen.

Compared with this example, in real life the optimization problem will be much more complicated, with (1) many more candidate tasks for risk mitigation, (2) more categories of constraints, (3) a single task with multiple constraints, (4) a possible random distribution of benefit values instead of a deterministic value. However, the problem remains a linear constrained optimization problem that can be solved with the proper mathematical tools.

Recommendations. Even for a complicated prioritization problem, the benefit and constraint information can be summarized in a similar format, as shown in TABLE 3.

Based on the optimization results, different combinations of risk mitigation tasks can be recommended for implementation. These combinations, along with their pros and cons, should be presented to the client for decision-making. It is also good practice to include the following information in the summary to enable easier decision-making:

- Plant area
- System and subsystem
- Criticality ranking and primary driver (operational vs. EHS).

The proposed procedure can help prioritize risk mitigation tasks identified from equipment strategy development. The procedure takes advantage of the valuable information previously obtained from the criticality assessment and the FMEA, determines the most value-added risk mitigation tasks—given the constraints of labor and financial resources—and helps the plant owner make data-driven decisions.

Prioritizing risk mitigation tasks can be complicated, as the results are often affected by many factors, including equipment operating conditions, maintenance effectiveness and condition monitoring capabilities. A more extensive study should be conducted to provide customized solutions that fit each plant's conditions. In some cases, for example, relatively simple solutions (such as an operator's round) may prove effective. It is also worth mentioning that precision-driven maintenance,[2] although not included as a risk mitigation strategy in this article, may have significant potential for future reliability improvement. HP

LITERATURE CITED

[1] Apelgren, R., "Use P-F intervals to map, avert failures," *Reliability Plant*, July 2019.
[2] Troyer, D., "A proactive lifestyle for your machines—Focus on FLAB," *Machinery and Equipment MRO*, August 2020.

TONG ZOU is a Senior Engineering Specialist at T.A. Cook Consultants. He has more than 16 yr of reliability engineering experience in the power generation, automotive, oil and gas and petrochemical industries. Dr. Tong's expertise includes reliability-centered maintenance, system and component reliability analysis, equipment life data analytics and reliability-based design optimization. Since joining T.A. Cook, he has worked on client projects focusing on reliability improvement.

MIKE RHODES, MANAGING EDITOR
Mike.Rhodes@HydrocarbonProcessing.com

Nickel-iron-chromium alloy in bar and hollow bar

Sandvik, a developer and producer of advanced stainless-steels, special alloys, titanium and other high-performance materials, has launched Sanicro® 825 (FIG. 1), the company's first-ever nickel-iron-chromium alloy in bar and hollow bar, for improved performance in corrosive, high-temperature environments.

Sanicro 825 (UNS NO8825) extends the company's growing Sanicro portfolio of nickel alloys and austenitic stainless-steels for aggressive wet, corrosive and high-temperature, pressure, acidic and seawater conditions.

A high-strength alloy with a minimum 40% nickel content, Sanicro 825 has excellent corrosion resistance to acids and alkalis, superior resistance to stress corrosion cracking (SCC) and good corrosion resistance to phosphoric, nitric, sulfuric and organic acids, and seawater, caustic chloride alkalis and ammoniac media.

Stable and easy to machine and weld, the new alloy is ideal for use in a wide range of components and installations, including heat exchangers, evaporators, offshore piping systems, seawater coolant, valves and flanges. It serves a multitude of industries, including oil and gas, chemical, petrochemical, pulp and paper, pickling equipment, nuclear fuel processing and food processing.

Available in 3 m–7 m lengths with an outside diameter (OD) ranging from 20 mm–60 mm, Sanicro 825 offers a cost-effective alternative to superalloys, such as Alloy 625 and Alloy 718. Its chemical formulation has been tailored within EN, UNS and ASTM standards.

New smartphone for Division 2

Pepperl+Fuchs ecom, a leading manufacturer of mobile devices rated for hazardous areas, offers a new mobile solution for frontline workers in Division 2 areas: the Ex-Cover Pro D2. Building on the strengths of the Samsung Galaxy XCover Pro, the Ex-Cover Pro D2 has been certified for use in potentially volatile settings and is designed to help those in the oil and gas, chemical, petrochemical and pharmaceutical industries to work faster and more efficiently, while also operating safely. It offers the durability frontline workers need with integrated features, like Samsung Knox customization and management capabilities, push-to-talk, barcode scanning and more to help users streamline workflows.

The Ex-Cover Pro D2 is durable and specifically designed for hazardous work environments where collaboration, productivity, data security and employee safety are paramount. The device's IP68 rating means it can handle dust, dirt, sand and water. It can withstand drops of up to 1.5 m without a case, and its MIL-STD 810G certification makes it reliable in extreme altitudes, humidity and other severe environmental conditions.

The rugged and thoughtfully designed Ex-Cover Pro boasts a 6.3-in. edge-to-edge display with Gorilla® Glass 5 to deliver a heavy-duty, high-quality viewing experience. Glove Mode also offers enhanced touch capabilities with gloves and in wet conditions. Ex-Cover Pro D2 comes with the latest Android™ 10 operating system and Samsung One UI 2.0 user interface, ensuring intuitive operation. Long battery life means the Pro lasts as long as the work does, providing > 14 hr of power. When out servicing a long route, field personnel can easily replace the battery with a spare to keep the phone going for as long as needed.

The Ex-Cover Pro features push-to-talk and walkie talkie integrations with platforms like Microsoft Teams, enabling workers to be highly productive outside the office and in tougher environments. With its built-in functionalities, as well as software and hardware solutions, the Ex-Cover Pro D2 can easily be set up and customized to suit the needs of any Division 2 industry. The multi-purpose device

FIG. 1. Sandvik's Sanicro® 825 nickel-iron-chromium alloy in bar and hollow bar.

is NFC-ready with enhanced security and reliability features from TEEgris, making it an excellent mobile point of sale (mPOS) system.

The Ex-Cover Pro D2 comes as an unlocked device, and is compatible with AT&T and Verizon in the U.S., as well as with Bell and TELUS in Canada. Pepperl+Fuchs collaborated with Samsung on the design and certification of the Ex-Cover Pro D2.

Continuously monitoring the state of liquids

A new radio wave-based analysis technology, developed by the Finnish high-tech company Collo, makes it possible to continuously monitor the state of any liquid in industrial processes (FIG. 2), be it thick slurries, resins, adhesives, coatings, emulsion, water or any other fluid.

Collo's technology is based on an electromagnetic resonator that emits a continuous radio frequency field into the liquid. The signal reacts to interferences caused by different components, chemicals and phases in the liquid. The analyzer immediately warns if the process is disturbed in any way so that the process can be adjusted according to the online data.

The sensors can be placed anywhere in the process to optimize the use of raw materials and chemicals in critical process

FIG. 2. Collo radio wave-based analysis technology.

FIG. 3. The ASCO™ Series RCS fully assembled pilot valve system.

steps. The analyzer monitors the process constantly, compared to manual samples that provide a delayed snapshot of the process status at a given time. The advantage of real-time monitoring is that it takes away the guesswork when adjusting the process, which in turn saves chemicals, materials, energy and time.

The Collo Analyzer simultaneously measures eight proprietary parameters from a liquid, which together form the liquid's fingerprint. If these characteristics are changed during processing—for example, if unwanted solids are formed or the chemical balance is negatively impacted—the analyzer shows the changes so that corrective measures can be made immediately.

Unlike generic measurement techniques, Collo doesn't just measure the liquids, but combines data with sophisticated analytics, providing actionable information for improved process performance. For optimal result, analytics are adjusted for each liquid application.

Once adjusted, the same system can be replicated in similar processes. This is especially beneficial for customers that have a vast number of identical liquid processes, as they are able to achieve significant economies of scale with Collo. The analyzer is very low-maintenance, as the sensor is not sensitive to dirt and does not require cleaning.

As Collo's technology displays real-time measurements, it is possible to continuously adjust the process according to the results. Process deviations are identified immediately and before they cause issues in the process or decrease its performance. For example, resin mixtures in electrical components insulation processes require a correct level of viscosity. If the critical stages can be analyzed online, the process will be steadier, resulting in less scrapped parts or faulty components shipped to customers, and decreased waste and energy and materials use.

Programmable digital chart recorder

Bristol Instruments introduces the OMR 700 digital data recorder. This instrument is expandable from 4–96 input channels and can record from 2 hr to 132 yr of data, depending on the number of channels and frequency of data acquisition.

Operated from a color touchscreen display, the OMR 700 data recorder has intuitive controls. The signal data is stored and displayed, and the instrument can be configured to display data as bar graphs or line graphs—each with numeric values or only numeric values. The display is sealed against ingress to IP64 and an optional housing is available rated at IP67.

The data recording rate is as fast as 1 millisecond and can be set as infrequently as 10 min. Input or output modules can be mixed and matched in the eight available I-O slots. I-O cards for the OMR 700 have up to 12 analog inputs per module. Up to four analog outputs or 10 digital outputs per module can be accommodated, and data outputs are another option.

The OMR 700 recorder can be connected to a PC through 10/100BaseT Ethernet. Data can be stored in binary or CSV formats. Besides OMR data viewer software, included with OMR 700, Excel can be used to view and manage CSV data.

Data recording can be based on time periods, an assigned button press or custom trigger events set by the user. Pre-triggers can also be set to define how many values are stored before a triggering event.

OMR 700 analog input types include: eight DC voltage ranges, four DC current ranges, AC voltage, current, power and frequency inputs, Pt, Ni and Cu RTDs, nine thermocouple input types, including J and K, as well as strain gauge inputs. Accuracy for analog inputs is as accurate as ± 0.15% of range, depending on card type. Digital inputs include 12 V–30 V, frequency and up/down counters. Counters measure as wide a range as 0.1 Hz–1 MHz.

The OMR 700 digital data recorder accepts supplied power between 80 V and 250 V AC/DC. All analog modules are fully isolated from the internal bus and some are galvanically isolated between channels as well as outputs.

Redundant control pilot valve system

The ASCO™ Series RCS (redundant control system) is a fully assembled pilot valve system that provides high process reliability while maintaining required plant safety levels. It achieves a higher level of process safety and reliability by using a redundant, fault-tolerant architecture, high diagnostic coverage and automated testing. The ASCO Series RCS (FIG. 3) can be used in SIL 3 applications and helps mitigate spurious and nuisance trips.

In the process control industry, uptime is everything. The need for dependable, on-demand shutdown solutions to maintain safety and allow for easy maintenance is critical to running a productive, efficient operation. The ASCO Series RCS operates without any single point of failure that might otherwise result in an unplanned closure of the process valve.

The ASCO Series RCS also allows for

individual solenoid valve testing, maintenance or replacement without bypassing, meaning there is no interruption to critical process functions. Since this keyed bypass functionality allows online maintenance and testing without process interruption, it can also help mitigate unnecessary nuisance trips.

Automated, online testing (SOV and PST) available with the ASCO Series RCS helps improve safety while also increasing reliability. Diagnostic feedback from either a pressure switch or a TopWorx GO™ Switch allows the ASCO Series RCS to be used in SIL 3 applications, where it can help greatly reduce spurious trip rates.

Available in both 2oo2 and 2oo3 architectures, the ASCO Series RCS provides everything a user needs—from basic safety and reliability to advanced diagnostics—and features some of the industry's highest flowrates.

With ASCO Series RCS, all necessary features are already built in, resulting in both time and money savings from not having to build the system in the field, while gaining the critical benefits of improved safety and reliability. From emergency shutdown and burner management systems to high-integrity pressure protection and flaring systems, the ASCO Series RCS is a safe, reliable and efficient choice for process valve diagnostics and actuation.

Alternative design for shaft end connections in compliance within API STD 671

Riverhawk Co., a provider of engineered tooling and solutions for turbomachinery and rotating equipment, has announced that its Hydraulic Shrink Disc, an alternative design for shaft end connections that utilizes a clamping force on the hub, is now an acceptable alternative to traditional shaft end connections as defined in the newest release (5th Ed.) of the American Petroleum Institute (API) standard 671 (API STD 671).

API STD 671 specifies the requirements for high-performance couplings for the transmission of power between the rotating shafts of two machines in special purpose applications. These applications include petroleum, petrochemical and natural gas industries.

The Hydraulic Shrink Disc is a legacy Riverhawk product that has been used as a replacement hub on shafts for other similar applications, including (but not limited to) generator, pumps and refrigeration applications. The Hydraulic Shrink Disc operates by using hydraulic pressure that activates a clamping force that squeezes the hub on the shaft vs. the typical dilation and pull-up designs. It can also replace the keyed and spline mounted hubs. Another key advantage of the Hydraulic Shrink Disc is its ability to provide a reduced overhung moment by allowing the use of smaller diameter shafts to transmit the same amount of torque.

Clamped shaft end connections is an emerging technology that has become more popular with end users as well as original equipment manufacturers (OEMs) because it has been solving issues commonly found among traditional shaft end connections. HP

Technology and Business Information for the Global Gas Processing Industry

GAS PROCESSING & LNG

GasProcessingNews.com | MAY/JUNE 2021

TREATING AND NGL

TURBOMACHINERY

Special Supplement to
HYDROCARBON PROCESSING®
Pipeline & Gas Journal

SPECIAL FOCUS: PIPELINES AND TRANSPORT

TURBOMACHINERY

HEAT EXCHANGE

TREATING AND NGL

LNG

BACK TO BASICS

DEPARTMENTS

COLUMNS

Cover Image: Two overlapping ends of a pipe string are raised and cut on a pipe-lay ship before they are welded together for the Nord Stream 2 pipeline from Russia to Germany. Photo courtesy of Nord Stream 2 and Axel Schmidt.

H_2 blending into gas networks for "greener" methane

A. BLUME, Editor-in-Chief

Facing regulatory uncertainty, competition from renewable energy and increasing calls for decarbonization, natural gas pipeline operators are studying the blending of hydrogen (H_2) into their networks to produce lower-carbon methane and test their equipment's capability for handling H_2/methane blends.

In Europe, Australia and the U.S., trial projects are studying blends of 5%–20% H_2 and methane for use in regional gas networks. For example, a group of 23 European gas infrastructure companies plan to build a dedicated, affordable H_2 transport network from modified gas infrastructure. This project, referred to as the European Hydrogen Backbone, is set to span 7,200 mi (11,600 km) by 2030 and 24,670 mi (39,700 km) across 21 countries by 2040.

Meanwhile, Australia's natural gas pipeline owners are looking to future-proof their A$75 B of assets by conducting tests to blend H_2 with natural gas. Some Australian states are pushing for a 10% H_2 blend in gas pipelines by 2030, which can be safely accommodated without modification to infrastructure or appliances.

The U.S. government's HyBlend project is examining the long-term effects of H_2 at different blends on metal and polymer piping and pipeline materials to determine the costs of upgrading existing pipeline networks to make the shift. Technical challenges of blending H_2 into gas networks include the risk of leakage related to possible H_2 embrittlement of metal, the risk of explosion from using H_2 in appliances at blends of greater than 25%, compatibility issues with existing compressors, and H_2's lower energy density compared with natural gas. Blends of up to 15% H_2 are anticipated to require only moderate modifications to infrastructure, but blends of 20% H_2 and higher could present more difficult conversion challenges.

Furthermore, Sempra Energy is carrying out a series of demonstration projects in the U.S. to test various blends of H_2 in pipeline segments of polyethylene, steel and a combination of the two. Sempra subsidiary Southern California Gas Co. is also conducting a study with technology developed by HyET Hydrogen to strip and compress pure H_2 from natural gas blends (FIG. 1).

For more H_2 technology and projects news, please subscribe to our new technical journal, *H2Tech,* and visit H2-Tech.com. **GP**

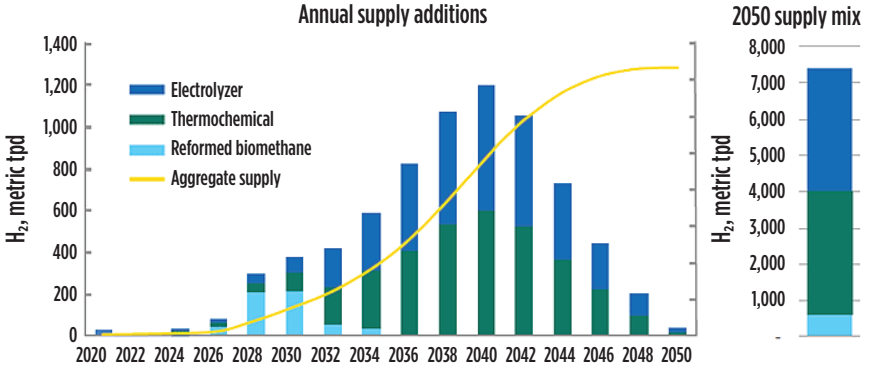

FIG. 1. Projected buildout of California H_2 supply, 2020–2050. Source: University of California–Irvine.

GAS PROCESSING & LNG
www.GasProcessingNews.com
P. O. Box 2608
Houston, Texas 77252-2608, USA
Phone: +1 (713) 529-4301
Fax: +1 (713) 520-4433
Editorial@GasProcessingNews.com

PUBLISHER
Catherine Watkins

EDITORIAL
Editor-in-Chief
Adrienne Blume

Managing Editor
Mike Rhodes

Editor-in-Chief/Associate Publisher, *Hydrocarbon Processing*
Lee Nichols

MAGAZINE PRODUCTION
Vice President, Production
Sheryl Stone

Manager, Advertising Production
Cheryl Willis

Manager, Editorial Production
Angela Bathe Dietrich

Assistant Manager, Editorial Production
Melissa DeLucca

Artist/Illustrator
David Weeks

Graphic Designer
Krista Norman

ADVERTISING SALES
See Sales Offices, page 42.

Gulf Energy

President/CEO
John Royall

CFO
Alan Millis

Vice President, Upstream and Midstream
Andy McDowell

Vice President, Finance and Operations
Pamela Harvey

Vice President, Production
Sheryl Stone

Vice President, Downstream
Catherine Watkins

Other Gulf Energy Information titles include: *H2Tech, Hydrocarbon Processing®, World Oil®, Petroleum Economist©, Pipeline & Gas Journal* and *Underground Construction.*

Scotland launches biomethane refueling

CNG Fuels has started building Scotland's first public access renewable biomethane heavy goods vehicle (HGV) refueling station, which will allow fleet operators to run their vehicles on low-carbon fuel, support net zero plans and save money.

The station, located at the Eurocentral industrial estate off the M8 near Bellshill, will refuel up to 450 lorries per day when it opens in November 2021, enabling HGVs to make low-carbon deliveries across Scotland. Most of England and Wales is already within a 300-mi round trip of a biomethane refueling station, and the new facility will put Inverness and Aberdeen within this range.

Renewable biomethane is the lowest-carbon, most cost-effective alternative to diesel for HGVs—it is 35%–40% cheaper and cuts vehicle greenhouse gas emissions by up to 85%. From 2021, CNG Fuels will dispense fully carbon-neutral fuel by sourcing biomethane from manure.

Excelerate, ExxonMobil, Albania study LNG terminal

Excelerate Energy LP, ExxonMobil LNG Market Development Inc. and the Republic of Albania have agreed to conduct a feasibility study for the potential development of an LNG project at the Port of Vlora in Southern Albania.

Under the MOU, Excelerate will conduct a study to explore the potential of an integrated LNG-to-power solution that includes developing an LNG import terminal, converting and/or expanding the existing Vlora thermal power plant, and establishing small-scale LNG distribution to Albania and the surrounding Balkans region.

Albania relies on hydropower plants, which can become unreliable during times of drought. LNG would bring reliable, affordable, and cleaner energy to the region and complement Albania's hydropower-based electricity production. ExxonMobil will identify opportunities to support the supply of LNG into Albania. The project pre-feasibility report is expected to be delivered in Q3 2021, while the targeted startup for the LNG import project could be as early as 2023.

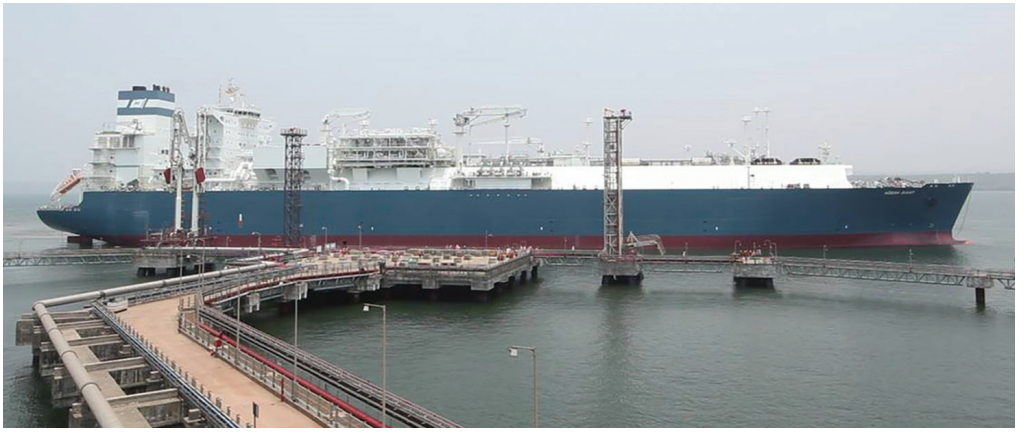

India welcomes first FSRU

India's first floating storage and regasification unit (FSRU), the *Höegh Giant,* arrived at H-Energy's Jaigarh Terminal in Maharashtra on April 12, sailing from Keppel Shipyard in Singapore. The arrival of the FSRU marks a new chapter in India's mission for accelerated growth of LNG infrastructure. The country aims to increase the share of natural gas in its energy mix from the present 6% to 15% by 2030.

The 2017-built *Höegh Giant* has storage capacity of 170,000 m^3 and installed regasification capacity of 750 $MMft^3d$ (equivalent to about 6 MMtpy). H-Energy has chartered the FSRU for a 10-yr period. *Höegh Giant* will deliver regasified LNG to the 56-km-long Jaigarh-Dabhol natural gas pipeline, connecting the LNG terminal to the national gas grid.

The facility will also deliver LNG through truck-loading facilities for onshore distribution and is capable of reloading LNG onto small-scale LNG vessels for bunkering services. H-Energy intends to develop a small-scale LNG market in the region, using the FSRU for storage and reloading LNG onto smaller vessels.

Novatek to offer 60% stake in Arctic LNG 2

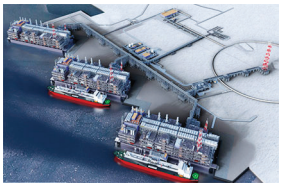

Russian independent LNG producer Novatek is offering up to a 60% stake in its Arctic LNG 2 project as collateral for long-term financing of the project. Novatek seeks to raise $11 B in external financing and aims to secure the funds by the first half of 2021.

The $21-B project, which received final investment approval in 2019, is expected to be launched in 2023 and to reach its full capacity of almost 20 MMtpy in 2026. The project's equity partners include Total, China National Petroleum Corp., China National Offshore Oil Corp., Mitsui & Co. and Japan Oil, Gas and Metals National Corp. In January 2021, Russia's Sberbank approved financing of up to €3 B ($3.5 B) for the Arctic LNG 2 project.

Australia's gas supply gap delayed to 2026

Plans by billionaire Andrew Forrest to ready an LNG import terminal by 2022 mean that Australia will not suffer a gas supply shortfall until 2026—2 yr later than previously forecast, according to Australian Energy Market Operator (AEMO). AEMO also noted that existing Victorian production is declining faster than previously projected.

Gas producers' forecasts for maximum daily capacity from existing, committed and anticipated southern fields in 2023 are nearly 20% lower at present than they were 1 yr ago. Gas fields in the Gippsland Basin, which largely supplies the southern states, are becoming exhausted and losing flexibility to ramp up output during peak winter demand. LNG imports and gas storage will be needed to cover peak demand.

Forrest's privately owned Squadron Energy won state approval to build an LNG import terminal at Port Kembla in New South Wales, with a startup target of late 2022. AEMO's forecast did not include a controversial LNG import terminal proposed by AGL Energy, which is awaiting approval from the Victorian government. If approved, AGL expects to start importing gas by mid-2023. AEMO also highlighted growing uncertainty in its demand forecasts as manufacturers switch away from carbon-based fuels to renewable power and hydrogen.

Ghana's Tema LNG terminal to receive first cargo

Tema LNG terminal in Ghana, the first offshore LNG receiving terminal in sub-Saharan Africa, was scheduled to receive its first LNG cargo at the end of May. Tema LNG, consisting of separate regasification and storage vessels, is backed by Helios Investment Partners and Africa Infrastructure Investment Managers.

A long-term supply deal between Royal Dutch Shell and Ghana National Petroleum Corp. supports the project. As of the time of publication, the terminal was ready for operation and was awaiting an agreement between Shell and Ghana National Petroleum Corp. on the first delivery date.

The terminal received its floating regasification unit (FRU), built by Jiangnan Shipbuilding, in January. The LNG FRU is designed for a regasification capacity of around 1.7 metric MMtpy of LNG and will be in operation for approximately 20 yr.

The FSU will work in conjunction with an upgraded, 127,500-m^3 LNG carrier to deliver 250 $MMsft^3d$ of natural gas. It will also provide facilities to bunker, reload or breakbulk LNG. Spanish LNG terminal operator Reganosa will run and maintain the terminal.

Occidental unit to transport CO_2 from Texas LNG project

Oxy Low Carbon Ventures, a subsidiary of Occidental Petroleum, will offtake and store the CO_2 captured from NextDecade Corp.'s planned Rio Grande LNG export plant at the Port of Brownsville, Texas. Oxy will move CO_2 from the Rio Grande LNG project and permanently sequester it in an underground geologic formation in the Rio Grande Valley.

NextDecade expects the carbon-capture-and-storage (CCS) project at Rio Grande to reduce permitted CO_2 emissions at the plant by more than 90%. The company also anticipates achieving a final investment decision (FID) on a minimum of two trains at Rio Grande LNG in 2021 and the CCS project soon after the FID is taken on the plant.

Rio Grande is one of 14 North American projects awaiting FID in 2021. Most of the FIDs were carried over from 2020, postponed by the COVID-19 pandemic. Another project at Brownsville, Annova LNG, decided in March to halt development of its proposed LNG export terminal due to changes in the global LNG market.

Woodfibre LNG signs second BP deal for LNG plant

Canadian LNG developer Woodfibre LNG has signed a second agreement to sell LNG from its proposed export plant in British Columbia to a unit of oil major BP. That puts the plant a step closer to getting built in a market that has seen some cancellations in recent months, but not many new projects.

Woodfibre will sell 0.75 MMtpy of LNG to BP Gas Marketing Ltd. over 15 yr on a FOB basis. The agreement will increase BP's total LNG offtake to 1.5 MMtpy from Woodfibre's proposed 2.1-MMtpy plant. Woodfibre could take a final investment decision in 2021, which would put the plant on track to produce first LNG in 2025 at a cost of around C$1.6 B–C$1.8 B.

Over the past two months, Annova, another LNG developer, stopped work on its export plant in Brownsville, Texas, and Pembina paused development of its Jordan Cove project in Oregon.

Sempra likely to delay Texas Port Arthur LNG decision to 2022

U.S. energy company Sempra Energy will likely move its planned final investment decision (FID) on the Port Arthur LNG export plant in Texas from 2021 to 2022, according to company executives. The Port Arthur project is one of 13 North American LNG export projects that was expected to take an FID in 2021. Most of those were carried over from 2020, and several were also carried over from 2019.

In addition to Port Arthur, Sempra, which owns part of the operating Cameron LNG plant in Louisiana, is building an export plant at its Costa Azul LNG import facility in Mexico and is developing second phases for Cameron and Costa Azul.

Global LNG demand has increased every year since 2012 and hit record highs every year since 2015, mostly due to fast-rising demand in Asia. However, in recent years, global gas buyers have been slow to sign new long-term contracts needed to finance the multibillion-dollar projects due to overbuilding of LNG export terminals in 2019, COVID-19 demand destruction and the collapse of global natural gas prices in 2020, as well as the U.S.-China trade war during former U.S. President Trump's administration.

Analysts expect global LNG demand to grow by about 3%–5% each year between 2021 and 2025. That projected growth rate, however, is much lower than the 11%–12% yearly increases seen from 2017–2019.

Cheniere, Shell deliver carbon-neutral LNG to Europe

U.S. LNG company Cheniere Energy supplied a carbon-neutral cargo of LNG to Royal Dutch Shell as part of a long-term agreement, joining a list of sellers neutralizing emissions as more buyers commit to environmental targets. The carbon-neutral LNG cargo was supplied from Cheniere's Sabine Pass facility in Louisiana and delivered to Europe in early April, with offsets bought from Shell's global portfolio of nature-based projects.

Consumers are increasingly paying a premium to have emissions neutralized from the wellhead through consumption. In March, Russian energy giant Gazprom said it had delivered its first carbon-neutral shipment to Europe. Pavilion signed a long-term contract with Chevron Corp. earlier this year and one with Qatar Petroleum in late 2020 requesting data on greenhouse gas emissions. Last year, China National Offshore Oil Corp. bought from Shell its first cargoes with offset carbon emissions.

Cheniere exported a record of 133 cargoes of LNG in Q1, despite having part of its facilities down for a few days during the winter storm in February. The company operates five LNG processing units at its Corpus Christi terminal. A sixth train at Sabine Pass is almost 1 yr ahead of schedule and could start production before the end of 2021.

Total presses ahead with Papua LNG, sees 2023 decision

French energy group Total has agreed with the Papua New Guinea government to proceed with an LNG project in the country, which had been delayed due to the pandemic, with a final investment decision due in 2023.

Total added in a statement that it would re-mobilize teams involved in the project. Total and its partners, ExxonMobil Corp. and Oil Search Ltd., had initially planned to develop Papua LNG in tandem with an expansion of ExxonMobil's PNG LNG terminal in a $13-B project adding three new production units at the PNG LNG plant, to help save billions of dollars.

However, Exxon has not agreed to terms sought by the Papua New Guinea government for the P'nyang gas development that would help feed the expansion, as Papua New Guinea Prime Minister James Marape pushed for bigger benefits for the country from the deal. Instead, Total's Papua LNG project will go ahead with two new production units to be built at the PNG LNG site, fed by the Elk Antelope gas fields.

Africa's floating LNG sector looks to regain footing post-pandemic

S. OIRERE, Contributing Writer

The drive to harness natural gas reserves in Africa is supporting low-emissions energy generation and effective monetization of marginal and small gas fields. This has created space for investment in floating liquefied natural gas (FLNG) and floating storage and regasification (FSRU), although the sector is still in its infancy.

COVID-19 slows gas developments. The pace of natural gas exploration, production and processing in sub-Saharan Africa was gaining momentum prior to the COVID-19 pandemic, which slowed or disrupted project progress in many areas from early 2020. Due to national lockdowns and restricted international travel, some gas production and processing operations in Africa were disrupted or delayed as the project owners and partners mapped out how to maneuver the pandemic disruption. Prior to the COVID-19 outbreak, Africa's total proven natural gas reserves had surpassed 509.6 Tft^3, equivalent to 7.3% of the world's total proven reserves, according to International Gas Union (IGU) estimates.

As gas production and processing projects pick up again post-pandemic, interest in the construction and operation of FLNG facilities is expected to grow in Nigeria, Ghana, Cameroon, Senegal, Mozambique and Equatorial Guinea. The countries' respective national oil companies are seeking partnership with mid-capacity independents to launch FLNG systems to gain footing in global LNG markets and meet local demand for gas supply.

Due to financial constraints and difficulties in mobilizing adequate investment resources for increased offshore natural gas production, greater focus has been placed on assets in shallow waters or onshore, but with capacity to connect them to nearshore liquefaction facilities. The following sections showcase projects that are in operation or under development.

Nigeria licenses first FLNG. The emerging FLNG market in Africa is largely concentrated in countries that have a mix of ultra-deep and deepwater, midwater and shallow-water natural gas blocks, with Nigeria becoming the latest to license its first FLNG project.

The country's State Department of Petroleum Resources recently awarded a license to establish an FLNG production facility to indigenous firm UTM Offshore Ltd. The facility will have a capacity of 1.2 MMtpy and process 176 MMsft^{3}d of natural gas and condensate from the mature Yoho field. UTM Offshore has not specified if it will order a new FLNG unit for the project or utilize an existing vessel. The project will contribute to the Nigerian government's initiative to severely curb gas flaring in the country.

Tema LNG ramps up. In neighboring Ghana, a new FSRU vessel has been developed at the Port of Tema. Owned by Access LNG, the floating regasification terminal was developed by a JV of London-based Helios Investment Partners, a leading Africa-focused private investment firm; and German LNG infrastructure developer Gasfin Development SA.

Unlike FLNG projects that target the development of marginal and small natural gas reserves, Ghana's floating LNG project will be used to support electricity generation.

The 95-m FSRU was built at China's CSSC Jiangnan Shipyard and fitted with two IMO type C tanks for a storage capacity of 28,000 m^3. It was delivered to Ghana in January 2021. The FSRU's annual regasification capacity is approximately 1.7 MMtpy of LNG, with a lifespan of 20 yr. The FSRU and the floating storage unit (FSU) have a combined storage capacity of 145,000 m^3–160,000 m^3.

The Emerging Africa Infrastructure Fund (EAIF) announced a $31-MM boost for the project after signing an agreement with Access LNG. The investment will contribute to reducing carbon emissions from the project, contributing to Ghana's long-term energy needs, and strengthening its economic stability and economic development efforts.

According to Ogbemi Ofuya, a Partner at Helios Investment Partners, the Tema project "…positions the energy sector in Ghana for both growth and environmental sustainability so that when the world recovers from COVID-19, Ghana will have the energy infrastructure needed to help it compete."

***Hilli Episeyo* develops stranded reserves.** An FLNG nearshore the coast of Cameroon has been developed under a partnership of Golar LNG, Perenco and Cameroon's national oil company, Société Nationale des Hydrocarbures (SNH). The FLNG will offer a low-cost, fast-tracked solution for stranded gas projects that are too small to justify a large-scale LNG development.

FIG. 1. The Greater Tortue Ahmeyim project, led by BP, Kosmos Energy, Petrosen and SMHPM, will produce 2.5 MMtpy of LNG at a nearshore hub on the maritime border of Senegal and Mauritania. Photo: BP.

Perenco operates the Sanaga South and Ebome gas fields, which hold an estimated 500 Bft^3 of gas offshore Cameroon. In 2016, Perenco and SNH signed a 10-yr deal with Golar LNG to develop Sanaga South's remaining LPG reserves for the Cameroonian market and LNG for international consumers. Subsequently, Perenco and SNH made the decision to fully develop the country's LNG market with the support of the FLNG *Hilli Episeyo,* the world's first converted LNG FPSO, now owned and operated by Golar Hilli Corp., a subsidiary of Golar LNG Ltd.

The conversion of a 1975 Moss LNG carrier with a storage capacity of 125,000 m^3 to an FLNG facility was carried out at the Keppel Shipyard in Singapore under a $735-MM contract. Keppel chose Black & Veatch as the topside subcontractor to supply the liquefaction technology. Gazprom subsidiary Gazprom Marketing & Trading Singapore Pte Ltd. (GM&TS) will purchase all of the LNG produced by the *Hilli Episeyo* for export.

Tortue FLNG eyes startup next year. A similar floating gas system is being developed for Senegal and Mauritania. The Greater Tortue Ahmeyim project (**Fig. 1**) is designed to produce gas from a deepwater/midwater FPSO to an FLNG vessel at a nearshore hub on the maritime border of the two countries.

BP, Kosmos Energy, Senegalese national oil company Petrosen and Mauritanian national oil company SMHPM are collectively developing the Greater Tortue Ahmeyim project. The FLNG's designed capacity is 2.5 MMtpy, with total recoverable gas in the field estimated to be around 15 Tft^3.

Outlook for African FLNG. Other major projects that have boosted Africa's FLNG market at different levels of implementation include the $8-B Coral South FLNG project in Mozambique. The project is listed as the world's first ultra-deepwater FLNG facility, with a capacity to liquefy more than 3.3 MMtpy of natural gas.

Also, in Equatorial Guinea, UK-based Ophir Energy and OneLNG, a JV of Golar LNG and Schlumberger, are attempting to revive a floating LNG terminal with an estimated annual capacity of 2.5 MMtpy.

Although Africa's FLNG market is still under development, optimism about its future growth is abundant. Oil and gas major Shell expects global LNG demand to double to 700 MMtpy by 2040 as gas plays a significant role in shaping a lower-carbon energy system. Shell's Integrated Gas and New Energies Director, Maarten Wetselaar, presented the following outlook: "While we see weak market conditions today due to record new supply coming in, two successive mild winters and the Coronavirus situation, we expect equilibrium to return, driven by a combination of continued demand growth and reduction in new supply coming onstream until the mid-2020s." **GP**

SHEM OIRERE is a freelance journalist based in Nairobi, Kenya. He has spent more than 10 yr covering various sectors of Africa's economy, and has had numerous articles published in several international publications and websites. He earned a higher degree in journalism from the London School of Journalism, and is also a member of the Association of Business Executives (ABE).

EastMed pipeline faces technical challenges, competition

E. GERDEN, Contributing Writer

The outcome of the EastMed pipeline project—a planned, 1,900-km (1,180-mi), subsea pipeline that would supply Europe with 9 Bm^3y–12 Bm^3y of natural gas from the Eastern Mediterranean—is being closely watched by many on the global stage. If built, it would be the world's longest and deepest subsea gas pipeline and provide considerable energy resources to European markets.

Partners eye fast track to 2025. Greece, Cyprus and Israel signed an agreement in January 2020 for the EastMed pipeline to pump offshore gas between Israel and Cyprus to Greece, and then to Italy and other Southeast European countries. The three stakeholder countries plan to take a final investment decision (FID) by 2022 on the €6-B project. The consortium hopes to develop the pipeline as soon as 2025, in an effort to fast-track Europe's diversity of gas resources.

Proposed pipeline reroute. In contrast to the original pipeline plan, Greece and Egypt are discussing the possibility of changing the pipeline route due to technical and economic difficulties. Delek Drilling and Chevron, the operators of Israel's Leviathan field (**FIG. 1**), have announced their intention to boost gas supplies to the Egyptian market, further calling into question prospects for the EastMed pipeline.

According to Derek Drilling, proven and probable reserves of the Leviathan field are 377 Bm^3, with another 270 Bm^3 classified as promising resources, as of July 2020. The known reserves are insufficient to fill the original pipeline route.

Instead of running to Cyprus through an offshore pipeline, the newly proposed pipeline route would run from Israel's Leviathan gas field to Egypt by land and then to the Greek island of Crete, passing through the Greek-Egyptian Exclusive Economic Zone. Gas would be liquefied at Egypt's Damietta and Idku LNG terminals near Port Said. The gas then would be transported as LNG to Europe.

The project reroute would promote Egypt's status as a regional gas hub and provide an opportunity for Israel to gain direct access to the European gas market. However, even if Egypt is added to the project, EastMed's feasibility relies heavily on potential new discoveries of gas reserves in the region.

Reroute raises tensions. The proposed reroute heightens political tensions between Cyprus and Turkey, as Cyprus would be left out of the new pipeline route, leaving Turkey to advance its interests in the Eastern Mediterranean. Turkey's requests for inclusion have so far largely been ignored by regional players. More recently, however, Israel has expressed a desire to cooperate with Turkey on natural gas exports.

Conduit to Egypt threatens EastMed. A second pipeline project by Israel and Egypt may threaten the EastMed project and double Israel's gas exports to Egypt. Israel started exporting gas to Egypt in early 2020 through an existing pipeline that runs offshore before crossing the Sinai Peninsula overland.

Now, the two countries have proposed a new, $6-B–$7-B, subsea pipeline to send gas to be liquefied in Egypt before being exported to the EU. The capacity of the pipeline could reach 10 Bm^3y at the initial stage, with a possible expansion to 20 Bm^3y. The construction of the pipeline is expected to take only 1 yr–2 yr.

Up to $235 MM could be invested in the construction of the second export pipeline to increase gas supplies to Egypt, which is boosting gas exports from its own fields, including Zohr. Egypt also has spearheaded the establishment of the East Mediterranean Gas Forum, which includes Cyprus, Greece, Israel, Italy, Jordan and Palestine.

FIG. 1. Israel's Leviathan gas field, operated by Delek Drilling and Chevron. Photo: Teckhnoblog.

Pipeline challenges to Russian gas. Both the EastMed pipeline and the newly proposed pipeline from Israel to Egypt threaten Russian state-owned Gazprom's expansion into Southern Europe's gas markets over the next decade. The pipeline projects would also negatively affect Russian independent producer Novatek, which supplies 80% of the gas from its Yamal LNG flagship project to the EU market.

Regardless of whether the proposed pipeline projects go ahead, Europe will still rely on Russian gas. For this reason, the startup of Gazprom's delayed Nord Stream 2 gas pipeline from Russia to Germany is of critical importance for Russia and European consuming countries. The pipeline was delayed as some companies were forced to withdraw from construction efforts under threat of U.S. sanctions; however, Nord Stream 2 is now on track for completion in 2021/2022 and was 92% finished as of late March. **GP**

EUGENE GERDEN is an international contributing writer specializing in the global oil refining and gas industry. He has been published in a number of prominent industry publications.

Use a seven-step procedure to mark piping CMLs

A. ANWER and **K. ALAM,** ADNOC Gas Processing, Ruwais, Abu Dhabi, UAE

Piping is considered one of the most valuable assets in any hydrocarbon processing facility. Many meters of piping run through these facilities, transporting process fluid from one unit to another. The integrity of piping systems is as important as that of any other asset in the facility; however, when studying piping systems of different sizes, metallurgy and lengths, it is important to consider inspection plans that are not only effective but also efficient with respect to the effort required. Marking more condition monitoring locations (CMLs) than necessary wastes time and effort, but marking far fewer CMLs than needed puts piping integrity at risk.

Several guidelines are available to define the CMLs on a given piping system; however, the plant inspector has the ultimate control over defining, inspecting and redefining the CMLs throughout the piping life. This is a continuous process (FIG. 1), and balance can be achieved only after at least one full round of design life is finished with no loss of process containment. Data from similar operators may help achieve a balance to the piping inspection, which is normally the first step in defining CMLs for any piping system. A stepwise approach in defining, inspecting and redefining CMLs on any piping system is detailed in the following sections.

Step 1: Data from similar operators. Sharing data between industries and companies worldwide is not uncommon, but it can be difficult to organize. Nonetheless, if a data-sharing arrangement can be made, information from similar service operation can help in many ways.

Of significant usefulness are comparable CMLs marking data for piping systems in similar service. These provide a quick start for other operators to launch this continuous process. If already normalized for a given piping system at a hydrocarbon processing facility, verified CMLs can save massive effort for a new operator. However, if such data is not available or not easily obtained, then this step can be skipped.

Step 2: Identification of credible damage mechanisms. Information on credible damage mechanisms must be obtained before starting work to define the CMLs on any piping system. If a risk study has already been performed for the facility, then this document may contain the relevant information.

Step 3: Define inspection tasks. Inspection tasks must be defined after information on credible damage mechanisms is made available. These inspection tasks can provide a way forward for marking appropriate CMLs. In most cases, inspection tasks for piping include measuring the wall thickness to identify different forms of corrosion. Most CMLs are marked to perform ultrasonic inspection tasks.

Step 4: Corrosion rate determination. When designing a piping system, an initial design corrosion rate is always considered to define the lifespan of a piping system. This critical information defines the corrosion allowance. For all piping systems, the initial design corrosion rate must be tabulated to determine the actual corrosion rate.

To determine the actual corrosion rate, initial marking of CMLs should be done only on baseline thickness locations, if available. If baseline thicknesses have not been measured, then CMLs should be defined at bare minimum locations to enable the inspector to determine the actual corrosion rate.

The initial inspection frequency can be increased so that this exercise can be completed. A round of three inspections should be sufficient for accurately calculating the corrosion rate of any piping system.

Step 5: CMLs placement. An inspector must evaluate the placement of CMLs based on several factors:

- Credible damage mechanism
- Inspection task
- Design corrosion rate/allowance
- Piping geometry
- Piping accessibility.

Services that are not safety-critical upon loss of process containment should be separated and, by default, only one CML in each 60-m run of piping should be defined. However, all other services that are declared process-critical should be examined in detail, considering the previously listed factors.

Any damage mechanism that is general in nature should result in fewer CMLs; however, damage mechanisms may change with changes in piping geometry or piping tags, resulting in varying process conditions and more CMLs, as a general rule. A single run of piping with similar process conditions throughout, with no changes to temperature, flow or other process conditions, does not need to be inspected at many locations. Conversely, piping runs with many branches bring changes to existing process conditions, which may impact the credible damage mechanism and require inspection at multiple locations.

FIG. 1. General work view of a piping inspection.

FIG. 2. Inspection port shown as an example for CML reading.

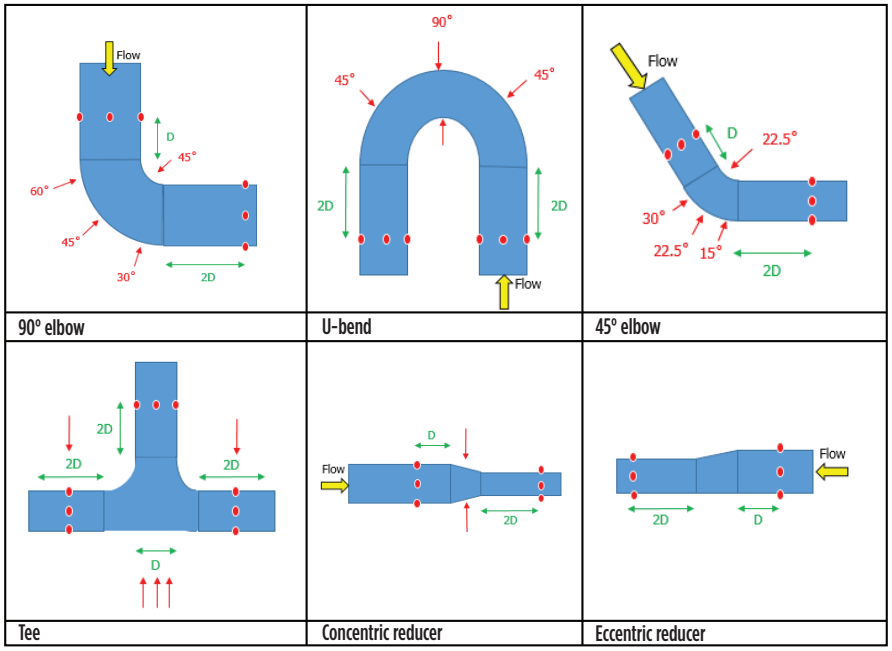

FIG. 3. Typical TMLs for different piping fittings.

The type of inspection task to be performed on a given CML also impacts the total number of CMLs. Ultrasonic thickness inspection, the most common task performed on piping, gives only the data related to corrosion or pressure boundary thickness. Other necessary inspections may include temperature monitoring at desuperheater locations or profile radiography to search for debris accumulation at piping deadlegs. CMLs to monitor such conditions are specific and largely unlimited. Wall thickness measurements, obtained through ultrasonic thickness testing, can be limited or controlled to some extent.

During the project design phase, the definition of corrosion allowance for any piping system is given after carefully studying the anticipated corrosion rate of the metallurgy put into service, with reference to a defined design life. The corrosion allowance definition should be respected; however, it should also be reviewed and verified—this is the core work of the inspection team monitoring the piping systems.

When CMLs are defined for corrosive services, an appropriate metallurgy and corrosion allowance combination for the design life must also be in place. Careful attention must be paid to the verification of this combination through minimum CMLs.

Step 6: Field marking. CML markings on isometrics should be replicated as closely as possible in the field. This becomes especially important when data must be analyzed and CMLs must be redefined. Inaccuracy in positioning the CMLs can result in incorrect or irrelevant readings for the analysis. When looking into the records of any industry, the data from a single, incorrectly located CML can be seen to follow an erroneous pattern over time.

Field marking of CMLs is of utmost importance and can be achieved through many ways, including in-house resources or external support. Insulation demands more work than bare piping; however, it should be kept in mind that marking CMLs is a one-time activity for as long as the CMLs remain the same. Solutions (FIG. 2) are available for each marking requirement including piping, thin insulation, thicker insulated tanks, vessels, hot service and even cryogenic processes.

Step 7: Performing inspection on CMLs. After CMLs are defined, the core business of recording the actual readings starts. How to take these readings is of utmost importance. A more relative term used for thickness recording is thickness monitoring locations (TMLs). If a CML is defined only for thickness monitoring, then TMLs can be defined for that specific CML.

Each CML can have multiple TMLs. As a general rule, along a 360° band of piping, readings should be recorded at each quadrant, with each reading representing a single TML. Different recommendations are available to define TMLs on different CMLs in piping. One recommended definition for different piping configurations and fittings is shown in FIG. 3.

Marking CMLs for all piping groups provides a baseline work for evaluating and maintaining piping integrity. When performing this marking work, each step as defined above should receive proper attention. Ignoring any of the seven recommended steps may lead to recording incorrect data that may not be representative of the piping integrity. **GP**

ASHFAQ ANWER is an Inspection Engineer working in gas processing in Ruwais, Abu Dhabi, UAE. He has more than 14 yr of professional inspection experience in ammonia-urea complexes, petrochemical units, and oil and gas industries. He has extensive expertise in material selection, corrosion mapping and control, fitness-for-service studies, defining inspection framework and implementing inspection plans for old and new units.

KAISER ALAM is an Inspection, Corrosion and Metallurgy Specialist with more than 7 yr of experience in static equipment inspection, fitness for service, material selection, and inspection strategies and procedures. His experience is predominantly in the downstream oil and gas industry in the Middle East.

Evaluate ERW and SAW pipes for onshore buried gas pipelines

S. ZARDYNEZHAD, TurboTech Consulting Corp., Calgary, Alberta, Canada

The question of whether to use electric resistance welding (ERW) pipe or submerged arc welding (SAW) pipe for an onshore gas pipeline project arises frequently. Each type of pipe has different advantages and disadvantages, which should be studied in detail to make a rational and reliable decision.

The quick answer may be to perform an internet search for a comparison of the two types; however, most of the resources readily available on the internet about this subject are based on advertising and sales efforts. Good engineers use hard data and factual experience to make equipment purchasing decisions.

In this article, ERW and SAW pipes—the latter of which may be double (DSAW) or longitudinal (LSAW) style—for onshore gas pipelines are explained. A general comparison between ERW and DSAW/LSAW is developed. Finally, selection criteria are proposed to help engineers and project managers decide which type of pipe to use in their project. **Note:** This article does not recommend or address spiral SAW pipes for buried natural gas pipelines, as this type of pipe is not acceptable by many clients' specifications.

Examples of pipeline failure. Examples of pipeline failure for both ERW and DSAW/LSAW due to weld seam fracture illustrate the many possible causes for pipeline failure. Many similar failure examples for each type are available from different regions around the world. These incident reports suggest the need for bias-free studies to determine all potential factors and classify them as contributing causes, direct causes and root causes.

ERW seam weld failure.[1] Williams Gas Pipeline experienced an incident caused by a brittle failure. A long split along or near a seam weld caused a catastrophic failure of the 16-in. (outside-diameter, or OD) pipeline at 1.5 mi downstream of the compressor station. The pipeline was manufactured of API 5L Grade X46 ERW pipe.

FIG. 1 shows (a) a large piece of the failed ERW pipe containing the origin of failure, (b) the same piece marked with flow direction and the distance from the other end of the failed piece, and (c) a mockup reconstructed from the failed piece with a split along a seam. The white circle indicates the failure origin at 52.5 in. from the other end of the failed piece (upstream). The insert shows a photo of the fracture surface. FIG. 2 shows more detail of the fracture surface of the pipe.

DSAW/LSAW seam weld failure.[2] Enbridge experienced the rupture of a 34-in. (OD), API-5L-X52 crude oil pipeline and oil release near Cohasset, Minnesota. A fatigue crack along the DSAW/LSAW pipe's longitudinal seam weld generated during the transport of pipes caused the failure, based on the incident report.[2] The project used ERW pipe from Canadian

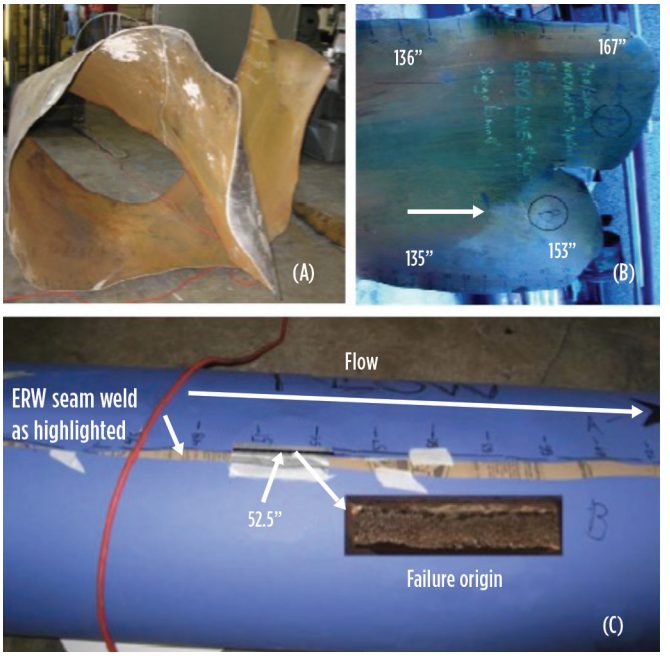

FIG. 1. The failed ERW pipe containing the origin of the failure and the reconstruction mockup for the failure.[1]

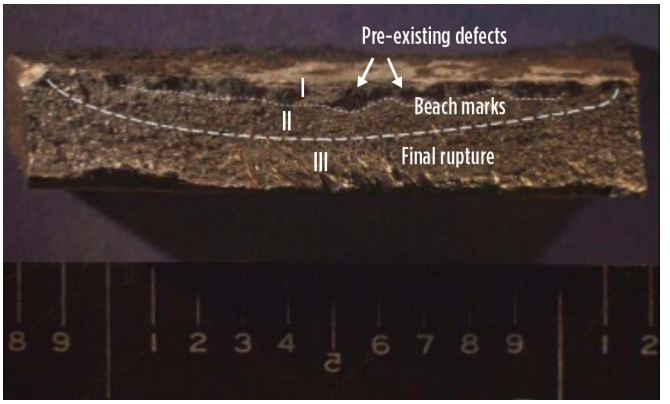

FIG. 2. Failure origin of the ERW pipe showing a three-zone feature: Zone 1: initiation sites, Zone 2: subcritical crack growth region, and Zone 3: final fracture area.[1]

TABLE 1. Comparison between ERW and DSAW/LSAW pipes

Parameter	ERW pipe characteristics	DSAW/LSAW pipe characteristics
Raw material note: Pipes should be normally fully killed, continuously cast steel	Normally hot coils.	Normally plate, but hot coils can also be used.
Grades	No difference; however, depending on the mill, market conditions and required thickness, there may be a limit on pipe production for specific grades. The mill's confirmation is required at an early phase of the project.	
Pipe size	Normally 1 NPS–26 NPS.	Normally 16 NPS–64 NPS; check with the mill for special-order pipe sizes.
Wall thickness	Since hot coils are used as the starting material, thinner wall-thickness pipe can be manufactured. The maximum thickness may reach 1 in.; however, mill confirmation and mill past production experience for similar service are recommended to be verified.	Normally 0.5 in.–2 in., depending on grade and pipe size; however, mill confirmation and mill past production experience for similar service are recommended to be verified.
Welding process	Two electrodes, usually copper, are used to apply pressure and current. The electrodes are disc-shaped and rotate as the material passes between them. This allows the electrodes to stay in constant contact with the material to make long, continuous welds.	In this method, a welding arc is submerged in welding flux. A continuous solid filler wire is fed from the outside. The pipe is first welded from the inside and then welded from the outside. The welds penetrate 100% of the pipe wall and produce a strong bond of the pipe material.
Weld seam surface quality	The weld seam is flat, which may cause difficulty and impact productivity of work during construction for field bending.	The weld seam is not flat, and is higher than the steel plate surface. The tolerance of the weld seam height should be agreed upon initially, as this impacts the pipe coating performance.
Weld seam defects	Lesser defects, but a high risk of oxide air in the seam, which impacts the chemical composition and microstructure.	Whether or not defects are present depend on the definition of defects, as well as on the pipe grade, pipe thickness, mill's quality control, etc.
Weld seam chemical composition	Since no filler metal is used to complete the weld seam, there is usually little difference in the chemical composition of the weld metal and the base metal. It is formed from the same material and is considered more homogenous in chemical composition with the base metal.	DSAW pipe requires a filler metal. When filler metal is used, the weld seam local region is somewhat different in chemical composition to that of the surrounding base metal.
Heat treatment of the weld seam	Normally, the weld seam is heat-treated before the shop hydrostatic test, creating a similar zone of microstructure. This must be confirmed by the mill, especially for sour service.	Normally, the weld seam is heat-treated before the shop hydrostatic test, creating a similar zone of microstructure. This must be confirmed by the mill, especially for sour service.
Weld seam length	The weld length of ERW pipe is the same as for DSAW/LSAW pipe; however, the risk of defects in the weld seam is lower than for DSAW/LSAW pipe.	The weld length of ERW pipe is the same as for DSAW/LSAW pipe.
Fracture toughness—pipe body	Impact testing commonly can be done by reputable mills up to M45.	
Fracture toughness—weld and heat-affected zone	Impact testing commonly can be done by reputable mills up to M45 for the fusion line. However, subject to the pipe grade, the specified toughness value and minimum metal design temperature (MDMT), some mills may have limitations.	
Pipe length	Reputable mills can produce either triple random lengths (approx. 18 m) or special-order quadruple random length (approx. 24 m).	Reputable mills can produce triple random lengths (approx. 18 m) with no jointers (girth weld) for DSAW/LSAW pipe, assuming availability of plate with suitable length at the time of order.
Y/T (yield to tensile) ratio	Reputable mills can produce pipe based on the pipe datasheet and specification.	
Pipe-making process productivity	Higher production productivity compares to that of DSAW/LSAW pipes, mainly because ERW pipes can form pipe continuously from an entire coil, while SAW plates are limited in length by the dimensions of the associated pipe-welding presses.	Lower production productivity compares to ERW pipes, mainly due to welding the pipe from the inside and outside.
Dimensional accuracy	Normally higher than DSAW/LSAW pipes.	Reputable mills can produce based on the agreed design tolerances.
Non-destructive testing	Normally, ultrasonic tests will be performed for the coil, weld and pipe as a whole. In addition, eddy current and magnetic particle testing may be carried out. Detail must be clarified with the mill before the order is placed.	Ultrasonic tests will be performed for the plate and weld. In addition, radiography will be performed for the weld seam and pipe ends. Magnetic particle testing may also be carried out. Detail must be clarified with the mill before the order is placed.

TABLE 1. Comparison between ERW and DSAW/LSAW pipes (CONT.)

Parameter	ERW pipe characteristics	DSAW/LSAW pipe characteristics
Tolerances	No difference in tolerance values between ERW and DSAW/LSAW pipes based on applicable standards (e.g., API or CSA). Reputable mills can produce pipe based on applicable codes, standards and specifications.	
Cost of production	ERW normally has lower cost of production; however, the total cost depends on other factors such as technical requirements, availability of the product at the time of order, the cost of plate/coils, market conditions, etc.	
Pipe-laying cost	As a result of high dimensional accuracy and the smooth weld surface of ERW pipes, lower costs can be expected in the pipe-laying process due to a reduction of workload in girth welding to join pipes, etc.	
Production in low-temperature region	Production of ERW pipe under extra-low temperature conditions is difficult.	
Heat and melting of the plate/coil	In the case of conventional ERW pipes, the outside and inside corner edges of the steel band heat and melt preferentially, resulting in non-uniform heating in the sheet thickness direction. In contrast, JFE Steel Corp.'s Mighty Seam material is heated and homogeneously melted in the wall-thickness direction.[5]	For DSAW pipes, plate edges are under the submerged arc welding during the welding operation, so its heat exchange and protection performance is relatively strong. The submerged welding process protects the steel from contamination by impurities in the air, such as oxygen.
Transportation fatigue cracking	Potential risk of pipe damage due to fatigue crack initiation during transportation by rail, truck and marine for both ERW and DSAW/LSAW. However, due to a narrow HAZ band, ERW pipe is less susceptible to fatigue load during transportation compared to DSAW/LSAW pipe.	
High-pressure application (> 100 barg design pressure)	Both ERW advanced pipe (e.g., JFE Steel Corp.'s Mighty Seam pipe[3]) and DSAW/LSAW pipe are similar in quality and lack of defects in the weld seams. For high-pressure gas transmission pipelines with design pressures of ≥ 100 barg, the author prefers to use DSAW/LSAW pipe from reputable pipe mills. This is mainly because the 100% weld penetration, radiographic testing, use of plate with homogeneous chemical composition, dual-weld configuration, use of electrodes and submerged welding process protect the steel edge from contamination of impurities and mitigate the risk of oxide inclusion to the weld.	

Phoenix Steel Products and DSAW/LSAW pipe from U.S.-based Kaiser Steel. All the longitudinal seam weld failures caused by fatigue cracks in the pipeline occurred in pipe manufactured by Kaiser Steel, as per the report[2] (FIG. 3).

ERW pipe background. ERW pipe is manufactured by cold-forming a sheet of steel into a cylindrical shape. A current is then passed between the two edges of the steel to heat it to a point at which the edges are forced together to form a bond without the use of welding filler material.[3]

Initially, this manufacturing process used low-frequency AC current to heat the edges. This low-frequency process was used from the 1920s until 1970. In 1970, the low-frequency process was replaced by a high-frequency ERW process that produced a higher-quality weld. Over time, the welds of low-frequency ERW pipe were found to be susceptible to selective seam corrosion, hook cracks and inadequate bonding of the seams, so low-frequency ERW is no longer used to manufacture pipe. The high-frequency process is still used to manufacture pipe for use in new pipeline construction.

In ERW pipe manufacturing, the weld seam is butt-welded after heating and melting the coil edges, using the Joule heat generated by passing a high-frequency current through the edges. At the seam of the butt weld, the welding beads on the pipe inside and outside surfaces are removed by online, full-length grinding, followed by seam heat treatment to improve the weld microstructure.

After ERW line pipes are cut to the specified length based on the purchase order (e.g., 6 m, 12 m or 18 m), the product undergoes the quality assurance process, which includes hydrostatic, ultrasonic and other non-destructive testing of the seam, as well as pipe body inspections of external appearance and dimensions.[4]

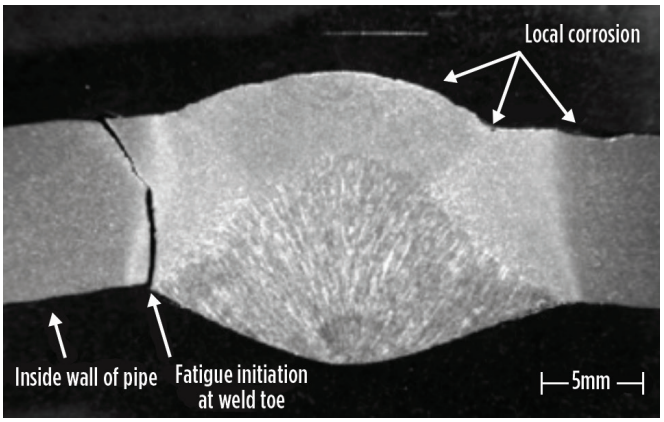

FIG. 3. Fatigue initiating at the toe of a weld on the interior surface of a DSAW/LSAW pipe.[2]

DSAW/LSAW pipes. DSAW/LSAW pipes are normally manufactured by continuous roll-forming of plate material into a tubular shape. The edges of the rolled plate are manipulated so that V-shaped grooves are formed on the interior and exterior surfaces at the locations of the seam and after tack welding. Butt-welding of the weld seam by submerged arc welding is done internally and then externally, followed by seam heat treatment to improve the weld microstructure.

After SAW line pipes are cut to the specified length based on the purchase order (e.g., 6 m, 12 m or 18 m), the product undergoes the quality assurance process, which includes hydrostatic, radiographic and ultrasonic testing of the seam, as well as pipe body inspections of external appearance and dimensions.[1]

Pipe produced by capable, reputable mills that is based on applicable codes and specifications should be subject to factual evaluation. The mill's experience in the production of each type of pipe must be requested and validated.

Comparison of ERW and DSAW/LSAW pipes. The author believes there is no general single option for pipe type (i.e., ERW vs. DSAW/LSAW) for use in large (> 16 nominal pipe size, or NPS) onshore gas pipelines that is correct and applicable for every application. Detailed study is needed based on the project constrains (i.e., costs, schedule, etc.), pipeline terrain, pipe specifications (e.g., grade, thickness, etc.), quality requirements, risks, pipe manufacturer's experience, client's pipe integrity experience, etc.

TABLE 1 gives a general comparison between ERW and DSAW/LSAW pipes for sizes above 16 in. onshore buried gas pipelines, based on the author's experience.

Proposed selection criteria. The selection between ERW and DSAW/LSAW pipes in a pipeline project requires detailed study, especially with regard to the mill's capability and experience. The author proposes the following steps for making a decision between ERW and DSAW/LSAW pipes:

1. Finalize critical operating and design parameters of the pipeline system, such as pressure, temperature, flowrate, minimum design metal temperature (MDMT), etc.
2. Conduct a reliable fracture control analysis based on the rich gas composition of the gas. The Battelle Two-Curve Method is a classic method that may be used.
3. Finalize the pipe grade, toughness and MDMT.
4. List the project constrains, including costs, schedule, quality, resources, risks, customer experience and preference, etc.
5. Conduct a market study and identify and manage the associated risks.
6. Decide on potential mills for the pipe manufacture and request their workload, past experience, production processes for different types of pipe, optional tests and inspections, etc.
7. Determine the evaluating parameters and associated weights.
8. Prepare a pipe datasheet based on two options (ERW and DSAW/LSAW) and send the datasheet with a material requisition to the potential mills.
9. As part of the quote for supply of line pipe, ask the manufacturer to submit a manufacturing procedure specification (MPS) document providing information on raw material, production process, inspection, test, etc. in detail.
10. Review the mill's quote and prepare technical and commercial evaluations in a bias-free atmosphere. Clarify unclear areas with the mills and a subject matter expert.
11. Consider a brainstorming session and ask for feedback from construction, the pipeline integrity team, shop inspectors, etc.
12. Conduct a cost-benefit analysis by considering the cost of risk and all key factors, rather than just the pipe cost quoted by the mills.

Recommendations. Many factors and risks must be considered in the selection of the final pipe type (between ERW and DSAW/LSAW) for an onshore buried natural gas pipeline project, based on the actual project requirements and conditions. The project manager should ensure that a bias-free engineering study has been conducted.

The author's conclusion is that for a pipe size of 16 in.–26 in., both ERW and SAW pipes are possible options for an onshore buried natural gas pipeline project. A final decision must be made based on a detailed study considering many factors besides the pipe cost. If a pipe longitudinal fails during operation, then the root causes, direct causes and contributing causes must be discerned.

The author believes that pipe produced by capable, reputable mills that is based on applicable codes, standards and specifications should be subject to factual evaluation and not personal judgment. The mill's experience in the production of each type of pipe in similar service, thickness, size and grade must be requested and validated. Engineers must ask for manufacturing procedure qualification testing (MPQT), manufacturing procedure specifications (MPS) and other standards.

Finally, continual advances in materials and welding techniques have resulted in dramatic improvements in the reliability of both ERW and DSAW/LSAW pipes. For high-pressure applications with design pressure of ≥ 100 barg, the author prefers DSAW/LSAW pipes, as discussed in the last row of TABLE 1.

Regardless of which type is selected, the risks of corrosion, fatigue and seam-related defects to the longitudinal weld seams of ERW and DSAW/LSAW pipes still exist. These defects should be monitored and identified through integrity assessments (e.g., hydrostatic tests, indirect assessments and direct assessments) and must be repaired when found. GP

LITERATURE CITED

[1] Limon, S. and D. Katz, "A ERW seam weld failure," Paper No. 08150, NACE International Corrosion Conference and Expo, 2008.
[2] U.S. National Transportation Safety Board, "Pipeline accident report: Rupture of Enbridge Pipeline and release of crude oil near Cohasset, Minnesota, July 4, 2002" NTSB/PAR-04/01, June 23, 2004.
[3] JFE Steel Corp., Line Pipe Catalog No. E1E-001-05.
[4] U.S. Department of Transportation, Pipeline & Hazardous Materials Safety Administration, "Fact sheet: Pipe manufacturing process," December 1, 2011, Online: https://primis.phmsa.dot.gov/comm/FactSheets/FSPipeManufacturingProcess.htm
[5] JFE Steel Corp., Technical Report No. 18, March 2013.

SHAHAB ZARDYNEZHAD is a registered senior mechanical/pipeline engineer in Alberta with more than 29 yr of experience working in the world's largest oil, gas and petrochemical projects. He has experience in many cross-country, long-distance pipeline projects including buried, aboveground, thermal, high-pressure, NGL and sour gas pipelines. He holds a BS degree in mechanical engineering from the University of Petroleum of Iran, an MS degree in industrial engineering from IUST Iran and MS degrees in project management and mechanical engineering (pipeline specialization) from the University of Calgary in Canada.

Pipelines update: PHMSA regulations and the PIPES Act of 2020

W. VANDIVER, NuGen Automation, Houston, Texas

With the reauthorization of the PIPES Act (i.e., Protecting our Infrastructure of Pipelines and Enhancing Safety Act of 2020), the oil and gas industry is in line for changes that will have an effect on nearly every pipeline operator. In addition to an increase in funding for the Pipeline and Hazardous Materials Safety Administration (PHMSA), the agency was given several mandates to issue final rules throughout the industry.

Many of the final rules have been a long time in coming and are the result of PHMSA's slow pace in responding to industry incidents and concerns. Now that the agency has deadlines, however, operators will be seeing changes in several sections of the 49 Code of Federal Regulations (CFR) Part 192 ("Transportation of natural and other gas by pipeline: Minimum federal safety standards") and 49 CFR Part 195 ("Transportation of hazardous liquids by pipeline") (FIG. 1).

In addition to a new disclosure consideration for pipelines facing violation penalties, the affected areas of operation are the new classification of idled pipelines, large-scale LNG facilities, onshore gas gathering lines and updated leak detection standards for gas pipelines, each of which are discussed with relation to events bringing about the mandate and how operators likely will be affected by the final rules.

PHMSA has some work to do, and operators will be feeling the effects in the coming years. In late 2020, former President Trump signed into law the reauthorization of the PIPES Act.[1] The original legislation, the PIPES Act of 2016, recently expired,[2] but the new version sets goals and objectives to further the government's efforts to build a safer industry through increased administration and rulemaking.

One of the most impactful benefits of the act is the increase in general funding for PHMSA safety programs through 2023, including an increase in personnel and federal grant programs.[3] However, many of the mandates will have a direct impact on operator compliance, and most regulation updates are slated to take place within the next 3 yr. With so much change on the horizon, operators will benefit from looking ahead to know what regulations might impact their operations.

Disclosure consideration. Among the changes brought about by the PIPES Act of 2020 is the addition of an operator's self-disclosure of an issue as part of violation considerations.[4] This amendment to considerations for civil penalties[5] is a benefit for operators. Moving forward, any civil penalties for violations relating to pipeline facility compliance regulations[6] and certain one-call notification regulations[7] will be calculated with the consideration of an operator's proactive attempts to correct known violations or self-disclosure of such violations before PHMSA discovers the violation on its own.

This amendment appears to be a form of reward to operators that not only take measures to correct compliance issues on their own but also to those that are honest about such issues with PHMSA via reporting. Moreover, the implication is that a lack of such behavior on the part of an operator facing civil penalties for violations is likely to be considered as well, meaning operators that wait until audits come around and cannot prove unawareness of violations are more likely to receive harsher penalties.

Final rule issuances. The PIPES Act of 2020 also requires PHMSA to issue several final rules within certain timeframes to increase safety standards across the oil and gas industry. While the list is extensive, many operators are likely to feel the effects of specific changes. In most cases, the mandates are a response to ongoing industry concern.

Idle pipelines. In 2019, the American Petroleum Institute (API), in conjunction with the Association of Oil Pipe Lines (AOPL), submitted a request for clarification of how certain amendments applied to idle pipelines, referring specifically to 49 CFR Part 195 in the final rule. However, PHMSA replied that such clarification was unnecessary because Pipeline Safety Regulations (PSR) did not consider "idle" an acceptable status for a pipeline, only "in-service/active" or "abandoned."

PHMSA went on to exemplify how "idle" pipelines could continue to pose safety risks and must be addressed as "active" pipelines.[8] The PIPES Act of 2020, however, not only defines "idle" pipelines but also addresses rulemaking regarding such assets. Specifically, pipelines now qualify as "idle" if they have ceased normal operations and will not resume service for at least 180 d, have been isolated from all product sources, and have either been purged or hold such a small volume of gas that no potential hazard exists.[9]

With the recognition of this classification, PHMSA is now required to provide regulation for such assets. The act states that PHMSA's final rule for how PSR ap-

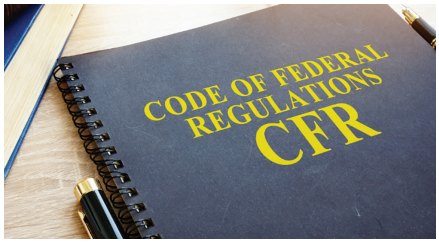

FIG. 1. The PIPES Act of 2020 will bring changes to several sections of 49 CFR 192 and 49 CFR 195 that will impact pipeline operators.

ply to idled pipelines must be issued within 2 yr.[10] For many operators, this will be a welcome addition to regulations, as they will not only be able to classify qualifying assets as "idle" instead of maintaining active pipeline compliance on such lines, but also will have more guidance on safety practices for idle pipelines.

Large-scale LNG facilities. In late 2020, the Government Accountability Office (GAO), which audits agencies on behalf of the U.S. Congress, released a report that examined federal regulations applicable to LNG facilities.[11] The report's chief finding was that LNG export facility regulations belonging to multiple agencies, including PHMSA, were out of date and lacking "current technical standards."[12]

In the case of PHMSA, relevant regulations were found to cite fire safety standards dating to 2001, despite the government recommendation that regulations that include technical standards be reviewed and updated accordingly every 3 yr–5 yr.[13] Specifically, the report identified that eight of nine standards relating to Part 193 and 45 of 55 regulations applying to natural gas facilities were outdated.[14]

Many critics say relevant PHMSA regulation updates are long overdue given a shift in the industry toward large-scale export LNG facilities.[15] On the heels of these findings—and in addition to an executive order that required PHMSA to update 49 CFR Part 193, which had received little attention since the 1980s[16]—it is no surprise that the PIPES Act now calls for PHMSA to update federal safety standards via a final rule for operating and maintaining large-scale LNG facilities, except for peakshaving facilities. This rule must be issued within 3 yr.

Operators can likely expect more specific regulations with stricter guidelines, as well as updated information pertaining to specific processes and procedures.

Onshore gas gathering lines. As recently as October 2019, PHMSA updated pipeline safety regulations for gas transmission pipelines, citing incidents that occurred over the past decade that resulted in several fatalities.[17] Meanwhile, API issued two standards in 2020 pertaining to the definition of gas gathering lines for regulation application and the operational practices for gas gathering pipelines after recognizing the need for more robust practices for gas gathering lines.[18]

Not as much movement as expected has been seen on PHMSA's part to update regulations pertaining to gas gathering pipelines, leading the PIPES Act to direct PHMSA to update minimum safety standards for onshore gas gathering pipelines as a final rule within 90 d. Operators should expect a revised set of minimum standards;[19] however, given the deadline, it is unlikely that PHMSA will be requiring radical changes, translating to a smoother updating process for operators.

Leak detection standards. Since 2003, PHMSA has spent an estimated $15.6 MM on leak detection research, with 87% applying to gas pipelines. Of this $13.57-MM portion, 75% applied to transmission lines, 68% applied to distribution lines, 59% applied to gathering lines and 3% applied to underground storage. Of that research, more than 80% focused on specific technologies.[20]

Moreover, as part of the Pipeline Safety, Regulatory Certainty and Job Creation Act of 2011, PHMSA was required to provide a report of leak detection systems (LDS) utilized by hazardous liquid pipeline facilities and transportation-related flowlines, along with their limitations and practicability.[21] In the same year, in response to a fatal gas transmission pipeline rupture and subsequent explosion, the National Transportation Safety Board (NTSB) issued a safety recommendation to PHMSA that operators of natural gas transmission and distribution lines be required to utilize LDS to assist in recognizing and locating leaks;[22] however, as of March 2020, PHMSA had not yet accomplished the provision of "a more comprehensive and effective leak detection system for the pipeline industry as a whole."[23]

Despite research and encouragement by other agencies, 49 CFR Part 192, which addresses gas transmission, distribution and regulated onshore gathering pipelines, makes mention of LDS only twice. In §192.935, which addresses operators' preventative and mitigative measures, the regulation mentions LDS as an additional measure,[24] while §192.620 states that LDS are an acceptable method of control for high-consequence areas for which response time to mainline valves exceeds 1 hour after an event is identified in a control room.[25]

Compared to the LDS sections specifically outlined in Part 195 for hazardous liquid pipelines, the regulations for gas pipelines are minimal. In an effort to make such regulations more robust and to reduce methane emissions, the PIPES Act of 2020 requires PHMSA to release a final rule within 1 yr that outlines more comprehensive LDS and repair programs for gas operators. To meet this goal, PHMSA must provide minimum performance standards with consideration for available technologies.[26] Operators should be prepared for updated regulation that is more specific as to acceptable leak detection methods, with considerations of the type and location of pipelines.

Additionally, while the PIPES Act refers to "advanced leak detection technologies," this includes commercially available technologies for continuous monitoring, as well as approved periodic survey methods. Therefore, while it is likely that CFR Part 192 will be brought closer to the level of specificity provided in CFR Part 195 for hazardous liquid pipelines, with potential regulations for computational pipeline monitoring, operators are more likely to find that their existing methods must be sharpened rather than replaced altogether.

While the reauthorization of the PIPES Act will certainly bring about change in the industry, it is important for operators to focus on how they can prepare for the new requirements, as well as the reasoning behind the updates. PHMSA regulations are not written and released overnight, and operators can be attentive to the development of new regulations and anticipate what resources will be needed to stay in compliance. However the regulations of the future affect them, operators must recognize that, as technology and operations evolve, so will the regulations that aim to keep our industry safe. **GP**

LITERATURE CITED

Complete Literature Cited available online at www.GasProcessingNews.com

WHITNEY VANDIVER is a Compliance Specialist at NuGen Automation LLC, where she specializes in control room management compliance and assists operators with state and federal CRM audits. Dr. Vandiver previously worked for a pipeline operating company in compliance-driven documentation and served as a volunteer editor for the drafting of API MPMS 18.2. She holds a BA degree from the University of Central Oklahoma and an MA degree and PhD, both in linguistics, from Purdue University.

Introduction to oil bearing turboexpander rotor dynamics

T. AVETIAN and L. E. RODRÍGUEZ, L.A. Turbine, Los Angeles, California

Turboexpanders are the ideal choice for processes with large pressure drops that require refrigeration or power recovery. Whereas a valve or orifice also can be used to effectively drop pressure, turboexpanders extract useful work from a flowing gas stream. Isentropic efficiencies as high as 90% are readily achieved with a turboexpander, resulting in much lower discharge temperatures.

Turboexpanders were introduced in the mid-1930s when the first machine was designed and implemented for air separation. The first unit for a natural gas application was designed and installed in the early 1960s. Over the years, many technological advances in design and manufacturing have allowed these machines to contribute to improvements in the efficiency of gas processing plants. Today, turboexpanders are standard in the natural gas industry for liquefaction and dewpoint control (FIG. 1). They are also used in the petrochemical industry for ethylene plants, air separation, refrigeration and power generation. Their relatively simple construction and hermetically sealed design generally lead to high reliabilities, with some plants operating the same units for many decades. Today, more than 5,000 turboexpanders are in operation worldwide.

Like a steam or gas turbine, a turboexpander is a rotating machine with an expansion turbine that converts the energy contained in a gas into mechanical work.[1] The work produced by the turbine is absorbed by a "loading" element that is mounted on the same shaft as the turbine. The loading element can be a dyno (oil brake), an electric generator or a centrifugal compressor stage. For the latter two, turboexpanders afford the opportunity to utilize energy that otherwise would not be available with a Joule–Thomson (J–T) valve. For instance, a compressor stage can be used as a pressure booster to meet a need in the process that otherwise would have necessitated a separate compressor driven by an electric motor or an engine.

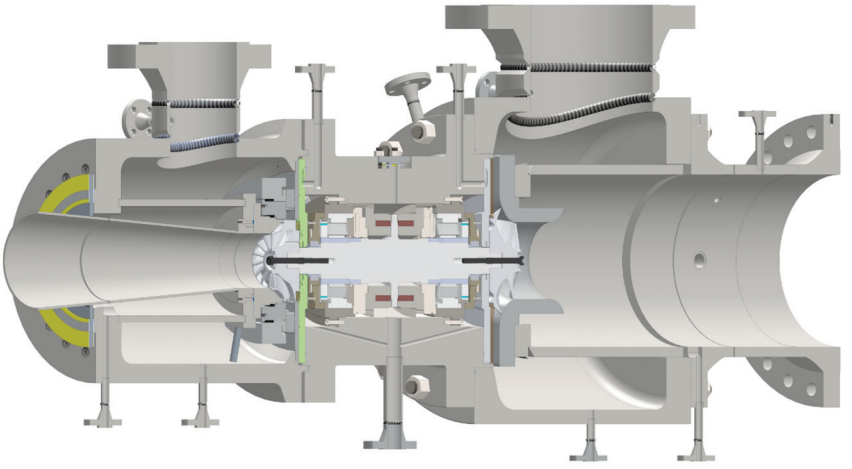

FIG. 1. Typical turboexpander design.

In the authors' experience, the more plant designers and end users understand about what is inside the "black box" of a turboexpander, the more successful they are when making critical decisions about their equipment. By being familiar with turboexpander rotor dynamic design, new machine designers and operators involved in a turboexpander project will be better equipped to fulfill their roles. The goal of rotor dynamic analysis is to ensure that catastrophic failure of a turboexpander does not occur due to vibration instabilities.

This article is meant to aid end users as they engage with turboexpanders, either at the procurement or operational stage, and offers an overview of turboexpander rotor dynamics, suggestions for what to look for from original equipment manufacturers (OEMs), and a case study describing the typical data presented in a turboexpander rotor dynamic design document.

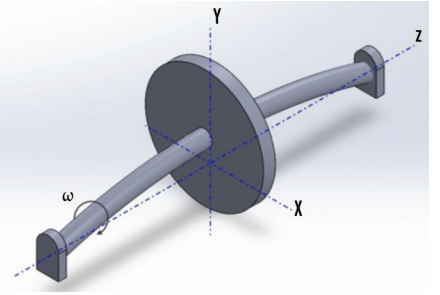

FIG. 2. Simplified rotor schematic.

The purpose of rotor dynamics. The field of rotor dynamics is concerned with the motions and associated forces of rotating shafts. In the study of rotor dynamics, emphasis is placed on five degrees of freedom, or types of motion, spanning lateral and torsional. Lateral motion is perpendicular to the shaft's rotation axis (the X–Y plane shown in FIG. 2). This includes translations in the X and Y directions and rotations about the X and Y axes. Torsional motion is rotation about the shaft's rotation axis—the Z axis. Axial motion in the Z direction is typically neglected for

machines supported in oil bearings, which is the focus of this article. **Note:** Axial motion in the Z direction is not neglected for active magnetic bearing control systems, where they can play a significant role.

Every turboexpander vibrates at some minimum level at least once per revolution because no rotor can be perfectly balanced. The OEM must, at a minimum, ensure that the design can tolerate the motions imposed by the residual imbalance in the rotor. Therefore, the primary objective of performing rotor dynamics analysis is to predict the motion of the rotor and ensure that the vibration levels are contained within acceptable limits.

Vibration limits may be set by available clearances between rotating and stationary components (e.g., bearings and seals), or by limitations on bearing load capacity. It is important to avoid operating near a critical speed, or natural frequency, to avoid very high amplitude vibrations and stresses.

Vibration limits can also be set by experience and empirical data. API-617, for instance, limits overall vibration to the lesser of 1 mil or $\sqrt{12{,}000/N_{mc}}$, where N_{mc} is the maximum continuous running speed of the machine. However, the OEM may find higher levels of vibration acceptable, depending on the type of bearing used, its clearances, and its stiffness and damping properties.

The term "critical speed" is worthy of comment. The definition of the term itself is not uniform across the industry. Therefore, it is important that the OEM and end user have a common understanding. For instance, API has slightly different definitions across different standards (e.g., API 616, API 617, etc.)

For the purpose of this article, the following definition is adopted: A critical speed is a shaft rotational speed at which the rotor bearing support system is in a state of resonance. This does not mean that a critical speed is necessarily an unstable operating point. A rotor running at a critical speed will normally run at elevated vibration levels. The level of vibration is inversely related to the amount of damping in the system. The level of magnification is known as the amplification factor. Rotor systems with sufficiently high damping, and therefore low amplification factor at around the critical speed, do not require any separation margin, or avoidance speeds, and therefore are typically ignored. As such, these sufficiently damped resonant frequencies are often not treated as critical speeds. Another reason for not considering sufficiently damped resonant frequencies is that they sometimes cannot be reproduced on the test stand.

Associated with critical speeds are their vibration modes, which are the shapes the shaft will take while running at a critical speed (**FIG. 3**). These mode shapes are commonly referred to as the first rigid (translatory or bouncing) mode, the second rigid (conical or rocking) mode, and the *n*th (first, second, third, etc.) bending mode.

It is not uncommon for engineering, procurement and construction companies (EPCs) or end users to request a rotor dynamics analysis report from the OEM for review during the design stage. The following section provides an overview of the components of such a report. For illustration purposes, results from an actual case study are included under each heading.

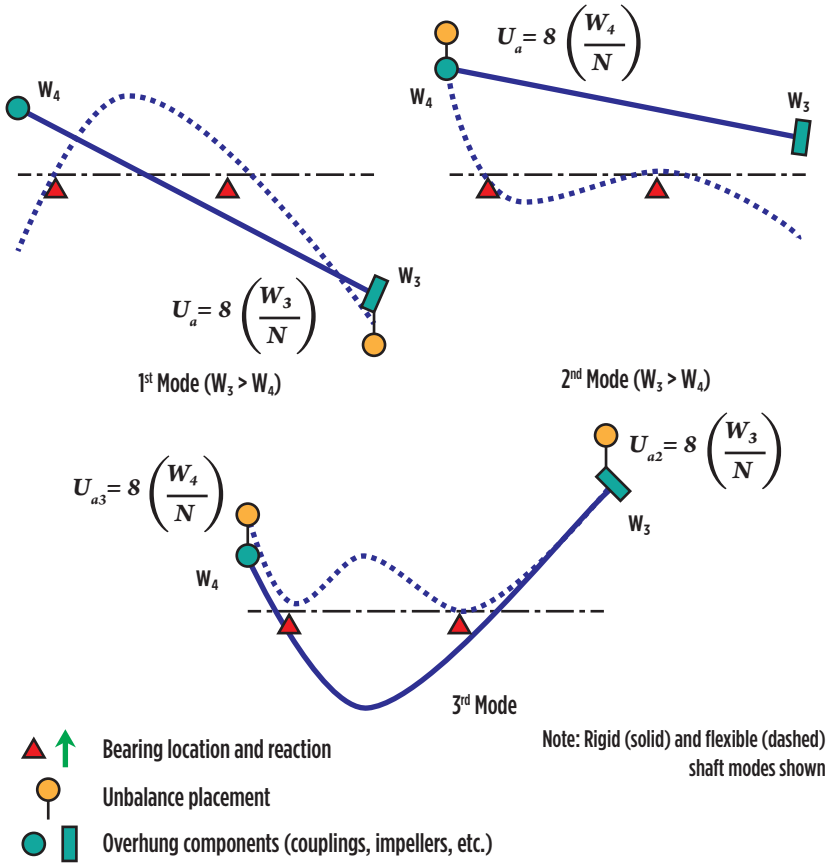

FIG. 3. Rotor mode shapes (from API 617).[2]

Case study machine. The machine in question is a 5,395-hp turboexpander processing approximately 170 MMsft^{3}d of natural gas feed (85.7% methane, 9.3% ethane, 2.5% propane, etc.) at a supply pressure and temperature of 865 psia and –27°F. The expander is loaded by a centrifugal compressor stage handling a flow of mostly methane (97.9%) at a flow rate of 285.61 MMft^{3}d and compressing at a pressure ratio of approximately 1.21. The rotor speed is 17,500 rpm at the design point, but it can fluctuate between +2.74% and –1.89% of that value, depending on the off-design operating conditions.

Rotor model. This machine was required to feature oil bearings. A rotor dynamic analysis (RDA) based on the finite-element technique was performed, using a commercial software to determine, among other issues, which design of radial oil bearings was most appropriate. The geometric model of the turboexpander rotor-bearing system is shown in **FIG. 4.**

The rotor consists of a solid shaft with one overhung wheel on each end. The wheels are computer numerical control (CNC) machined from forged aluminum alloy and attached to the shaft via a tight, slip-fit, polygon fit (which provides high

precision alignment during operation) and secured with a fastener (which prevents any axial displacement or loosening). Fully assembled, the rotor weighs 163 lb and is approximately 24 in. long. The shaft diameter at the bearing location is approximately 3 in.

The contribution of the wheels depends on their mass properties, namely weight, polar inertia (around the shaft axis), transverse inertia (across the shaft axis) and the location of the center of gravity. Those values are added to the "node" or "station," where the element is located on the shaft (see the legend in FIG. 4).

As for the bearings, their contribution consists of providing radial support stiffness to the rotor and attenuation of the vibrations. They are pictured in the model in FIG. 4 as springs. These are mathematically expressed as rotor speed-dependent stiffness and damping coefficient matrices.

Undamped critical speed (UCS) map. A UCS map is a plot of critical speeds vs. bearing stiffness (FIG. 5). This plot identifies the critical speeds and their mode shapes, as well as how they vary with different bearing stiffnesses. As such, the UCS map provides the designer with a starting point in the process to choose the type of bearing needed. For example, for a stiffer bearing, the designer may choose fixed-geometry bearings with tighter clearances, whereas for softer bearings, the choice may be tilting-pad or flexible-pivot bearings with larger clearances. The goal in choosing a bearing is to avoid potentially exciting a shaft's critical speed within the range of operating speeds required by the design of the turboexpander. FIG. 5 shows that a relatively softer bearing would be a better choice, considering that the critical speeds with stiffer bearings would be too close to the design speed.

Damped natural frequency (eigenvalue) map. A damped natural frequency map is a plot of natural frequencies (eigenvalues) vs. running speed (FIG. 6). It is produced with models of the bearings, seals and any other excitation phenomena incorporated. This plot is useful for checking the likelihood of exciting a natural frequency in the operating range, as well as evaluating potentially unstable operating points.

A common characteristic of turboexpanders is that their shafts have a low aspect ratio, meaning they are quite short relative to their diameter. As a result, the

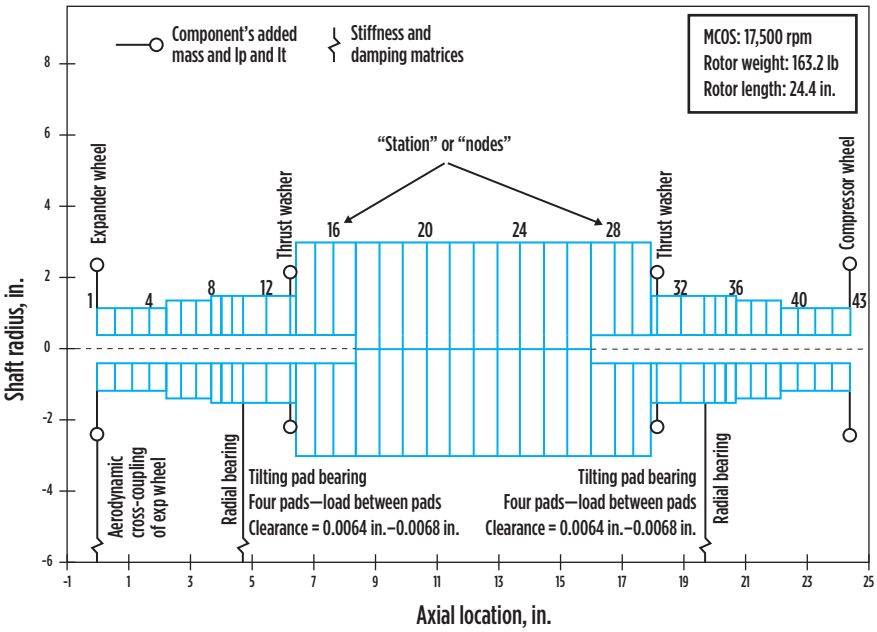

FIG. 4. Graphical depiction of the finite-element model for rotor dynamic simulations.

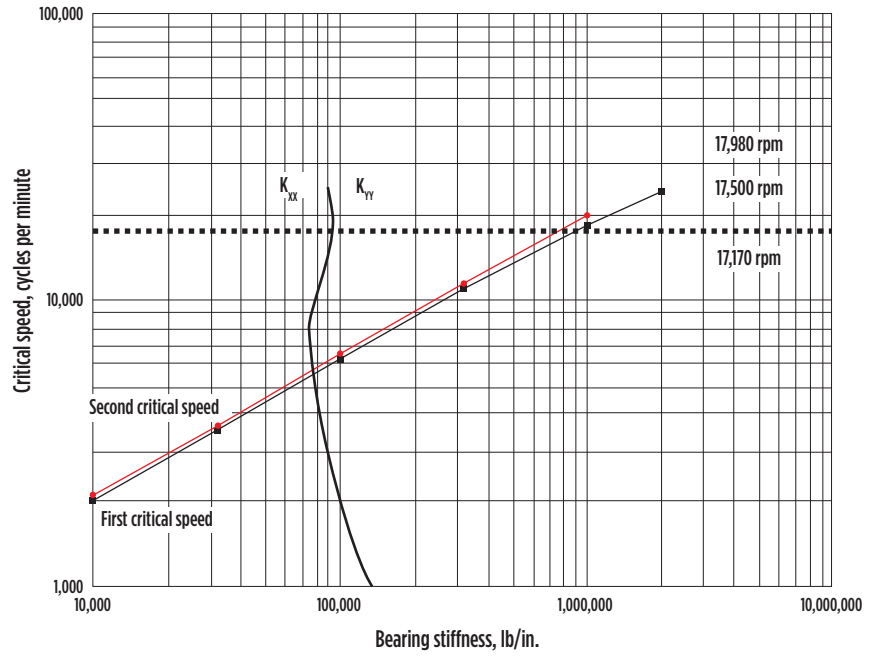

FIG. 5. Undamped critical speed map. K_{XX} and K_{YY} refer to the direct bearing stiffness in the horizontal and the vertical direction, respectively. In this case study, $K_{XX} = K_{YY}$.

natural frequency of the bending mode of these short, "stubby" shafts ends up much higher than their operating speeds or any excitation frequency. Therefore, from a rotor dynamics perspective, they are categorized as "stiff-shaft" designs.

The implication for stiff-shaft designs is that only the rigid body translational modes of vibration are of serious concern. These modes are greatly influenced by the design of the bearings. Smaller machines are usually equipped with tight-clearance, fixed-geometry bearings with high stiffness.

This yields a machine that does not have any critical speeds within its operating range. Larger rotors tend to utilize tilting-pad or flexible-pivot bearings and can be designed with larger clearances and lower stiffness. With this configura-

tion, the machine tends to pass through a highly damped natural frequency at very low speeds. Since the bearings are well damped, these points of operation are not considered critical speeds due to the low amplification factor.

Two predominant modes of vibration are observed within the speed range, namely a cylindrical and a conical mode (FIG. 7). These results show that the rotor system is well designed since the natural frequencies for both modes do not intersect the 1X excitation line. Such a condition would have indicated a potential resonance situation.

Stability analysis. It is not enough to know that damped natural frequencies do not cross the 1X excitation line. The designer must show that the bearing system is robust against the presence of destabilizing forces such as those induced by the areodynamic components, seals or bearings. It is also important to know how much damping is inherent in each vibration mode. Should insufficient damping be identified for a given mode shape, the rotor would be susceptible to high vibrations due to excitations such as unbalance. As mentioned previously, the bearings are the source of damping. However, the amount of "effective" damping is not the same for every mode. This is quantified by the so-called logarithmic decrement ("log dec") or, alternatively, the damping factor. Designers typically prefer using one of these parameters for their analysis, but both are representative of the same physical reality.

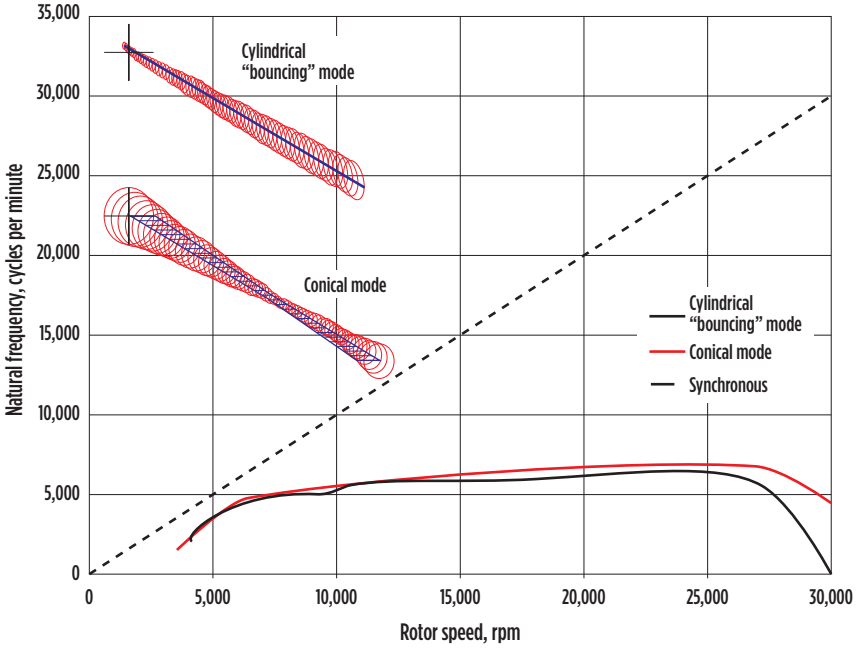

FIG. 6. Damped natural frequency map.

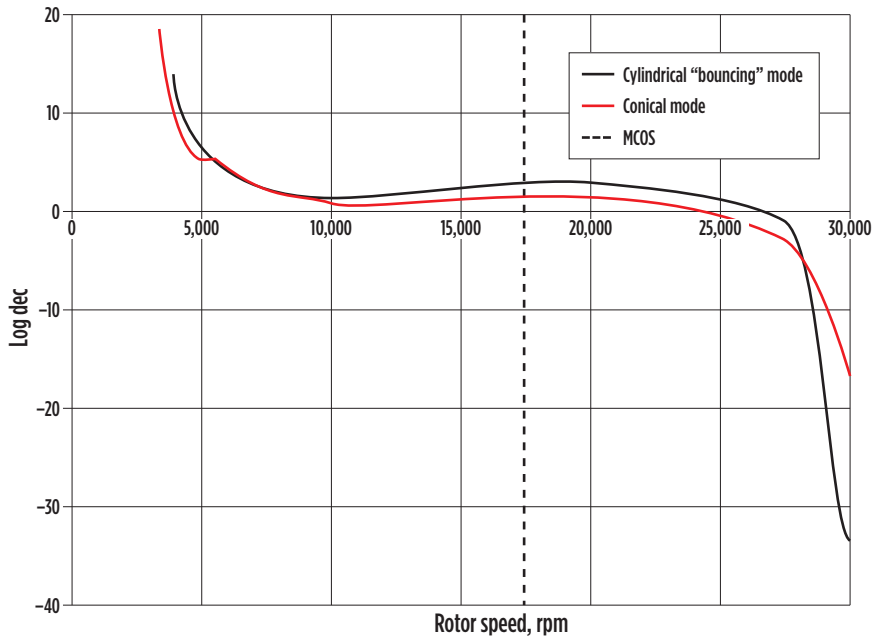

FIG. 7. Log dec plot.

FIG. 7 depicts the predicted log dec for the two predominant modes of vibration on this expander rotor. A minimum log dec of 0.1 implies that the system is sufficiently damped and can be considered stable. The data indicates that the log dec is positive for both modes from zero speed until MCOS. However, the log dec drops to negative values for speeds above 25,000 rpm, which indicates that the mode shape becomes unstable. This means that the system becomes self-exciting, and the vibrations will increase sharply. This is due to hydrodynamic effects in the oil film between the bearing and the shaft. This is clearly an undesirable condition, but it is not concerning in this case because the control system limits the maximum speed to protect the mechanical integrity of the machine.

Also, note that the aerodynamic forces experienced by the wheels are transferred to the rotor bearing system and can sometimes add significant excitation forces, which must be considered in the calculation. The mechanism of these aerodynamic effects is such that they generate a displacement that is orthogonal, and not parallel as intuition might suggest, to the aerodynamic force. This phenomenon is modeled in mathematical terms as cross-coupled stiffness and can have the capacity to induce undesirable unstable vibrations. In many turboexpander cases, the destabilizing forces generated in the expander wheel are more consequential than in the compressor wheels. FIG. 8 shows an example on a different turboexpander in which the amount of aerodynamic cross-coupling created a significant instability.[3]

Bearing loads. Both static and dynamic loads on bearings can be predicted and are necessary in ensuring that the

bearings, the bearing pedestals and the skid (i.e., the machine support structure) can handle the loads imposed on them.

Unbalance response plots. Until this point in the analysis, the designer has not accounted for excitation forces, such as unbalance. The unbalance in the rotor will generate a dynamic load at the same frequency as the rotation of the rotor (one excitation per revolution). The shape of the unbalance force will be related to the amount and distribution of unbalance (in terms of weight). Three unbalance weight configurations are typically considered in an analysis for any turbomachine, and they must follow API guidelines. The amount of balance is determined by the balancing tolerance applicable for each machine, and the unbalance weights are arranged spatially in such a way as to excite the predominant modes. A single weight in the middle of the rotor (which may be called a purely static unbalance) would tend to excite the cylindrical or bounding mode. A "couple" unbalance (i.e., one in which the weights are separated axially but opposite exactly 180°) will excite the conical or "hinging" mode.

The simulation in FIG. 9 shows the speed at which the vibration will peak as the rotor goes up in speed. This is the critical speed, and it is an important parameter to predict and monitor during field startup. The shape of the curve itself is important because it indicates the rate at which the vibration will increase as the machine ramps up. Well-damped, smoothly increasing curves with a wide base and a "dull" peak like the one pictured in FIG. 9 are preferable over one with a sharp and narrow peak. In the latter, which is a result of poor damping, the vibrations will quickly jump for a small increase of rotor speed, rendering the process of ramping up to speed somewhat unreliable and unpredictable. The shape of the curve is quantified by a parameter called "amplification factor." From an API 617 perspective, those speeds with amplification factors greater than 2.5 are considered critical speeds.

Another issue to consider is that the rotor must not run too close to the critical speed. The parameter to watch is the separation margin, which is the amount of separation between the critical speed (*Nc*) and the rated speed.

The data generated by the response analysis (i.e., vibration response magnitude and phase angle) can be validated with field measurements as long as the machine is equipped with proper instrumentation and data acquisition equipment, either in the field or in a factory test stand.

Clearance checks. The analysis must show that available clearances between rotating and stationary components are not exceeded, with considerations for margin. For instance, API 617 requires that shaft vibrations must not exceed more than 75% of minimum design diametral clearances.

In summary, a successful rotor dynamics analysis should ensure that the overall vibration levels will not exceed clearance or load limits, and that the overall rotor bearing system is stable throughout the operating speed range.

Conclusion. Rotor dynamics analysis is a key part of turbomachinery design. Ensuring that a rotor is stable and will operate within acceptable levels of vibration is necessary for long-term, reliable operation. API 617[2] can be referenced for reviewing such an analysis to make sure that all parties agree to what defines a suitable design.

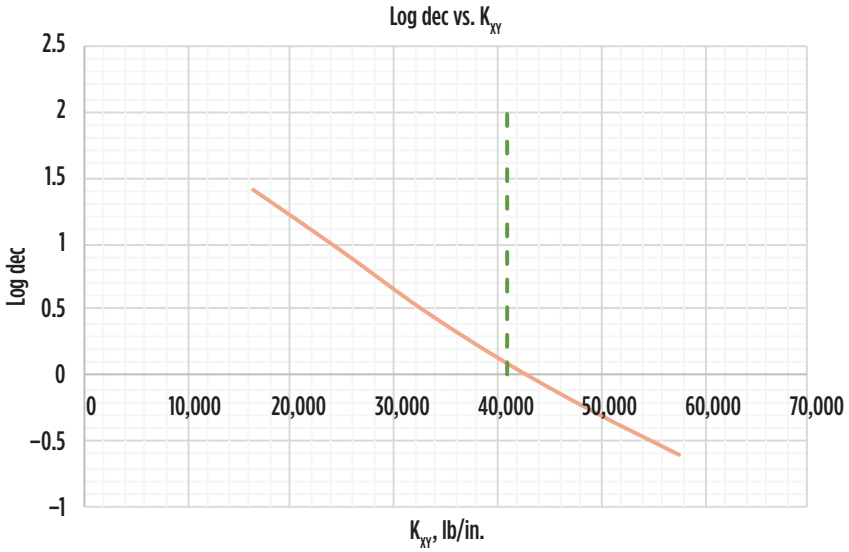

FIG. 8. Influence of cross-coupling stiffness in log dec. K_{XX} and K_{YY} refer to the direct bearing stiffness in the horizontal and the vertical direction, respectively. In this case study, $K_{XX} = K_{YY}$.

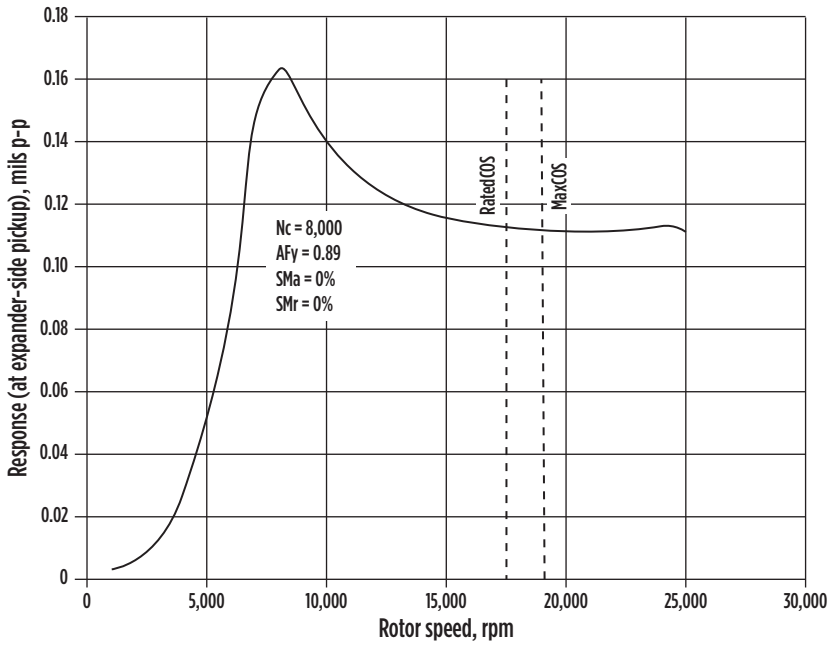

FIG. 9. Rotor dynamic response plot.

Ultimately, all rotor dynamic models should be verified on the test stand prior to operation in the field. Referring to a rotor dynamics analysis report during the evaluation of a mechanical run test is an important part of making sure that a machine has been manufactured and assembled according to design. More importantly, validation of the model on the test stand can provide assurance that the machine will operate as expected in field conditions.

As previously mentioned, the typical turboexpander should not present a significant rotor dynamic challenge for the OEM. These machines typically operate below significant shaft critical speeds, and minimal vibration can be expected given well-balanced components. In addition, instability is a rare issue with well-designed and manufactured bearings and seals.

After a machine has been commissioned, it is important for the operations team to collect vibration and bearing temperature data on a regular basis. These long-term trends prove invaluable when troubleshooting a vibration issue.

The most common rotor dynamics issue observed in the field is high synchronous vibration. Wearing components over time can contribute to rotor imbalance, steadily increasing vibration levels. Another common cause of imbalance increase over time is the formation of hydrates or other solids in expander wheels in cryogenic natural gas processing applications. Sudden, high levels of vibration can be attributed to major failures in either rotating components and/or bearings, such as blade loss in an impeller.

Other, more serious and difficult issues, such as rotor instability, will usually present themselves immediately during commissioning. These types of problems can be due to unforeseen (and unmodeled) process loads or poorly modeled rotor dynamics analysis. They are not easily solved by improving component balancing and usually require intensive efforts to redesign or add components, which can cause lengthy and expensive delays. For this reason, it is critical to ensure that a proper rotor dynamics analysis is performed during the design phase to rule out any possibility of rotor bearing instability. **GP**

LITERATURE CITED

[1] Avetian, T., "Fundamentals of turboexpander design and operation," *Gas Processing & LNG*, May/June 2020.

[2] American Petroleum Institute, "API Standard 617: Axial and centrifugal compressors and expander compressors," 8th Ed., 2014, API Publishing Services, Washington, D.C.

[3] Avetian, T., L. E. Rodríguez and J. Park, "Addressing high sub-synchronous vibrations in a turboexpander equipped with active magnetic bearings," Proceedings of the 48th Turbomachinery Symposium, 2019.

TADEH AVETIAN is Director of Engineering at L.A. Turbine, responsible for identifying and defining research and development projects, as well as directing turboexpander design for new and aftermarket equipment. Mr. Avetian is a California-registered professional engineer with BS and MS degrees in mechanical engineering from California State Polytechnic University of Pomona.

LUIS E. RODRÍGUEZ is a Design Engineer at L.A. Turbine, responsible for the mechanical design of turboexpanders. Prior to L.A. Turbine, he worked for 10 yr at Sulzer Turbo Services in La Porte, Texas. Mr. Rodriguez is a Texas-registered professional engineer with a BS degree from Universidad Simón Bolívar in Venezuela and an MS degree from Texas A&M University.

Improve gas-gas exchanger footprint and economics with a PSHE

R. BROAD, API Heat Transfer, Bretten, Germany; and A. BAYATI, McDermott, The Hague, the Netherlands

Plate-type heat exchangers are known for high heat transfer coefficients. As a result, they are compact and lightweight compared to conventional shell-and-tube (S&T) exchangers. Another advantage of plate-type exchangers is a lower fouling tendency due to higher wall shear stress; however, the construction of widely used exchangers, such as gasketed and bloc-type exchangers, limits their application to low and medium design pressures (typically less than 50 barg). The plate-and-shell heat exchanger (PSHE) combines the advantages of plate-type exchangers with the robustness of the S&T exchanger into one exchanger. Design pressure can rise to 400 barg for the PSHE.

This article focuses on a specific application in upstream facilities where weight reduction and smooth operation in turndown is always a concern. The design comparison, advantages and limitations between S&T exchangers and PSHEs are presented and discussed using an actual example.

Exchanger background. Gas-gas exchangers in gas treatment processes (FIG. 1) are usually the largest exchanger in an offshore plant, with special design criteria. In this article, the possibility of replacing conventional S&T exchangers with PSHEs is reviewed, and the advantages in this application are evaluated.

Due to the risk of hydrate formation in gas-gas exchangers, the design of S&T exchangers are required to meet certain criteria, which goes back to work done by P. W. Knight in 1975.[2] The satisfactory feedback from practice encourages designers to follow Knight's recommendations. Further studies by HTRI have demonstrated similar criteria.[3]

As per Knight's recommendation, three parameters play a crucial role in sizing a gas-gas exchanger:

- Maximum tube-side velocity (to prevent foaming and formation of unstable emulsion)
- Minimum tube-side velocity (to prevent hydrate formation)
- Maximum tube length per shell based on selected tube size

These three parameters determine the size and number of S&T exchangers. It is clear that the maximum gas velocity influences achievable heat transfer coefficient, while minimum velocity and maximum tube length determine the number of shells in series. To minimize the risk of separation, it is normal to select one tube pass.

The minimum velocity limit is recommended to prevent stratification inside tubes. This limit is usually easy to observe for design flow, but very difficult to adhere to during turndown conditions. To overcome the low velocity issue in turndown, a recycle line from the compressor discharge to the exchanger inlet has been considered by some designers to boost the velocity in turndown conditions and in late-life scenarios. This modification requires additional piping and creates energy losses.

Due to the smaller channel size, the corrugated plate and the flow direction constantly breaking up the boundary layer, the chance of stratification is unlikely with PSHE. Turndown can be handled without the additional recycle line, which reduces piping requirements and power consumption.

As per common practice, minimum approach temperature for an S&T exchanger should not be less than 5°C (preferably 8°C), while it can be as low as 2°C for the PSHE. This means lower compressor power consumption, which results in considerable savings of long-term operation costs.

Lighter equipment with a smaller footprint is always a challenging activity in offshore platform design. The following example demonstrates significant savings achieved by replacing an S&T exchanger with a PSHE.

Case study: Exchanger design comparison. The design of the S&T calculation is shown in FIG. 2; the design includes the highest velocity possible to maintain the minimum required velocity in turndown condition. This design also boosts the tube-side heat transfer coefficient, which is the main resistance.

Compact exchangers. In recent years, increased attention on environmental

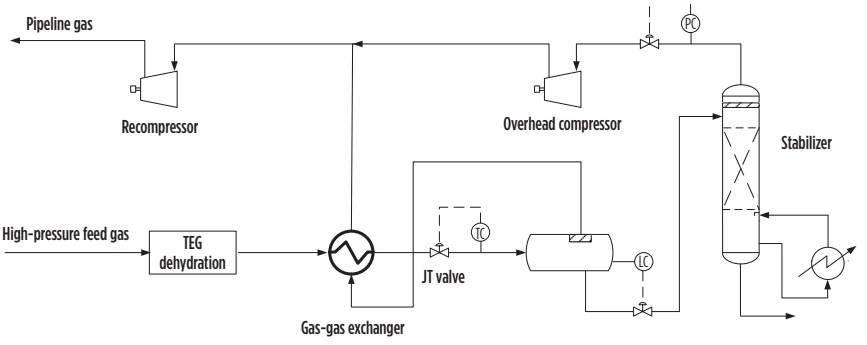

FIG. 1. Process flow for a gas-gas exchanger in a gas treatment facility.[1]

and economic sustainability has led many end-users to review the possibility of replacing very large S&T exchangers with more compact plate-type exchangers. In this application for a gas-gas exchanger, which includes high design pressure, the printed circuit heat exchanger (PCHE) and the PSHE are considered to be the most appropriate alternatives (FIG. 3).

In the authors' opinion, the PSHE appears to be the more attractive choice from the economic and maintenance points of view. The PSHE has larger channels and easy access to the plate pack. Feed gas entering the exchanger is usually clean because of upstream separation and filtration; however, fouling due to fine sand carryover has been reported.

PSHE construction. The construction of a PSHE is shown in FIG. 4. It essentially consists of a cylindrical plate pack within a round shell. The shell diameters range from 360 mm–1,600 mm. The plate pack is cylindrical, with circular plates of 0.8-mm thickness (depending on the design pressure and temperature), pressed with a pattern approximately 3 mm deep. The resulting heat exchange area is approximately 300 m^2/m^3—more than three times greater than an S&T type. As the U-value for a plate-type heat exchanger is more than twice that achieved in an S&T exchanger, the physical size is reduced by a factor of six or more.

The plate pack is held between circular, thick-walled plates. The plates are pressed from 316 grade stainless steel or higher, with accurate spacing obtained by the high points on adjacent ribbed plates. Alternate plates are welded at the plate-side ports to create "shell-side" passages, which are open to the annulus formed between the plate pack and the shell. The "plate-side" passages are connected by inlet and outlet headers through holes at the top and bottom of the plates, and the shell side is sealed with a circumferential weld around the rim. The diameter of these connectors, and of the plate-side connections on the front of the shell, are geometrically limited to limit the loss of the available plate area. The effective plate area between these connections is approximately two-thirds of the total circular plate area.

Reliability and maintenance. High-quality welding, plus accordion-like construction, makes the PSHE suitable for the larger temperature gradients experienced in startup, shutdown and process upsets.

The plate packs also have been tested for thermal transients, a common concern with all heat exchangers during start-up, shutdown and process upsets. Thermal cycling has been conducted between ambient and –168°C, at 80 barg, where an excess of 8,000 cycles was achieved before failure occurred. Then, 36,000 cycles were performed between ambient and 100°C, at which point the test was stopped and a burst was performed. The

HTRI

Output Summary Page 1

Released to the following HTRI Member Company:
MCDERMOTT

SI Units

See Data Check Messages Report for Informative Messages.
See Runtime Message Report for Warning Messages.

Process Conditions		Cold Shellside		Hot Tubeside	
Fluid name		Dry Process Gas			Wet Process Gas
Flow rate	(kg/s)		121.60		138.80
Inlet/Outlet Y	(Wt. frac vap.)	1.0000	1.0000	1.0000	1.0000
Inlet/Outlet T	(Deg C)	-19.62	-2.17	2.62	-12.76
Inlet P/Avg	(kPa)	4751.3	4706.9	6105.0	6072.8
dP/Allow.	(kPa)	88.932	100.00	64.514	100.00
Fouling	(m2-K/W)		0.000170		0.000260

Exchanger Performance					
Shell h	(W/m2-K)	1171.2	Actual U	(W/m2-K)	202.05
Tube h	(W/m2-K)	1375.3	Required U	(W/m2-K)	191.76
Hot regime	(--)	Sens. Gas	Duty	(MegaWatts)	5.5428
Cold regime	(--)	Sens. Gas	Eff. area	(m2)	5099.3
EMTD	(Deg C)	5.7	Overdesign	(%)	5.37

Shell Geometry			Baffle Geometry		
TEMA type	(--)	NEN	Baffle type		NTIW-Seg.
Shell ID	(mm)	1500.0	Baffle cut	(Pct Dia.)	15.42
Series	(--)	1	Baffle orientation	(--)	Perpend.
Parallel	(--)	1	Central spacing	(mm)	1520.0
Orientation	(deg)	0.00	Crosspasses	(--)	9

Tube Geometry			Nozzles		
Tube type	(--)	Low Fin	Shell inlet	(mm)	690.00
Tube OD	(mm)	19.050	Shell outlet	(mm)	690.00
Length	(m)	14.000	Inlet height	(mm)	193.50
Pitch ratio	(--)	1.3333	Outlet height	(mm)	234.54
Layout	(deg)	30	Tube inlet	(mm)	690.00
Tubecount	(--)	2441	Tube outlet	(mm)	690.00
Tube Pass	(--)	1			

Thermal Resistance, %		Velocities, m/s			Flow Fractions	
Shell	17.25		Min	Max	A	0.124
Tube	51.12	Tubeside	6.61	7.09	B	0.712
Fouling	21.71	Crossflow	3.34	4.09	C	0.074
Metal	9.92	Window	6.69	7.61	E	0.090
					F	0.000

FIG. 2. HTRI result for S&T exchanger design.

FIG. 3. Channel-size PCHE (left) vs. PSHE (right).

worn-in plate pack achieved the same results as a new plate pack.

PSHEs have been successfully used in many upstream, downstream, single-phase, condensing and boiling applications. Although the PSHE shell side is accessible for mechanical cleaning just like bloc-type exchangers, PSHEs are not recommended for applications with severe fouling tendency, where frequent mechanical cleaning is anticipated on the plate side.

Flow distribution. Shell-side flow distribution in a cross-flow arrangement is always a concern. Maldistribution due to flow bypass from the inlet to the outlet, which is seen in "X" type S&T exchangers, is minimal or less likely in a PSHE. Small channels of plate pack result in a reasonable pressure drop and, consequently, even flow distribution.

HTRI performed an extensive study of flow distribution in 2019.[4] The result is very satisfactory; channel-to-channel flow distribution was uniform for both the plate side and shell side in the example. Multiple inlets and outlets and reasonable pressure drop over the plate pack minimize the risk of shell-side maldistribution.

PSHE design for gas-gas exchanger.

The authors' recommended PSHE is shown in FIG. 5. Wet process gas (feed) is located on the shell side, and dry process gas (from the separator) is on the plate side. Glycol injection to the feed, which can be done in upstream pipe or directly inside the exchanger, helps prevent hydrate formation.

The authors offer several recommendations for designing a gas-gas exchanger as a PSHE:

- Maximum channel velocity is limited, as per Knight's recommendation.
- Minimum channel velocity is of minor concern, since the chance of stratification is nil.
- Glycol injection can be performed within the exchanger or at the inlet piping prior to the exchanger. A CFD analysis might be needed as further study to ensure even distribution of glycol over the entire plate pack.

Recommendations.

Compactness and reliability make PSHEs a suitable candidate for many non-severe fouling applications in onshore and offshore plants. It is a good fit in process and utility facilities, and can be used for debottlenecking and revamp by directly replacing an existing tube bundle with a plate pack.

Large, conventional S&T gas-gas exchangers in gas treatment facilities can be replaced with compact PSHEs, resulting in smaller footprint and a better economic and technical solution (TABLE 1). GP

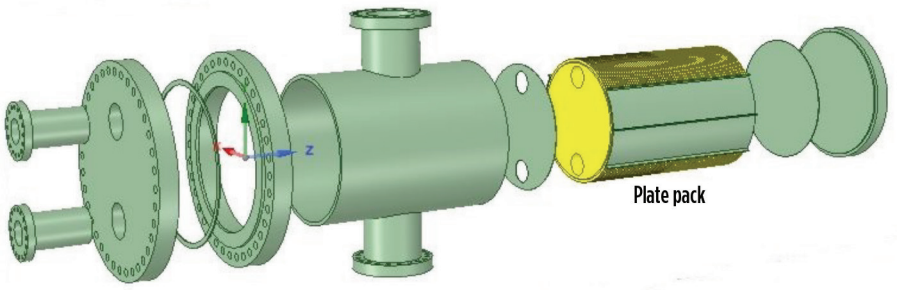

FIG. 4. PSHE exchanger construction.

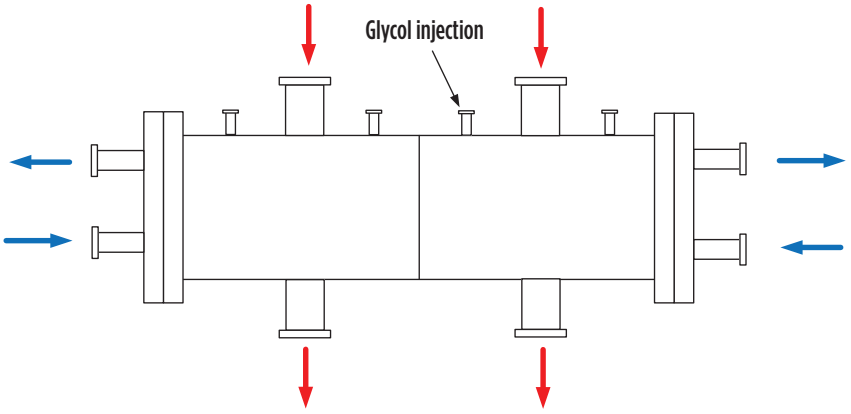

FIG. 5. PSHE for a gas-gas exchanger.

TABLE 1. Design comparison for PSHE vs. S&T exchanger

Heat exchanger type	Dimensions, mm	Approximate weight, kg	Price, € MM*	Minimum turndown, %
S&T	1,500 (inner diameter) × 14,000 (tube length)	100,000	1.8	45
PSHE	1,530 (inner diameter) × 3,000 (two plate packs)	28,000	1.3	No limit

*This is an indication for fabrication cost; transportation and installation cost are not included

LITERATURE CITED

[1] Mokhatab, S., A. Poe and J. Mak, *Handbook of Natural Gas Transmission and Processing*, 4th Ed., Gulf Professional Publishing, October 2018.

[2] Knight, W. P., "Plant operating data improve heat exchanger design," *Hydrocarbon Processing*, Vol. 54, Iss. 5, 1975.

[3] Nangia, K. K., J. W. Palen and J. Taborek, "Field data and performance analysis for gas-gas exchanger with glycol injection," HTRI Report STS-1, 1972.

[4] Farrell, K., "CFD simulation of plate and shell heat exchanger," HTRI Report PHE-22, 2019.

ROBERT BROAD is Business Development Manager–Systems at API Heat Transfer. He is a chartered chemical engineer, a Fellow of the Institution of Chemical Engineers and a member of both the International Register of Professional Engineers and the European Federation of National Engineering Associations. Mr. Broad has worked for more than 20 yr with compact heat exchangers, striving to use technology to reduce energy usage. He holds an MBA degree from Henley Management College in the UK.

ABDOLLAH BAYATI is Heat Transfer Subject Matter Expert at McDermott. He has more than 20 yr of experience in fabrication, thermal and mechanical design of heat exchangers for the oil and gas industry, both onshore and offshore. His journey through fabrication to design, along with academic study, has strengthened and encouraged him to explore new opportunities for technical and economic improvement. He holds a BS degree in heat transfer and fluid dynamics and an MS degree in energy engineering.

Energy savings for a propane refrigerant compressor using simulation

H. Y. NOH, Saudi Aramco, Yanbu, Saudi Arabia

Saudi Aramco's Yanbu fractionation plant utilizes deethanizers, depropanizers, debutanizers and an RVP column. These distillation columns are equipped with overhead air fan coolers, except for the deethanizer columns, which have a propane refrigerant closed-loop system. The system essentially consists of a steam-operated compressor, an air cooler, expansion valves, a refrigerant flash drum and an evaporator.

Propane refrigerant is highly compressed by the compressor, cooled by the air cooler and then flashed through the expansion valve in the refrigerant flash drum under medium pressure. Medium-pressure liquid propane is let down to further reduce pressure and is then vaporized in the evaporator, after being used as a cooling medium for the deethanizer overhead ethane vapor stream. The vaporized refrigerant is recycled back to the compressor, in addition to the low-pressure flashed vapor propane, through an overhead letdown valve after the refrigerant flash drum.

In two 1980s-era deethanizer modules, the existing compressors have a single suction side only. This configuration is inefficient in terms of compressor input energy because single suction is designed to receive only the combined low-pressure streams: one from the evaporator and one from the refrigerant flash drum. The newest module of the deethanizer at the propane refrigerant compressor has two different suctions.

Based on this information, a simulation[a] study was conducted to modify the old configuration to correspond to the newest module to determine whether energy improvement could be achieved.

Existing compressor design. The Yanbu fractionation plant receives C_2+ that is transferred to deethanizer columns for separation. Normal operating pressure in the columns is 390 psia, and the temperature required for near-pure ethane condensing on the overhead is approximately 41°F. **FIG. 1** shows the deethanizer overhead cooling system with typical operating conditions.

In the existing design mode, the overhead C_2 vapor stream is partially condensed by the liquid C_3 refrigerant system. The liquid refrigerant C_3 absorbs heat from C_2 and is converted into C_3 vapor. In the existing system, the low-pressure (61-psia) vapor from the evaporator is designed to combine with another low-pressure (61-psia), cloud-marked vapor stream from the flash drum (83 psia) in **FIG. 1.** Then, the combined stream is used as suction for the compressor. The refrigerant vapor is pressurized, fully condensed, subcooled and flashed. The propane refrigerant circulates in the closed loop.

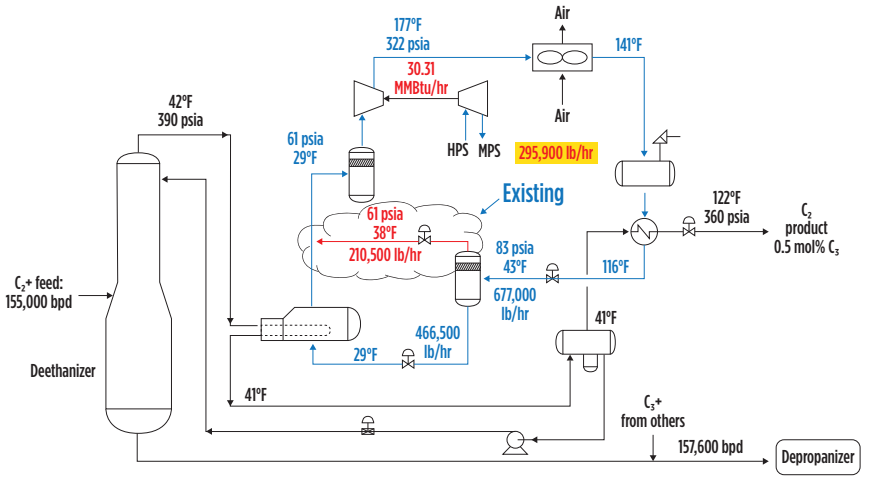

FIG. 1. Existing deethanizer overhead cooling system and required steam flowrate to turbine.

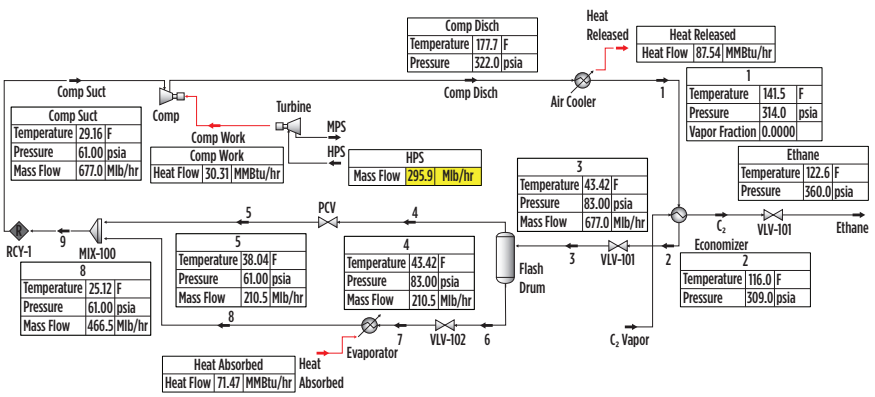

FIG. 2. Mass and energy balance for the existing design, using simulation.[a]

To run the system, power of 30.31 MMBtu/hr is supplied to the compressor by the steam turbine, which intakes high-pressure steam and exhausts medium-pressure steam. In this system, the required steam flowrate is 295,900 lb/hr.

To represent the system, modeling[a] was carried out as shown in **FIG. 2,** generating a good match to the design. The adiabatic efficiency of the compressor and the isentropic efficiency of the turbine were 75% and 70%, respectively.

Compressor design proposal. As shown in **FIG. 3,** the existing compressor has only a single suction on the left side. In the existing system, the single suction comes from the combined line—one for low-pressure (61-psia) vapor from the evaporator, and the other for a low-pressure (61-psia), cloud-marked vapor stream from the flash drum (83 psia), as shown in **FIG. 1.**

As stated, the newest module of the deethanizer propane refrigerant compressor has two different suctions on the right side. The low-pressure compressor suction line receives low-pressure vapor from the evaporator, but the compressor is designed to receive medium-pressure vapor propane directly from the flash drum without any letdown. Since there is no letdown after the refrigerant flash drum, some energy conservation in the compressor is anticipated.

Based on the configuration of the newest module, a simulation[a] was conducted to check for improvement to the compressor energy.

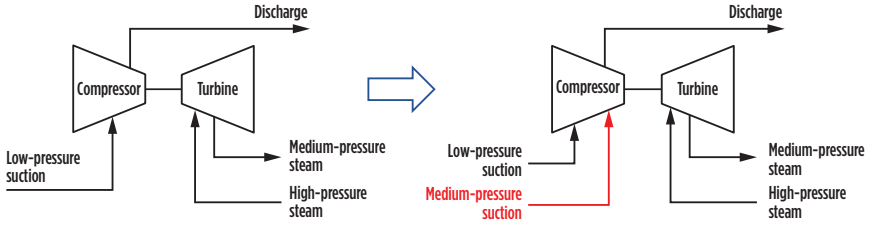

FIG. 3. Proposed compressor schematic.

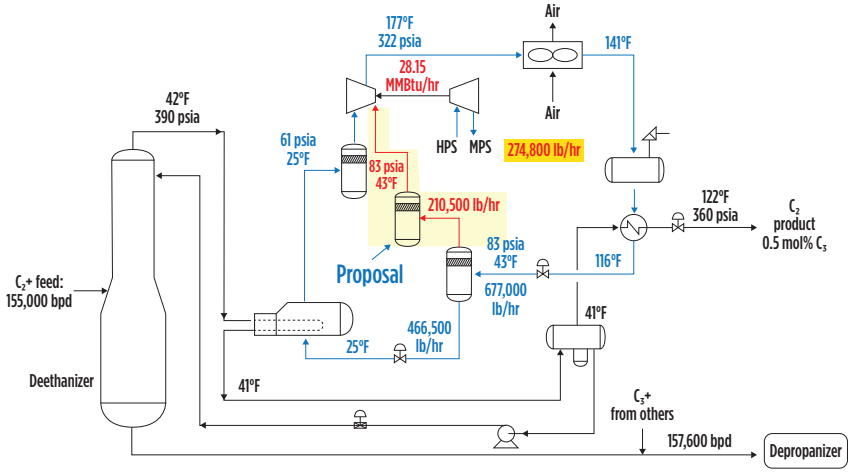

FIG. 4. Proposed deethanizer overhead cooling system and required steam flowrate with reduction to the turbine.

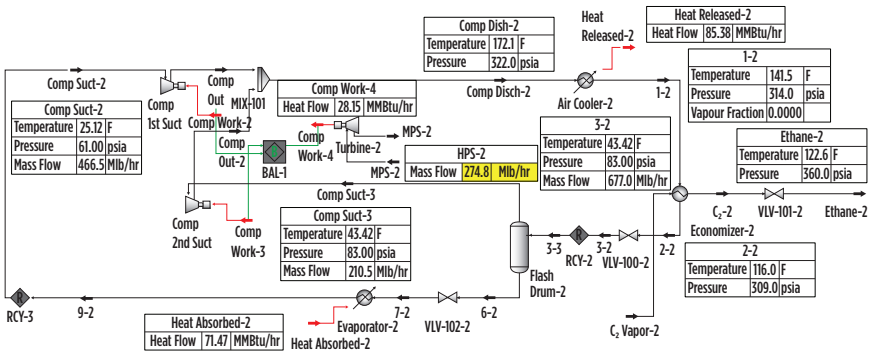

FIG. 5. Mass and energy balance for the proposed design, using simulation.[a]

Proposed design result. To follow the proposed design modification, the line in the cloud-marked vapor stream shown in **FIG. 1** needs modification. As the compressor requires medium-pressure (83-psia) C_3 vapor to the second suction, a change was made to the schematic (**FIG. 4**). Since the compressor does not accept entrained liquid with C_3 vapor, a knockout drum was added between the flash drum and the compressor.

Without letdown and at medium pressure for the recycle loop compressor, the required power to the compressor was reduced from 30.31 MMBtu/hr to 28.15 MMBtu/hr. Accordingly, the high-pressure steam intake and medium-pressure steam exhausts were reduced from 295,900 lb/hr to 274,800 lb/hr.

The same efficiencies for the compressor and turbine (75% adiabatic and 70% isentropic) were taken as in the existing system. **FIG. 5** shows the modeling result for steam savings in the refrigeration system when the medium-pressure C_3 flows into the compressor without letdown.

Recommendations. The study reveals that a high-pressure steam savings of 21,100 lb/hr per module can be achieved, which is equivalent to an energy savings of 7.1%. This initiative can be applied to the closed recycle loop.

The air cooler duty also can be reduced by 2.5%, since the compressor discharge temperature drops by 5°F, from 177°F (**FIG. 1**) to 172°F (**FIG. 4**). Reduction of air cooler duty is helpful for plant operation during very hot weather, especially in the Middle East. **GP**

NOTE

[a] Simulation and modeling performed using HYSYS

HAE YONG NOH is a Process Engineer at the Yanbu NGL Fractionation Department of Saudi Aramco. He has 12 yr of experience in the oil and gas industry and is a licensed professional engineer in chemical and mechanical engineering. Mr. Noh earned a BS degree in chemical engineering from Chung Ang University in Seoul, South Korea and an MS degree in interdisciplinary engineering from Purdue University in West Lafayette, Indiana, U.S.

Specifying trip valves is critical for LNG service

P. JESSEE, Valin Corp., Portland, Oregon

Appropriately specifying trip valves in the world of natural gas liquification is a critical element. Failing to do so effectively can risk the lives of operators and maintenance personnel working in close proximity to the equipment, and can sometimes cause irreparable damage to expensive turbomachinery.

LNG equipment overview. The process of liquefying natural gas has been in existence since the 19th century. By converting natural gas from a gaseous state into a liquid, it can more easily be transported to areas where natural gas pipelines do not reach.

According to the U.S. Energy Information Administration, the volume of natural gas in a liquid state is roughly 600 times smaller than its volume in a gaseous state in a natural gas pipeline. Some geographic areas of the U.S. store LNG onsite where there is a high demand for electricity at certain times. This demand typically revolves around extreme weather conditions or where pipeline delivery is limited. Natural gas also can be used in a liquid state as transportation fuel.

With such an essential end product, it stands to reason that the process for making it has been adequately refined over the years. The liquefaction of natural gas is achieved by lowering the temperature of the gas until it changes phase from vapor to liquid. The resulting LNG exists at a temperature of roughly –260°F. The process to take natural gas to this temperature is most often carried out in a series of turbocompressors. These turbocompressors increase the pressure and compress the gas, followed by an adiabatic expansion step that causes a dramatic reduction in temperature. The process is straightforward, but if certain precautions are not taken, disaster can ensue. One of these precautions is the inclusion of a trip valve.

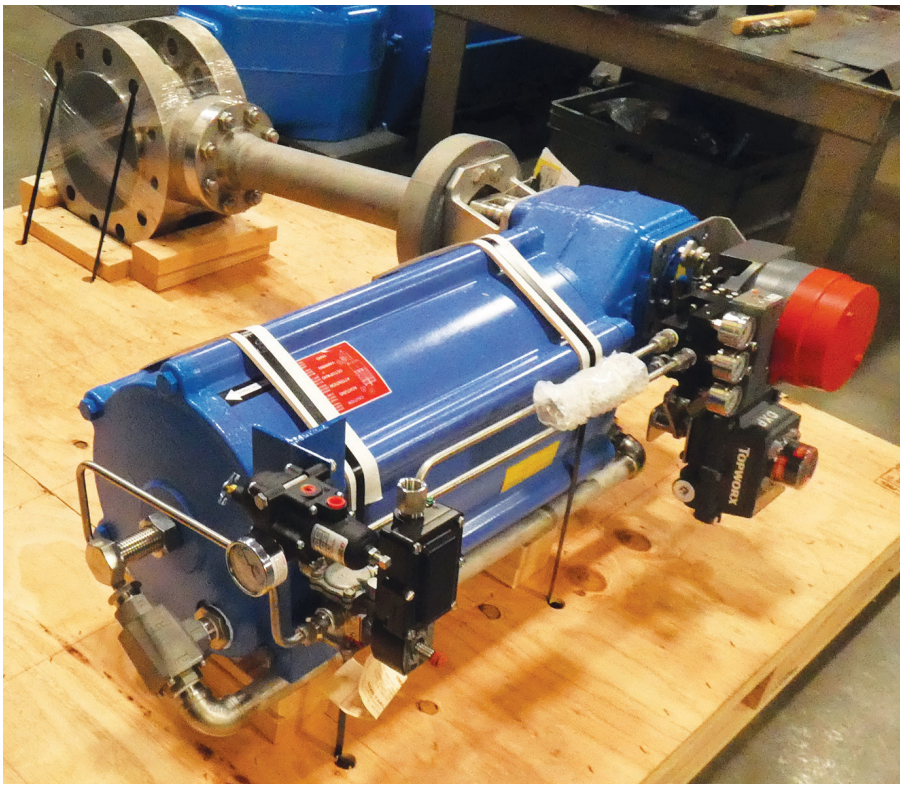

FIG. 1. A typical compressor trip valve assembly.

Turbine trip valves. A turbine trip valve (FIG. 1) should be present near each turbocompressor used in the natural gas liquefaction process. If the load on the turbocompressor stops for any number of reasons, then the trip valve is designed to completely cut off the flow. This prevents the turbine from over-revving and potentially damaging the equipment.

The turbine trip valve is an essential safety device that not only prevents catastrophic damage to extremely expensive capital equipment, but also protects the lives of those working near the turbocompressors. A turbine trip valve is unique among large valves due to the combination of the extreme temperature conditions it faces and the short time allowed for a turbine trip valve to cycle closed. In fact, it is common for trip valves to be required to cycle closed in 0.3 sec–2 sec, which can be difficult to achieve for large valves.

To properly specify these trip valves, a number of different factors must be considered. The first step is to understand the application requirements. These include the pressure, temperature, flows and media that are making their way through the valve.

In most cases, the required size will make a high-performance butterfly valve the best choice for a turbine trip valve.

Specification requirements. Some of the steps in properly specifying a turbine trip valve are similar to those taken in specifying any type of valve. The first is to determine how much fluid will be flowing through the valve. The actual flowrate will determine the size of the valve required for the job. In most cases, the required size will make a high-performance butterfly valve the best choice for this application.

Next, the typically low process temperatures must be taken into account. It is not unusual for natural gas trip valves to face design conditions below –100°C (–148°F). These cryogenic temperatures require thick piping insulation, and the valves need long stem extensions so that the critical stem sealing components are outside of the cold zone.

The next step is to determine the required torque, which is a function of the valve size, seat and bearing designs, as well as process temperatures and pressures. An analysis of the required torque and cycle speed will allow the calculation of the maximum rotational force that the long stem extension will need to withstand. It will also determine how much "shaft windup" will result.

Once the maximum rotational force is known, an actuator must be selected to provide the required torque. An adequate safety factor should be applied to accommodate process upsets, aging equipment, etc. The extremely fast required cycle times frequently make oversized air ports necessary.

Once the major components—the valve and actuator—have been selected, similar care must be used to select the control components. Similar to the computer modeling used to size and select a process valve, the pneumatic system also must be modeled to allow the selection of solenoid valves and quick exhaust devices to vent the air from the actuator quickly enough to meet the trip requirements. All sources of pressure loss must be accounted for, such as pipe nipples, compression fittings, elbows, tees and exhaust screens.

Other considerations. A few other important characteristics, if not recognized and addressed properly, can be problematic. For example, the combination of the mass of the moving components of the valve and actuator and the fast cycle speeds can cause the actuator to be damaged. In this case, shock-absorbing bumpers must be specified for the actuator travel stops.

The locality where the trip valve will be installed must be accounted for. All components must meet local piping codes and electrical certifications, and the ambient conditions may require sunshades, corrosion-resistant materials or coatings, air system "rebreathers" or heat tracing.

Testing. Finally, each trip valve assembly must be tested to verify that it meets all the system requirements. Most customers require certified material test reports to confirm that the critical pressure-retaining components are made from the alloys specified by the manufacturer. Other forms of nondestructive examination (e.g., X-rays, liquid penetrant tests, positive material inspection, etc.) also may be required by the customer.

After the trip valve system has been completely assembled, it must be tested and timed to verify that it meets the trip speed requirement. This step cannot be skipped, as computer modeling alone is not sufficient for this critical piece of safety equipment. This testing is typically done using data loggers and sensors. The sensors detect valve position and air pressure, allowing the test system to graph the valve through the complete cycle.

Heavy engineering is required to ensure that a trip valve will work properly and do the job needed. Understanding all of the conditions and requirements will ensure that a critical element is not overlooked that may lead to damaged equipment, unplanned shutdowns and potential injuries or deaths. **GP**

PETER JESSEE, P.E., is a Process Control Application Engineer for Valin Corp., having joined the organization in 1990. He has many years of experience in both technical and sales positions for industrial and commercial control systems, control valves, flowmeters and industrial instrumentation.

Sulfur recovery for gas processing plants

L. MICUCCI, Siirtec Nigi, Milan, Italy

Natural gas produced in gas fields is a mixture of hydrocarbons containing hydrogen sulfide (H_2S) and organic sulfur species (carbonyl sulfide, COS; carbon disulfide, CS_2; and mercaptans, RSH), along with other impurities. The content of the sulfur compounds spans 0.1 vol%–25 vol%, depending on field location and well age. These gases must be removed due to their toxic properties and adverse impacts on the environment. Therefore, gas processing facilities originate gas effluents rich in sulfur species, notably H_2S.

Since the sulfur species cannot be discharged to the atmosphere, they must be converted into elemental sulfur and recovered in liquid or solid form by means of a sulfur recovery unit (SRU). Eventually, the residual sulfur species contained in the offgases produced by SRUs are thermally oxidized and released to the atmosphere as SO_2 and H_2O.

Increased public environmental awareness has led to more severe restrictions on SO_2 emissions. In several parts of the world, a sulfur recovery efficiency as high as 99.9+%, which corresponds to 50 mg/Nm^3 of SO_2 at the stack tip, is required.

Moreover, restrictions are also required on the yearly quantity of SO_2 that can be discharged to the atmosphere. This constrains the number of startups and shutdowns a central processing facility (CPF) is allowed in a year. Consequently, SRUs have become vital for the operation of CPFs.

The regulatory framework, the variations of plant throughput required by well production schedules, and the possible presence of BTEX (benzene, toluene, ethylbenzene and xylene) in the SRU feed make the design and operation of an SRU a challenging task for a gas processing facility. A number of variables must be considered including gas pressure, temperature and composition; the quantity of sulfur species (H_2S, COS, CS_2 and RSH); the economic framework and the location of the gas field.

An SRU encompasses a set of processing units including an acid gas enrichment unit, a Claus unit, a tail gas treatment unit (TGTU), a sulfur degassing unit (DGS) and an oxidizing unit. **FIG. 1** shows a block diagram of the sulfur recovery island of an inland CPF processing natural gas from Mediterranean offshore wells.

Acid gas enrichment. A Claus unit must be fed with acid gas rich enough in H_2S for the flame of the thermal reactor to be stable. When the acid gas from the upstream sweetening unit contains more than 35 vol% of H_2S, it can be handled directly in the Claus reactor furnace without issue.

However, if the acid gas is lean (as often is the case in gas field development projects), then the H_2S concentration must be increased above 35 vol% by means of an acid gas enrichment unit. When the acid gas contains 15 vol%–20 vol% of H_2S, the enrichment can be attained through a regenerative absorption on MDEA aqueous solutions. (**Note:** The absorption process on alkanolamines was described in the fifth article of the "Back to Basics" series, published in the September/October 2020 issue.)

Below 15 vol%, formulated alkanolamines or hindered amines can be used to attain an enrichment ratio (the ratio of the H_2S content of the acid gas to the Claus unit and the H_2S content of the acid gas from the sweetening unit) greater than 3, while maximizing the CO_2 rejection (i.e., the CO_2 remaining in the offgas).

Alternatively, the desired enrichment can be pursued by recycling to the absorber part of the acid gas extracted from the regeneration tower. In this process setup, the H_2S in the feed can be controlled by adjusting the recycle flowrate, as shown in the dotted line of **FIG. 2.**

For large-scale gas plants, this configuration may be expensive due to large volumes of acid gas flows, which translate into large-diameter pipe and large valves.

Claus unit. The function of the Claus unit is to convert H_2S into elemental sulfur and water. This is accomplished by reacting H_2S with SO_2, according to the reversible reaction shown in Eq. 1:

$$2H_2S + SO_2 \leftrightarrow \tfrac{3}{x} S_x + 2H_2O \qquad (1)$$

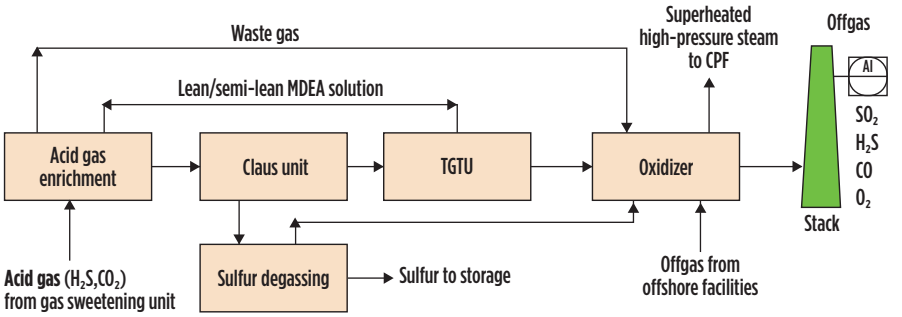

FIG. 1. Sulfur recovery island in a CPF processing offshore Mediterranean gas.

The kinetic of the Claus reaction would be too slow; therefore, it requires either catalysis or high temperature to occur. The SO_2 needed by the reaction is introduced into the chemical environment by burning one-third of the fed H_2S with atmospheric air through a Claus burner, as shown in Eq. 2:

$$H_2S + \tfrac{3}{2}O_2 \leftrightarrow SO_2 + H_2O \quad (2)$$

The oxidation reaction in Eq. 2, being strongly exothermic, develops a temperature higher than 1,000°C if the H_2S concentration in the acid gas is greater than 40 vol%.

An industrial Claus unit encompasses a thermal front end and a catalytic end. In the thermal stage, the acid gas and air are admitted into the thermal reactor (TR)—an internally refractory-lined pressure vessel—through a Claus burner. The enthalpy of the process gas exiting the TR at 1,000°C is recovered in the waste heat boiler (WHB) by rising medium-pressure or high-pressure steam. Most of the elemental sulfur formed in the thermal stage is condensed and recovered as liquid.

The process gas exiting the first sulfur condenser contains unreacted H_2S, SO_2, S, H_2O and N_2. This stream is directed into a "catalytic assembly" comprising a reheater, an adiabatic fixed-bed catalytic converter and a sulfur condenser. In the catalytic converter, the Claus reaction (Eq. 1) takes place at low temperature, and further elemental sulfur is yielded. To prevent the formed sulfur from condensing inside the catalyst pores, effluents from the previous condenser must be reheated to above the sulfur dewpoint in the reheater. The catalyst of a Claus unit is alumina (Al_2O_3). When the Claus unit is not integrated with a TGTU based on oxidized sulfur species reduction, and the acid gas contains COS and CS_2, a layer of titanium (TiO_2) catalyst is placed on the top of the alumina bed. The titanium catalyst promotes organic sulfur hydrolysis to CO_2 and H_2S.

The recovery of sulfur in a two- or three-stage conventional Claus plant is thermodynamically limited. Typical Claus plant recovery efficiencies are 90%–96% for a two-stage converter plant and 95%–98% for a three-stage reactor plant. Most Claus units are fitted with two catalytic converters (**FIG. 3**).

The key process variable of a Claus unit is the "air demand"—i.e., the H_2S/SO_2 ratio measured at the outlet of the plant. This variable is used to fine-tune the air flowrate to the burner in a way that ensures the optimum operation of the unit.

In a CPF, the acid gas flowrate and its composition can change over time. To provide the Claus unit with the operational flexibility needed to tackle these variations, in addition to the installation of feed and air preheaters to support the Claus operation, the thermal stage of the Claus unit must be designed to accommodate different operational modes, depending on the feedstock characterization.

These modes can be grouped into four categories: straight-through, split-feed, cofiring and fuel-support mode. In the straight-through mode, the entirety of the acid gas and airflow passes through the Claus burner. This mode is set for rich acid gases.

When the H_2S concentration falls below 35 vol%–40 vol%, the operation of

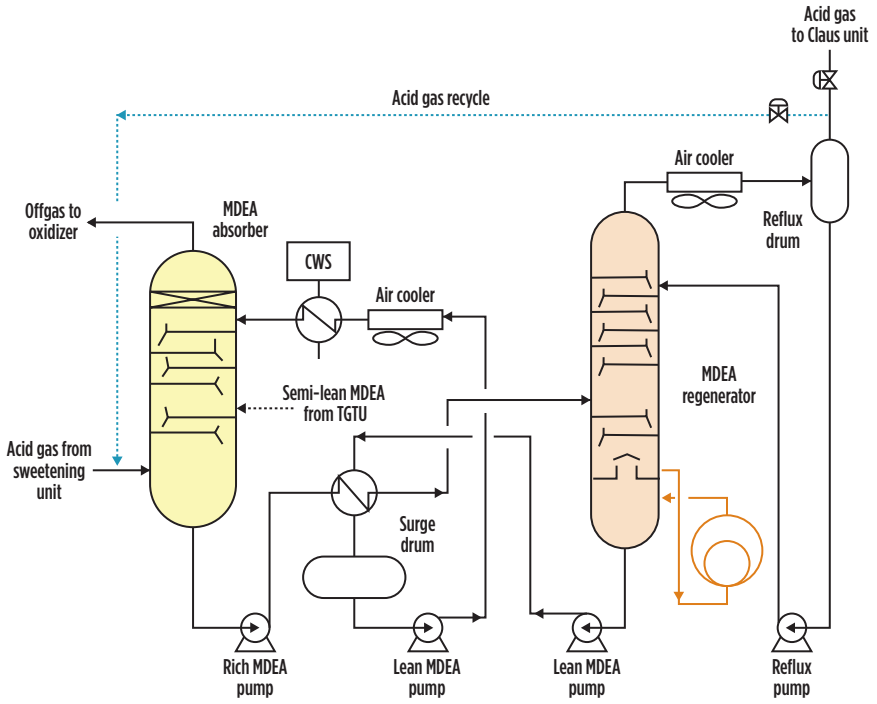

FIG. 2. Acid gas enrichment process flowsheet.

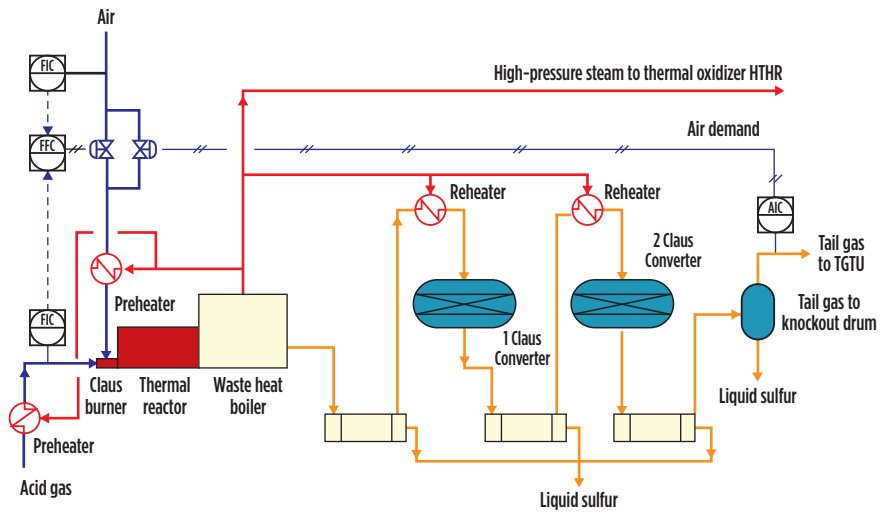

FIG. 3. Claus unit process flow diagram.

the Claus unit can be supported by activating the split-feed mode. In this case, a slipstream of the acid gas bypasses the burner and enters an intermediate point of the thermal reactor while the airflow passes through the burner. Since the bypassed acid gas is not involved in the oxidation step, the heat released by the reaction (Eq. 2) is transferred to a lesser mass. This entails a comparatively higher temperature. In this way, the temperature of the flame can be kept at the desired value simply by adjusting the slipstream flowrate. However, when natural gas contains BTEX, the split-feed mode cannot be used because the resulting formation of soot would foul the catalyst converters.

In cases where natural gas contains BTEX and/or when lean acid gas must be processed in the CPF, the operation of the Claus unit can be supported with the cofiring technique. In cofiring mode, a small quantity of a clean fuel gas is added to the thermal reactor to keep the temperature higher than 1,200°C, which is the temperature required for destroying BTEX inside the thermal reactor.

The fuel-support mode is a variation[a] of the cofiring technique to optimize the handling of very lean acid gas and BTEX bearing gas.

Tail gas treatment unit. The overall sulfur recovery efficiency of a Claus unit is in the range of 94%–98%, depending on the number of Claus catalytic converters. Therefore, Claus offgas still contains a sizeable quantity of SO_2, sulfides, COS and CS_2. These sulfur compounds must be removed if an overall SRU recovery of more than 99.9% is targeted.

Further removal of sulfur species can be accomplished by complementing the Claus unit with a TGTU. In many CPFs, the TGTU process is based on catalytic reduction of oxidized sulfur species back into H_2S by means of a reducing agent, such as H_2. The reducing agent is typically produced by burning a clean fuel gas in substoichiometric condition in an inline burner—a reducing gas generation (RGG) process.

SCOT (licensed by Shell), RAR (licensed by Kinetics Technology) and TopClaus (jointly licensed by Worley/Comprimo and Haldor Topsoe) are well-known commercial processes based on RGG. The HCR process (licensed by Sirtec Nigi) supplies reducing gas, exploiting the H_2S thermal dissociation ($H_2S \rightarrow S + H_2$) that naturally occurs inside the thermal reactor. In this way, the RGG—which is known to be a source of operational troubles—is no longer required.

In addition to the reduction of oxidized sulfur species, the reduction catalyst also promotes the hydrolysis of COS and CS_2. A Claus unit complemented with this kind of TGTU does not need titanium catalyst to destroy the organic sulfur.

A TGTU plant based on the reduction process consists of a catalytic reduction section followed by a quench step and H_2S extraction from offgas, as shown in FIG. 4. In this process, the Claus offgas is preheated to 240°C in a gas-gas heat exchanger by means of the high-pressure steam produced in the Claus waste heat boiler. The heated Claus offgas is then charged into a fixed-bed catalytic converter, where the hydrogenation reaction takes place. The offgas in this reactor contains N_2, H_2S, H_2O, CO_2 and traces of unreacted SO_2. After cooling to 40°C–45°C in the quench tower, the offgas is contacted by an aqueous solution of formulated MDEA, which absorbs the H_2S before the effluent is discharged to the atmosphere through an oxidizer (also

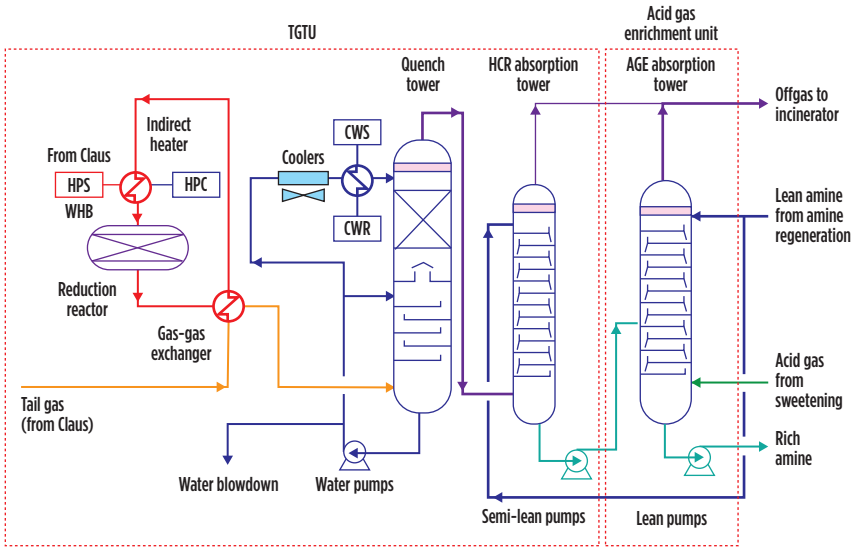

FIG. 4. Integrated tail gas cleanup process representing an integrated TGTU at a gas field development project.

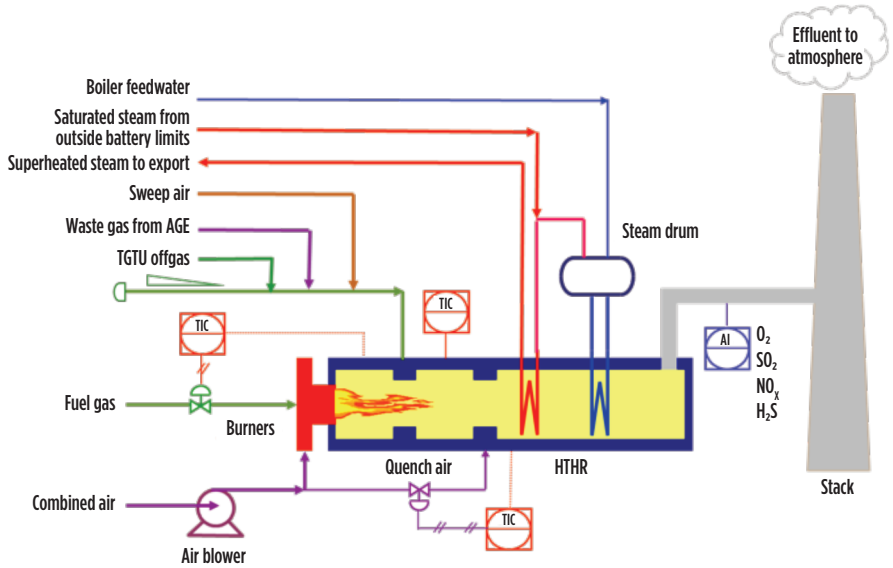

FIG. 5. Integrated thermal oxidizer.

referred to as an incinerator). The H_2S captured by the solvent is stripped in the regeneration tower of the acid gas enrichment section of the SRU and then sent back to the Claus unit, thereby achieving an overall sulfur recovery efficiency greater than 99.9%.

When only 99%–99.5% sulfur recovery efficiency is allowed, processes based on selective oxidation of H_2S to elemental sulfur can be used. The selective oxidation of H_2S is achieved by means of a catalyst that does not promote the Claus equilibrium reaction and prevents oxidation to SO_2 of the elemental sulfur formed via the reverse reaction of (1, FIG. 3). Other compounds in the process gas, such as COS and CS_2, are neither oxidized nor hydrolyzed. Well-known selective oxidation processes include SUPERCLAUS and EUROCLAUS (both licensed by Worley/Comprimo and Jacobs).

Thermal oxidizer (incinerator). The oxidizer/incinerator is the interface between the CPF and the environment. It receives offgases from both the enrichment section and the TGTU. It also receives the sweep air from the sulfur pit.

All these streams still contain "traces" of H_2S, COS and CS_2 that must be converted into less noxious compounds, such as SO_2, CO_2 and H_2O. Generally, these pollutants are destroyed by means of an oxidation process carried out at temperatures between 450°C and 650°C (up to 940°C when CO oxidation is required by local legislation) before being discharged to the atmosphere.

FIG. 5 shows an example of a thermal oxidizer installed in a large CPF. It includes several elements:

- A combustion chamber, where a fuel gas is burned with excess air to produce a flue gas hot enough to bring the offgas temperature to the desired level
- An oxidation chamber, where effluents are mixed and thermally oxidized
- A high-temperature heat recovery (HTHR) section, including a waste heat boiler and one or more superheating coils for rising high-pressure steam.

For small-scale CFP, the quantity of high-pressure steam that can be produced may not justify the investment in HTHR. In these cases, the hot effluent is routed toward the atmosphere through the stack after having been quenched with secondary air in the quench chamber of the oxidizer.

Liquid sulfur degassing. Liquid sulfur is formed in the condensers and collected in a pit by gravity. In the condensers, liquid sulfur is in equilibrium with its vapor; therefore, it dissolves a small quantity of H_2S. Under the condenser operating conditions, the dissolved H_2S reacts with elemental sulfur to form polysulfides (H_2S_x, with $x > 1$). These H_2S_x slowly and naturally decompose to form sulfur and H_2S. Liquid sulfur, if not degassed, would be risky due to the release of flammable, toxic, corrosive H_2S.

In a sulfur degassing system, hot air (sweeping air) can be used as a catalyst for the H_2S_x decomposition and as a stripping agent for H_2S. The H_2S concentration in the degassed liquid sulfur is specified at less than 10 ppmw, which is generally accepted as a safe concentration.

Several commercial liquid degassing systems exist, one of which is the Shell Degassing process. In this system, hot air is bubbled below an open box submerged in the liquid sulfur to create a natural circulation flow that promotes H_2S_x decomposition and H_2S stripping.

Other processes use hot air as the stripping agent and the promoter/catalyst for the H_2S_x decomposition. These processes accomplish the degassing operation in an out-of-pit pressure vessel fitted with mass transfer equipment. Among these are D'GAAS (licensed by Fluor) and SN Degassing (licensed by Siirtec Nigi).

Material and energy integration. An SRU encompasses several intertwined process units, with each one achieving a specific function involving heat exchange and material transformation. The ways in which these specific functions are interwoven affects the service factor of the materials stream and the energy efficiency, which ultimately impacts the economics of a CPF.

In general, the Claus unit produces approximately 2,300 kg–3,000 kg of steam per ton of recovered liquid sulfur. When the waste heat boiler is designed to produce high-pressure steam at 45 barg and greater, this steam can be used not only to supply the Claus captive users (feed preheaters, the reheaters and the plant steam tracing), but also to supply energy to the reducing catalyst of the TGTU through a condensing steam heat exchanger with significant cost advantages over the traditional gas-gas heat exchanger or inline burners.

Moreover, the net valuable high-pressure steam produced in the SRU block can be used by other steam users of the CPF in exchange for the less-valuable steam at 3.5 barg that is needed by the SRU's MDEA regenerator.

The acid gas load of the MDEA withdrawn from the absorber bottom of the TGTU is in the range of 0.12 mol/mol–0.15 mol/mol; significant pickup capability for a lean MDEA solution remains (**note:** the load of an MDEA solution is generally 0.45 mol/mol–0.5 mol/mol). This residual pickup capacity can be exploited to reduce the overall MDEA circulation flowrate in the SRU, which entails a further reduction of CAPEX and OPEX due to the reduced duties of the heat exchangers and the electric power requirement of the pumps. This material integration is achieved by feeding the above stream to an intermediate tray of the enrichment absorption tower (FIG. 4), where it is transformed into rich MDEA.

The thermal and material integrations of the processes inside the SRU maximize the thermodynamic efficiency and streams utilization, with economic benefits both in terms of CAPEX and OPEX. GP

NOTE

[a] Variation introduced by Siirtec Nigi

LORENZO MICUCCI is a Senior Director at Siirtec Nigi SpA. He has more than 30 yr of experience in the engineering and contracting industry, most of which have been spent in the natural gas sector. In 2001, he joined Siirtec Nigi in Milan, where he directed the process design and operations department and the research and development department. During his time as R&D head, three patents have been granted to Siirtec Nigi, two of which have been implemented on an industrial scale. At present, he is the Senior Director of the technology and marketing departments. Mr. Micucci also worked for Saipem (Snamprogetti) as a Plant Designer for integrated gasification combined cycle and gas-to-liquids plants. He holds an MS degree in chemical engineering from the University of Bologna in Italy and is enrolled as a Qualified Engineer in the Register of Milan Order of Engineers.

Waga Energy to deploy RNG technology in Quebec

Waga Energy has been enlisted by the Mauricie Residual Materials Management Board to deploy its landfill gas-to-renewable natural gas (RNG) technology at the Saint-Étienne-des-Grès landfill in Quebec, Canada. The green gas produced will be purchased by gas distributor Énergir for injection into its gas grid onsite. The landfill gas-to-RNG project, which will run for at least 20 yr, will be the first in Canada to use the WAGABOX technology, which was developed to recover landfill gas as biomethane.

The recovered biomethane will be upgraded into grid-compliant RNG by a WAGABOX gas treatment unit built onsite. The landfill gas at Saint-Étienne-des-Grès was previously captured and burned in a flare. Designed to process 3,400 m^3/hr of biogas, the WAGABOX unit will produce 468,000 GJ/yr of renewable gas, corresponding to the consumption of 8,000 local households and preventing the release of 23,000 tpy of CO_2 into the atmosphere. The project is scheduled to be completed by 2022.

Servomex upgrades flammable gas analyzer

Servomex's SERVOPRO MultiExact 4200 analyzer provides high-specification multi-gas analysis of flammable gas samples and trace contaminants in applications including HyCO, syngas, hydrogen production and gas transfer applications.

Utilizing paramagnetic, infrared and gas filter correlation sensing technologies, the MultiExact 4200 analyzer measures up to four gas streams simultaneously, with percentage measurements for O_2, CO_2 and CO. It can also be configured to measure percentage CH_4 and ppm-level CO, CO_2, CH_4 and N_2O.

The analyzer has a built-in LCD screen and provides alarm, fault and calibration logs. An automatic calibration option reduces ongoing operational requirements. Other benefits include minimal maintenance requirements and a low cost of ownership.

GTT upgrades NO96 technology

GTT has developed the NO96 Super+, an evolution of the NO96 Cargo Containment System (CCS), which has received an approval in principle from Bureau Veritas.

The NO96 Super+ technology integrates insulating reinforced polyurethane foam panels instead of plywood boxes to reduce the heat ingress inside the tank. Glass wool flat joints are also inserted between adjacent foam panels to optimize the behavior of the system and ensure it the best thermal performance.

These modifications allow GTT to further reduce the evaporation of the cargo during operations, with NO96 Super+ offering a guaranteed boiloff rate of 0.085 vol%/d for a standard LNG carrier with a capacity of 174,000 m^3. Further reductions down to 0.08 vol%/d are possible for larger capacities, such as 200,000 m^3.

BW LNG signs digitalization deal

BW LNG has signed a deal with Kongsberg Digital and Alpha Ori Technologies for a digitalization partnership to realize digital capabilities that enhance efficiency and reduce the environmental footprint of LNG carriers (LNGCs) and floating storage and regasification units (FRSUs).

The agreement encompasses several projects, including utilizing a common data management platform and developing a maritime digital twin and digital processing models. The aim of the partnership is to enable the acceleration of technologies needed for future-ready LNG carriers and FSRUs by leveraging Kongsberg Digital's data infrastructure technology, Vessel Insight, together with Alpha Ori's SMARTShip digital applications and BW LNG's operational expertise and assets for piloting a maritime digital twin and a real-time decision-support system.

A pilot project has been established to develop and test a maritime digital twin developed for the BW Magna FSRU, utilizing the Vessel Insight data infrastructure, Kognifai digital platform and maritime simulators from Kongsberg Digital, as well as value-adding expert applications from Alpha Ori. The pilot will illustrate an example of the benefits of digitalization for the industry.

Silverstream Technologies completes LNGC trials

Clean technology company Silverstream Technologies announced that its pioneering air lubrication system, the Silverstream System, has delivered significant fuel and emissions savings during testing on the Shell-chartered 170,000-m^3 LNG carrier *Methane Patricia Camila.*

Following operational testing of the retrofitted technology, Silverstream and Shell's engineers demonstrated 6.6% net savings generated by the Silverstream System. The technology was tested at various vessel speeds during *Methane Patricia Camila's* normal operations, to calculate fuel and emissions savings.

The Silverstream System enables fuel and emissions efficiencies through its unique design. The technology produces a thin layer of microbubbles along the full flat bottom of the vessel, reducing frictional resistance between the water and the hull.

The system was successfully retrofitted on the 2010-built LNGC during its October 2020 planned dry docking at the Sembcorp Marine Admiralty Shipyard in Singapore. From design through to installation, the system was reviewed and approved by ABS in accordance with its guidance note for air lubrication technology.

Honeywell enables large U.S. CCS project

Wabash Valley Resources LLC has selected a range of Honeywell UOP technologies to capture and sequester up to 1.65 MMtpy of CO_2 and to produce clean H_2 energy from a repurposed gasification plant in West Terre Haute, Indiana. The project is expected to be one of the largest carbon sequestration initiatives in the U.S. to date.

UOP will provide technology licenses, basic engineering and specialty equipment including a modular MOLSIV molecular sieve dehydration unit, a modular Ortloff CO_2 fractionation unit and a Polybed pressure swing adsorption (PSA) unit to sequester CO_2 and process synthesis gas from the gasification unit. The Ortloff CO_2 fractionation technology will produce a high-purity liquid CO_2 stream while separating an H_2-rich stream that will be purified by the PSA unit. The CO_2 stream will be sent for permanent geological storage.

Chart, ABB to standardize controls for LNG, biogas, H_2

Chart Industries has signed a development and commercial MOU with ABB to support Chart's modular offerings for LNG, H_2, biogas, water treatment and carbon-capture projects.

Chart and ABB have complementary offerings and share a drive for clean energy, water and industrial applications. Their partnership will modularize solutions in key emerging segments to drive down cost and minimize risks.

As part of the MOU, ABB will develop standard modular controls, automation, power supply and telecoms solutions for a number of Chart offerings:

- H_2 and LNG plants with significant electrical content
- Transform Materials' plants, a sustainable chemical company with a patented net-carbon-negative process to cost-effectively produce high-purity acetylene and H_2
- BlueInGreen water treatment dissolution skids
- Carbon-capture plants.

Chart Industries is a provider of technology, equipment and services related to LNG, H_2, biogas and carbon capture, among others. ABB is a global technology company that energizes the transformation of society and industry to achieve a more productive, sustainable future.

X-Gas leads in next-generation sustainable fuel transport

The X-gas project is a series of unconventional, medium-capacity LNG/gas bunkering tankers designed by Knud E. Hansen. The flagship design of the project is a 126.5-m vessel with a total cargo capacity of 9,000 m^3, split between two Type C tanks. The platform is highly customizable and can be tailored to accommodate a range of tank capacities, as well as various containment systems including membrane tanks.

A unique feature of the X-gas platform is a low-profile, forward deck house. This enables the vessel to safely approach and pull alongside cruise ships with low-hanging lifeboats. It also minimizes the need for ballast during cargo transfer. Lastly, the forward deck house allows for larger cargo tanks without impeding bridge visibility.

For improved maneuvering and safety, the design features two propulsion thrusters aft and two bow thrusters, as well as an autodocking system. The design also features a fuel-efficient diesel electric power and propulsion plant. Integrated with the propulsion plant is an energy storage system with a lithium-ion battery bank. Boiloff gas from the cargo tanks is captured and consumed in the dual-fuel engines, and waste heat from the engine cooling water is converted to electric and thermal power.

GAS PROCESSING & LNG

Catherine Watkins, Publisher
+1 (713) 520-4421
Catherine.Watkins@HydrocarbonProcessing.com
www.GasProcessingNews.com

NORTH AMERICA

NORTH HOUSTON, SUGAR LAND, NORTH TEXAS, UPPER MIDWEST
Jim Watkins
+1 (713) 525-4632
Jim.Watkins@GulfEnergyInfo.com

WEST HOUSTON, CENTRAL TEXAS, ALBERTA, NEW MEXICO
Brett Stephen
+1 (713) 525-4660
Brett.Stephen@GulfEnergyInfo.com

DALLAS, MIDWEST/CENTRAL U.S.
Josh Mayer
+1 (972) 816-6745
Josh.Mayer@GulfEnergyInfo.com

WESTERN U.S., BRITISH COLOMBIA
Rick Ayer
+1 (949) 366-9089
Rick.Ayer@GulfEnergyInfo.com

SOUTHEAST HOUSTON, GULF COAST & SOUTHEAST U.S.
Austin Milburn
+1 (713) 525-4626
Austin.Milburn@GulfEnergyInfo.com

NORTHEAST U.S., EASTERN CANADA
Merrie Lynch
+1 (617) 594-4943
Merrie.Lynch@GulfEnergyInfo.com

OUTSIDE NORTH AMERICA

AFRICA
Dele Olaoye
+1 (713) 240-4447
Africa@GulfEnergyInfo.com

BRAZIL
Evan Sponagle
Phone: +55 (21) 2512-2741
Mobile: +55 (21) 99925-3398
Evan.Sponagle@GulfEnergyInfo.com

CHINA, HONG KONG
Iris Yuen
China: +86 13802701367
Hong Kong: +852 69185500
China@GulfEnergyInfo.com

WESTERN EUROPE
Hamilton Pearman
+33 608 310 575
Hamilton.Pearman@GulfEnergyInfo.com

INDIA
Manav Kanwar
+91 (22) 2837 7070
India@GulfEnergyInfo.com

ITALY, EASTERN EUROPE
Riccardo R.C. Laureri
Office: +39 02 2362500
Mobile: +39 335 6962477
Riccardo.Laureri@GulfEnergyInfo.com

JAPAN
Yoshinori Ikeda
+81 (3) 3661-6138
Japan@GulfEnergyInfo.com

KOREA
YB Jeon
+82 (2) 755-3774
Korea@GulfEnergyInfo.com

RUSSIA, FSU
Lilia Fedotova
+7 (495) 628-10-33
Lilia.Fedotova@GulfEnergyInfo.com

UK, SCANDINAVIA, IRELAND, MIDDLE EAST
Brenda Homewood
Phone: +44 (0) 1622 297123
Brenda.Homewood@GulfEnergyInfo.com

CORPORATE, FULL ACCESS SUBSCRIPTION AND CLASSIFIED SALES
J'Nette Davis-Nichols
+1 (713) 520-4426
Jnette.Davis-Nichols@GulfEnergyInfo.com

ADVERTISER INDEX